



---

# EMPIRE

## modular system for nuclear reaction calculations

(version: 3.1 Rivoli)

M. Herman

NNDC, Brookhaven National Laboratory, Upton, USA

e-mail: mwherman@bnl.gov

R. Capote

NDS, International Atomic Energy Agency, Vienna, Austria

V. Zerkin,

NDS, International Atomic Energy Agency, Vienna, Austria

A. Trkov

Jožef Stefan Institute, Ljubljana, Slovenia

H. Wienke

affiliation ...

M. Sin,

University of Bucharest, Bucharest, Romania

B.V. Carlson

ITA/Centro Tecnico Aeroespacial, Sao Jose dos Campos, Brazil

C. Mattoon

Lawrence Livermore National Laboratory, Livermore, USA

Young-Sik Cho

Korea Atomic Energy Research Institute, Daejeon, South Korea

June 3, 2011

---



EMPIRE is a modular system of nuclear reaction codes, comprising various nuclear models, and designed for calculations over a broad range of energies and incident particles. The system can be used for theoretical investigations of nuclear reactions as well as for nuclear data evaluation work. A projectile can be a photon a nucleon, a light or heavy ion. The energy range starts just above the resonance region in the case of a neutron projectile, and extends up to few hundred MeV for heavy ion induced reactions. The code accounts for the major nuclear reaction models, such as optical model, Coupled Channels and DWBA (ECIS06), Coupled Channels' Soft-Rotator (OPTMAN), Multi-step Direct (ORION + TRISTAN), NVWY Multi-step Compound, exciton model (PCROSS and DEGAS), hybrid Monte Carlo simulation (DDHMS), and the full featured Hauser-Feshbach model including the optical model for fission. Heavy ion fusion cross section can be calculated within the simplified coupled channels approach (CCFUS). A comprehensive library of input parameters based on the RIPL-3 library covers nuclear masses, optical model parameters, ground state deformations, discrete levels and decay schemes, level densities, fission barriers, and  $\gamma$ -ray strength functions. Effects of the dynamic deformation of a fast rotating nucleus can be taken into account in the calculations (BARFIT, MOMFIT). The results can be converted into the ENDF-6 format using the accompanying EMPEND code. Modules of the ENDF Utility Codes and the ENDF Pre-Processing codes are applied for ENDF file verification. The package contains the full EXFOR library of experimental data in computational format C4 that are automatically retrieved during the calculations. Publication quality graphs can be obtained using the powerful and flexible plotting package ZVView. Interactive plots with ZVView comparing experimental results with calculations can be produced with ENDVER modules. The graphic user interface, written in Tcl/Tk is linked to the rest of the system through bash-shell (UNIX) scripts and provides for easy operation of the system.

(Mike to add a paragraph on the resonance module and the covariances).



# Contents

<b>1</b>	<b>Introduction</b>	<b>10</b>
<b>2</b>	<b>Models</b>	<b>13</b>
2.1	Fusion/reaction cross section . . . . .	13
2.2	Coupled-Channels Code ECIS . . . . .	15
2.3	Coupled-Channels Code OPTMAN . . . . .	17
2.4	Multi-step Direct . . . . .	17
2.4.1	Outline of the theory . . . . .	17
2.4.2	Notes on RPA-Description of Transition Strength Functions . . . . .	22
2.4.3	Implementation of ORION and TRISTAN codes in EMPIRE . . . . .	24
2.5	Multi-step Compound . . . . .	25
2.5.1	Conditional level densities . . . . .	26
2.6	$\gamma$ -emission in Multi-step Compound . . . . .	28
2.7	Coupling between MSC and MSD . . . . .	31
2.8	Exciton model . . . . .	32
2.9	Monte Carlo Preequilibrium . . . . .	36
2.10	Compound Nucleus . . . . .	38
2.10.1	Level densities . . . . .	40
2.10.2	Nuclear deformation and moments of inertia . . . . .	48
2.10.3	Fission barriers . . . . .	50
2.10.4	Dissipation effects . . . . .	51
2.10.5	$\gamma$ -ray emission . . . . .	52
2.11	Width fluctuation correction . . . . .	54
2.12	Photoabsorption . . . . .	56
2.13	Fission . . . . .	58
2.13.1	Fission barriers . . . . .	58
2.13.2	Transmission mechanisms . . . . .	60
2.13.3	Decay probabilities . . . . .	62
2.13.4	Input/output . . . . .	63
2.14	Binding energies . . . . .	67
2.15	Model compatibility . . . . .	67
2.16	Spectra of recoils . . . . .	69
2.17	Exclusive spectra . . . . .	71

<b>3</b>	<b>Code</b>	<b>72</b>
3.1	Directory structure . . . . .	72
3.2	Installation . . . . .	74
3.3	Array dimensions . . . . .	76
3.4	Parameter libraries . . . . .	78
3.4.1	Masses ( <i>empire/RIPL-2/masses/mass-frdm95.dat</i> ) . . . . .	78
3.4.2	Discrete levels ( <i>empire/RIPL-2/levels/zxxx.dat</i> ) . . . . .	79
3.4.3	Optical model parameters ( <i>empire/RIPL-2/optical/om-data/om-parameter-u.dat</i> ) . . . . .	83
3.4.4	Excited-level deformation parameters ( <i>empire/RIPL-2/optical/om-data/om-deformations.dat</i> ) . . . . .	91
3.4.5	Experimental Giant Dipole Resonance parameters ( <i>empire/RIPL-2/gamma/gdr-parameters-exp.dat</i> ) . . . . .	91
3.4.6	Calculated Giant Dipole Resonance energies and widths ( <i>empire/RIPL-2/gamma/gdr-parameters-theor.dat</i> ) . . . . .	92
3.4.7	Tabulated HF-BCS level densities ( <i>empire/RIPL-2/densities/total/level-densities-hfbcs/zxxx.dat</i> ) . . . . .	93
3.4.8	Experimental fission barriers ( <i>empire/RIPL-2/fission/fis-barrier-exp.dat</i> ) . . . . .	93
3.4.9	Fission barriers and saddle point deformations based on the ETFSI model ( <i>empire/RIPL-2/fission/fis-barrier-etfsi.dat</i> ) . . . . .	94
3.4.10	Tabulated level densities at saddle points ( <i>empire/RIPL-2/fission/fis-levden-hfbcs-inner/zxxx.dat</i> and <i>empire/RIPL-2/fission/fis-levden-hfbcs-outer/zxxx.dat</i> ) . . . . .	95
3.4.11	Level density parameters ( <i>empire/data/ldp.dat</i> ) . . . . .	97
3.4.12	Ground state deformations ( <i>empire/data/deflib.dat</i> ) . . . . .	97
3.4.13	Fission barriers ( <i>empire/data/fisbar.dat</i> ) . . . . .	97
3.4.14	Neutron resonances ( <i>empire/data/resonances.endf</i> ) . . . . .	98
3.5	Flow of the calculations . . . . .	98
3.6	List of EMPIRE modules . . . . .	100
3.7	Executing EMPIRE . . . . .	104
3.7.1	"runE" sequence (Run EMPIRE) . . . . .	105
3.7.2	"format" sequence . . . . .	105
3.7.3	"verify" sequence . . . . .	106
3.7.4	"process" sequence . . . . .	106
3.7.5	"run" sequence . . . . .	107
3.7.6	Script mode . . . . .	107
3.7.7	GUI mode . . . . .	112
3.8	ENDF formatting . . . . .	119
3.8.1	EMPEND Input instructions . . . . .	121
3.9	Fitting Optical Model Parameters . . . . .	123
3.10	Input/Output files . . . . .	124
3.10.1	*.inp (INPUT.DAT; main input) . . . . .	124



3.10.2	*.lst (LIST.DAT; lengthy output)	136
3.10.3	*.out (OUTPUT.DAT; short output)	138
3.10.4	*.fus (FUSION)	138
3.10.5	*.lev (LEVELS)	138
3.10.6	*-lev.col (TARGET_COLL.DAT)	139
3.10.7	*-inp.fis (FISSION.INP)	140
3.10.8	FISSION.OUT	141
3.10.9	*-omp.rtpl (OMPAR.RIPL)	141
3.10.10	*-omp.dir (OMPAR.DIR)	141
3.10.11	*.endf (OUTPUT.ENDF)	142
3.10.12	*-s.endf	142
3.10.13	*.exf (EXFOR.DAT)	142
3.10.14	*.c4 (empire/util/x4toc4/c4.dat)	143
3.10.15	*.ps (empire//util/plotc4/plot.ps)	144
3.10.16	*-cum.ps	144
3.10.17	*-ompfit.lst (FIT.OUT)	144
3.10.18	*.x42c4_lst (empire/util/x4toc4/x4toc4.lst)	144
3.10.19	*.x42c4_errs (empire/util/x4toc4/errors)	144
3.10.20	Log files	144
3.11	Plotting capabilities	145
3.11.1	ZVView	146
3.12	Plans for further development	147
<b>4</b>	<b>Working notes</b>	<b>149</b>
4.1	Avoiding problems	149
4.2	Fitting discrete levels	149
4.3	Handling OM potentials	151
4.3.1	DWBA with RIPL OMP	152
4.3.2	Coupled-Channels with RIPL spherical OMP	153
4.3.3	Coupled-Channels with RIPL Coupled-Channels OMP for inelastic scattering	153
4.3.4	Complete Coupled-Channels with RIPL CC OMP for inelastic scattering	154
4.4	Use of level densities	154
4.5	Parameter tuning	155
4.6	Description of test cases	168
	<b>Appendix ChangeLog</b>	<b>174</b>

# 1 Introduction

The first version of EMPIRE code was released in 1980. This code originally contained the Hauser-Feshbach theory and the classical HYBRID model to account for the preequilibrium effects. The width fluctuation correction was implemented in terms of the HRTW approach [1, 2]. Since that time, the code has been continuously developed. Adding the FKK Multi-step Compound mechanism [3] lead to the EMPIRE-MS version. Subsequently, the NVWY formulation of the Multi-step Compound mechanism [4] was implemented in the HMS-EMPIRE. This version also included combinatorial calculations of particle-hole level densities. In addition, a version for heavy ion induced reactions (EMPIRE HI) was developed.

EMPIRE-2 is a totally new release of the code. Contrary to the preceding developments, which largely consisted in adding new features without changing the structure of the code, the present version has been rewritten from scratch, using different programming concepts. Taking advantage of the relaxed memory limitations, all intermediate files were eliminated, which together with careful coding of the most crucial parts of the code, increased the speed of the program by a factor of 20. The new code is projected to be general and flexible, and can be applied to the calculation of neutron capture in the keV region, as well as for heavy ion (HI) induced reactions at several hundreds of MeV. All dimensions in the main code are set up through the parameter statements contained in the separate file, which is included wherever appropriate, making any adjustment of the code to the actual problem and/or computer straightforward. The code has a modular structure. Each module performs a well defined task and communicates with other modules through a set of global COMMONS which are included in most of the subroutines. This assures access to all the resources throughout the code, and facilitates adding new features and mechanisms.

EMPIRE makes use of several codes, written by different authors, which were converted into subroutines and adapted for the present use. In most cases, the modifications concerned input/output interface and never affected the physical model contained in the original source. The following codes are incorporated in the present version of EMPIRE:

<b>ECIS06</b>	Coupled-Channels and DWBA code by J. Raynal [5],
<b>CCFUS</b>	simplified Coupled-Channels calculation of HI fusion cross section by C.H. Dasso and S. Landowne [6],
<b>ORION &amp; TRISTAN</b>	TUL [7] approach to Multi-step Direct by H. Lenske [8],
<b>DEGAS</b>	exciton model with angular momentum conservation and $\gamma$ emission [9] by E. Běťák and P. Obložinský,

**DDHMS** Monte Carlo simulation of the preequilibrium decay by M.B. Chadwick [10]

**BARMOM** fission barriers and moments of inertia by A. Sierk [11].

The reader is referred to the original papers for a more detailed description of these incorporated codes. Furthermore, the package includes the following stand-alone codes:

**EMPEND** converts EMPIRE results into ENDF-6 format (written by A. Trkov),

**ENDRES** merges existing resonance parameters into ENDF-6 formatted file produced by EMPEND (written by A. Trkov),

**X4TOC4** converts experimental data retrieved from EXFOR into computational C4 format (written by D.E. Cullen) [12],

**C4SORT** sorts experimental data in the computational C4 format file by MAT/MF/MT numbers and incident energy (written by A.Trkov) [13],

**FIXUP** used to reconstruct redundant cross sections MT=4, 103, and 107 (Program of the Pre-Pro series, written by D.E. Cullen) [12],

**LEGEND** reconstructs tabular linearly interpolable angular distributions from ENDF data in different format representations (Program of the Pre-Pro series, written by D.E. Cullen) [12],

**LSTTAB** tabulates ENDF and EXFOR data in PLOTTAB format (module of ENDVER package, written by A.Trkov) [13],

**SIXTAB** converts ENDF file MF6 to Law 7 representation (module of ENDVER package, written by A.Trkov) [13],

**PLOT C4** plots comparison between EMPIRE results and EXFOR data (written by D.E. Cullen and A. Trkov) [13],

**CHECKR** performs format checking of the ENDF-6 formatted file (ENDF Utility codes, written by Ch. Dunford)

**FIZCON** performs physics check of the ENDF-6 formatted file (ENDF Utility codes, written by Ch. Dunford)

**PSYCHE** performs more physics checking of the ENDF-6 formatted file (ENDF Utility codes, written by Ch. Dunford)

**LINEAR** converts MF=3 (cross sections) in an ENDF file into a linear-linear interpolable form (Program of the Pre-Pro series, written by D.E. Cullen) [12]

<b>PLTLST</b>	prepares a list of data types in the EXFOR data-base that can be compared to quantities in the ENDF files (module of ENDVER package, written by A.Trkov) [13],
<b>RECENT</b>	reconstructs the resonance contribution to the cross sections in an ENDF file into linearly interpolable form (Program of the Pre-Pro series, written by D.E. Cullen) [12]
<b>SIGMA1</b>	Doppler broadens neutron induced cross sections in an ENDF file (Program of the Pre-Pro series, written by D.E. Cullen) [12]
<b>STANEF</b>	Standardizes ENDF-6 formatted file (ENDF Utility codes, written by Ch. Dunford)
<b>zvvdxd</b>	Produces plots of angular distributions, spectra and double differential cross sections using ZVView package (written by V. Zerkin).
<b>c4zvd</b>	ZVView plotting package by V. Zerkin [14].

The next chapter outlines nuclear reaction models used in the code. Both, the structure of the code and the input/output files are described in Chapter 3. Use of the code, the role of input parameters, and a few typical examples of input files are discussed in Chapter 4.

## 2 Models

### 2.1 Fusion/reaction cross section

The reaction cross section is calculated in terms of transmission coefficients  $T_l^a(\epsilon)$  using the expression

$$\sigma_a(U, J, \pi) = \frac{\pi}{k^2} \frac{(2J+1)}{(2I+1)(2i+1)} \sum_{S=|I-i|}^{I+i} \sum_{l=|J-S|}^{J+S} f(l, \pi) T_l^a(\epsilon), \quad (2.1)$$

where  $k$  is the wave number of relative motion,  $i, I, J$ , and  $S$  indicate projectile, target, compound nucleus, and channel spin, respectively, and  $l$  is the orbital angular momentum of the projectile  $a$ . The function  $f(l, \pi)$  ensures parity conservation. It is unity if  $p*P*(-1)^l = \pi$  and zero otherwise. Here  $p$ ,  $P$ , and  $\pi$  are projectile, target, and compound nucleus parities and  $\epsilon$  and  $U$  stand for the projectile and compound nucleus energy.

For projectiles with mass numbers  $A < 5$  the transmission coefficients entering Eq. 2.1 are calculated using optical model routine ECIS06[5] unless an external file FUSION exists. In the latter case, the spin distribution of the Compound Nucleus is constructed from this file.

The heavy ion fusion cross section is calculated using Eq. 2.1 with transmission coefficients determined according to one of the following methods:

- (i) Simplified Coupled-Channels approach [6] (CCFUS code). Inelastic excitations and transfer reaction channels are treated as independent modes which couple to the initial ground state. The corresponding wave equations are approximately uncoupled by diagonalizing the interaction at the barrier. The total transmission probability is then obtained by summing over the distribution of transmission probabilities for the eigenbarriers, with weights given by the overlap of the initial state with the eigenchannels. This is a default option. It takes into account coupling of the excited collective states in the target and projectile. A detailed description of the method can be found in the original reference [6].
- (ii) Distributed fusion-barrier model [15]. This method accounts for the effective lowering of the one-dimensional fusion barrier by allowing for the additional dimension and assuming that the barrier distribution in the added dimension can be represented by a truncated Gaussian. Thus the fusion barrier distribution  $f(B')$  can be characterized by the mean energy  $B$ , the standard deviation

$\sigma_B$ , and the truncation parameter  $t$ , and is written as

$$f(B') = n_0 \exp\left(\frac{B - B'}{2\sigma_B^2}\right)^2 \quad (2.2)$$

for  $|B - B'| < t\sigma_B$  and  $f(B') = 0$  otherwise. The parameter  $t$  defines the lowest possible value of the fusion barrier and  $n_0$  is the normalization factor ensuring that the integral of Eq. 2.2 is 1. The fusion probability for a given angular momentum  $l$  is given by a convolution of the barrier distribution  $f(B')$  and the transmission coefficient  $T_l(E - B')$

$$p(E, l) = \int_{-\infty}^{\infty} f(B') T_l(E - B') dB'. \quad (2.3)$$

The transmission coefficient in the Hill-Wheeler approach [16] reads

$$T_l(E - B') = \{1 + \exp[-2\pi(E - B' - E_{rot})/(\hbar\omega)]\}^{-1}, \quad (2.4)$$

with  $E_{rot}$  being rotation energy at angular momentum  $l$ . The distributed fusion-barrier option in EMPIRE allows for the extra-push energy that can be specified in the input and added to the fusion barrier. The latter, if not specified in the input, is by default calculated using BAR subroutine of CCFUS (see above).

- (iii) Fusion cross sections for each  $l$  read from the external file *FUSION* (\*.fus). The code converts them into transmission coefficients to be used in Eq.2.1. The existence of the *FUSION* (\*.fus) file overrides all input dispositions regarding fusion determination.  
NOTE: *FUSION* (\*.fus) file refers to a single incident energy, therefore only one energy at a time can be calculated.
- (iv) Total fusion cross section specified in input (single incident energy only).
- (v) Critical angular momentum  $l_{cr}$  for compound nucleus formation specified in input (single incident energy only).

In the latter two cases the transmission coefficients are assumed to be of the form

$$T_l^a(\epsilon) = \frac{1}{1 + \exp(-\frac{l_{cr}-l}{\delta l})}, \quad (2.5)$$

where  $\delta l$  is an input parameter. If the total fusion cross section is specified in the input, then the code adjusts  $l_{cr}$  in order to reproduce the requested value.

## 2.2 Coupled-Channels Code ECIS

ECIS [5] is a well known and highly respected code for calculations within the generalized optical model and Coupled-Channels model (CC). These are important for modeling reactions on deformed nuclei and, in particular, for the correct description of a strong population of collective discrete levels in the inelastic scattering. ECIS-95 was added to EMPIRE as its new extensive module by R. Capote in February 2001 and replaced with the ECIS06 version in EMPIRE-3.1. Symmetric rotational, vibrational-rotational and harmonic-vibrational CC modes are available. The implementation features automatic preparation of the ECIS06 input. It uses the RIPL-2 [17] optical model segment and resorts to the RIPL-2 discrete level schemes and to the deformation parameters (quadrupole deformations  $\beta_2$ ) only if these are not included in the optical model parameter set available from RIPL-2. Since EMPIRE has no table of vibrational (dynamical) deformations, these are defined in a somewhat ad hoc manner as 0.15 for quadrupole and 0.05 for octupole vibrations.

Calculations can be performed for the majority of deformed nuclei including rotational and vibrational, even-even and even-A with integer spins, as well as odd-A with half-integer spins. Vibrational even-even nuclei and even-A are also covered. The only exceptions are vibrational odd-A nuclei. In these cases automatic construction of the file with collective levels is not possible and the user must prepare the corresponding file manually.

Once ECIS06 is invoked, the code prepares several interim files to be read by EMPIRE. In most cases, the code prepares two additional files:

TARGET\_COLL.DAT, collective levels and their deformations to be used by the rotational or vibrational CC. In the case of vibrational model the phonon structure of the levels is also read from this file (in the case of the rotational model this information is ignored).

OMPAR.DIR, parameters of the Optical Model Potential (OMP) to be used in the inelastic channel (discrete collective levels). OMP parameters may be selected via a new keyword DIRPOT (similar to OMPOT, but only for the inelastic channel). This information is supplemented by the parameters read from the *\*-lev.col* file.

ECIS06 can be invoked by the EMPIRE in three different ways, using input directive DIRECT. The default value (DIRECT=0) calls the spherical optical model and suppresses calculation of direct reactions to the discrete levels. The remaining options have the following meaning:

DIRECT 1. Population of discrete, collective levels in the inelastic scattering is calculated using the Coupled-Channels model. The direct cross sections are exact but spherical transmission coefficients  $T_l$  are used for subsequent preequilibrium and HF calculations in the whole energy grid. These results are re-normalized at the  $T_l$  level by taking into account direct component. The total, elastic, absorption and the inelastic cross sections are

taken from the CC calculations if a true Coupled-Channel Optical Model Potential (CC-OMP) is being used (otherwise, in the case of the Spherical OMP (S-OMP), only inelastic cross sections are accepted).

The option DIRECT=1 is fairly fast, though some accuracy may be lost compared to the DIRECT=2 option described below. In general, it should perform well for the weakly coupled levels. For strong coupling, such as in the highly deformed rotational bands in heavy nuclei, it should be used with caution. It is the recommended option if accuracy is not a critical issue and the appropriate CC-OMP is available.

DIRECT 2. Population of discrete, collective levels in the inelastic scattering is calculated within the CC as above. Importantly, the CC is used consistently, considering the ground state and the coupled levels, to calculate all necessary transmission coefficients for subsequent preequilibrium and HF calculations. These CC transmission coefficients define absorption cross section that is available for the preequilibrium and HF decay. The absorption cross section sums up with the direct cross sections to collective levels to the reaction cross section. DIRECT=2 is an exact option that considers flux decrease due to the collective excitations at the level of  $T_l$ . In the first run with DIRECT=2,  $T_l$  values are calculated for the whole energy grid. These values are stored in the file *\*.tl* for further use. Although the first run takes quite a lot of time, all successive runs are much faster. It should be noted that file *\*.tl* can be used for successive runs only if no changes were made to the files *\*-lev.col* and *\*-omp.rtpl*. For each incident energy in the input file, there is one *\*.tl* file stored in the *work* directory. The DIRECT=2 is a recommended option for accurate calculations whenever an appropriate CC-OMP is available.

DIRECT 3. Population of discrete collective levels in the inelastic scattering is calculated using the DWBA method providing approximate direct cross sections. The spherical transmission coefficients  $T_l$  are used for the whole energy grid in subsequent preequilibrium and HF calculations. These results are renormalized at the  $T_l$  level by taking into account direct component. This option is fairly fast, though some accuracy may be lost. In general, it should perform well for weakly coupled levels. For a strong coupling, such as in the highly deformed rotational bands in heavy nuclei, it should be used with caution. The DWBA option has an advantage if the suitable CC-OMP is not available. In such a case, one can use S-OMP parameters in the DWBA calculations tuning inelastic cross sections by adjusting dynamical deformations of collective levels in file *\*-lev.col*.



## 2.3 Coupled-Channels Code OPTMAN

(insert text here)

## 2.4 Multi-step Direct

The approach to statistical Multi-step Direct reactions is based on the Multi-step Direct (MSD) theory of preequilibrium scattering to the continuum originally proposed by Tamura, Udagawa and Lenske [7]. Since then, the approach has been revised, especially the part related to statistical and dynamical treatment of nuclear structure.

The evolution of the projectile-target system from small to large energy losses in the open channel space is described in the MSD theory with a combination of direct reaction (DR), microscopic nuclear structure and statistical methods. As typical for the DR-approach, it is assumed that the closed channel space, i.e. the MSC contributions, have been projected out and can be treated separately within the Multi-step Compound mechanism.

### 2.4.1 Outline of the theory

In the MSD theory the effective Hamiltonian in the open channel space is divided into an energy averaged optical model part  $H^{opt}$ , describing the relative motion of projectile  $a$  and target  $A$ , the intrinsic Hamiltonian  $H^{intr}$  of the asymptotically separated nuclei and the residual effective projectile-target interaction  $V^{res}$  leading to non-elastic processes

$$H = H^{opt} + H^{intr} + V^{res} \quad . \quad (2.6)$$

Both  $H^{opt}$  and  $V^{res}$  are non-hermitian operators. To a large extent the imaginary parts are related to the flux absorbed into the closed channels, but those open channels which are not treated explicitly are also contributing.

The ORION code solves the Lippmann-Schwinger equation for the open channel T-matrix where the  $n^{th}$ -order term

$$T_{\gamma 0}^{(n)} = \langle \chi_E^{(-)} | (\gamma | V^{res} (G^{chan}(E) V^{res})^{n-1} | 0) | \chi_0^{(+)} \rangle \quad (2.7)$$

describes the  $n$ -step transition from the entrance channel with incoming scattering wave  $\chi_0^{(+)}$  and the ground state configuration  $|0\rangle = |aA\rangle$  to an exit channel  $\gamma$  with outgoing wave  $\chi_E^{(-)}$  at the energy  $E$  [18, 19].  $G^{chan}(E)$  is the Green's function for the channel. The scattering waves are optical model wave functions. They are weakly energy dependent on a scale much larger than the one on which the intrinsic states  $\gamma$  vary. The MSD approach treats the residual projectile-target interactions perturbatively. In this sense, MSD theory is a “weak coupling” description of continuum scattering.

In order to describe the statistical content of pre-equilibrium spectra the real states  $\gamma$  are expanded into  $n$ -particle and  $n$ -hole model states  $c$ . Explicitly,  $H^{intr}$  is chosen as

$$H^{intr} = H_0^{intr} + V^{intr} \quad . \quad (2.8)$$

The states  $c$  are eigenstates of  $H_0^{intr}$  and the residual interaction  $V^{intr}$  couples states from different particle-hole classes only. It is assumed that the configuration mixing between  $np-nh$  classes is stochastic in nature and leads to a random distribution of amplitudes with mean value zero [19]. When the density matrix is averaged over a finite energy interval, e.g. with a Lorentzian or Gaussian  $g(x)$  of full width  $\Delta$  large compared to the mean level spacing,

$$\hat{\rho}(E) = \int dE' g(E - E') \hat{\rho}_{micro}(E) \quad (2.9)$$

the coherence of the basis states is lost. As a result, the density matrix becomes a statistical matrix

$$\hat{\rho}(E) = \sum_n \hat{\rho}_n(E). \quad (2.10)$$

The summation extends over the  $np - nh$  classes with

$$\hat{\rho}_n(E) = \sum_{c=[npnh]} |c\rangle P_c(E) \langle c| \quad (2.11)$$

and the probability per energy to find the system in the configuration  $c$  is given by the spectroscopic densities,

$$P_c(E) = -\frac{1}{\pi} \text{Im} \left[ \int dE' g(E - E') \langle c | G^{intr}(E') | c \rangle \right], \quad (2.12)$$

with  $G^{intr}(E)$  being the intrinsic Green's function.

The statistical operators carry further properties which are important for the physical content of the description. Integrating  $P_c(E)$  over an interval  $\Delta E$  one obtains the spectroscopic factor for the configuration  $c$  in  $\Delta E$ . Irrespective of the representation, i.e. in either the  $\gamma$  or the  $c$  basis, the trace of  $\hat{\rho}(E)$ , Eq. 2.9, gives the total level density at energy  $E$ . The partial level density of  $np - nh$  states is determined by  $\text{tr}(\hat{\rho}_n)$  (Eq. 2.11).

Similar to the chaining and never-come-back hypotheses of [3] the interference terms  $n \neq k$  are neglected by assuming that in each step the reaction is dominated by transitions into configurations with the highest level density at a given excitation energy. This means, that we neglect de-excitation and re-scattering processes which decrease or leave the  $ph$ -number unchanged, respectively. With this assumption the cross section becomes an incoherent super-position of  $n$ -step contributions

$$\frac{d^2\sigma}{d\Omega dE} = \sum_n \frac{d^2\sigma^{(n)}}{d\Omega dE}, \quad (2.13)$$

where the multi-step cross sections are defined as

$$\frac{d^2\sigma^{(n)}}{d\Omega dE} = \sum_{c=[npnh]} P_c(E) |T_{c0}^{(n)}|^2. \quad (2.14)$$

Expanding  $V^{res}$  into multi-poles  $V_\lambda$  and noting that only  $1p-1h$  configurations are directly excited in a one-step process the  $\sigma^{(1)}$  is determined by an average over transitions into the  $1p-1h$  states  $c$  around excitation energy  $E$  with form factors

$$F_\lambda^{c0} = (c|V_\lambda|0). \quad (2.15)$$

Rather than treating each transition separately it is sufficient to consider averages over the microscopic form factors. Thus,  $V^{res}$  is represented in terms of state independent multipole form factors  $F_\lambda$  and nuclear transition operators  $O_\lambda$

$$V^{res}(r, \xi) = \sum_\lambda F_\lambda(r) O_\lambda(\xi). \quad (2.16)$$

Here,  $r$  denotes the relative motion coordinate and  $\xi = (\xi_a, \xi_A)$  are the intrinsic coordinates including spin and isospin, respectively. The multipole form factors  $F_\lambda$  in turn are related to  $O_\lambda$ . In a self-consistent approach they are obtained by averaging  $V^{res}$  over  $O_\lambda$ :

$$F_\lambda(r) = (c|O_\lambda^\dagger \hat{\rho}(E) V^{res}|c)/S_\lambda(E, c). \quad (2.17)$$

Here, the general case of a transition starting from an arbitrary state  $c$  is considered which appears in the intermediate steps of higher order multi-step processes. For one-step reactions the initial state is the ground state  $c = 0$ . By normalization to the transition strength function  $S_\lambda$

$$(c|O_{\lambda'}^\dagger \hat{\rho}(E) O_\lambda|c) = \delta_{\lambda\lambda'} S_\lambda(E, c) \quad (2.18)$$

the dependence of the form factor on the internal state is removed to a large extent.  $S_\lambda$  is the nuclear response function for the external operator  $O_\lambda$  describing the transition rate per unit energy from the state  $c$  into the ensemble of states  $c'$  centered at energy  $E$ .

The above relations are appropriate for one-step reactions where  $c$  is the ground state. However, in higher steps  $c$  is an arbitrary intermediate  $np-nh$  state which is summed over in the cross section. Thus, for multi-step scattering the form factor, Eq.2.17 actually utilizes a too microscopic picture. The statistical aspects in multi-step transitions are taken fully into account by the average multipole form factors

$$F_\lambda = \frac{tr(\hat{\rho} O_\lambda^\dagger \hat{\rho} V^{res})}{tr(\hat{\rho} O_\lambda^\dagger \hat{\rho} O_\lambda)}, \quad (2.19)$$

which are independent of the initial state and the multi-step order, respectively. In the applications of the theory these global form factors together with the response functions of Eq.2.18 are used.

With the above results the one-step cross section is expressed as

$$\frac{d^2\sigma^{(1)}}{dE d\Omega} = \sum_\lambda S_\lambda(E) \overline{\frac{d\sigma^{(1)}}{d\Omega}}|_\lambda, \quad (2.20)$$

where  $\overline{\sigma^{(1)}}$  is a reduced DWBA cross section calculated with the average form factors (Eq.2.17).

The multi-step part of the theory is discussed here for two-step reactions only. The state-independent and slowly varying two-step amplitudes read

$$T_{\lambda_1, \lambda_2}^{(2)} = \langle \chi_E^{(-)} | F_{\lambda_2} G^{opt} F_{\lambda_1} | \chi_\alpha^{(+)} \rangle, \quad (2.21)$$

with  $G^{opt}$  being Green's function for the optical model potential. The nuclear structure information is now contained completely in

$$(0 | O_{\lambda'_1}^\dagger G^{(intr)\dagger}(E'_1) O_{\lambda'_2}^\dagger \hat{\rho}(E) O_{\lambda_2} G^{(intr)}(E_1) O_{\lambda_1} | 0). \quad (2.22)$$

By definition, the exit channel configurations are  $2p - 2h$  states which are excited from  $1p - 1h$  states  $c_1$ . Also in the first step only  $1p - 1h$  states  $a$  are excited. Therefore, we only have to consider the  $1p - 1h$  reduced parts of the two Green functions.

To a good approximation the dependence of  $S_{\lambda_2}(E, c_1)$  on  $c_1$  can be replaced by a dependence on  $E_1$  by considering that the spectroscopic strength usually is located in the vicinity of the unperturbed energy. Theoretically, this is achieved by taking the average over the response functions belonging to states  $c_1$  at energy  $E_1$

$$\begin{aligned} S_\lambda(E, E_1) &= \frac{\sum_{c_1} P_{c_1}(E_1) S_\lambda(E, c_1)}{\sum_{c_1} P_{c_1}(E_1)} \\ &= \frac{tr(\hat{\rho}_1(E_1) O_\lambda^\dagger \hat{\rho}(E) O_\lambda)}{tr(\hat{\rho}_1(E_1))}. \end{aligned} \quad (2.23)$$

The final result for the two-step MSD cross section is of very intuitive structure

$$d^2\sigma^{(2)}/dEd\Omega = \sum_{\lambda_1 \lambda_2} \int dE_1 S_{\lambda_2}(E, E_1) S_{\lambda_1}(E_1, 0) \overline{\frac{d\sigma^{(2)}}{d\Omega}}(E, E_1) |_{\lambda_1 \lambda_2}. \quad (2.24)$$

$\overline{\sigma^{(2)}}$  is an averaged cross section defined in terms of the  $T^{(2)}$ -matrix elements (Eq.2.21, which describes two-step scattering wave-mechanically as a coherent quantal process. The total response of the intrinsic system at energy loss  $E$  is contained in the first and second step transition strength functions. The folding accounts for the partitions of the total energy  $E$  into one- and two-step parts such that  $E$  is conserved.

In the present version of the code only one- and two-step MSD contributions are considered. In most cases it is a good approximation to use the ground state response functions also for the second step but at an energy shifted by the amount of total energy loss in the first step. This corresponds to the assumption that the structure of excited nuclei is close to the structure of the ground state as far as single particle occupancies and other mean-field properties are concerned.

Summarizing this section, the statistical properties of pre-equilibrium spectra are used to eliminate interference contributions at various places. Physically, this corresponds to

the neglect of certain intrinsic correlation functions which only would be observable at an energy resolution of the order of the average level spacing. This leads to a representation of pre-equilibrium cross sections as an incoherent super-position of multi-step contributions. The statistical treatment is introduced in a minimal way, namely referring only to the intrinsic systems while multi-step scattering is described quantum-mechanically as a coherent process at all steps.

### Updated formalism in TRISTAN

In the previous version of the EMPIRE nuclear single-particle energies and wave functions used in TRISTAN were obtained from a spherical Nilsson Hamiltonian with standard parameters. Pairing correlations were accounted for by the BCS method in the constant gap approximation. The resulting two-quasi-particle (2qp) excitation energies and wave functions determine the uncorrelated 2qp multipole nuclear Green functions  $G_L^{2qp}(\varepsilon)$ . The uncorrelated  $2qp$  response function for an external one-body multipole field  $U_L = v(r)Y_L$  is then  $\chi_L^{2qp}(\varepsilon) = \langle c | U_L^\dagger G_L^{2qp}(\varepsilon) U_L | c \rangle$ ,  $|c\rangle$  being an initial reference state. In the RPA schematic model a separable residual particle-hole interaction is assumed of the form  $V^{sep}(1, 2) = \sum_L \kappa_L U_L(1) U_L(2)$ . Then the quasi-particle RPA (QRPA) correlated response function for the operator  $U_L$  is obtained from the Bethe-Salpeter (B-S) equation [20]:

$$\chi_L^{QRPA}(\varepsilon) = \chi_L^{2qp}(\varepsilon) + \kappa_L \chi_L^{2qp}(\varepsilon) \chi_L^{QRPA}(\varepsilon) \quad (2.25)$$

The multipole spectroscopic strength function of multipolarity  $L$  is  $S_L(\varepsilon) = -Im\chi_L^{QRPA}(\varepsilon + i\Gamma/2)/\pi$ ,  $\Gamma$  being the spreading width. In the current version of EMPIRE we use the TRISTAN module modified according to Ref. [21]. A quadrupole deformation term, taken from the EMPIRE input, has been added to the nuclear Hamiltonian. As the nuclear Hamiltonian is now non-diagonal in the spherical Nilsson basis the  $2qp$  wave functions are, in contrast with the degenerate case, not eigenfunctions of the angular momentum squared  $L^2$ . Consequently the uncorrelated  $2qp$  multipole nuclear Green functions are not diagonal with respect to  $L$ . However, because of the symmetry with respect to the deformation axis both parity  $\pi$  and angular momentum projection  $K$  onto this axis are still conserved. The uncorrelated  $2qp$  multipole response function for the external one-body field  $U_{L,K} = v_{L,K}(r)Y_L^K$  then becomes:

$$\chi_{L,K}^{2qp}(\varepsilon) = \langle c | \sum_{L'} U_{L,K}^\dagger G_{L,L',K}^{2qp}(\varepsilon) U_{L,K} | c \rangle = \langle c | U_{L,K}^\dagger G_{L,L,K}^{2qp}(\varepsilon) U_{L,K} | c \rangle \quad (2.26)$$

The QRPA correlated response function is obtained in the schematic RPA from the B-S equation for each  $K$  [22]:

$$\chi_{L,K}^{QRPA}(\varepsilon) = \chi_{L,K}^{2qp}(\varepsilon) + \kappa_{L,K} \chi_{L,K}^{2qp}(\varepsilon) \chi_{L,K}^{QRPA}(\varepsilon) + [off - diagonal terms in L] \quad (2.27)$$

The calculation of the multipole spectroscopic strength function  $S_L$  now involves a summation over  $K$  of  $Im\chi_{L,K}^{QRPA}$ . It can be shown that the contributions of the off-diagonal

terms in the B-S equation to the spectroscopic strength function are negligibly small compared to the diagonal terms.

Calculations accounting for nuclear deformation in MSD nicely reproduce the data in the direct continuum region while the "spherical" calculations underpredict the same data. It should be stressed that, except for adjustment of dynamic deformations used in the coupled-channel calculations and the fission input, these results were obtained without any adjustment of the MSD part of the calculations. In the IAEA evaluation for  $^{232}\text{Th}$  the missing strength in the continuum region of the neutron spectrum was filled up with a large number of fictitious collective levels embedded in the continuum. Similar approach has also been used in other ENDF/B-VII evaluations for important actinides, such as  $^{235,238}\text{U}$  and  $^{239}\text{Pu}$ . The "deformed" MSD approach allows to achieve similar result on a physically more sound basis. The method is computationally faster and has been implemented as a default in the current version of the EMPIRE code.

### 2.4.2 Notes on RPA-Description of Transition Strength Functions

In the MSD approach continuum scattering is considered as a sequence of  $1p-1h$  transitions and the transition strength functions, Eq. 2.18, correspond to response functions of an external one-body operator acting repeatedly on a nucleus. A reliable description of one-body response functions is provided by the Random Phase Approximation theory [23, 24] (RPA). In RPA the whole series of  $1p-1h$  interaction diagrams is summed exactly. Thus, an essential contribution to the intrinsic correlations is treated explicitly. In the notation of Section 2.4.1 they are part of  $H_0^{intr}$ . Thus, the  $ph$ -classes are built from correlated basis states. This justifies also the *ansatz* of Eq. 2.8 where  $V^{intr}$  was defined as to act only between  $ph$ -classes.

An important advantage for a reliable description of pre-equilibrium spectra is that RPA accounts for collective and non-collective features on the same theoretical footing [24, 25, 19, 18, 26]. The approach describes at the same time the large amount of weakly excited background states and the strongly excited giant resonances (*GR*) in the continuum together with low-lying surface vibrations. It is clear that the response functions do not suffer from double counting of transition strength which appears if collective states are treated separately. Important quantities like energy weighted sum rules are known to be conserved by RPA. Also the enhancement of the response due to ground state correlations is included.

In view of a large number of  $p-h$  configurations which are needed in order to describe nuclear spectra over a range of excitation energies of several tens of *MeV* a fully microscopic calculation is of little use. In accordance with the statistical description of cross section statistical considerations are also incorporated into the structure calculations. Instead of solving the RPA-eigenvalue problem by direct diagonalization it is more appropriate to consider the average properties of excitations. The Green function approach to RPA [24, 19] provides the proper theoretical basis for such a description.

For a general formulation, applicable also to open shell nuclei, the quasi-particle RPA (QRPA) is used. Thus, a BCS ground state and a canonical transformation to quasi-

particles is assumed [27]. The excitations are then given in terms of two quasi-particle ( $2qp$ ) rather than by  $1p-1h$  configurations. Furthermore, in order to account for the self-energies the  $2qp$  energies are taken to be complex by adding a state dependent damping width  $\Gamma_\alpha^\downarrow$ . The response functions include inelastic events only and are calculated in linear response theory. Formally, the response functions entering into the MSD-calculation are expressed through the RPA polarization propagator  $\chi^{RPA}(E)$

$$S_\lambda(E, 0) = -\frac{1}{\pi} \text{Im}[\chi^{RPA}(E)]. \quad (2.28)$$

In higher steps, where the transition starts from a state  $c \neq 0$ , the  $1p1h$  densities and response functions on the background of an already excited nucleus are required. At excitation energies per particle which are well below the Fermi energy the structure remains close to the ground state. Since this is the region of main interest for pre-equilibrium scattering Eq.2.28 is used also in two-step and higher order reactions at the appropriate excitation energy. The average response functions, Eq.2.23, are approximated by

$$S_\lambda(E, E_1) \simeq S_\lambda(E - E_1, 0), \quad (2.29)$$

where it is assumed that  $S_\lambda$  depends only on energy difference  $E - E_1$  which corresponds to the relative excitation energy. The form factors of Eq.2.19 are found to be given by folding  $V^{res}$  with  $\overline{\rho}_\lambda$ . Thus, the theory leads to a transparent and consistent description of nuclear structure and reaction dynamics which accounts for the microscopic and the statistical aspects of pre-equilibrium reactions.

The code TRISTAN assumes  $O_\lambda = \kappa_\lambda U_\lambda$ , where the radial part of  $U_\lambda$  is chosen as the derivative of the ground state potential and the coupling constants  $\kappa_\lambda$  are treated as empirical parameters. This phenomenological approach to RPA is widely used in structure calculations and has been found to give reliable results for response functions [25, 28].

The MSD response functions are calculated with single particle levels from a spherical Nilsson Hamiltonian with standard parameters. The ground state is obtained from a BCS calculation in the “fixed gap approximation” with  $\Delta_p = \Delta_n = 12.0/\sqrt{A}$  MeV for protons and neutrons. This also allows a realistic description of open-shell nuclei. Correspondingly, the response functions are calculated with quasi-particle RPA (QRPA).

Multipole fields with a radial shape  $\sim r^\lambda$  are taken. The coupling constants  $\kappa_\lambda$  are determined such that excitation energies of low-lying surface oscillations and of the Giant Dipole Resonance are reproduced.

The  $2qp$ -spreading width  $\Gamma_\alpha^\downarrow$  which describes in a global way the internal nuclear dissipation of the model states is parametrized as

$$\Gamma_\alpha^\downarrow = \Gamma_0 \left( \frac{1}{1 + \exp((E_\alpha - E_{thr})/a)} - \frac{1}{1 + \exp((-E_\alpha - E_{thr})/a)} \right) \quad (2.30)$$

an odd function of  $E_\alpha$ . The parameters  $\Gamma_0$ ,  $E_{thr}$ ,  $a$  are taken equal to the width and energy of the giant dipole resonance. The maximum  $l$ -transfer  $\lambda$  is internally set between 1 and 4 depending on the maximum  $l$  contributing to the reaction cross section.

In EMPIRE-3.1 fitting of the coupling constants  $\kappa_\lambda$  has been improved to minimize their fluctuations with changing incident energy.

### 2.4.3 Implementation of ORION and TRISTAN codes in EMPIRE

Implementation of ORION and TRISTAN codes in EMPIRE involves a few modifications that facilitate operation of the codes. The common input parameters (such as incident channel configuration and optical model parameters) are passed to ORION and TRISTAN directly from the EMPIRE. The parameters that are specific to ORION and TRISTAN are set to default values in EMPIRE and transmitted when ORION and TRISTAN are called. The latter parameters can be modified by the user in the optional input to EMPIRE. However, a default MSD calculation can be performed without any additional input.

EMPIRE takes care of multiple calls of ORION with appropriate energy losses (Q-triangle). In the first set of calls, a standard averaged form factor is used. Then EMPIRE calls ORION calculations with the compressional form factor, which is more appropriate for  $\lambda = 0$  momentum transfer. The tables resulting from both sets of calculations are merged in such a way that all  $\lambda = 0$  momentum transfers are calculated with the compressional form factor while the remaining ones are determined with the standard form factor. The extension of the original version of ORION to the compressional form factor for  $\lambda = 0$  was performed according to the suggestions by H. Lenske)

The TRISTAN code has been modified to automate blocking of the shell model orbital by the unpaired nucleon. In the stand alone version of the code this orbital must be specified in the input. Since the orbitals are reordered during the calculations two runs are necessary (the first one without blocking to identify a correct orbital). In the version of TRISTAN that is included in EMPIRE this preliminary calculation is performed internally, whenever necessary, and the blocking is set up.

Results of the MSD calculations are sensitive to the coupling constants  $\kappa_\lambda$ . By default, these are determined such that excitation energies of low-lying  $2^+$ ,  $3^-$ , and  $4^+$  collective levels be reproduced. The code identifies the lowest discrete levels with the above spins and uses them for fitting coupling constants  $\kappa_\lambda$ . However, not always the lowest levels are the collective ones. If this happens, the user has to fix the energies of these levels in the input file. The energy of the Giant Dipole Resonance is used to determine the  $\kappa_1$  parameter. For  $\lambda = 0$  transitions the self-consistent coupling constant is used by default. Also in  $\lambda = 0$  and  $\lambda = 1$  cases user may choose to provide the respective energies in the input. Each of the coupling constants can also be set to the self-consistent value.

It should be noted that actual implementation of the TRISTAN code does not allow for treatment of the charge exchange channels. Therefore, the MSD cross sections and double-differential spectra can only be calculated for the inelastic scattering. It should be stressed, however, that due to the collective nature of the MSD approach, its contribution to the inelastic scattering is much bigger than to the charge-exchange channels and thus the latter ones can be calculated with the exciton model DEGAS (see Section 2.8) or Monte Carlo approach (see Section 2.9) with reasonable accuracy.



## 2.5 Multi-step Compound

The modeling of Multi-step Compound (MSC) processes follows the approach of Nishioka et al. (NVWY) [4]. Like most of the precompound models, the NVWY theory describes the equilibration of the composite nucleus as a series of transitions along the chain of classes of closed channels of increasing complexity. In the present context, we define the classes in terms of the number of excited particle-hole pairs ( $n$ ) plus the incoming nucleon, i.e. excitons. Thus the exciton number is  $N = 2n + 1$  for nucleon induced reactions. Assuming that the residual interaction is a two-body force only neighboring classes are coupled ( $\Delta n = \pm 1$ ).

According to NVWY, the average MSC cross-section leading from the incident channel  $a$  to the exit channel  $b$  is given by

$$\frac{d\sigma_{ab}}{dE} = (1 + \delta_{ab}) \sum_{n,m} T_n^a \Pi_{n,m} T_m^b, \quad (2.31)$$

which also has to be summed over spins and parities of the intermediate states and where we have omitted kinematic and angular-momentum dependent factors. The summation includes all classes  $n$  and  $m$ . The transmission coefficients  $T_n^a$  describing the coupling between channel  $a$  and class  $n$  are given as

$$T_n^a = \frac{4\pi^2 U_n^a}{(1 + \pi^2 \sum_m U_m^a)^2}, \quad (2.32)$$

where  $U_n^a = \rho_n^b < W_{n,a} >$  is microscopically defined in terms of the average bound level density  $\rho_n^b$  of class  $n$ , and in terms of the average matrix elements  $W_{n,a}$  connecting channel  $a$  with the states in class  $n$ . The probability transport matrix  $\Pi_{mn}$  is defined via its inverse,

$$(\Pi^{-1})_{nm} = \delta_{nm}(2\pi\rho_n^b)(\Gamma_n^\downarrow + \Gamma_n^{ext}) - (1 - \delta_{nm})2\pi\rho_n^b \overline{V_{n,m}^2} 2\pi\rho_m^b. \quad (2.33)$$

in terms of the mean squared matrix element  $\overline{V_{n,m}^2}$  coupling states in classes  $n$  and  $m$ , the average spreading width  $\Gamma_n^\downarrow$  of states in class  $n$ , and the average total decay width  $\Gamma_n^{ext}$  in class  $n$ . The spreading width  $\Gamma_n^\downarrow$  is again related to the mean squared matrix element  $\overline{V_{n,m}^2}$

$$\Gamma_n^\downarrow = 2\pi \sum_m \overline{V_{n,m}^2} \rho_m^b. \quad (2.34)$$

Under the chaining hypothesis  $\overline{V_{n,m}^2}$  couples only neighboring classes ( $\overline{V_{n,m}^2} = 0$  unless  $|n - m| = 1$ ). The decay width  $\Gamma_n^{ext}$  is determined by the sum of the transmission coefficients  $T_n^a$  over all open channels

$$\Gamma_n^{ext} = (2\pi\rho_n^b)^{-1} \sum_a T_n^a. \quad (2.35)$$

More explicitly  $\Gamma_n^{ext}$  may be expressed through the energy integral of the product of transmission coefficients and level densities

$$\Gamma_n^{ext} = (2\pi\rho_n^b)^{-1} \sum_{\alpha} \sum_{m=n-1}^{m=n+1} \int T_{n \rightarrow m}^{\alpha}(\varepsilon) \rho_m^b(E - Q_p - \varepsilon) d\varepsilon. \quad (2.36)$$

Here,  $\varepsilon$  stands for the ejectile  $p$  energy,  $Q_p$  for its binding in a composite system, and  $\alpha$  symbolically accounts for the angular momentum coupling of the residual nucleus spin, ejectile spin and orbital angular momentum to the composite nucleus spin. Again, due to the chaining hypothesis, only those emissions which change class number by  $|n-m| \leq 1$  are allowed. We note that, unlike the FKK[3] formulation, in the NVWY theory transmission coefficients  $T_{n \rightarrow m}$  carry two class indexes.

Following Ref. [29] the microscopic quantities  $\langle W_{n,a} \rangle$  and  $\overline{V_{n,m}^2}$  are expressed in terms of the macroscopic ones. To define  $\langle W_{n,a} \rangle$  EMPIRE uses Eq. 2.32 and equates it to the optical model transmission coefficient. The matrix element  $\overline{V_{n,m}^2}$  is related to the imaginary part of the optical model potential  $W(\epsilon)$  using Eq. 2.34 with  $\Gamma_n^{\downarrow} = 2W(\epsilon)$ . To evaluate  $\Gamma_n^{\downarrow}$ ,  $W(\epsilon)$  has to be averaged over the probability distribution of particles and holes. Once the matrix  $\Pi^{-1}$  is determined it is inverted numerically and used in Eq. 2.31 to calculate MSC emission spectra.

EMPIRE decides whether the MSC calculation should be followed by the Hauser-Feshbach one or not. If the number of MSC classes considered is high enough so that the equilibrium class is included in the MSC chain the code restricts calculations to the MSC mechanism only. To this end, the matrix element  $\overline{V_{n,n+1}^2}$  of Eq. 2.33, responsible for the transition to a next higher class, is set to zero for the highest class. This closes the “leakage” of flux from the MSC, which normally would be treated in the frame of the Hauser-Feshbach model. Thus, the whole flux entering the composite nucleus is consistently treated within the MSC mechanism. This approach is certainly attractive from the theoretical point of view. On the practical side, however, there are severe drawbacks. The most important is that, so far, the discrete levels in a residual nucleus are not treated in the MSC formalism. In fact, EMPIRE, when using MSC mechanism, totally ignores the discrete level region. In addition, the particle-hole level densities, as used in the MSC, are less realistic than their counterparts used in the Hauser-Feshbach model. The latter ones have been carefully adjusted to the experimental data, especially in the low energy region, while the particle-hole level densities, in most cases, make use of an equidistant spacing model with  $g=A/13$ . Therefore, it is recommended to use a few (3 to 5) MSC classes, which are generally sufficient to grasp the most important part of the MSC spectrum and to delegate the rest of the decay to the Hauser-Feshbach model.

### 2.5.1 Conditional level densities

Following Ref. [30], the conditional density of states having all  $p$  particles bound (i.e. below the binding energy  $B$ ) reads

$$\rho_{ph}^B(E) = \frac{g^{p+h}}{p!h!} \sum_{i=0}^I \binom{p}{i} (-1)^i \frac{(E - iB)^{p+h-1}}{(p+h-1)!} \quad (2.37)$$

for  $IB < E \leq (I+1)B$ , with  $I = 0, 1, \dots, (p-1)$ , and

$$\rho_{ph}^B(E) = \frac{g^{p+h}}{p!h!} \sum_{i=0}^{p-1} \sum_{m=0}^{h-1} \binom{p}{i} (-1)^i \frac{[(p-i)B]^{p+m}}{(p+m)!(h-1-m)!} (E-pB)^{h-1-m} \quad (2.38)$$

for  $E > pB$ . The superscript  $B$  indicates that quantity refers to the bound states embedded in the continuum. For excitation energies lower than the Fermi energy, which is approximately 40 MeV, it is not necessary to consider any additional limitations for the energies of the hole states. For the higher energies, the depth of the potential well have to be taken into account. Relevant formulas were reported in Ref. [31], but for the time being these were not implemented in the EMPIRE code.

Using Eqs. 2.37 and 2.38 one can calculate energy dependence of the average escape width and of the damping width, which both depend on  $\rho_{ph}^B(U)$ . These factors were originally introduced by Feshbach, Kerman, and Koonin as the  $Y$ -functions (see p.462 of Ref.[3]). These functions define the density of final states accessible to different transition modes compatible with two-body interaction ( $\Delta n = -1, 0, +1$ ). For the  $\Delta = -1$  transition one obtains:

$$Y_n^{n-1} = \frac{\rho_{21}^B(E-U) \rho_{p-2,h-2}^B(U)}{\rho_{ph}^B(E)}. \quad (2.39)$$

The accessible state density for the  $\Delta = 0$  transition reads

$$\begin{aligned} Y_n^n &= Bg^2h \frac{\rho_{p-1,h}^B(U)}{\rho_{ph}^B(E)} \\ &+ \alpha \frac{1}{2}(h+1)(h+2) \frac{g}{\rho_{ph}^B} \left[ \frac{U-E+2B}{h+2} g \rho_{p-2,h+1}^B(U) \right. \\ &\left. + \beta \rho_{p-2,h+2}^B(E-2B) - \rho_{p-2,h+2}^B(U) \right], \end{aligned} \quad (2.40)$$

with  $\alpha = 1$  for  $E \leq 2B+U$ ,  $\beta = 1$  for  $E > 2B$ , and both equal to 0 elsewhere. The density of states available for the creation of the particle-hole pair is

$$Y_n^{n+1} = g \frac{1}{2} h(h+1) \frac{\rho_{p,h+1}^B(U)}{\rho_{ph}^B(E)} \quad (2.41)$$

The most complicated expression describes damping width

$$\begin{aligned} Y_n^{n+1} \downarrow &= g \frac{(h+1)(h+2)}{\rho_{ph}^B(E)} \left\{ \frac{1}{2} h \rho_{p,h+2}^B(E) - \alpha \frac{1}{2} h \rho_{p,h+2}^B(E-B) \right. \\ &+ (h+3) \frac{1}{2} \rho_{p-1,h+3}^B(E) - \frac{1}{2} \alpha \left[ (h+3) \rho_{p-1,h+3}^B(E-B) \right. \\ &\left. \left. + \frac{B^2 g^2}{2(h+2)} \rho_{p-1,h+1}^B(E-B) + Bg \rho_{p-1,h+2}^B(E-B) \right] \right\}, \end{aligned} \quad (2.42)$$

with  $\alpha$  equal 1 for  $E > B$  and 0 for  $E \leq B$ .

## 2.6 $\gamma$ -emission in Multi-step Compound

The emission of  $\gamma$  in the Multi-step Compound mechanism is treated in terms of the model proposed by Hoering and Weidenmueller [32]. Application follows the paper by Herman *et al.* [33]. The model assumes that  $\gamma$  emission occurs through the deexcitation of the Giant Dipole Resonance (GDR) built within MSC classes. Following Brink-Axel hypothesis [34, 35, 36] each nuclear state serves as the basis of a GDR excitation with identical properties. Moreover, the Tamm-Dancoff approximation is used and GDR is represented as a linear combination of correlated 1p-1h states. Each MSC class  $M$ , now characterized also by its spin  $J$ , splits into four sub-classes  $M_n$ . The states in subclasses  $M_n$ , with  $n=1, 2$  and  $3$  contain GDR built on states in class  $M-1$  with spins  $J-1$ ,  $J$ , and  $J+1$ , respectively, and opposite parity. The states in class  $M_4$  are pure single particle excitations and contain no GDR.

The pure MSC-contribution to the cross section is obtained while neglecting the GDR built on the ground state, which leads to the non-statistical direct-semidirect process. The theory [32] allows for the inclusion of direct-semidirect in the formalism. However, the implementation of direct-semidirect in the EMPIRE is oversimplified and has been disabled. On the other hand, an option is provided to start MSC calculations right from the first class. This approach lacks formal justification but brings the model closer to the treatment of  $\gamma$  emission in the classical preequilibrium models.

The average MSC cross section is given by

$$\overline{\sigma_{a,\gamma}^{MSC}} = T_{a,Mm} \Pi_{Mm,Nn} T_{Nn,\gamma}, \quad (2.43)$$

where

$$\begin{aligned} (\Pi^{-1})_{Mm,Nn} = & 2\pi\rho_{Mm}v_{Mm,Nn}2\pi\rho_{Nn} \\ & + \delta_{M,N}\delta_{m,n}2\pi\rho_{Mm}(\Gamma_{Mm}^{\uparrow} + \Gamma_{Mm}^{\downarrow}) \end{aligned} \quad (2.44)$$

and  $T_a = \sum_{Mm} T_{aMm}$  are the optical model transmission coefficients.

The transmission coefficients for the  $E1$ - $\gamma$  channel are defined, as for the particle channel, in terms of the unitarity deficit of the average  $S$ -matrix.

$$T_{\gamma} = 1 - \left| \overline{S_{\gamma\gamma}} \right|^2. \quad (2.45)$$

This is directly proportional to the strength function  $f(E)$ , which can be written as a function of the absorption cross section, yielding

$$T_{\gamma}^{E1} = \frac{1}{2\pi} \sigma_{abs}(E_{\gamma}^{E1}) \frac{(E_{\gamma}^{E1})^2}{(\hbar c)^2}. \quad (2.46)$$

The absorption cross section has a Lorentzian form and is given by

$$\sigma_{abs}(E_\gamma^{E_1}) = \sigma_{res} \frac{(E_\gamma^{E_1})^2 \Gamma_{res}^2}{((E_\gamma^{E_1})^2 - E_{res}^2)^2 + (E_\gamma^{E_1})^2 \Gamma_{res}^2}. \quad (2.47)$$

For the resonance energy  $E_{res}$ , the resonance width  $\Gamma_{res}$ , and the peak cross section  $\sigma_{res}$ , the experimental or systematics data are used as input parameters. As in the case of particle emission, the average matrix element  $v_{Mm,Nn}$  coupling non-collective states of two exciton classes is determined from the imaginary part of the optical model potential.

Next, we will analyze the individual matrix elements  $(\Pi^{-1})_{Mm,Nn}$ . We begin by investigating the non-diagonal block  $(\Pi^{-1})_{Mm,(M+1)n} = 2\pi\rho_{Mm}v_{Mm,(M+1)n}^2 2\pi\rho_{(M+1)n}$ , i. e., the transition from a state in exciton class  $M$  to a state in the next higher exciton class  $(M+1)$ . There are four different types of matrix elements:

- decay of a GDR,
- the single particle transitions leaving the GDR unchanged,
- transitions among non-collective states,
- GDR creation.

Computation of these four types of matrix elements is discussed below.

(i) The matrix element  $(\Pi^{-1})_{Mm,(M+1)4}$ ,  $m = 1, 2$  or  $3$  describes the decay of a GDR via coupling to the next higher exciton class. This process is responsible for the spreading width of the GDR. In colliding with a bound particle the GDR loses its coherence and the bound particle is excited into an excited state thus creating another particle-hole state. This matrix element can be written as

$$2\pi\rho_{Mm}v_{Mm,(M+1)4}^2 2\pi\rho_{(M+1)4} = 2\pi\rho_{Mm}\Gamma_{GDR}^\downarrow. \quad (2.48)$$

For the width of the GDR the experimental value is used. Unfortunately, there is little literature on how this width is separated into spreading and decay width. It is known that for heavy nuclei the spreading width is dominant, whereas for light nuclei the reverse is true. For  $^{208}\text{Pb}$  approximately 90% of the width is due to the spreading width. For  $^{16}\text{O}$ , on the other hand, 90% of the width is due to the decay width [37]. This separation can be entered into the calculations as an input parameter. The result depends only weakly on this coefficient. The level densities  $\rho_{Mm}^{J,\pi}(E)$  for  $m=1,2,3$  are given by the exciton level densities  $\rho_{M-1}^{(J-1),-\pi}(E - E_{GDR})$ ,  $\rho_{M-1}^{J,-\pi}(E - E_{GDR})$  and  $\rho_{M-1}^{(J+1),-\pi}(E - E_{GDR})$ , respectively. These correspond to the level densities of the non-collective states on which GDR is built. Implicitly, all of them are for bound configurations.

(ii) The matrix element  $(\Pi^{-1})_{Mm,(M+1)n}$ ,  $m, n=1, 2, 3$  describes the transition of a GDR-state in class  $M$  to a GDR-state in class  $(M+1)$ . In such a transition the GDR is not affected and is just a "spectator". This is again a consequence of the two-body nature of the residual interaction. The subclasses 1, 2, 3 differ only in the angular momenta

of the non-collective states the GDR is built on. Since a transition among these states must not change the angular momentum this part is diagonal in the subclass indices, i. e.  $(\Pi^{-1})_{Mm,(M+1)m} \neq 0$ , only. Thus, these matrix elements are given by

$$(\Pi^{-1})_{Mm,(M+1)m} = 2\pi\rho_{Mm}v_{n.c.}^2.2\pi\rho_{Mm \rightarrow (M+1)m}^{acc}, \quad (2.49)$$

where  $\rho_{Mm}^J(E)$ ,  $m=1,2,3$ , is the exciton level density  $\rho_{M-1}^{(J',-\pi)}(E - E_{GDR})$  with  $J' = (J - 1), J, (J + 1)$   $\rho_{Mm \rightarrow (M+1)m}^{acc}(E)$ ,  $m=1, 2, 3$  are the accessible state densities  $\rho_{(M-1),J \rightarrow M,J'}^{acc}(E - E_{GDR})$  with  $J' = (J - 1), J, (J + 1)$ , respectively.  $v_{n.c.}$  stands for the average transition matrix element between two non-collective states of neighboring exciton classes.

(iii) The matrix element  $(\Pi^{-1})_{M4,(M+1)4}$  describes transitions between non-collective states only. The matrix element is again expressed through the average transition strength  $v_{n.c.}$  between two non-collective states

$$(\Pi^{-1})_{M4,(M+1)4} = 2\pi\rho_{M4}(E)v_{n.c.}^2.2\pi\rho_{M4 \rightarrow (M+1)4}^{acc}(E). \quad (2.50)$$

(iv) The matrix element  $(\Pi^{-1})_{M4,(M+1)m}$  with  $m = 1, 2$ , and 3 describes the creation of a GDR in the next higher exciton class. In the current version of EMPIRE the total GDR width is taken to describe this process<sup>1</sup>. However, the creation of a GDR is possible only if a particle or a hole has enough energy to create the GDR state. This is another consequence of the two-body nature of the residual interaction. A particle with the excitation energy of the GDR resonance is generally unbound. Thus, only a hole can contribute. The probability for a hole to have the required energy  $\epsilon$  within the configuration with the total exciton number  $(p + h)$  is given by

$$P(\epsilon) = N \frac{\rho(p, h - 1, E - \epsilon)}{\rho(p, h, E)}, \quad (2.51)$$

where  $\rho(p, h - 1, E - \epsilon)$  is the level density of the remaining excitons after removing a hole of the energy  $\epsilon$ .  $\rho(p, h, E)$  is the total level density at energy  $E$  for  $(p + h)$  excitons.  $N$  is the normalization constant.

$$\frac{1}{N} = \int_0^E \frac{\rho(p, h - 1, E - \epsilon)}{\rho(p, h, E)} d\epsilon = \frac{\rho(p, h - 1, E)}{\rho(p, h, E)(p + h - 1)}. \quad (2.52)$$

Hence, the probability for a hole to have the energy  $E \geq E_{GDR}$  is given by

$$\begin{aligned} \int_{E_{GDR}}^E P(\epsilon) d\epsilon &= \frac{(p + h - 1)}{\rho(p, h - 1, E)} \int_{E_{GDR}}^E \rho(p, h - 1, E - \epsilon) d\epsilon \\ &= \frac{\rho(p, h - 1, E - E_{GDR})}{\rho(p, h, E)}. \end{aligned} \quad (2.53)$$

---

<sup>1</sup>This may overestimate creation rate of the GDR. Other approaches are to use non-collective matrix element or the GDR width split among the neighboring classes. To activate these possibilities the user has to edit MSC-NVWY.f file and uncomment adequate lines in both of the following ranges 1028-1036 and 1093-1106.

Collecting everything yields

$$(\Pi^{-1})_{M4,(M+1)m} = 2\pi\rho_{M4}(E)\Gamma_{GDR}^{\downarrow} \frac{\rho(p, h-1, E-E_{GDR})}{\rho(p, h, E)}. \quad (2.54)$$

Thus, all four types of matrix elements within the block  $(M, M+1)$  have been determined. The matrix element  $(\Pi^{-1})_{(M+1)m,Mn}$  is obtained using the symmetry properties of the matrix  $\Pi^{-1}$ . The diagonal elements of this matrix are then obtained by summation:

$$(\Pi^{-1})_{Mm,Mm} = \sum_{n=1}^4 (\Pi^{-1})_{Mm,(M+1)n} + \sum_{n=1}^4 (\Pi^{-1})_{Mm,(M-1)n} + \sum_c T_{Mm,c}. \quad (2.55)$$

The matrix  $\Pi^{-1}$  is inverted numerically and used in Eq.2.43 to calculate  $\gamma$ -emission spectra.

## 2.7 Coupling between MSC and MSD

The NVWY theory includes a possibility of feeding higher MSC classes directly from the MSD chain, in addition to the normal transitions between bound states of increasing complexity. This process is taken in to account by a double sum over classes in the cross section formula (Eq.2.31). The second sum over  $n$  refers to the contribution of different classes to the particle emission, while the first one (over  $m$ ) corresponds precisely to the population of various classes directly from the open channel space rather than through the transitions along the MSC chain. This effect is included in the EMPIRE code by distributing the incoming channel transmission coefficient over different MSC classes. For the time being, it is done according to phase space and global coupling arguments requiring that the incoming flux splits between the first MSD and MSC classes in proportion to the respective state densities and to the average value of the squared matrix elements coupling unbound to unbound ( $\langle V_{uu}^2 \rangle$ ) and unbound to bound states ( $\langle V_{ub}^2 \rangle$ ). Introducing  $R = \langle V_{ub}^2 \rangle / \langle V_{uu}^2 \rangle$ , denoting the optical model transmission coefficient by  $T_{om}$ , the density of bound and unbound states in class  $n$  by  $\rho_n^b$  and  $\rho_n^u$  respectively, and their sum by  $\rho$ , the transmission coefficient populating the first MSC class may be written as

$$T_1 = T_{om} \frac{\langle V_{ub}^2 \rangle \rho_1^b(E)}{\langle V_{ub}^2 \rangle \rho_1^b(E) + \langle V_{uu}^2 \rangle \rho_1^u(E)} = T_{om} \frac{R}{(R-1) + \frac{\rho_1(E)}{\rho_1^b(E)}} \quad (2.56)$$

The same reasoning may be applied to the flux remaining in the open space, which may enter the MSC chain in subsequent steps of the reaction. Assuming  $R$  to be independent of the class number the transmission coefficient  $T_n$  populating the  $n^{th}$  MSC class is written as

$$T_n = \left( T_{om} - \sum_{i=1}^{n-1} T_i \right) \frac{R}{(R-1) + \frac{\rho_n(E)}{\rho_n^b(E)}} \quad (2.57)$$

If the MSD option is selected the absorption cross section available to MSC ( $\sigma_{abs}$ ) is reduced by the total MSD emission cross section ( $\sigma_{MSD}$ ) in order to ensure flux conservation and becomes:

$$\sigma_{abs}(J) = \sigma_{OM}(J) \left( 1 - \frac{\sigma_{MSD}}{\sigma_{OM}} \right), \quad (2.58)$$

where  $\sigma_{OM}$  is optical model reaction cross section and  $J$  stands for the compound nucleus spin.

The MSD emission populates residual nucleus continuum. Spin distribution of this population is assumed to be proportional to the spin distribution of  $1p$ - $1h$  states shifted by the spin of the target ground state. This approximation is imposed by the current structure of the ORION code which performs summations over angular momentum in the incident channel, thus making exact angular momentum coupling impossible. Choice of the  $1p$ - $1h$  spin distribution reflects dominant contribution of the first step of the MSD, which leaves the residual nucleus in the 2-exciton state.

The MSD cross section to the discrete states is distributed arbitrary among  $2+$ ,  $3-$ , and  $4+$  states with relative weights 4:2:1 respectively and inversely proportional to the squared distance between the energy of the populated level and the energy of the level to which field parameters in the response functions were fitted. In the case of an odd nucleus all levels with spins that differ from  $2+$ ,  $3-$ , and  $4+$  by  $1/2$  are assumed to belong to the respective spin multiplet. There was no attempt to treat MSD population of discrete levels more accurately as this kludge can be removed by using strict Coupled-Channels calculations.

## 2.8 Exciton model

This module was incorporated to improve  $(n, \gamma)$  reactions for fast neutrons and to add the capability of predicting spectra for the charge-exchange reactions that are not provided by the current implementation of the MSD model (ORION & TRISTAN). DEGAS is the exciton model code with angular-momentum conservation written by E. Běták as an improved version of the code PEGAS [9] by E. Běták and P. Obložinský. DEGAS was implemented in EMPIRE by P. Obložinský (BNL) in February 2001. Certain features of the DEGAS code were intentionally disabled for compatibility with other models present in the EMPIRE code. Thus,  $\gamma$ -cascade has been limited to primary  $\gamma$ s in the composite nucleus and multiple preequilibrium emissions have been blocked. In particular, DEGAS treatment of the equilibrium emission was disabled and left to the Hauser-Feshbach model coded in EMPIRE.

Within the above simplifications DEGAS solves the classical (apart of spin) set of master equations



$$\begin{aligned}
\frac{dP(E, J, n, t)}{dt} = & P(E, J, n-2, t)\lambda^+(E, J, n-2) \\
& + P(E, J, n+2, t)\lambda^-(E, J, n+2) \\
& + P(E, J, n, t) [\lambda^+(E, J, n) + \lambda^-(E, J, n) + L(E, J, n)] \\
& + \sum_{J', n', x} \int P(E', J', n', t)\lambda_x \left( [E', J', n'] \rightarrow [E, J, n] \right) d\varepsilon,
\end{aligned} \tag{2.59}$$

where  $P(E, J, n, t)$  is the occupation probability of the composite nucleus at the excitation energy  $E$ , spin  $J$  and the exciton number  $n$ ,  $\lambda^+$  and  $\lambda^-$  are the transition rates for decay to neighboring states, and  $L$  is the total integrated emission rate for particles (protons  $\pi$  and neutrons  $\nu$ ) and  $\gamma$ -rays. Note, that the last term ensures coupling of different spins. The nucleon emission rate per energy and time is

$$\lambda_{\pi, \nu}([E, J, n] \rightarrow [U, S, n-1]) = \frac{1}{h} \frac{\omega(n-1, U, S)}{\omega(n, E, J)} \Re_{\pi, \nu}(n) \sum_{j=|S-1/2|}^{S+1/2} \sum_{l=|J-j|}^{J-j} T_l(\varepsilon), \tag{2.60}$$

where  $\omega(n, E, J)$  is the particle-hole state density,  $T_l$ s are the transmission coefficients of the emitted nucleon, and  $\Re_x(n)$  is a fraction of  $x$ -type nucleons in the  $n$ -th stage. The particle-hole state density is

$$\omega(n, E, J) = \frac{g(gE - A_{p,h})^n}{p!h!(n-1)!} R_n(J), \tag{2.61}$$

where  $g$  is the single-particle level density,  $p$  and  $h$  are number of particles and holes ( $n = p + h$ ), and  $A_{p,h}$  is the Pauli correction term. The spin distribution reads

$$R_n(J) = \frac{2J+1}{2} \exp\left(-\frac{(J+1/2)^2}{2\sigma_n^2}\right), \tag{2.62}$$

with  $\sigma_n$  being the spin cut-off parameter ( $\sigma_n^2 = (0.24 + 0.0038E)nA^{2/3}$ ). Treatment of the intranuclear cascade rates follows the FKK [3] approach. The energy and spin dependence are assumed to factorize

$$\lambda^\pm(E, J, n) = \frac{2\pi}{\hbar} |M|^2 Y_n^\downarrow X_{nJ}^\downarrow, \tag{2.63}$$

where  $|M|^2$  is the energy part of the average squared transition matrix element of the residual interaction,  $Y_n^\downarrow$  is the energy part of the density of accessible final states, and the  $X_{nJ}^\downarrow$  factor takes care of angular momentum coupling. The latter two read

$$Y_n^\downarrow = \frac{g}{2(n+1)} \frac{(gE - A_{p+1,h+1})^{n+1}}{(gE - A_{ph})^{n-1}}, \tag{2.64}$$

and

$$X_{nJ}^\downarrow = \frac{1}{R_n(J)} \sum_{j_4 Q} R_1(Q) \tilde{F}(Q) R_{n-1}(j_4) \Delta(Qj_4J), \tag{2.65}$$

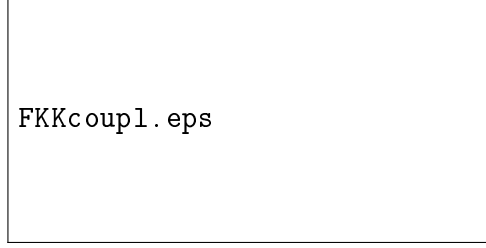


Figure 2.1: Angular momentum coupling in the intranuclear transitions.

with  $\Delta(Qj_4J) = 1$  for  $|Q - j_4| \leq J \leq Q + j_4$  and 0 otherwise. The function  $\tilde{F}(Q)$  is given by

$$\tilde{F}(Q) = \sum_{j_3 j_5} (2j_5 + 1) R_1(j_5) (2j_3 + 1) F(j_3) \begin{pmatrix} j_5 & j_3 & Q \\ \frac{1}{2} & 0 & -\frac{1}{2} \end{pmatrix}^2, \quad (2.66)$$

and the angular momentum density of the pair of states is

$$F(j_3) = \sum_{j_1 j_2} (2j_1 + 1) R_1(j_1) (2j_2 + 1) R_1(j_2) \begin{pmatrix} j_1 & j_2 & j_3 \\ \frac{1}{2} & -\frac{1}{2} & 0 \end{pmatrix}^2. \quad (2.67)$$

Notation of spins ( $j_i$ ,  $J$  and  $Q$ ) is defined in Fig. 2.1

The averaged squared matrix element  $|M|^2$  is related to the spin-independent estimate of Kalbach [38]

$$|M_{nonspin}|^2 = K A^{-1/3} \varepsilon^{-1}, \quad (2.68)$$

where  $\varepsilon = E/n$  is the energy per single exciton. The more complicated expressions [38] are used if  $\varepsilon$  is outside the 7-15 MeV range. In the current, spin-dependent formulation the averaged squared matrix element is chosen in such a way that, after performing additional averaging over spin, the non-spin value is recovered

$$|M|^2 \langle X_{nJ}^\downarrow \rangle = |M_{nonspin}|^2. \quad (2.69)$$

For the  $K$  constant the standard value of 100 MeV<sup>3</sup> is adopted.

The coding of  $\gamma$ -emission makes use of the Brink-Axel hypothesis [34, 35, 36] and Giant Dipole Resonance  $\gamma$ -ray strength function for the  $E1$  transitions. In the angular momentum coupling formalism the  $\gamma$  emission rate  $\lambda_\gamma$  from an  $n$ -exciton state is

$$\lambda_\gamma ([E, J, n] \rightarrow [E - E_\gamma, S, n]) = \frac{E_\gamma^2 \sigma_{GDR}(E_\gamma)}{3\pi^2 \hbar^3 c^2} \frac{b_{nS}^n \omega(n, E - E_\gamma, S)}{\omega(n, E, J)}, \quad (2.70)$$

if emission of a  $\gamma$  occurs with no change in the exciton number, or

$$\lambda_\gamma ([E, J, n] \rightarrow [E - E_\gamma, S, n - 2]) = \frac{E_\gamma^2 \sigma_{GDR}(E_\gamma)}{3\pi^2 \hbar^3 c^2} \frac{b_{n-2,S}^n \omega(n - 2, E - E_\gamma, S)}{\omega(n, E, J)}, \quad (2.71)$$

in the case of annihilation of one particle-hole pair. The photoabsorption cross section  $\sigma_{GDR}(E_\gamma)$  is written in the Lorentzian form

$$\sigma_{GDR}(E_\gamma) = 53.2mb \frac{NZ}{A} \frac{E_\gamma^2 \Gamma^2}{(E_\gamma^2 - E_{GDR}^2)^2 + E_\gamma^2 \Gamma^2}, \quad (2.72)$$

with  $\Gamma = 5$  MeV and

$$E_{GDR} = 29 \sqrt{(1 + 2/A^{1/3}) / A^{1/3}} [MeV]. \quad (2.73)$$

The branching ratios are

$$b_{nS}^{nJ} = \frac{y_m^n x_{mS}^{nJ}}{y_m^m x_{mS}^{mJ} + y_m^{m+2} x_{mS}^{m+2,J}}, \quad (2.74)$$

where

$$\begin{aligned} y_n^n &= gn, \\ y_n^{n+2} &= g^2 \varepsilon, \end{aligned} \quad (2.75)$$

and the spin coupling terms read

$$\begin{aligned} x_{nS}^{nJ} &= \frac{3(2J+1)}{R_n(S)} \sum_{j_1 j_2 j_3} (2j_1+1) R_1(j_1) (2j_2+1) R_1(j_2) R_{n-1}(j_3) \\ &\times \left( \begin{array}{ccc} j_2 & 1 & j_1 \\ \frac{1}{2} & 0 & -\frac{1}{2} \end{array} \right)^2 \left\{ \begin{array}{ccc} j_2 & j_3 & S \\ J & 1 & j_1 \end{array} \right\}^2 \end{aligned} \quad (2.76)$$

and

$$x_{nS}^{n+2,J} = \frac{2J+1}{2S+1} \sum_{j_1 j_2} (2j_1+1) R_1(j_1) (2j_2+1) R_1(j_2) \left( \begin{array}{ccc} j_2 & j_1 & 1 \\ \frac{1}{2} & -\frac{1}{2} & 0 \end{array} \right)^2 \Delta(S1J). \quad (2.77)$$

The spin labeling is explained in Fig. 2.2.

DEGAS solves the set of master equations (Eq. 2.59) and calculates integrals of occupation probabilities

$$\tau(E, J, n) = \int_0^\infty P(E, J, n, t) dt, \quad (2.78)$$

and preequilibrium emission cross sections

$$\frac{d\sigma_x}{d\varepsilon_x} = \sum_{J_c, J_r, n} \int \sigma(E_c, J_c) \tau(E_c, J_c, n) \lambda_x([E_c, J_c, n] \rightarrow [E_r, J_r, n-1]) dE_r. \quad (2.79)$$

Here, subscripts  $c$  and  $r$  refer to the composite and residual nuclei respectively.

Performance of the DEGAS code with regard to the  $\gamma$ -channel was tested by the Bratislava-Ljubljana collaboration [39]. It was demonstrated, by comparing practically all available



Figure 2.2: Diagram of spin coupling functions  $x_{nS}^{nJ}$  (left) and  $x_{nS}^{n+2,J}$  (right) for  $\gamma$  emission. The dotted lines represent  $\gamma$ s.

experimental data for (n, $\gamma$ ) and (p, $\gamma$ ) excitation functions in the incident energy range 8-20 MeV, that DEGAS results are very close to the more microscopic direct-semidirect (DSD) capture model. These excitation functions show relatively broad bell-shape form with a peak around the GDR energy, which is about 1 mb for (n, $\gamma$ ) and about 0.6 mb for (p, $\gamma$ ) reactions.

In addition to the already mentioned improvement of the charge-exchange reaction channel DEGAS can also be used to calculate (n,n') cross sections offering an alternative to the MSD/MSC approach.

The actual implementation of DEGAS is restricted to preequilibrium emission from stages with  $n = 1, 3, 5$ , and  $7$  excitons in the first composite nucleus. Emission of  $\gamma$ s, neutrons, and protons is considered (but only  $\gamma$ -emission is allowed from the  $n = 1$  stage).  $\gamma$ -cascade is blocked and only primary  $\gamma$ s are calculated. Being an independent development, DEGAS does not follow the EMPIRE style of having all dimensions set via the PARAMETER statement. It allows for up to 150 energy bins and 25 spins. While the spin limitation can be normally ignored (at least for not too high energies) user has to ensure that no more than 150 energy bins (NEX) are requested in the EMPIRE input when the DEGAS option is selected. Generally, all necessary input parameters are transferred automatically from EMPIRE to DEGAS, and the user does not need to provide any additional data.

## 2.9 Monte Carlo Preequilibrium

The Hybrid Monte-Carlo Simulation (HMS) approach to the preequilibrium emission of nucleons is the third precompound model included in EMPIRE (the other two are MSD&MSC and the exciton model (DEGAS)). The original HMS model has been formulated by M. Blann [40] as a hybrid model [41, 42, 43, 44] inspired version of the intranuclear cascade approach. Contrary to other classical preequilibrium models, this approach avoids multi-exciton level densities, which were shown by Bisplinghoff [45] to be used inconsistently in

the exciton and in the hybrid formulations. The HMS model has a number of attractive features. First of all, there are no physical limits on a number of preequilibrium emissions (apart from energy conservation). With the addition of linear momentum conservation by M.Chadwick and P. Obložinský (DDHMS), the model provides a nearly complete set of observables. These include cross sections for the production of residuals, light-particle double-differential spectra and spectra of recoils. Spin and excitation-energy dependent populations of residual nuclei can also be obtained, an essential feature for coupling the preequilibrium mechanism to the subsequent Compound Nucleus decay. The binding energies in the HMS model are thermodynamically correct. This is a clear improvement over the intranuclear cascade model, although exact account, typical of the Compound Nucleus model, is still out of reach. The DDHMS model proved to perform very well up to at least 250 MeV, extending energy range of the EMPIRE applicability to the desired limit.

The calculation flow in the DDHMS model can be summarized in terms of the following steps:

1. draw collision partner for the incoming nucleon (2p-1h state created)
2. draw energy ( $\varepsilon$ ) of the scattered nucleon (if bound go to step 5)
3. draw scattering angles for both particles
4. decide whether the scattered nucleon will be emitted, re-scattered or trapped
  - a) if emitted appropriate cross section is augmented
  - b) if re-scatters additional particle-hole is created and we return to step 2
  - c) if trapped, go to step 5
5. draw excitation energy of a particle in the remaining 1p-1h configuration (between  $0 \div (U - \varepsilon)$ ), if unbound go to step 3, if bound choose another existing 1p-1h pair and repeat step 5.

All excitons (including holes) are treated on equal footing and each of them is given a chance to interact or being emitted with *a priori* equal probability. The cascade ends when all excitons are bound. Below, we summarize various probability distributions which are used in concert with a random number generator.

For choosing a collision partner it is assumed that the unlike interaction is 3 times more probable than the like one ( $\sigma_{np} = 3\sigma_{nn}$ ). Thus, for the incident neutron we have  $P_{nn}$  and  $P_{np}$  for the probability of exciting neutron and proton respectively

$$P_{nn} = \frac{(A - Z)}{(A - Z) + 3Z}, \quad (2.80)$$

$$P_{np} = 1 - P_{nn} \quad (2.81)$$

and similarly for the incident proton

$$P_{pp} = \frac{Z}{Z + 3(A - Z)}, \quad (2.82)$$

$$P_{pn} = 1 - P_{pp}. \quad (2.83)$$

The energy distribution of the scattered particles  $P(\varepsilon)$  is given by the ratio of the  $(n-1)$ - and  $n$ -exciton level densities  $\rho_n$

$$P(\varepsilon)d\varepsilon = \frac{\rho_{n-1}(E - \varepsilon)g}{\rho_n(E)}d\varepsilon, \quad (2.84)$$

with  $n = 2$  or  $3$  and

$$\rho_2(E) = \frac{g(gV)}{2} \text{ if } E > V, \quad (2.85)$$

$$\rho_2(E) = \frac{g(gE)}{2} \text{ if } E \leq V, \quad (2.86)$$

$$\rho_3(E) = \frac{g^3 [V(2E - V)]}{4} \text{ if } E \geq V. \quad (2.87)$$

Here,  $V$  is a potential well depth. The emission probability is calculated as

$$P_\nu(\varepsilon - Q) = \frac{\lambda_c(\varepsilon - Q)}{\lambda_c(\varepsilon - Q) + \lambda_+(\varepsilon)}, \quad (2.88)$$

with the emission rate being

$$\lambda_c(\varepsilon - Q) \sim \frac{\sigma_\nu(\varepsilon - Q)(\varepsilon - Q)(2S + 1)\mu_\nu}{g}. \quad (2.89)$$

$\sigma_\nu$  is an inverse reaction cross section,  $Q$  is a binding energy,  $g$  is a single particle density,  $S$  denotes nucleon spin, and  $\mu_\nu$  stands for the reduced nucleon mass. Following the hybrid model,  $\lambda_+(\varepsilon)$  is calculated from the mean free path of a nucleon in nuclear matter.

The version which is actually implemented in EMPIRE has been coded by M. Chadwick and extended to double-differential cross sections in collaboration with P. Obložinský [10].

## 2.10 Compound Nucleus

The statistical model used in the EMPIRE is an advanced implementation of the Hauser-Feshbach theory. The exact angular momentum and parity coupling is observed. The emission of neutrons, protons,  $\alpha$ -particles, and a light ion is taken into account along with the competing fission channel. The full  $\gamma$ -cascade in the residual nuclei is considered. Particular attention is dedicated to the determination of the level densities, which can be calculated in the non-adiabatic approach allowing for the rotational and vibrational enhancements. These collective effects are gradually removed above a certain energy. Level densities acquire dynamic features through the dependence of the rotational enhancement on the shape of a nucleus.

In the frame of the statistical model of nuclear reactions the contribution of the Compound Nucleus (CN) state  $a$  with spin  $J$ , parity  $\pi$ , and excitation energy  $E$  to a channel  $b$  is given by the ratio of the channel width  $\Gamma_b$  to the total width  $\Gamma_{tot} = \sum_c \Gamma_c$  multiplied by the population of this state  $\sigma_a(E, J, \pi)$ . This also holds for secondary CNs that are formed due to subsequent emissions of particles. The only difference is that while the first CN is initially excited to the unique (incident channel compatible) energy, the secondary CNs are created with excitation energies which spread over the available energy interval. Each such state contributes

$$\sigma_b(E, J, \pi) = \sigma_a(E, J, \pi) \frac{\Gamma_b(E, J, \pi)}{\sum_c \Gamma_c(E, J, \pi)} \quad (2.90)$$

to the cross section. These have to be summed over spin  $J$  and parity  $\pi$ , and integrated over excitation energy  $E$  (in case of daughter CN) to obtain observable cross sections. The particle decay width is given by

$$\Gamma_c(E, J, \pi) = \frac{1}{2\pi\rho_{CN}(E, J, \pi)} \sum_{J'=0}^{\infty} \sum_{\pi'} \sum_{j=J'-J}^{J+J'} \int_0^{E-B_c} \rho_c(E', J', \pi') T_c^{l,j}(E - B_c - E') dE', \quad (2.91)$$

where  $B_c$  is the binding energy of particle  $c$  in the compound nucleus,  $\rho$  is the level density, and  $T_c^{l,j}(\epsilon)$  stands for the transmission coefficient for particle  $c$  having channel energy  $\epsilon = E - B_c - E'$  and orbital angular momentum  $l$ , which together with the particle spin  $s$  couples to the channel angular momentum  $j$ . For the discrete levels (characterized by the energy  $E_i$ , spin  $J_i$ , and parity  $\pi_i$ ) the level density  $\rho(E, J', \pi')$  reduces to  $\delta(E - E_i)\delta_{(J', J_i)}\delta_{(\pi', \pi_i)}$ .

The fission width reads

$$\Gamma_f(E, J, \pi) = \frac{1}{2\pi\rho_{CN}(E, J, \pi)} \int_0^{E-E_{sad}(J)} \rho_f(\epsilon, J, \pi) T_f^{HW}(E - E_{sad}(J) - \epsilon) d\epsilon, \quad (2.92)$$

where  $E_{sad}(J)$  is the energy of the saddle point with angular momentum  $J$ . The parity selection rules are implicit in Eqs. 2.91 and 2.92. The energy of the saddle point is given by the sum of the fission barrier  $B_f(J)$  and the rotational energy of the nucleus at spin  $J$ . Since nuclei at the saddle point are known to have a strong prolate deformation, with the angular momentum vector perpendicular to the symmetry axis, the rotational energy contribution to the saddle point energy is given by

$$\frac{\hbar^2 J(J+1)}{2(\mathfrak{S}_{\perp})_{sad}}. \quad (2.93)$$

Here  $\mathfrak{S}_{\perp}$  is a moment of inertia perpendicular to the symmetry axis calculated by the BAR-MOM routine [11]. In the Hill-Wheeler approximation the fission transmission coefficient  $T_f^{HW}$  is given by

$$T_f^{HW}(E - E_{sad}(J) - \epsilon) = \frac{1}{1 + \exp[-\frac{2\pi}{\hbar\omega}(E - E_{sad}(J) - \epsilon)]}. \quad (2.94)$$

By default,  $\hbar\omega = 1$  MeV is taken. This formulation is adequate for heavy ion induced reactions but needs refinement in the case of fission induced by low energy nucleons. This shortcoming will be removed in the later versions of the code.

### 2.10.1 Level densities

EMPIRE accounts for various models describing level densities and includes several respective parameterizations. In each case equal parity distribution  $\rho(E, J, \pi) = \frac{1}{2}\rho(E, J)$  is assumed.

Choice of the proper representation depends on a case being considered. For the nucleon induced reactions, with CN excited up to about 20 MeV, the Gilbert-Cameron approach is recommended. It assures the most accurate description of level densities in the energy range up to the neutron binding energy. The collective effects are included in the level density parameter  $a$ , providing reasonable estimate of the level densities as long as damping of the collective effects is irrelevant. The relatively low angular momentum introduced by the incident projectile justifies neglect of dynamical effects. However, these effects have to be taken into account in case of the heavy ion induced reactions and/or higher excitation energies. In these cases, the dynamic approach which accounts for the shape-dependent collective enhancements, their damping with increasing energy, and the temperature dependence of the  $a$ -parameter should be adopted.

#### Gilbert-Cameron approach

The Gilbert-Cameron approach [46] splits excitation energy in two regions. Different functional forms of level densities are applied in each of them. At low excitation energies (below the matching point  $U_x$ ) the constant temperature formula is used

$$\rho_T(E) = \frac{1}{T} \exp[(E - \Delta - E_0)/T], \quad (2.95)$$

where  $T$  is the nuclear temperature,  $E$  is the excitation energy ( $E = U + \Delta$  with  $\Delta$  being the pairing correction), and  $E_0$  is an adjustable energy shift. Above  $U_x$  the Fermi gas formula is applied

$$\rho_F(U) = \frac{\exp(2\sqrt{aU})}{12\sqrt{2}\sigma(U)a^{1/4}U^{5/4}}. \quad (2.96)$$

The level density parameter  $a$  is assumed to be energy independent. The spin cut-off factor  $\sigma(U)$  is given by

$$\sigma^2(U) = 0.146A^{2/3}\sqrt{aU}. \quad (2.97)$$

Three model parameters,  $T$ ,  $U_x$ , and  $E_0$ , are determined by the requirement that the level density and its derivative are continuous at the matching point  $U_x$ , and by fitting cumulative number of discrete levels with the integral of Eq. 2.95. The first of the conditions implies



$$\frac{1}{T} = \sqrt{a/U_x} - \frac{3}{2U_x}. \quad (2.98)$$

The code will not(!) stop if the discrete level scheme is incompatible with the level density parameter  $a$  (i.e., there is no real solution to Eq. 2.98). It is essential that only complete level schemes are used for the determination of  $T$  and  $E_0$  parameters. With increase in the excitation energy, some levels escape experimental detection. Numbers of the levels that are supposed to form a complete set is read by EMPIRE (starting with version 2.17) directly from the file containing discrete levels (*empire/data/RIPL/levels/Z\*.DAT*). This database makes part of the RIPL-2 library [47].

Cumulative plots of discrete levels along with the constant temperature fits, can be inspected by choosing the FITLEV option in the input. For each nucleus involved in the calculations an appropriate plot is created and stored in the *CUMULPLOT.PS* (\*-*cum.ps*) file which can be viewed once the calculations are done (NOTE: this option requires “gnuplot” packet and “ps2ps” which is a part of the “ghostscript”).

Calculations can be performed using constant level density parameter  $a$  read from the input file. No energy dependence is allowed in such a case. Alternatively, one of the built in systematics can be used. The latter ones account for the shell effects, which fade-out with increasing energy implying energy dependence of the  $a$  parameter. The general form of this dependence was proposed by Ignatyuk [48]

$$a(U) = \tilde{a}[1 + f(U)\frac{\delta W}{U}], \quad (2.99)$$

where  $\delta W$  is the shell correction,  $\tilde{a}$  is the asymptotic value of the  $a$ -parameter and

$$f(U) = 1 - \exp(-\gamma U). \quad (2.100)$$

The three relevant systematics available in EMPIRE are:

- (i) Ignatyuk *et al.* [48]:  $\tilde{a} = 0.154A + 6.3 \cdot 10^{-5}A^2$  and  $\gamma = -0.054$
- (ii) Arthur [49]:  $\tilde{a} = 0.1375A - 8.36 \cdot 10^{-5}A^2$  and  $\gamma = -0.054$
- (iii) Iljinov *et al.* [50]:  $\tilde{a} = 0.114A + 9.80 \cdot 10^{-2}A^{2/3}$  and  $\gamma = -0.051$

We stress again that Gilbert-Cameron approach does not account explicitly for the collective enhancements of the level densities. These are included implicitly in the  $\tilde{a}$  when fitting neutron resonance spacings. Such an approach leads to the over-estimation of the level densities above, say, 20 MeV. This deficiency can be overcome using the dynamic approach described below.

### Dynamic approach

The dynamic approach to the level densities is specific to the EMPIRE code. It takes into account collective enhancements of the level densities due to nuclear vibration and rotation. The formalism uses the super-fluid model below critical excitation energy (when the EMPIRE specific parametrization of the level density parameter is selected) and the

Fermi gas model above. Differently from other similar formulations, the latter one accounts explicitly for the rotation induced deformation of the nucleus, which becomes spin dependent (see Section 2.10.2). The deformation enters level densities formulas through moments of inertia and through the level density parameter  $a$  that increases with increase in the surface of the nucleus.

Assuming that the prolate nuclei rotate along the axis perpendicular to the symmetry axis the explicit level density formulas reads

$$\begin{aligned} \rho(E, J, \pi) = & \frac{1}{16\sqrt{6\pi}} \left( \frac{\hbar^2}{\mathfrak{I}_{\parallel}} \right)^{\frac{1}{2}} a^{1/4} \sum_{K=-J}^J \left( U - \frac{\hbar^2 K^2}{2\mathfrak{I}_{eff}} \right)^{-\frac{5}{4}} \\ & \exp \left\{ 2 \left[ a \left( U - \frac{\hbar^2 K^2}{2\mathfrak{I}_{eff}} \right) \right]^{\frac{1}{2}} \right\}. \end{aligned} \quad (2.101)$$

In the case of the oblate nuclei which are assumed to rotate parallel to the symmetry axis we have

$$\begin{aligned} \rho(E, J, \pi) = & \frac{1}{16\sqrt{6\pi}} \left( \frac{\hbar^2}{\mathfrak{I}_{\parallel}} \right)^{\frac{1}{2}} a^{1/4} \\ & \sum_{K=-J}^J \left( U - \frac{\hbar^2 [J(J+1) - K^2]}{2|\mathfrak{I}_{eff}|} \right)^{-\frac{5}{4}} \\ & \exp \left\{ 2 \left[ a \left( U - \frac{\hbar^2 [J(J+1) - K^2]}{2|\mathfrak{I}_{eff}|} \right) \right]^{\frac{1}{2}} \right\}. \end{aligned} \quad (2.102)$$

$a$  is a level density parameter,  $J$  is a nucleus spin and  $K$  its projection,  $E$  is the excitation energy and  $U$  is the excitation energy less pairing ( $\Delta$ ). The effective moment of inertia  $\mathfrak{I}_{eff}$  is defined in terms of the perpendicular  $\mathfrak{I}_{\parallel}$  and parallel  $\mathfrak{I}_{\perp}$  moments through the difference of their inverses

$$\frac{1}{\mathfrak{I}_{eff}} = \frac{1}{\mathfrak{I}_{\parallel}} - \frac{1}{\mathfrak{I}_{\perp}}. \quad (2.103)$$

The saddle-point moments of inertia are calculated using Sierk's routine MOMFIT [11], which provides a fit to the advanced liquid-drop model calculations.

It should be stressed that Eqs. 2.101 and 2.102 include summation over projection of the angular momentum  $K$  and thus automatically account for the rotational enhancement. The yrast line is obtained, setting level densities to 0 whenever the rotational energy becomes larger than  $U$ . In addition to the rotational enhancement the model accounts also for the vibrational enhancement, which is, however, less important. To this end Eqs. 2.101 and 2.102 are multiplied by  $K_{vib}$

$$K_{vib} = \exp \left\{ 1.7 \left( \frac{3m_0 A}{4\pi \hbar^2 S_{drop}} \right)^{2/3} T^{4/3} \right\} \quad (2.104)$$

with  $S_{drop} = 17/4\pi r_0^2$  and  $r_0 = 1.26$ .

Damping of the rotational enhancement is achieved by multiplying Eqs. 2.101 and 2.102 by

$$1 - Q_{rot} \left( 1 - \frac{1}{\hbar^2 / \mathfrak{I}_\perp t} \right) \quad (2.105)$$

Following Junghans *et al.* [51]  $Q_{rot}$  is assumed to be deformation independent

$$Q_{rot} = \frac{1}{1 + \exp \left( -\frac{E_{cr}}{d_{cr}} \right)} - \frac{1}{1 + \exp \left( -\frac{E - E_{cr}}{d_{cr}} \right)} \quad (2.106)$$

with  $E_{cr} = 40$  MeV and  $d_{cr} = 10$  MeV. The two terms in Eq. 2.106 ensure that  $Q_{rot} = 0$  at  $E = 0$  and tends to 1 for  $E \rightarrow \infty$ . We note that  $\hbar^2 / \mathfrak{I}_\perp t$  is approximately equal to the rotational enhancement and therefore multiplication of the level densities by Eq. 2.105 actually removes rotational enhancement when  $Q_{rot} = 1$ .

As nuclear temperature  $T$  increases the vibrational enhancement is damped by multiplying Eqs. 2.101 and 2.102 by the factor

$$Q_{vib} = \exp^{-1} \left( 1 - \frac{T - T_{1/2}}{DT} \right). \quad (2.107)$$

$T_{1/2} = 1$  MeV and  $DT = 0.1$  MeV are taken as default.

When EMPIRE-specific parametrization of the level density parameter  $a$  is selected (see below) the low-energy part of level densities is calculated in terms of the super-fluid (BCS) model [52]. With the pairing gap  $\Delta = 12/\sqrt{A}$  the critical temperature  $T_{crt}$  is

$$T_{crt} = 0.567\Delta. \quad (2.108)$$

The critical value of the level density parameter  $a$  is then determined by the iteration procedure

$$a_{crt}^{(0)} = \tilde{a} (1 + \gamma \delta_W) \quad (2.109)$$

$$U^{(n)} = a_{crt}^{(n)} T_{crt}^2 \quad (2.110)$$

$$a_{crt}^{(n+1)} = \tilde{a} \left[ 1 + \frac{\delta_W}{U^{(n)}} (1 - \exp(-\gamma U^{(n)})) \right]. \quad (2.111)$$

$\tilde{a}$  is the asymptotic value of the level density parameter. Eqs. 2.110 and 2.111 are iterated until the condition

$$\frac{|a^{(n+1)} - a^{(n)}|}{a^{(n+1)}} < 0.001 \quad (2.112)$$

is fulfilled. The condensation energy  $E_{cond}$ , critical energy  $U_{crt}$ , a critical value of the determinant  $Det_{crt}$ , and critical entropy  $S_{crt}$  are defined by the following expressions

$$E_{cond} = 1.5a_{crt}\Delta^2/\pi^2, \quad (2.113)$$

$$U_{crt} = a_{crt}T_{crt}^2 + E_{cond}, \quad (2.114)$$

$$Det_{crt} = \left(\frac{12}{\sqrt{\pi}}\right)^2 a_{crt}^3 T_{crt}^5, \quad (2.115)$$

$$S_{crt} = 2a_{crt}T_{crt}. \quad (2.116)$$

At excitation energies below  $U_{crt}$  (i.e., in the energy range where the BCS model applies) we define the parameter  $\varphi$

$$\varphi = \sqrt{1 - U/U_{crt}}, \quad (2.117)$$

which allows to express all thermodynamical quantities in terms of their critical values

$$T = 2T_{crt}\varphi \ln^{-1}\left(\frac{\varphi+1}{1-\varphi}\right), \quad (2.118)$$

$$S = S_{crt}T_{crt}(1-\varphi^2)/T, \quad (2.119)$$

$$Det = Det_{crt}(1-\varphi^2)(1+\varphi^2)^2. \quad (2.120)$$

The parallel and orthogonal moments of inertia below the critical temperature  $T_{crt}$  are

$$\mathfrak{S}_{\parallel}^{BCS} = \mathfrak{S}_{\parallel}T_{crt}(1-\varphi^2)/T \quad (2.121)$$

and

$$\mathfrak{S}_{\perp}^{BCS} = \frac{1}{3}\mathfrak{S}_{\perp} + \frac{2}{3}\mathfrak{S}_{\perp}T_{crt}(1-\varphi^2)/T \quad (2.122)$$

respectively (see the following section for the definitions of  $\mathfrak{S}_{\parallel}$  and  $\mathfrak{S}_{\perp}$ ). Using these results squares of the effective spin cut-off parameters are defined as

$$\begin{aligned} \sigma_{eff}^2 &= \mathfrak{S}_{\parallel}^{BCS}T & \text{for } \alpha_2 < 0.005, \\ \sigma_{eff}^2 &= \left(\mathfrak{S}_{\parallel}^{BCS}\right)^{1/3} \left(\mathfrak{S}_{\perp}^{BCS}\right)^{2/3} T & \text{for } \alpha_2 > 0.005, \end{aligned} \quad (2.123)$$

with  $\alpha_2$  being ground state deformation. The BCS level densities are calculated according to the expression

$$\rho_{BCS}(U, J) = \frac{2J+1}{2\sqrt{2\pi}\sigma_{eff}^3\sqrt{Det}} \exp\left(\frac{S - J(J+1)}{2\sigma_{eff}^2}\right) \quad (2.124)$$

Finally, Eq. 2.124 is corrected for rotational and vibrational collective effects in the non-adiabatic mode (i.e., including their damping with increasing temperature), that results in

$$\rho(U, J) = \rho_{BCS}(U, J)Q_{rot}^{BCS}K_{rot}Q_{vib}K_{vib}. \quad (2.125)$$

The vibrational enhancement  $K_{vib}$  and its damping  $Q_{vib}$  are given by Eqs. 2.104 and 2.107 respectively. The rotational enhancement is

$$K_{rot} = \mathfrak{S}_{\perp} T \quad (2.126)$$

and is damped with the function

$$Q_{rot}^{BCS} = 1 - Q_{rot} \left( 1 - \frac{1}{\mathfrak{S}_{\perp} T} \right), \quad (2.127)$$

where  $Q_{rot}$  has been defined by Eq. 2.106. A somewhat unusual form of Eq. 2.127 is due to the fact that while Eqs. 2.101 and 2.102 contain rotational enhancement intrinsically, Eq. 2.124 does not. Therefore, action of the damping function has to be reversed.

In the dynamic treatment of the level densities the level density parameter  $a$  can be determined using one of the following 3 methods:

(i) **EMPIRE-specific:**  $a$  is assumed to be energy (temperature) dependent and calculated following Ignatyuk *et al.* [48] as

$$a(U) = \tilde{a} [1 + f(U) \frac{\delta_W}{U}], \quad (2.128)$$

where  $\delta_W$  is the shell correction and  $\tilde{a}$  is the asymptotic value of the  $a$ -parameter given by,

$$\tilde{a} = \eta A + \zeta A^{2/3} F_{surf}(R_{max}/R_{min}), \quad (2.129)$$

and

$$f(U) = 1 - \exp(-\gamma U). \quad (2.130)$$

Compared to the original formulation of Ignatyuk *et al.* [48], there is an additional factor  $F_{surf}(R_{max}/R_{min})$  in Eq. 2.128. It accounts for the dependence of the level density parameter on nuclear deformation. This factor is a function of the ratio of nuclear axes  $R_{max}$  and  $R_{min}$  and was provided by Igor Gontchar [53] in a tabular form .

The level density  $a$ -parameters at neutron binding energy  $a_{B_n}$  were extracted using Eqs. 2.101 through 2.107 from average neutron resonance spacings  $D_{obs}$  compiled by Iljinov *et al.* [50]. These  $a$  values were fitted with Eqs. 2.128 through 2.130 to obtain  $\eta$ ,  $\zeta$ , and  $\gamma$  parameters. Depending on the choice of shell-corrections the two sets of parameters were derived. For the Nix-Moller shell corrections [54] the parameters are:

$$\begin{array}{ll} \eta = 0.094431 & \eta = 0.117113 \\ \xi = -0.08014 & \xi = -0.09939 \text{ for } Z \geq 85 \\ \gamma = 0.075594 & \gamma = 0.094447 \end{array} \quad (2.131)$$

When Myers-Swiatecki shell-corrections are being used the parameters become:

$$\begin{array}{ll} \eta = 0.052268 & \eta = 0.067645 \\ \xi = 0.13395 & \xi = 0.173358 \text{ for } Z \geq 85 \\ \gamma = 0.093955 & \gamma = 0.121465 \end{array} \quad (2.132)$$

Actually, EMPIRE looks in the *data/ldp.dat* file for the experimental values of the  $a$ -parameter. Experimental results are given priority over the systematics prediction. The average ratio of the experimental values to the results of Eq. 2.129 is used to normalize systematics predictions for the nuclei for which there are no experimental results. This way a sort of the "local systematics" is constructed for the nuclei involved in the calculation run. In both cases, level densities below  $U_{crt}$  are calculated in the frame of the super-fluid model [52] with the pairing gap  $\Delta = 12/\sqrt{A}$ .

When using EMPIRE-specific method, the cumulative plots of discrete levels along with the model predictions, can be produced by choosing the FITLEV option in the input. For each nucleus involved in the calculations an appropriate plot is produced and stored in the CUMULPLOT.PS file, which can be inspected after the run is over (NOTE: this option requires "gnuplot" packet and "ps2ps" which is a part of the "ghostscript").

(ii) **fit to the shell-model s.p.s.:** energy dependent level density parameters for about 4000 nuclei were deduced [55] directly from the spacings of the shell-model single particle states (s.p.s.) calculated by Moller and Nix [54, 17]. The level density parameter  $a$  was parametrized as

$$a(U) = a_1 + a_2 e^{-a_3 U} \quad (2.133)$$

with  $a_1$ ,  $a_2$ , and  $a_3$  coefficients contained in the file *data/nparac.dat*. When this option is used Eqs. 2.101 through 2.107 are applied at all energies, down to the discrete level region. No adjustment to the experimental level densities or to discrete levels is performed. This method should not be used in the vicinity of shell closures.

(iii)  **$a=A/\text{constant}$ :** level density parameter  $a$  is assumed to be energy independent and proportional to the mass number. Typically, it is taken as  $A/8$  but can be specified in the input file. Also in this case Eqs. 2.101 through 2.107 are applied down to the discrete levels and no adjustment to experimental data is performed. This method is not recommended and is included only because of its wide use in the heavy ion calculations.

### Hartree-Fock-BCS approach

EMPIRE can read precalculated level densities from the RIPL-2 library, which contains tables of level densities [56] for more than 8000 nuclei calculated in the frame of the Hartree-Fock-BCS approach. These microscopic results include a consistent treatment of shell corrections, pairing correlations, deformation effects and rotational enhancement. The results were re-normalized to the experimental  $s$ -wave neutron resonance spacings and adjusted to the cumulative number of discrete levels, so that the degree of accuracy is comparable to the phenomenological formulae.

Using the partition function method, the state density can be obtained as

$$\omega(U) = \frac{e^{S(U)}}{(2\pi)^{3/2} \sqrt{Det(U)}}. \quad (2.134)$$

Entropy  $S$  and excitation energy  $U$  are derived from the summation over single particle levels and  $Det$  stands for the determinant. Pairing correlations are treated within

the standard BCS theory in the constant- $G$  approximation with blocking. Consequently single-particle energies are replaced by their quasi-particle equivalents with BCS equations determining gap parameter  $\Delta$  and the chemical potential  $\lambda$ . Spherical and deformed nuclei are treated in a distinct mode. The level density for spherical nuclei is simply related to the state density (Eq. 2.134)

$$\rho_{sph}(U, J) = \frac{2J+1}{2\sqrt{2\pi^3}} e^{-J(J+1)/(2\sigma^2)} \omega(U), \quad (2.135)$$

while for deformed nuclei the formula is similar to the one used in the EMPIRE-specific level densities (Eqs. 2.101 and 2.102)

$$\rho_{def}(U, J) = \frac{1}{2} \sum_{K=-J}^J \frac{1}{\sqrt{2\pi\sigma^2}} e^{-[J(J+1)/(2\sigma_{\perp}^2) + K^2(1/\sigma^2 - 1/\sigma_{\perp}^2)/2]} \omega(U), \quad (2.136)$$

in which  $\sigma$  is the spin cut-off parameter and  $\sigma_{\perp}$  the perpendicular spin cut-off parameter, both affected by the pairing correlations, and  $\sigma_{\perp}$  being related to the perpendicular moment of inertia. It should be stressed that similarly to Eq. 2.101 and 2.102, Eq. 2.136 comprises rotational enhancement. As in the case of EMPIRE-specific level densities, this enhancement has to disappear with increasing excitation energy. To this end, a phenomenological damping function  $f_{dam}$  is introduced

$$f_{dam}(U) = \frac{1}{1 + e^{(U-E_{def})/d_U}} \left[ 1 - \frac{1}{1 + e^{(\beta_2 - \beta^*)/d\beta}} \right]', \quad (2.137)$$

which contains energy and deformation dependent factors. The deformation energy is the difference between the energy in the spherical configuration and at the equilibrium deformation. The parameter  $d_U$  describes how fast the sphericity is recovered at energies above  $E_{def} = E_{sph} - E_{eq}$ .  $\beta^*$  defines an actual deformation when moving between spherical and deformed shape. The above parameters were taken as  $d_U = 2.5$  MeV,  $\beta^* = 0.15$  and  $d\beta = 0.01$ . With this damping function the level density formula reads

$$\rho(U, J) = [1 - f_{dam}(U)] \rho_{sph}(U, J) + f_{dam}(U) \rho_{def}(U, J). \quad (2.138)$$

HF-BCS calculations depend on the single-particle schemes used to determine the thermodynamic quantities, in particular on the single-particle state density around the Fermi energy. The calculations under discussion are based on schemes obtained using the Hartree-Fock method with MSk7 Skyrme type force. These single-particle levels perform very well in predicting nuclear masses and other ground state properties, which increases the confidence in the level densities calculated by this approach. As mentioned earlier, final results were adjusted to resonance spacings at the neutron binding energy and to the cumulative number of discrete levels by applying shift to the excitation energy and a multiplicative factor to the entropy. Therefore, no further phenomenological adjustment needs to be performed by EMPIRE.

Level density tables contain numerical values for 30 spins and extend up to 150 MeV, which sets limits on their possible utilization, although spin restriction should not be an issue for nucleon induced reactions.

Before concluding this section we would like to note certain affinity between the HF-BCS and the default, EMPIRE-specific, level densities. Both approaches use the BCS model at low energies, incorporate rotational enhancement directly into the level density formula, and apply phenomenological (although functionally different) damping of rotational effects. Both take into account deformation effects (in EMPIRE-specific densities these are not only temperature but also spin dependent), and are adjusted to the available experimental information. The EMPIRE-specific densities also include a vibrational enhancement factor. However, the most essential difference between the two approaches is the use of a phenomenological  $a$ -parameter and closed formula in the EMPIRE-specific approach, while HF-BCS level densities are derived directly from the microscopic single-particle schemes. The latter approach is expected to be more reliable away from valley of stability.

### 2.10.2 Nuclear deformation and moments of inertia

The shape of each nucleus affects such parameters as the Giant Dipole Resonance, level density parameters  $a$  and rotational enhancement of the level densities. This shape is estimated by the code by summing up ground state deformation and dynamic deformation induced by the rotation of the nucleus. The ground state deformation is read from the file *data/nix-moller.dat* [54], and the dynamic deformation is taken to be proportional to the square of the angular momentum  $I$ . Ground state deformation  $\alpha_{g.s.}$  is damped with the increasing nuclear temperature, since nuclei are known to become spherical at high excitation energies. The dynamic deformation  $\alpha_{2dyn}$  is calculated following Vigdor and Karwowski [57]

$$\alpha_{2dyn} \approx b(-1.25y/(1-x)), \quad (2.139)$$

where  $b$  is treated as an adjustable parameter. The angular momentum parameter  $y$  is given by

$$y = 1.9249I(I+1)\frac{I(I+1)}{\eta A^{7/3}} \quad (2.140)$$

and the fissility parameter is given by

$$x = 0.01965\frac{Z^2}{\eta A}, \quad (2.141)$$

where  $\eta$  is the neutron-proton difference term

$$\eta = 1 - 1.7826(N-Z)^2 A^{-2}. \quad (2.142)$$

Accordingly, the deformation is parametrized as



$$\alpha_2(T, I) = \alpha_{g.s.} h(T) + \alpha_{2dyn} \quad (2.143)$$

where  $h(T) = 1/\{1 + \exp[(T-2)/0.5]\}$  damps the ground state deformation with increasing excitation and reduces the value by 50% at temperature  $T = 2$  MeV. This value seems a reasonable estimate corresponding to about 50 MeV of excitation energy. Obviously, such a procedure is an approximation, but a more rigorous approach (e.g. using Cranking Model to determine potential surface minima at different spins and temperatures) would require prohibitive calculation times, due to the large number of intermediate nuclei involved. However, we believe that the approximation used is sufficient to provide the leading term of the effect. We note that when using this prescription, a nucleus that is deformed in the ground state will tend (at low spins) to become spherical with increasing energy. This is because of the temperature damping of the ground state and negligible contribution of the dynamic deformation at low spins. On the other hand, for  $b > 0$ , a prolate nucleus will tend to become spherical and eventually oblate with increasing angular momentum. Qualitatively, such behavior agrees with the results of the more rigorous calculations [58].

Moments of inertia for the yrast states (not the saddle-point) are calculated for deformation  $\alpha_2(T, I)$  using expressions proposed by Vigdor and Karwowski [57]

$$\begin{aligned} \mathfrak{I}_{\parallel} = \mathfrak{I}_0(1 - \alpha_2 + 0.429\alpha_2^2 + 0.268\alpha_2^3 - 0.212\alpha_2^4 \\ - 1.143\alpha_2\alpha_4 + 0.494\alpha_2^2\alpha_4 + 0.266\alpha_4^2) \end{aligned} \quad (2.144)$$

$$\begin{aligned} \mathfrak{I}_{\perp} = \mathfrak{I}_0(1 + 0.5\alpha_2 + 1.286\alpha_2^2 + 0.581\alpha_2^3 - 0.451\alpha_2^4 \\ + 0.571\alpha_2\alpha_4 + 1.897\alpha_2^2\alpha_4 + 0.700\alpha_4^2) \end{aligned} \quad (2.145)$$

with the rigid-sphere moment of inertia

$$\mathfrak{I}_0/\hbar^2 = 0.01448A^{5/3} \text{ MeV}^{-1}, \quad (2.146)$$

and

$$\alpha_4 = \frac{\alpha_2^2(0.057 + 0.17x + c_2y) + c_3\alpha_2y}{1 - 0.37x - c_1y}. \quad (2.147)$$

The coefficients  $c$  are

$$\begin{array}{ll} c_1 = -0.266 & c_1 = -0.70 \\ c_2 = -0.896 & \text{for } \alpha_2 < 0 \quad c_2 = 0.663 \quad \text{for } \alpha_2 > 0. \\ c_3 = -0.571 & c_3 = 0.286 \end{array} \quad (2.148)$$

The three principal-axis moments of inertia for the saddle-point are calculated with the routine MOMFIT [11] by Sierk. MOMFIT is a fit to moments of inertia calculated in 1983-1985 by Sierk at Los Alamos National Laboratory, using Yukawa-plus-exponential double-folded nuclear energy, exact Coulomb diffuseness corrections, and diffuse-matter moments of inertia. The parameters of the model are those derived by Moller and Nix in

1979:  $r_0 = 1.16$  fm,  $a_s = 21.13$  MeV,  $\kappa_s = 2.3$ , and  $a = 0.68$  fm. The diffuseness of matter and charge distributions used correspond to a surface diffuseness parameter of 0.99 fm.

It should be stressed that the above mentioned computations of moments of inertia are valid up to the liquid drop stability limit. Both calculation methods (MOMFIT and expressions proposed by Vigdor and Karwowski [57]) will provide this limit. As a default, the code will restrict calculations to the partial waves below the liquid drop stability limit (even if the fusion cross section extends above this value). The user can increase this limit to the  $l$ -value at which the fission barrier disappears (including shell correction) or to specify a value in the input. In both cases, the rigid sphere moments of inertia will be taken above the liquid drop stability limit.

### 2.10.3 Fission barriers

The liquid-drop spin dependent fission barriers for  $19 < Z < 102$  are calculated using the BARFIT subroutine [11], which also provides ground state energies and the compound nucleus stability limit with respect to fission (i.e., spin value at which liquid-drop fission barrier disappears). BARFIT consists of a fit to the barriers calculated by Sierk within the rotating droplet model, using Yukawa-plus-exponential double folded nuclear energy, exact Coulomb diffuseness corrections, and diffuse-matter moments of inertia. The calculated barriers for  $l = 0$  are accurate to a little less than 0.1 MeV. The output from the BARFIT subroutine is a little less accurate. Errors may be as large as 0.5 MeV but the characteristic uncertainty is in the range of 0.1-0.2 MeV. The values of ground state energy are generally approximated to within about 0.1-0.2 MeV. The approximate value of the stability limit is nearly always within  $0.5\hbar$  of the calculated one.

For nuclei with  $Z \geq 102$  the recent parametrization of the Thomas-Fermi fission barriers at zero spin is used [59] .

$$B_f(J = 0) = S(N, Z)F(X), \quad (2.149)$$

where  $S$  is proportional to the nominal surface energy of the nucleus, and is given by

$$S = A^{2/3}(1 - kI^2), \quad (2.150)$$

with  $I = (N - Z)/A$  and  $k = 1.9 + (Z - 80)/75$ . The fissility is proportional to the ratio of the nominal Coulomb and surface energies of a sphere:

$$X = Z^2/A(1 - kI^2). \quad (2.151)$$

The function  $F$  is

$$\begin{aligned} F(X) &= 0.000199749(X - X_0)^3 & \text{for } X_1 \leq X \leq X_0 \\ F(X) &= 0.595553 - 0.124136(X - X_1) & \text{for } 30 \leq X \leq X_1 \end{aligned} \quad (2.152)$$

with  $X_0 = 48.5428$  and  $X_1 = 34.15$ . These formulae predict vanishing barriers for nuclei with  $Z \geq 110$ . Spin dependence is not provided by Eqs. 2.149-2.152. The EMPIRE code assumes that angular momentum dependence calculated with BARFIT for  $Z=102$  and  $A=256$  is also valid for the heavier nuclei.

The full fission barrier is a sum of the liquid-drop part and the shell correction  $\delta_W$  taken with the opposite sign. The latter is assumed to gradually disappear with spin  $J$  and temperature  $T$  so that the fission barrier becomes

$$B_f(T, J) = B_{ld}(J) - f(T) g(J) \delta_W. \quad (2.153)$$

The temperature fade-out function was found [60] to be

$$\begin{aligned} f(T) &= 1 & \text{for } T < 1.65 \text{ MeV} \\ f(T) &= e^{1.066(1.65-T)} & \text{for } T \geq 1.65 \text{ MeV}. \end{aligned} \quad (2.154)$$

For the angular momentum fade-out the following formula is used [60]

$$g(J) = \frac{1}{1 + \exp[(J - J_{1/2})/\Delta J]} + d \cdot \exp[(J - J_G)^2/\Delta J_G^2], \quad (2.155)$$

where the first term accounts for the overall decrease of the shell correction due to the increasing nuclear deformation, while the second one (of Gaussian type) permits the inclusion of fluctuations characteristic of the particular nucleus. The parameters  $J_{1/2}$  and  $\Delta J$  vary slowly with the mass number. Typical values for heavy nuclei are about 20-25 for  $J_{1/2}$  and 2-3 for  $\Delta J$ . The Gaussian correction can be used only if the relevant parameters can be determined from the experimental data.

#### 2.10.4 Dissipation effects

The fission process is delayed by the dissipation effects. They are treated in an approximate, time-independent approach [61, 62, 63], which takes into account: (i) the stationary limit of Kramers [63] and (ii) the exponential factor [62] applied to the Kramers' fission width to account for the transient time after which the statistical regime is reached. The classical Hill-Wheeler fission width  $\Gamma_f^{HW}$  (Eq. 2.92) is modified to obtain Kramers limit

$$\Gamma_f^K = \Gamma_f^{HW} (\sqrt{1.0 + (\beta_v/2\hbar\omega)^2} - \beta_v/2\hbar\omega) \quad (2.156)$$

where  $\beta_v$  is the reduced dissipation coefficient and  $\omega$  describes the potential curvature at the fission saddle point. In addition, the fission width is reduced to account for the transient time needed to form a saddle point [62]

$$\Gamma_f = \Gamma_f^K \exp\left(-1.51768\tau \sum_x \Gamma_x\right), \quad (2.157)$$

where  $x$  runs over all particle channels and  $\tau$  is given by

$$\begin{aligned} \tau &= \beta_v^{-1} \ln(10 \frac{B_f}{T}) & \text{for } \beta_v < 3.2 \cdot 10^{-21} \text{ s}^{-1} \\ \tau &= 0.19531 \beta_v \ln(10 \frac{B_f}{T}) & \text{for } \beta_v \geq 3.2 \cdot 10^{-21} \text{ s}^{-1} \end{aligned} \quad (2.158)$$

$T$  is a nuclear temperature, and  $\beta_v = 3.2 \cdot 10^{-21} \text{ s}^{-1}$  is assumed to separate under-damped and over-damped motion.

### 2.10.5 $\gamma$ -ray emission

The E1, E2, and M1 transitions are taken into account in the statistical model (Hauser-Feshbach) calculations. An arbitrary mixture of the Weisskopf single-particle model [64] and of the Giant Multipole Resonance model (Brink-Axel hypothesis [34, 35, 36]) can be used. Relative contributions of both approaches are defined by the input parameter  $t$ . The transmission coefficients for a  $\gamma$ -ray emission are written as

$$T_{Xl} = (1 - t)T_{Xl}^{Weiss} + tT_{Xl}^{GMR}, \quad (2.159)$$

where  $Xl$  denotes different multipolarities and the  $t$ -parameter adopts values between 0 and 1. However, the default value  $t = 1$  (i.e., pure GMR) is normally used. The Weisskopf estimates  $T_{Xl}^{Weiss}$  defined by the equations:

$$T_{E1}^{Weiss} = C_{E1} 4.599^{-7} A^{2/3} E_\gamma^3 [MeV^{-3}], \quad (2.160)$$

$$T_{M1}^{Weiss} = C_{M1} 1.3^{-7} E_\gamma^3 [MeV^{-3}], \quad (2.161)$$

$$T_{E2}^{Weiss} = C_{E2} 3.54^{-13} A^{4/3} E_\gamma^5 [MeV^{-5}]. \quad (2.162)$$

$E_\gamma$  denotes the  $\gamma$ -ray energy and  $A$  is the nuclear mass. The coefficients  $C_{Xl}$  can be used to adjust theoretical estimates to the experimental data.

The Brink-Axel hypothesis allows the cross section for photoabsorption by an excited state to be equated with that of the ground state. Introducing the  $\gamma$ -ray strength function  $f_{Xl}(E_\gamma)$ , the transmission coefficient can be written as

$$T_{Xl}^{GMR} = 2\pi f_{Xl}(E_\gamma) E_\gamma^{2l+1}. \quad (2.163)$$

The Giant Dipole Resonance (GDR) shape is generally described by the sum of two Lorentzians with energy-dependent width. The  $\gamma$ -ray strength function is given by the expression

$$f_{E1}(E_\gamma) = \sum_{i=1}^2 \sigma_i \Gamma_i \left[ \frac{E_\gamma \Gamma_i(E_\gamma, T)}{(E_\gamma^2 - E_i^2)^2 + E_\gamma^2 \Gamma_i(E_\gamma)^2} + \frac{0.7 \Gamma_i 4\pi^2 T^2}{E^5} \right], \quad (2.164)$$

where  $\sigma_i$ ,  $\Gamma_i$ , and  $E_i$  are the peak cross section, the width, and the energy of the  $i$ -th hump of the GDR, and the energy dependent width is given by

$$\Gamma_i(E_\gamma, T) = \Gamma_i \frac{E_\gamma^2 + 4\pi T^2}{E_i^2}. \quad (2.165)$$

By default, the parameters of the GDR are estimated from the systematics based on the Dietrich and Berman compilation [65], containing 150 experimental data for nuclei ranging from mass  $A = 51$  up to  $A = 239$ . The deformation parameter  $\delta=0.064$  is the limit for considering a nucleus to be “nearly spherical”. GDR parameters for the deformed nuclei ( $\delta > 0.064$ ), are given by the following expressions:

$$E_2 = 50A^{-0.232} [MeV] \quad (2.166)$$

$$\ln(E_2/E_1) = 0.946\delta \quad (2.167)$$

$$\Gamma_1 = (0.283 - 0.263\delta)E_1 [MeV] \quad (2.168)$$

$$\Gamma_2 = (0.35 - 0.14\delta)E_2 [MeV] \quad (2.169)$$

$$\sigma_1 = 3.48A/\Gamma_1 [mb] \quad (2.170)$$

$$\sigma_2 = 1.464A^{4/3}/\Gamma_2 [mb] \quad (2.171)$$

where  $\Gamma$  and  $\sigma$  are the GDR width and peak cross section respectively, while subscripts 1 and 2 refer to the lower- and higher-energy GDR humps. The particular feature of the present systematics is the deformation independent energy of the second GDR hump ( $E_{2GDR}$ ).

Separate systematics was performed for the “nearly spherical” nuclei, because “deformed nuclei systematics” in the  $\delta = 0$  limit does not adequately describe the GDR parameters for spherical and slightly deformed nuclei. The following expressions were proposed for nuclei with  $\delta \leq 0.064$ :

$$E_{GDR} = (49.336 + 7.34\delta)A^{-0.2409} [MeV] \quad (2.172)$$

$$\Gamma_{GDR} = 0.3E_{GDR} [MeV] \quad (2.173)$$

$$\sigma_{GDR} = 10.6A/\Gamma_{GDR} [mb] \quad (2.174)$$

More details on these systematics will be published in a separate paper [66]. By default, the deformation is spin dependent as is the shape of GDR. An input option is provided to suppress this dependence and use ground state deformation.

It is also assumed that the systematics holds for the GDR built on the highly excited states with large angular momentum, like those produced in the HI reactions. However, the code allows for an additional increase of the GDR width with the excitation energy [67]. This increase cannot be deduced from the analysis of the database [65] containing GDRs built on the ground state but has to be added on top of the derived systematics giving

$$\Gamma = \Gamma_{syst} + c E_x^{1.6}, \quad (2.175)$$

where the index *syst* stands for the result of the systematics, and  $E_x$  is the excitation energy of the excited nucleus. This dependence (with  $c = 0.0026$ ) was obtained for Sn isotopes [67] and has been accepted in the code.

The following default parameters have been adopted for the Giant Quadrupole Resonance (GQR):

$$E_{GQR} = 63A^{-1/3} [MeV] \quad (2.176)$$

$$\Gamma_{GQR} = 6.11 - 0.012A [MeV] \quad (2.177)$$

$$\sigma_{GQR} = 0.00015 \frac{Z^2 E_{GQR}^2}{A^{1/3} \Gamma_{GQR}} [mb] \quad (2.178)$$

The GQR energy is taken after Ref. [68] while the GQR width and peak cross section are taken from Ref. [69].

The default parametrization of the spin-flip Giant Monopole Resonance follows Bohr and Mottelson [25]

$$E_{GMR} = 41A^{-1/3} [MeV] \quad (2.179)$$

$$\Gamma_{GMR} = 4.0 [MeV] \quad (2.180)$$

$$\sigma_{GMR} = 1.0 [mb] \quad (2.181)$$

EMPIRE-3.1 includes also series of E1  $\gamma$ -ray strength functions proposed in RIPL-2 [47]. We refer to the RIPL-2 TECDOC available at [www-nds.iaea.org/RIPL-2/handbook/ripl2.pdf](http://www-nds.iaea.org/RIPL-2/handbook/ripl2.pdf) for detailed description of these advanced approaches.

## 2.11 Width fluctuation correction

The Hauser-Feshbach model assumes that there are no correlations among various reaction channels contributing to the formation and decay of a certain compound nucleus state  $J^\pi$ . An obvious case for which this assumption breaks down is the elastic channel, for which entrance and exit channels are the same. This correlation leads to an increase of the elastic channel cross section compared to the Hauser-Feshbach predictions. At higher incident energies, at which the elastic channel is one among many inelastic ones, this increase can be safely neglected. However, if there are only a few open channels the increase of the elastic channels turns out to have serious consequences on other channels (particularly on inelastic scattering and capture).

One of the models which allows these effects to be taken into account has been proposed by Hofmann, Richert, Tepel and Weidenmueller [1] (HRTW). In the case of no direct reaction contribution, the averaged  $S$ -matrix element connecting channels  $a$  and  $b$  can be written as

$$\langle S \rangle_{ab} = \delta_{ab} e^{i\zeta_{ab}} (1 - T_a)^{1/2}, \quad (2.182)$$

where

$$T_a = 1 - |< S >_{aa}|^2 \quad (2.183)$$

is an optical model transmission coefficient. The HRTW model assumes that the Compound Nucleus (CN) cross sections **factorize** and can be expressed through a product of the channel dependent quantities  $\xi$ . This would be the famous Bohr's assumption if not for the elastic enhancement factor  $W_a$ , which has been introduced by HRTW in order to account for the elastic channel correlation

$$< \sigma_{ab}^{fl} > = \xi_a \xi_b \quad a \neq b \quad \text{and} \quad < \sigma_a^{fl} > = W_a \xi_a^2. \quad (2.184)$$

Setting

$$\xi_a = \frac{V_a}{\sqrt{\sum_c V_c}} \quad (2.185)$$

we get for the CN cross section

$$\sigma_{ab}^{CN} \equiv < \sigma_{ab}^{fl} > = V_a V_b \left( \sum_c V_c \right)^{-1} [1 + \delta_{ab} (W_a - 1)]. \quad (2.186)$$

Taking into account that the incoming flux has to be conserved (unitarity condition) we find the relation between  $V$ s, the elastic enhancement factor ( $W_a$ ), and the transmission coefficient ( $T_a$ )

$$V_a = T_a \left[ 1 + \frac{V_a}{(\sum_c V_c)} (W_a - 1) \right]^{-1}. \quad (2.187)$$

This equation can be solved for  $V_a$  by iteration once all  $W_a$  are known. The current version of EMPIRE uses  $W_a$  derived from the analysis of numerically generated sets of  $S$ -matrices [2]. This exercises was tailored to the cases that include many weak channels coupled to a few strong channels, which is typical of neutron capture reactions. The resulting formula for the elastic enhancement factor is

$$W_a = 1 + 2 [1 + T_a^F]^{-1} + 87 \left( \frac{T_a - T_{ave}}{\sum_c T_c} \right)^2 \left( \frac{T_a}{\sum_c T_c} \right)^5, \quad (2.188)$$

with

$$F = 4 \frac{T_{ave}}{\sum_c T_c} \left( 1 + \frac{T_a}{\sum_c T_c} \right) \left( 1 + 3 \frac{T_{ave}}{\sum_c T_c} \right)^{-1}, \quad (2.189)$$

which completes formulation of the model.

The widths fluctuation correction has been added by Herman to improve code performance at low incident energies. The theory requires that each  $J^\pi$  state in the highest energy bin of the first CN is treated separately. In order to define physical elastic channels the fusion cross section to a given  $J^\pi$  capture state is decomposed into  $l$  components (actual version of EMPIRE uses  $T_l$  rather than  $T_{lj}$ ). In the first sweep  $T_l$ s for all channels are stored and elastic channels recorded. In the second sweep  $V_l$  and HF-type denominator are

calculated, and the enhancement is applied to the elastic channels. Finally, the third sweep is needed to normalize partial widths and calculate cross sections. For practical reasons, the channels are divided into strong ( $T_l \geq 0.0001$ ) and weak ones ( $T_l < 0.0001$ ). The effective transmission coefficients ( $V_a$ ) for the strong channels are calculated by iteration until the requested accuracy is achieved, while only one iteration is applied to obtain  $V_a$  for the weak channels. Particle channels are treated explicitly while  $\gamma$ -channels are lumped into one or more fictitious channels. By default, the HRTW model is applied below 5 MeV incident energy. Users have the option to apply it at all energies or to turn it off.

## 2.12 Photoabsorption

A model of photonuclear reactions must account for the different reaction mechanisms involved in the initial photonuclear excitation process and the subsequent decay of the excited nucleus by particle and gamma-ray emission. At low energies, below about 30 MeV, the Giant Dipole Resonance (GDR) is the dominant excitation mechanism, where a collective bulk oscillation of the neutrons against the protons occurs. At higher energies, up to approximately 150 MeV, photoabsorption on a neutron-proton pair (a quasi-deuteron, QD), which has a large dipole moment, is the dominant mechanism.

In EMPIRE, the photoabsorption cross section is calculated as the sum of two components[70],

$$\sigma_{abs}(E_\gamma) = \sigma_{GDR}(E_\gamma) + \sigma_{QD}(E_\gamma).$$

The GDR component,  $\sigma_{GDR}(E_\gamma)$ , is given by a Lorentzian shape, with parameters describing the total absorption of the giant dipole resonance. The expression used is given in detail in 2.9.5, but takes the basic form

$$\sigma_{GDR}(E_\gamma) = \sum_i \sigma_i \frac{(E_\gamma \Gamma_i)^2}{(E_\gamma^2 - E_i^2)^2 + (E_\gamma \Gamma_i)^2},$$

where  $\sigma_i$ ,  $E_i$  and  $\Gamma_i$  are the GDR peak cross section, energy and width, respectively. The summation is limited to  $i = 1$  for spherical nuclei, while for deformed nuclei the resonance is split and one uses  $i = 1, 2$ . As a rule, the parameters are derived from fits to experimental data or from systematics[47].

The QD component,  $\sigma_{QD}(E_\gamma)$ , is taken from the model of Chadwick *et al.* [71], which uses a Levinger-type theory. It relates the nuclear photoabsorption cross section to the experimental deuteron photodisintegration cross section,  $\sigma_d(E_\gamma)$ , as

$$\sigma_{QD}(E_\gamma) = L \frac{NZ}{A} \sigma_d(E_\gamma) f(E_\gamma).$$

Here, the Levinger parameter was derived as  $L = 6.5$  and  $f(E_\gamma)$  is the Pauli-blocking function, which reduces the free deuteron cross section  $\sigma_d(E_\gamma)$  to account for Pauli blocking of the excited neutron and proton by the nuclear medium. The experimental deuteron



photodisintegration cross section was parametrized as

$$\sigma_d(E_\gamma) = 61.2 \frac{(E_\gamma - 2.24)^{3/2}}{E_\gamma^3},$$

with  $E_\gamma$  in MeV and  $\sigma_d$  in mb. The Pauli-blocking function was found by Chadwick *et al.* to be a multidimensional integral whose solution could be well approximated in the energy range 20 – 140 MeV by the polynomial expression

$$\begin{aligned} f(E_\gamma) = & 8.3714 \times 10^{-2} - 9.8343 \times 10^{-3} E_\gamma + 4.1222 \times 10^{-4} E_\gamma^2 \\ & - 3.4762 \times 10^{-6} E_\gamma^3 + 9.3537 \times 10^{-9} E_\gamma^4, \end{aligned}$$

with  $E_\gamma$  in MeV. In Ref. [71], the Pauli-blocking function was not parametrized below 20 MeV, where it tends to zero, or above 140 MeV, where it tends to unity. As the contribution needs to be defined at all energies considered, EMPIRE follows the example of Ref. [70] and uses an exponential shape,  $f(E_\gamma) = \exp(-D/E_\gamma)$ , for energies below 20 MeV and above 140 MeV, with  $D = 73.3$  MeV for  $E_\gamma < 20$  MeV and  $D = 24.2$  MeV for  $E_\gamma > 140$  MeV. This form has the correct behavior in that it tends to zero at  $E_\gamma = 0$  and to unity for large  $E_\gamma$ , and is continuous with the previous equation at 20 and 140 MeV.

Preequilibrium reaction mechanisms become important for incident photon energies above 10 to 15 MeV. In the photoabsorption mechanisms described above, the initial nuclear excitation can be understood in terms of particle-hole excitations ( $1p1h$  for the GDR;  $2p2h$  or  $2p1h$  for QD processes) and thus it is natural to use a preequilibrium theory of particle-hole processes to describe the preequilibrium emission and damping to equilibrium during the evolution of the reaction. Such models can be used to calculate photonuclear reactions for incident photons with energies up to about 140 MeV, which is the threshold for pion production. At present, EMPIRE permits the calculation of preequilibrium emission in photonuclear reactions using either the exciton model module PCROSS or the Hybrid Monte-Carlo Simulation module HMS. Both implementations of photoabsorption represent the GDR fraction as an initial  $1p1h$  excitation and the QD fraction as an initial  $2p2h$  excitation. The implementation of photoabsorption in PCROSS does not take into account the correlation of the two holes created through the QD mechanism, which would require an initial configuration closer to a  $2p1h$  one than to a  $2p2h$  one [70]. The implementation in HMS takes this correlation into account in a manner consistent with the model of Ref. [71].

Following the possible emission of preequilibrium particles, the remaining nuclear system reaches equilibrium, after which it decays by sequential particle or gamma-ray emission (or possibly fission) until the nuclear ground state is reached. In EMPIRE, the Hauser-Feshbach theory is used to calculate cross sections for these processes.

Much more information on photonuclear reactions can be found in Ref. [70], which served as the basis for this brief description of these processes.

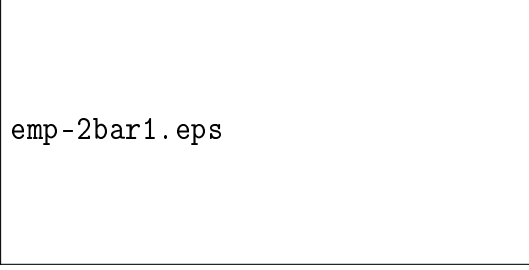


Figure 2.3: Double-humped fission barriers

## 2.13 Fission

The relation used in the statistical model for the fission cross section calculation is

$$\sigma_{a,f}(E) = \sum_{J\pi} \sigma_a(EJ\pi) P_f(EJ\pi), \quad (2.190)$$

where  $\sigma_a(EJ\pi)$  is the population of the fissioning nucleus in the state  $EJ\pi$  and  $P_f(EJ\pi)$  represents the fission probability. Depending on the type of particle which induces fission, EMPIRE-3.1 offers two formalisms (selected by the directive input FISSHI) to calculate fission probability. The default value (FISSHI = 0) selects the optical model for fission (or its simplified version) to calculate fission induced by light particles or photons, FISSHI = 1 selects the Sierk model adequate for heavy ion induced fission, and FISSHI = 2 turns off any fission calculation.

The default option (FISSHI = 0) describes transmission through single-, double- and triple-humped fission barriers starting from sub-barrier excitation energies up to about 200 MeV. For multi-humped barrier, an expression for the fission probability is derived in the frame of the optical model for fission. In case of double-humped barrier, the expression is generalized for the case of multi-modal fission. For light actinides, a triple-humped fission barrier with a shallow tertiary well, which accommodates undamped vibrational states can be employed. This fission model can provide good description of experimental data (including gross vibrational resonant structure at sub-barrier energies), reasonably good predictive power and improved methodology for determination of fission barrier parameters.

### 2.13.1 Fission barriers

The optical model for fission considers the possible transmission mechanisms using a complex potential ( $V_f = V + iW$ ) to describe the uni-dimensional multi-humped fission barrier (Figures 2.3, 2.4).

The real part of the barriers, associated with the discrete transition states, are parameterized as a function of the quadrupole deformation using smoothly joined parabolas

$$V_i(\beta) = E_{fi} + (-1)^i \frac{1}{2} \mu \hbar^2 \omega_i^2 (\beta - \beta_i)^2, \quad (2.191)$$

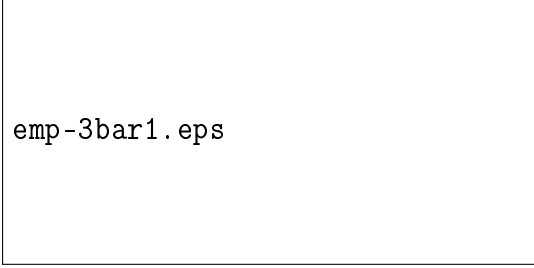


Figure 2.4: Triple-humped fission barriers

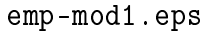


Figure 2.5: Double-humped fission barriers used in multi-modal calculations

where  $i = 1$  for a single barrier, runs from 1 to 3 for a two-humped barrier, and from 1 to 5 for a three-humped one. The energies  $E_{fi}$  represent maxima of  $V_i$  in odd regions (humps) and minima in even regions (wells),  $\beta_i$  are the corresponding abscissae, the harmonic oscillator frequencies  $\omega_i$  define the curvature of each parabola and  $\mu$  is the inertial mass parameter, assumed independent of  $\beta$  and approximated by the semi-empirical expression  $\mu \approx 0.054A^{5/3}MeV^{-1}$ , where  $A$  is the mass number. The discrete transition states are rotational levels built on vibrational or non-collective band-heads, characterized by a given set of quantum numbers (angular momentum  $J$ , parity  $\pi$  and angular momentum projection on the nuclear symmetry axis  $K$ ) with excitation energies

$$E_i(J, K, \pi) = E_{fi} + \epsilon_i(K, \pi) + \frac{\hbar^2}{2I_i}[J(J+1) - K(K+1)], \quad (2.192)$$

where  $\epsilon_i(K, \pi)$  are the excitation energies of the band-heads, and  $\hbar^2/2I$  are inertial parameters (the Coriolis term for  $K = 1/2$  is neglected). To each transition state associated is a parabolic barrier with the height  $E_i(J, K, \pi)$  and the curvature  $\hbar\omega_i$ . The transition state spectrum consists of a discrete part below a certain energy  $E_{ci}$  and a continuum described by the level density functions  $\rho_i(EJ\pi)$ .

Assuming Brosa's channel concept and the hypothesis that the bifurcation points appear in the deformation region corresponding to the second minimum [72], different discrete and continuous spectra for the transition states at the outer saddle are considered for each mode. This is illustrated in Figure 2.5 for two modes known as super-long symmetric (SL) and standard asymmetric (S1).

For the case of a triple-humped barrier, it is reasonable to assume that with increasing excitation energy the shell effects, which cause splitting of the outer hump, decrease and the outer humps lump into a single one. Therefore, in the present formalism the triple-humped barriers are only associated with the discrete transition states. Accordingly, the continuum contribution to the fission coefficient is calculated considering a double-humped barrier with the second peak representing a single barrier equivalent to the two outer humps (Figure 2.4). The parameters of the equivalent barrier are determined by imposing equal transmission.

The negative imaginary potential  $iW$  is introduced in the deformation range corresponding to the second well for both double- and triple-humped barriers to simulate damping of the class II vibrational states, hence, the absorption of the incoming flux in this well [73, 74, 75]. For the triple-humped barrier the tertiary well is supposed to be shallow enough to neglect damping of class III vibrational states. The strength  $W$  depends quadratically on deformation and increases with the excitation energy

$$W(\beta) = -\alpha[E - V(\beta)] \quad (2.193)$$

The input parameter  $\alpha$ , which controls the strength of the imaginary part of the fission potential, should be chosen to fit the width of the resonances in sub-barrier fission cross section and to be consistent with physical values for the transmission coefficients at higher energies.

In the following sections we shall denote humps with capital letters A,B,C ( $i=1,3,5$ ) and wells with Roman figures II ( $i=2$ ) and III ( $i=4$ ).

### 2.13.2 Transmission mechanisms

Figure 2.6 shows the transmission mechanisms through a double-humped fission barrier for excitation energies below both humps and above at least one of them. The incoming flux can be transmitted directly through the barrier or can be absorbed in the isomeric well. The fraction absorbed in the isomeric well can: (i) be re-emitted in the fission channel (indirect prompt fission), (ii) return back to a class I state or (iii) undergo  $\gamma$ -transition to the isomeric state. The isomeric state, in turn, can decay by delayed (isomeric) fission or by shape transition to class I states.

Similar transmission mechanisms are encountered in the case of the triple-humped barrier (Figure 2.7), the main difference consisting in replacing the transmission through a single outer hump by the direct transmission through the second and third hump. The transmission coefficients through the humps ( $T_A, T_B, T_C$ ), for direct transmission ( $T_{dir}, T_{BC}$ ) and absorption in the isomeric well ( $T_{abs}$ ) are calculated in WKB approximation for complex potentials [73, 74, 76]. In the simplest version of the model (FISOPT=0), the transmission coefficients through the humps ( $T_A, T_B, T_C$ ) of a barrier corresponding to a particular discrete transition state, are calculated with Hill-Wheeler formula

$$T_{ij}(EKJ\pi) = \frac{1}{1 + \exp\{-(2\pi/\hbar\omega_i)[E - E_i]\}} \quad i = A, B, C. \quad (2.194)$$

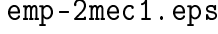


Figure 2.6: Transmission mechanisms through a double-humped fission barrier

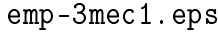


Figure 2.7: Transmission mechanisms through a triple-humped fission barrier

The total transmission coefficient through a hump is sum of two contributions corresponding to the discrete and continuous part of the transition state spectrum

$$T_i(EJ\pi) = \sum_{K \leq J} T_i(EKJ\pi) + \int_{E_{ci}}^{\infty} \frac{\rho_i(\varepsilon J\pi) d\varepsilon}{1 + \exp \left[ -\frac{2\pi}{\hbar\omega_i} (E - V_i - \varepsilon) \right]} = A, B \quad (2.195)$$

Increasing the excitation energy, the strength of the imaginary potential increases and the entire flux transmitted through the inner hump is absorbed in the second (isomeric) well ( $T_{abs} \rightarrow T_A$ ), and the direct transmission through the entire barrier disappears ( $T_{dir} \rightarrow 0$ ). Therefore, the direct fission occurs only for sub-barrier excitation energies and occurs only through discrete channels

$$T_{dir}(EJ\pi) = \sum_{K \leq J} T_{dir}(EKJ\pi), \quad (2.196)$$

while the absorption in the isomeric well occurs through all fission channels. In full  $K$ -mixing approximation all the discrete channels with the same  $J\pi$  contribute irrespective of their  $K$  value to the total absorption coefficient. The continuum fission channels contribute at higher energies, where the class II states are completely damped and the entire flux transmitted through the inner barrier is absorbed in the isomeric well

$$T_{abs}(EJ\pi) = \sum_{K \leq J} T_{abs}(EKJ\pi) + \int_{E_{cA}}^{\infty} \frac{\rho_A(\varepsilon J\pi) d\varepsilon}{1 + \exp \left[ -\frac{2\pi}{\hbar\omega_A} (E - V_A - \varepsilon) \right]} \quad (2.197)$$

In the case of the triple-humped barrier, the total direct transmission through the outer humps is the sum of the transmissions through discrete barriers and the continuum built above the equivalent barrier

$$T_{BC}(EJ\pi) = \sum_{K \leq J} T_{BC}(EKJ\pi) + \int_{E_{ceq}}^{\infty} \frac{\rho_{eq}(\varepsilon J\pi) d\varepsilon}{1 + \exp \left[ -\frac{2\pi}{\hbar\omega_{eq}} (E - V_{eq} - \varepsilon) \right]} \quad (2.198)$$

### 2.13.3 Decay probabilities

#### Double-humped barrier, multi-modal fission

The most general expressions used in Empire for the fission probability calculation were derived extending the procedure of Back [73] for multi-modal fission. For a particular mode ( $m$ ), the decay probabilities for direct ( $P_{dir}$ ), indirect ( $P_{ind}$ ), and delayed ( $P_{iso}$ ) fission read (the dependence on  $EJ\pi$  is implicit)

$$P_{dir,m} = \frac{T_{dir,m}}{\sum_m T_{dir,m} + \sum_d T_d} \left( 1 - \frac{1}{a} \right) \quad (2.199)$$

$$P_{ind,m} = \frac{T_{B,m}}{\sum_m T_{B,m} + T_{\gamma II}} \cdot \frac{1}{a} \quad (2.200)$$

$$P_{iso,m} = \frac{R_{f,m}^{iso} T_{\gamma II}}{\sum_m T_{B,m} + T_{\gamma II}} \cdot \frac{1}{a} \quad (2.201)$$

In order to preserve unitarity the decay probability for competing channels ( $P_d$ ) takes the form

$$P_d = \frac{T_d}{\sum_m T_{dir,m} + \sum_d T_d} \left( 1 - \frac{1}{a} \right) \quad (2.202)$$

where:

$$a = \left[ 1 + b^2 + 2b \coth \left( \frac{T_A + \sum_m T_{B,m} + T_{\gamma II}}{2} \right) \right]^{1/2}$$

$$b = \frac{(\sum_m T_{dir,m} + \sum_d T_d)(T_A + \sum_m T_{B,m})}{T_{abs}(\sum_m T_{B,m} + T_{\gamma II})}$$

$T_{\gamma II}$  represents  $\gamma$ -decay transmission coefficient in the isomeric well and  $R_f^{iso}$  is the branching ratio for fission of the isomeric state. In the present version of the code,  $T_{\gamma II}$  and consequently the isomeric fission are considered negligible and are not calculated. The fission probability for mode  $m$  reads

$$P_{f,m} = P_{dir,m} + P_{ind,m} + P_{iso,m} \quad (2.203)$$

and the total fission probability is obtained by summing over all modes:

$$P_f = \sum_m P_{f,m} \quad (2.204)$$

At over-barrier energies the class II vibrational states become completely damped, the entire flux penetrating the inner barrier is absorbed in the isomeric well ( $T_{abs} \rightarrow T_A$ ), the direct transmission disappears ( $T_{dir} \rightarrow 0$ ), the population probability of the isomeric state becomes negligible ( $T_{\gamma_{II}} \rightarrow 0$ ) and the decay widths of the class II state exceed the distance between them ( $\coth[(T_A + \sum_m T_{B,m} + T_{\gamma_{II}})/2] \rightarrow 1$ ). In these conditions, the fission probability becomes

$$P_{f,m} = \frac{T_{B,m}}{\sum_m T_{B,m}} \cdot \frac{1}{1+b} = W_m \cdot \frac{T_f}{T_f + \sum_d T_d} \quad (2.205)$$

where  $W_m$  is the mode weight ( $W_m = T_{B,m} / \sum_m T_{B,m}$ ) and  $T_f$  is the total fission coefficient

$$T_f = \frac{T_A \sum_m T_{B,m}}{T_A + \sum_m T_{B,m}} \quad (2.206)$$

The decay probability through a competitive channel  $d$  recovers the well-known form

$$P_d = \frac{T_d}{T_f + \sum_d T_d} \quad (2.207)$$

### Triple-humped barrier, single-mode fission

In the case of a triple-humped fission barrier with a shallow tertiary well, accommodating undamped vibrational states, the fission probability is given by the previous formulae (particularized for single-mode fission) where the transmission coefficient through the outer hump  $T_B$  is replaced by the direct transmission coefficients through the outer humps  $T_{BC}$ .

### Single-humped fission barrier

In this simple case, the fission coefficient is given by the transmission coefficient through a parabolic barrier ( $T_f = T_A$ ).

#### 2.13.4 Input/output

The fission subroutine FISFIS can be invoked by Empire in two different ways using the input directive FISOPT.

- FISOPT = 0 (default option) corresponds to the simplified version of the model and requires the minimum fission input. It's the only possible option for the single-humped barrier and is recommended for multi-humped barrier at over-barrier excitation energies for all fissioning nuclei or for odd-odd fissioning nuclei for the entire energy range. It considers the humps of the fission barrier to be completely decoupled and approximated by independent parabolas (Figure 2.8), therefore no information about the wells and the imaginary potential are needed. The fission probability is given by

$$P_f = \frac{T_f}{T_f + \sum_d T_d} \quad (2.208)$$

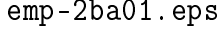


Figure 2.8: Fission barrier parametrization and transmission mechanisms corresponding to  $\text{FISOPT} = 0$  option

with

$T_f = T_A$	single-humped barrier
$T_f = T_A T_B / (T_A + T_B)$	double-humped barrier
$T_f = T_A T_B T_C / (T_A + T_B T_C)$	triple-humped barrier

- $\text{FISOPT} = 1$  selects the optical model for fission which may be applied for the multi-humped barriers at any excitation energy, but requires complete information about the complex fission potential. The parameter  $\alpha$  in eq.(2.193) can be defined by a parabolic energy dependence whose coefficients can be chosen by the user. This option is recommended for multi-humped barriers at excitation energies lower or around their heights, especially for even-even fissioning nuclei, but can not be used for single barriers. The fission coefficients and the decay probabilities for fission and for the competitive channels are calculated using the formulae presented in the previous section.

The fission input parameters can be automatically retrieved from the built-in systematics and/or libraries, or can be provided by the user. For example, the parameters of the fundamental fission barrier are chosen by EMPIRE according to the value of the input directive FISBAR:

- $\text{FISBAR} = 0$  (default value) The heights of the fission barrier calculated within the Extended Thomas-Fermi plus Strutinsky Integral (ETFSI) method are retrieved from RIPL-2 [47]. This compilation includes fission barriers (and level densities at saddles) for 2301 nuclei with  $78 < Z < 120$ . For the single-humped barriers the code considers for the width the default value  $\hbar\omega_A = 1.00$  MeV. For the double-humped barriers, the following default values (in MeV) for the widths of the humps are provided by the code:

$\hbar\omega_A = 1.04$	$\hbar\omega_B = 0.60$	even-even nuclei
$\hbar\omega_A = 0.80$	$\hbar\omega_B = 0.52$	odd-A nuclei
$\hbar\omega_A = 0.65$	$\hbar\omega_B = 0.45$	odd-odd nuclei



Because no information about the wells are provided, this option can not be used in conjunction with  $\text{FISOPT} = 1$ .

- $\text{FISBAR} = 1$  The heights and widths are retrieved from an internal library where the user can store the desired barrier parameters. It's the only option which can be used in conjunction with  $\text{FISOPT} = 1$ , and the only one allowing for a triple-humped fission barrier. The internal library (*empire/data/fisbar.dat*) contains the following quantities for each included nuclide:  $Z$  (atomic number),  $A$  (mass number),  $\text{NRPARAB}$  (number of parabolas describing the fission barrier),  $\text{NRWELL}$  (number of wells),  $V_i, \hbar\omega_i$  (heights and widths of humps,  $i$  runs from 1 to  $\text{NRPARAB}-\text{NRWELL}$ ),  $V_j, \hbar\omega_j$  (depth and widths of wells,  $j$  runs from 1 to  $\text{NRWELL}$ ).
- $\text{FISBAR} = 2$  is similar to  $\text{FISBAR} = 0$ , excepting that the code retrieves from RIPL-2 'experimental' heights of the fission barriers rather than theoretical ETFSI results.

Above the fundamental fission barrier whose parameters are selected by  $\text{FISBAR}$ , there are the barriers associated with the transition states. There are two options concerning the transition state spectrum controlled by  $\text{FISDIS}$ :

- $\text{FISDIS} = 0$  (default value) The entire transition state spectrum is considered continuous and described by the level densities at saddles.
- $\text{FISDIS} = 1$  The transition state spectrum has a discrete part. A maximum number of NFDIS rotational band-heads states can be considered. Each band-head is characterized by excitation energy (with respect to the fundamental barrier), spin projection on the symmetry axis and parity. The widths of the parabolas which define barrier associated to a certain transition state are also input parameters. By default they are equal to the widths of the fundamental barrier. If  $\text{FISOPT} = 1$  then the number of discrete transition states and their spin projection-parity sequence should be the same for every hump and well. When creating the fission input, EMPIRE introduces four discrete states only to help the user to input his own values. The maximum number of discrete band-heads is 30. On each band-head EMPIRE builds rotational levels according to 2.192. The default values for the inertial parameters agree with RIPL-2 recommendations (the perpendicular moments of inertia are equal to  $100\hbar^2/\text{MeV}$  for the inner barrier and  $200\hbar^2/\text{MeV}$  for the outer barrier).

There are two available options for the level density at saddles

- $\text{FISDEN}=0$  Microscopic Hartree-Fock-BCS calculations of level densities at saddles retrieved from RIPL-2.
- $\text{FISDEN}=1$  (default value) The level densities at saddles are calculated using the same Empire-specific dynamical approach as used for normal states (BCS + modified Fermi Gas) except for the following differences:

- equilibrium deformation is replaced by the saddle deformation,
- pairing at saddles is parameterized following RIPL-2 as  $\Delta_f = 14A^{1/2}$ ,
- shell corrections at saddles are calculated as recommended in RIPL-2:

$$\delta W_A = \begin{cases} 2.6 & Z \leq 97 \\ 2.6 - 0.1(Z - 97) & Z > 97 \end{cases} \quad (2.209)$$

$$\delta W_B = \begin{cases} 0.6 + 0.1(Z - 97) + 0.04(N - 143) & Z < 97 \\ 0.6 + 0.04(N - 143) & Z \geq 97 \end{cases} \quad (2.210)$$

- collective enhancements corresponding to the nuclear shape asymmetry at each saddle are calculated following the prescription in RIPL-2. The following shape asymmetries can be considered:  
 bff=1 axial, mirror symmetry  
 bff=2 axial asymmetry, mirror symmetry  
 bff=3 axial symmetry, mirror asymmetry  
 bff=4 axial, mirror asymmetry

For both options (FISDEN = 0, 1) energy dependence of level densities can be adjusted by multiplying level densities with a quadratic function  $a_0 + a_1E + a_2E^2$  with coefficients chosen by the user.

Depending on the value of the input quantity FISMOD, Empire performs single- or multi-modal fission calculations:

- FISMOD = 0 (default value) Single-mode fission is considered.
- FISMOD = 1, 2 A number of FISMOD+1 fission modes are considered by introducing for each mode a complete set of outer barrier parameters, including discrete and continuous transition state spectra. The maximum number of modes is 3, but it can be increased by modifying NFISMOD in *empire/source/global.h*. By default, except the symmetry, the parameters of all outer barriers are identical, leaving to the user the responsibility of finding proper parameters. In the present version of the code this option is not valid for the triple-humped fission barrier.

Initial EMPIRE run creates a fission input file *-inp.fis*, which user can modify if parameter adjustment is required. The parameters adjustable by the user are:

- -  $V_i$  - maxima (and minima) of the real part of the fission potential
- -  $\beta_i$  - corresponding deformations
- -  $(\hbar^2/2I)_i$  - inertial parameters
- -  $w_j$  - the polynomial coefficients defining the parameter which controls the strength of the imaginary potential (if FISOPT = 1)

- - the number of discrete states (rotational band-heads) for each hump and well
- -  $\epsilon_i$ ,  $K$  - the excitation energy and spin projection of the transition states
- -  $\hbar\omega_i$  - the associated barrier's width
- -  $V_{eq}$ ,  $\hbar\omega_{eq}$  the height and width of the equivalent barrier (if triple-humped barrier is considered)
- -  $bff_i$ ,  $\delta W_i$ ,  $\Delta_{fi}$ ,  $\gamma_i$ ,  $\tilde{a}_{fi}/\tilde{a}$  - asymmetry type of nuclear shape, shell correction, correlation factor (pairing), damping parameter in Ignatyuk's formula, branching ratio of asymptotic values of  $a$  parameter for saddle and normal states (if FISDEN = 1)
- -  $a_j$  the polynomial coefficients adjusting level densities at saddles.

The fission cross section for each fissioning nucleus and the total fission cross section are printed in EMPIRE output files. More detailed fission results corresponding to the last incident energy of the run are stored in the file FISSION.OUT. Beside input parameters, it contains fission half-life, level density related quantities at critical energy (if FISDEN = 1), fission coefficients for each spin and parity, fission cross sections and weights for all individual modes, and total fission cross section. Such a set of data is provided for each fissioning nucleus.

## 2.14 Binding energies

Binding energies are internally calculated using masses recommended by Audi *et al.* [77] whenever available. Otherwise the theoretical predictions of Moller and Nix [54] are used.

## 2.15 Model compatibility

Possible inclusions of different preequilibrium models in a single calculation run rises a problem of double-counting. The current version of EMPIRE has 5 modules for preequilibrium decay: MSD, MSC, DEGAS and HMS and PCROSS. While MSD and MSC describe different reaction mechanisms and are complementary, neither of them is compatible with DEGAS, HMS or PCROSS. Therefore, neither of the latter three can be used together with MSD or MSC in the same exit channel. Also DEGAS, HMS and PCROSS mutually exclude each other. However, these models can be combined if used in different exit channels, e.g., neutron inelastic scattering may be calculated using MSD&MSC while the emission of protons can be treated within the exciton model using PCROSS. We also note that summing  $\gamma$ -emission spectra from more than one of the three possible mechanisms (MSC (GST=1 option), DEGAS, and PCROSS) would be obvious multiple-counting and must be avoided.

An additional complication is introduced by the possibility of using ECIS06, which calculates Coupled-Channel contributions to the collective discrete levels. In general, these

contributions are so strong that adding those provided by the exciton model leave the results practically unchanged. Thus, ECIS06 can be considered compatible HMS since the latter does not include collective excitations. By the same token ECIS06 is not compatible with MSD as both include collectivity of discrete levels. However, ECIS06 and MSD can be combined providing that only the continuum contribution from the MSD is retained.

To avoid double-counting when combining different models EMPIRE applies the following priorities:

**ECIS06** provides inelastic scattering to collective levels independently of the settings for the remaining models.

**MSD** provides inelastic continuum independently of other settings. Inelastic to the discrete levels is suppressed if ECIS06 is active. Note the provision for the second-chance preequilibrium emission after MSD.

**MSC** results are taken for the inelastic to the continuum. Charge-exchange to the continuum is accepted if not suppressed by use of DEGAS, HMS or PCROSS.

**DEGAS** provides inelastic and charge-exchange to the continuum if MSD and MSC are not active. Otherwise, only the charge-exchange contribution is used. Gamma emission from DEGAS is used if not provided by the MSC.

**HMS** provides inelastic and charge-exchange to the continuum and to discrete levels if MSD and MSC are not active. Otherwise only the charge-exchange contribution is used. Suppresses DEGAS results for particle emission if such was calculated. HMS does not provide  $\gamma$ -rays, thus DEGAS or MSC results are adopted.

**PCROSS** provides inelastic and charge-exchange to the continuum if these are not provided by any of the above listed models. Provides  $\gamma$ -emission if not suppressed by  $\gamma$ -emission from MSC or DEGAS. Provides preequilibrium emission of clusters independently of settings for other models.

This scheme allows the user to activate any combination of reaction mechanisms while the code ensures the internal consistency of calculations. Overlapping contributions from various models are summed up and the Compound Nucleus contribution is added in all cases. A concise summary explaining use of the models is printed as a table at the beginning of the lengthy output *\*.lst*. An example is reproduced below:

#### Use of preequilibrium models

		-----					
Exit	channel	ECIS	MSD	MSC	DEGAS	HMS	PCROSS
neut.	disc.	0	1	0	0	0	0
neut.	cont.	0	1	1	0	0	0
prot.	disc.	0	0	0	1	0	0
prot.	cont.	0	0	0	1	0	0

gammas	0	0	0	1	0	0
alpha cont.	0	0	0	0	0	1

1 indicates that the contribution of the model is included, and 0 means that it is not calculated or ignored. In the above example, MSD, MSC, DEGAS and PCROSS were invoked, and priority rules caused DEGAS neutron contribution to be suppressed as well as all PCROSS contributions except emission of clusters.

Selecting DIRECT =1 (or 2 or 3), MSD=1, MSC=1, PCROSS=1 is supposed to give the best results at low incident energies (say up to 30 MeV). At higher incident energies the preference should be given to the HMS model, which accounts for the multiple preequilibrium emission. When selecting appropriate models the user should take into account that not all of them provide the same set of observables. In particular, DEGAS is missing angular distributions, which are calculated by the HMS. On the other hand, preequilibrium  $\gamma$ -emission can be obtained from DEGAS, PCROSS or MSC but not from HMS. Finally, we note that DEGAS is the only preequilibrium model with proper angular momentum coupling.

## 2.16 Spectra of recoils

Energy spectra of recoils are calculated taking into account correlations between the excitation energy of the nucleus and the emission energy of the particle. In order to do so, the recoil energies are followed throughout the deexcitation cascade. A recoil spectrum is ascribed to each excitation energy bin for each nucleus involved in the decay chain. Emission of a particle depletes the spectrum bin of the parent and accumulate in the recoil spectrum bin of the daughter nucleus.  $\gamma$  emissions are assumed to produce no recoil but shift respective portions of the recoil spectrum to the the lower excitation energy bin in the same nucleus. Transitions to discrete levels are summed directly to the ground state recoil spectrum, since particle emission from discrete levels is not considered and  $\gamma$ -emission does not change the recoil spectrum. At the end of the decay cascade all the recoil spectra for energy bins embedded in the continuum are null, and the final result is given by the ground state recoil spectra.

The following assumptions are made in the course of these calculations:

- Particle emission from a nucleus at a certain excitation energy is independent of the actual recoil energy of the nucleus. The center of mass motion of a nucleus (recoil) is assumed to have no effect on the emission of particles, as the latter involves internal degrees of freedom. Statistically, any emission depletes the recoil spectrum of the parent uniformly, so that for each emission the whole recoil spectrum corresponding to the parent energy bin is reduced by a constant factor.
- Compound Nucleus emissions are isotropic and uncorrelated between each other. However, forward peaked angular distributions of nucleons emitted through the preequilibrium or direct mechanisms and the center of mass motion of the first Compound

Nucleus are retained and taken into account in constructing recoil spectra. We note that recoils are given in the laboratory system.

Ejectile emission energy is denoted by  $\varepsilon$ , excitation energy by  $E$ , nucleus recoil energy by  $e$ , and  $r$  and  $p$  subscripts are used to mark residuals and parent nuclei respectively. The  $d\sigma(e, E)/de$  stands for the recoil spectrum at the excitation energy  $E$  summed over spin and parity. Consider a single emission of an ejectile with energy  $\varepsilon$ ; the contribution of this emission to the recoil spectrum of the residual can be quantified. We apply momentum conservation in binary reactions to calculate the “recoil kick” energy ( $\Delta e$ ) for this single emission event

$$\Delta e = \frac{m_{ejc}}{m_r} \varepsilon, \quad (2.211)$$

in which  $m_{ejc}$  and  $m_r$  are the ejectile and recoil mass respectively. Similarly, the contribution to the residue recoil spectrum is obtained from the emission spectrum by applying the reverse factor

$$\frac{d\sigma(\Delta e, E_r)}{d(\Delta e)} = \frac{m_r}{m_{ejc}} \frac{d\sigma(\varepsilon, E_r)}{d\varepsilon}. \quad (2.212)$$

The recoil energy of the residue is obtained by adding the ejectile momentum and the momentum of the parent nucleus vectorially. We can express the residue recoil energy  $e_r$  through the “recoil kick” (Eq. 2.211) and the recoil energy of the parent  $e_p$  before emission

$$e_r(e_p, \theta) = \Delta e + e_p + 2\sqrt{\Delta e \cdot e_p} \cos(\theta), \quad (2.213)$$

where  $\theta$  is the angle between the momentum of the parent and the “recoil kick”. Thus the contribution to the recoil spectrum in the residue can be defined as

$$\frac{d\sigma(e_r, E_r)}{de_r} = \int_0^\infty \int_0^\pi \delta(e_r - e_r(e_p, \theta)) \left[ \frac{d\sigma(e_p, E_p)}{de_p} \right]_n \frac{d\sigma(\Delta e, E_r, \theta)}{d(\Delta e)} \sin(\theta) d\theta de_p. \quad (2.214)$$

where the  $\delta$  function ensures selection of the correct recoil energy and the square brackets  $[\ ]_n$  around the parent recoil spectrum indicate that the integral was normalized to unity:

$$\int_0^\infty \frac{d\sigma(e_p, E_p)}{de_p} de_p = 1. \quad (2.215)$$

Integration in Eq. 2.214 is limited by the range of possible recoil energies. We note that Eq. 2.214 distributes the recoil cross section related to a single emission event over various recoil energies. The reason for this spread is two-fold: (i) vectorial coupling of momenta and (ii) recoil spectrum of the parent nucleus. Even in the case of a delta-function parent spectrum (the first CN), the residual spectrum covers the range from  $\Delta e + e_p - 2\sqrt{\Delta e \cdot e_p}$  to  $\Delta e + e_p + 2\sqrt{\Delta e \cdot e_p}$ , as results from Eq. 2.213. The  $d\sigma(\Delta e, E_r, \theta)/d(\Delta e)$  is assumed to be isotropic ( $\theta$  independent) except for the MSD and direct inelastic contributions, for which angular distributions are preserved in Eq. 2.214. The recoil spectrum of the Compound Nucleus is single valued and differs from zero only at the energy of the Center of Mass motion. This is also the first-parent spectrum to which Eq. 2.214 is sequentially

applied. We note that Eq. 2.214 refers to the emissions of a single type ejectile with a given emission energy. Eq. 2.214 is applied to all possible emissions including summation over different ejectile types and parent/residue excitation energies.

## 2.17 Exclusive spectra

EMPIRE may rearrange emission spectra to conform to the ENDF representation, which require that for a given reaction all pertinent subsequent emissions are summed up to produce effective spectra (for each ejectile) associated with the reaction. For example, neutron spectrum from the (n,2n) reaction should contain a sequence of two neutron emissions, which is followed by the  $\gamma$ -cascade only. Thus the contribution of the first neutron should be subtracted from the (n,n) and added to the (n,2n) spectrum.

A new algorithm for calculation of the exclusive spectra has been developed and implemented in EMPIRE-3.1. It is based on the concept of the 'population spectra', also used for the recoils, and avoids approximations inherent in the previous method. The new algorithm is more precise, never produces negative cross sections, and can treat an arbitrary number of emissions.

*To be completed*

## 3 Code

### 3.1 Directory structure

The full version of EMPIRE-3.1 has the following directory structure:

- **empire**
  - **source** - source of the EMPIRE code divided into modules and Makefile
  - **data** - library of input parameters (files: *ldp.dat*, *nparac.dat*, *resonances.endf*, *fisbar.dat*)
  - **RIPL-2** - RIPL-2 library (the same structure as original RIPL-2 CD-ROM[47])
    - **levels** - discrete levels for nuclei with Z from 0 up to 109
    - **densities**  $\Rightarrow$  **total**  $\Rightarrow$  **level-densities-hfbcs** - tables of level densities calculated within Hartree-Fock-BCS approach
    - **optical**  $\Rightarrow$  **om-data**  $\Rightarrow$  data relevant to optical model calculations (files: *om-parameter-u.dat*, *om-index.txt*, *om-references.txt*, *om-deformations.dat*)
    - **gamma** - data relevant to  $\gamma$ -strength functions (files: *gdr-parameters-exp.dat*, *gdr-parameters-theor.dat*, *deflib.dat*)
    - **fission** - data relevant to fission (files: *fis-barrier-etfsi.dat*, *fis-barrier-exp.dat*)
    - **masses** - nuclear masses, g.s. deformations and abundances (files: *abundance.dat*, *gs-deformations-exp.dat*, *mass-frdm95.dat*)
  - **work** - input and output files
  - **scripts** - bash and Tcl/Tk scripts
  - **x4cd** - complex package containing full EXFOR loaded into MySQL database, MySQL server, and retrieval system including stand-alone GUI
  - **EXFOR** - EXFOR library, index file (X4-INDEX.TXT) and retrieval tools (obsolete in 3.1)
    - **subent/xx/xxxx** - sub-directories with EXFOR sub-entries (optional, obsolete in 3.1)
  - **util** - utility codes
    - **empend** - converts EMPIRE results into the ENDF format



- **c4sort** - sorts experimental data in the computational format file
- **fixup** - reconstructs redundant MT sections
- **legend** - calculates linearly interpolable angular distributions
- **lsttab** - tabulates ENDF and EXFOR data in PLOTTAB format
- **sixtab** - converts ENDF File 6 into Law 7 representation
- **x4toc4** - converts retrieved EXFOR data into the computational format
- **plotc4** - plots the comparison between calculated and experimental data
- **c4zvd** - ZVView plotting package
- **checkr** - ENDF-6 format checking
- **endres** - merges resonance parameters from file \*-res.endf into the new ENDF-6 formatted file containing EMPIRE results to produce full evaluation
- **fizcon** - more ENDF-6 format checking
- **psyche** - ENDF-6 file physics checking
- **linear** - makes all cross section in File 3 linearly interpolable
- **pltlst** - prepares a list of experimental data for the selected nuclide that can be compared to the data reconstructed from an ENDF file (the list file has identical format as the report file from PLOT4)
- **recent** - reconstructs cross sections from the resonance parameters
- **sigma1** - Doppler broadens cross sections in the resonance range
- **stanef** - standardizes ENDF-6 formatted file
- **zvvddx** - plots angular distributions, energy spectra and double-differential cross sections using package
- **auxiliary** - icons and pictures
- **doc** - documentation (includes this manual)

The *empire* directory can be placed anywhere within the file system. For the correct functioning of the system scripts the internal structure of the *empire* directory must be preserved. The user may choose to create additional *work* directories, e.g., for each separate project or reaction studied. In such a case the additional directories may have any name but must be on the same level as the *work* sub-directory (i.e., they must be sub-directories of *empire*).

## 3.2 Installation

The distribution of EMPIRE consists of five *.tgz* files and the installation script *setup-emp*. The *.tgz* files contain

- *empire-2-xx.tgz* - (*xx* standing for the current version of the code) contains EMPIRE source, parameter library, *work* sub-directory, PREPRO2000 and ENDVER packages, and format checking codes (mandatory).
- *x4cd.tgz* - EXFOR library of experimental data (... appropriate text is needed) format.
- *HFBCS-lev-dens.tgz* - contains files with tabulated level densities calculated in the frame of the HF-BCS approach. Size of this file after decompression is about 145 Mb. Users who do not intend to use this option for level densities may choose not to install them.
- *fis-lev-den.tgz* - contains files with tabulated level densities at inner and outer fission barrier calculated in the frame of the HF-BCS approach. Users who do not intend to use this option for level densities may choose not to install them.
- *X4-2-17.tgz* - obsolete Fit is (... appropriate text is needed)

Out of these files only *empire-2-xx.tgz* is required to run calculations, *x4cd.tgz*, *HFBCS-lev-dens.tgz*, and *fis-lev-den.tgz* are optional and *X4-2-17.tgz* is redundant if *x4cd.tgz* can be used.

The easiest recommended way of installing EMPIRE is using the *setup-emp* script, which guides the user through the installation procedure. The script can be used to install sources downloaded from the Web sites as well as those provided on the CD-ROM. The script can be placed anywhere in the file system and can be invoked by typing:

*setup-emp*

at the shell prompt. The three *.tgz* files are assumed to be located in the same directory. The installation script allows the target directory to be selected and files to be installed. It also compiles all of the package using the default g77 FORTRAN compiler or any other compiler specified by the user (the compiler itself must already be installed on the system). Considering the size of the *X4-2-xx* and *HFBCS-lev-dens*, the install script offers a possibility of using plain ASCII versions of both libraries as stored on the CD-ROM. The *setup-emp* script tries to set up links to the CD-ROM directories when the user decides to skip installation of any of the two libraries. This option saves considerable amount of disk space at the price of the increased time needed for reading the data. Also, the CD-ROM with EMPIRE-2-xx distribution has to be mounted during calculations blocking a CD-ROM drive.

EMPIRE can also be installed manually. To this end the *empire-2-xx.tgz* file has to be uncompressed and untarred with the following commands (on UNIX systems):

```
gunzip empire-2-xx.tgz
tar xvf empire-2-xx.tar
```

or with a single command

```
tar xvzf empire-2-xx.tgz
```

on the systems which allow such an action (e.g., Linux). The same should be done with the *X4-2-xx.tgz* and *HFBCS-lev-dens.tgz* files if the user chooses to install them. The three *.tgz* files must be located in the same directory. The decompressed files will be placed according to the directory structure described in the previous section, with *empire* directory on the level of the *.tgz* files. The whole package can be compiled by invoking *Compile* script in the *empire* directory. This will execute the *make* command in the following sub-directories:

- *empire/source/*
- *empire/util/(all sub-directories)*

Users have to ensure that FORTRAN compiler is called properly. To this end, one should edit *Makefile* files in the above mentioned directories and fix calls to FORTRAN compiler. By default *g77* of Linux is used. Several other typical options are included in the *Makefile* files. These are commented with the *#* character in the first column. Users should remove this character on the line corresponding to the desired compiler and comment a line with *g77* instead. Systems that do not allow for the *make* utility will have to compile all *.f* and *.c* files manually using something like

```
fort *.f *.c -o empire
```

in the *empire/source/* directory. The utility executables should be named after their respective directories, i.e., *plotc4*, *x4toc4*, etc.. In most cases this is achieved with the *-o* option as in the example above. This syntax may differ for various compilers. Note that *empire/source/* sub-directory contains a file *pipe.c*, which is written in C-language. Modern FORTRAN compilers are usually integrated with the C-compiler and should compile C code properly. If this is not the case a native C-compiler has to be used for *pipe.c* and the resulting object file has to be linked manually with the objects of FORTRAN modules.

For full functionality EMPIRE requires the following software:

- FORTRAN 77 compiler or higher
- C-compiler
- gnuplot

- ghostscript (including ghostview and ps2ps)
- awk (gawk)
- bash shell
- Tcl/Tk, itcl

However, only the generic FORTRAN 77 and C compilers are needed to perform basic calculations. The C-compiler can be eliminated by replacing calls to the *PIPE* subroutine by *SYSTEM* available as subroutine or function in most FORTRAN 90/95 compilers. We stress that all the remaining components are freely available on the Internet for practically any operating system (including UNIX and MS Windows).

### 3.3 Array dimensions

All the dimensions are set in the *dimension.h* file and can be changed if necessary. Those parameters which may require modifications in everyday use of the code are listed first.

NDNUC	maximum number of nuclei involved in the calculation
NDEJC	number of ejectiles (must be 3 or 4)
NDEX	maximum number of energy bins in the continuum discretization
NDLW	maximum number of partial waves to be considered in calculations
NDTL	maximum number of partial waves when calculating transmission coefficients (can be less than NDLW)
NDMSCS	number of steps in Multi-step Compound
NDLV	maximum number of discrete levels in any nucleus
NDBR	maximum number of branching ratios for each level
NDHRTW1	maximum number of strong ( $T_l > 0.0001$ ) channels, which are stored and treated explicitly in HRTW
(the following parameters <b><i>should not</i></b> be changed unless you know what you are doing!)	
NDHRTW2	=10 maximum number of elastic channels for a single $J^\pi$ (used in HRTW)
NDAFIS	=1 number of asymmetric fission channels (not used)
NDVOM	=7 maximum number of coefficients to describe real optical model potential depth

---

NDWOM	=7 maximum number of coefficients to describe imaginary optical model potential depth
NDVSO	=7 maximum number of coefficients to describe spin-orbit optical model potential depth
NDRVOM	=3 maximum number of coefficients to describe real optical model potential radius
NDRWOM	=3 maximum number of coefficients to describe imaginary optical model potential radius
NDRVSO	=3 maximum number of coefficients to describe spin-orbit optical model potential radius
NDETL	=NDEX+5 maximum number of energy bins for transmission coefficients
NDECSE	=NDEX maximum number of energy bins for energy spectra
NDEREC	=NDECSE maximum number of energy bins for recoil spectra
NDERO	=NDEX maximum number of energy bins for level densities
NDANG	=19 maximum number of angles in MSD
NDCC	=10 maximum number of Coupled-Channels in CCFUS
NDROP	=7 maximum number of parameters for the determination of level densities in the Gilbert-Cameron approach
NDGDRPM	=10 maximum number of parameters for GDR shape determination
NDGQRPM	=8 maximum number of parameters for GQR shape determination
NDGMRPM	=8 maximum number of parameters for GMR shape determination
NDKNTR	=3 maximum number of control parameters
NDREGIONS	=6 number of exit channels considered in the IDNA matrix defining use of the models (neut. disc., neut. cont., prot. disc., prot. cont., $\gamma$ , clusters)
NDMODELS	=6 number of reaction models considered in the IDNA matrix (CC, MSD, MSC, DEGAS, HMS, PCROSS)
NDDEFCC	=6 maximum order of deformation for collective levels
NDCOLLEV	=35 maximum number of collective levels taken into account in the ECIS06 calculations

NMAse	=9066 number of nuclei in tables of ground state properties
NFMOD	=3 maximum number of fission modes
NFisEN	=55 number of energies for which level densities at saddles are given in RIPL-2
NFisJ	=30 number of spins for which level densities at saddles are given in RIPL-2
NFPARAB	=5 maximum number of parabolas which can be used in the fission barrier parameterization
NFHUMP	=3 the maximum number of humps above which there is a continuum of levels
NFISENMAX	=400 maximum number of energy bins for level densities at saddles (for FISDEN=1)

## 3.4 Parameter libraries

Input parameters are stored in two distinct areas reflecting their origin - original EMPIRE input library can be found in the *empire/data* directory, while the result of the IAEA co-ordinated project RIPL-2[47] are stored in the *empire/RIPL-2* folder. The latter directory follows structure and content of the RIPL-2 library, although files not used by EMPIRE are omitted. Accordingly, RIPL-2 documentation can be consulted for more details. The advent of the more complete and more up to date RIPL-2 database has reduced the original *empire/data* library to a few EMPIRE-specific files and neutron resonance parameters from ENDF/B-VII.0.

### 3.4.1 Masses (*empire/RIPL-2/masses/mass-frdm95.dat*)

Combined set of experimental [77] and predicted ground state properties. The atomic mass excesses and nuclear ground-state deformations are tabulated for 9066 nuclei ranging from neutron and proton up to  $[Z=136, A=339]$ . Calculations are based on the finite-range droplet macroscopic model and the folded-Yukawa single-particle microscopic model [78]. The values of only nine constants are determined directly from a least-squares adjustment to the ground-state masses of 1654 nuclei ranging from O-16 to  $[Z=106, A=263]$  and to 28 fission-barrier heights. The error of the mass model is 0.669 MeV for the entire region of nuclei considered, but is only 0.448 MeV for the region  $N$  greater than or equal to 65. Included are microscopic corrections  $E_{mic}$  that correspond to the difference between the total binding energy and the spherical macroscopic (droplet) energy.

Each record of the file contains:

<b>Z</b>	charge number
<b>A</b>	mass number

<b>El</b>	element symbol
<b>fl</b>	flag corresponding to 0 if no experimental data available 1 for a mass excess recommended by Audi&Wapstra (1995) 2 for a measured mass from Audi&Wapstra (1995)
<b>Mexp</b>	experimental or recommended atomic mass excess in MeV of Audi&Wapstra (1995)
<b>Mth</b>	calculated FRDM atomic mass excess in MeV
<b>Emic</b>	calculated FRDM microscopic energy in MeV
<b>beta2</b>	calculated quadrupole deformation of the nuclear ground-state
<b>beta3</b>	calculated octupole deformation of the nuclear ground-state
<b>beta4</b>	calculated hexadecapole deformation of the nuclear ground-state
<b>beta6</b>	calculated hexacontatetrapole deformation of the nuclear ground-state

The corresponding FORTRAN format is (2i4,1x,a2,1x,i1,3f10.3,4f8.3)

### 3.4.2 Discrete levels (*empire/RIPL-2/levels/zxxx.dat*)

EMPIRE-2.17 is the first version to contain a preliminary discrete level library prepared by the Budapest group for the RIPL-2 project and linked to EMPIRE by R. Capote. ENSDF of 1998 has been used as a main source of data [79, 80]. The preliminary Budapest library contains 2546 nuclear level schemes, with at least 1 known level, within mass range  $A=1-266$  and  $Z=0-109$ . The basic set includes 113346 levels (out of which 8554 have unknown level energies denoted with +X or +Y) and 159323  $\gamma$ -transitions. The total number of levels with unique spin is 12956, and there are an additional 8708 levels with uncertain spin or parity assignment.

The level schemes were analyzed using constant temperature fits to the cumulative plots for all nuclei with at least 30 known levels in order to determine the cut-off energy ( $E_{max}$ ) and the corresponding cumulative number of levels ( $N_{max}$ ) up to which schemes can be assumed complete and suitable for reaction calculations. These results were extended to cover all remaining nuclei using the nuclear temperature inferred from the above analysis. The energy  $U_c$ , corresponding to the highest level with known and unique spin and parity assignment in the ENSDF, was subsequently determined for all nuclei.

For the purpose of reaction calculations the library was completed by estimating data missing in the basic ENSDF set:

- unique spins and parities for all levels below the cutoff energy  $E_{max}$  were generated by (i) analyzing  $\gamma$ -transitions (3560), (ii) drawing from the assumed spin distribution (3551), and (iii) selecting from the list suggested in ENSDF (6280).

- 21595 Internal Conversion Coefficients (ICC) for electromagnetic transitions available in the original ENSDF data set were supplemented with 92634 ICCs calculated by cubic spline interpolation of values tabulated by Hager and Seltzer for the K, L, and M shells and by Dragoun, Plajner, and Schmetzler for the N+O+... shells.
- if ENSDF reported de-exciting transitions from a level but did not specify the decay modes, 100% electromagnetic decay was assigned to the level. If other decay modes were indicated, the percentage of the electromagnetic mode was obtained from the available information on the decay modes and flagged by %IT or %G in the data files.

Details concerning the above assignments will be published in the RIPL-2 documentation.

Because of the considerable size, the library of nuclear levels is divided into files named *Zxxx.DAT*, where “*xxx*” stands for the atomic number with trailing zeros retained. Each file contains decay data for a single element. Isotopes inside the file are ordered according to the increasing mass number *A*. The format consists of three types of records: (i) identification, (ii) level, and (iii) gamma. Each isotope begins with an identification record such as the one shown below for the case of <sup>22</sup>Mg (here and elsewhere, a heading in italic has been introduced to facilitate explanation of the fields and is not part of the original file):

<i>SYMB</i>	<i>A</i>	<i>Z</i>	<i>Nol</i>	<i>Nog</i>	<i>Nmax</i>	<i>Nc</i>	<i>Sn[MeV]</i>	<i>Sp[MeV]</i>
22Mg	22	12	17	18	9	4	19.382000	5.497000

The FORTRAN format statement (a5,i5,2f12.6) is used to read the following quantities:

<b>SYMB</b>	mass number with symbol of the element
<b>A</b>	mass number
<b>Z</b>	atomic number
<b>Nol</b>	number of levels in the decay scheme
<b>Nog</b>	number of gamma rays in the decay scheme
<b>Nmax</b>	maximum number of levels up to which the level scheme is complete (by default EMPIRE uses MIN(Nmax, NDLV) levels limited to 40 when the ENDF option is invoked)
<b>Nc</b>	number of a level up to which spins and parities are unique
<b>Sn</b>	neutron separation energy in MeV
<b>Sp</b>	proton separation energy in MeV



The identification record is followed by the level record, which in turn is followed by the pertinent gamma records if decay of the level is known. This combination is repeated for all levels in a given isotope. An example below shows level records for the ground state and the first excited state in  $^{22}\text{Mg}$ :

<i>Nl</i>	<i>El</i> [MeV]	<i>s</i>	<i>p</i>	<i>T<sub>1/2</sub></i> [s]	<i>Ng</i>	<i>J</i>	<i>unc</i>	<i>spins</i>	<i>nd</i>	<i>m</i>	<i>percent</i>	<i>mode</i>
1	0.000000	0.0	1	3.86E+00	0			0+	1	=	100.0000	%EC+%B+
2	1.246300	2.0	1	2.10E12	1			2+	0			

The related format is

(i3,1x,f10.6,1x,f5.1,i3,1x,(e10.2),i3,1x,a1,1x,a4,1x,a18,i3,10(1x,a2,1x,f10.4,1x,a7)).

Each level record may contain the following quantities:

<b>Nl</b>	sequential number of a level
<b>El</b>	energy of the level in MeV
<b>s</b>	level spin (unique). Whenever possible unknown spins up to $E_{max}$ were inferred using statistical methods. Unknown and undetermined spins are entered as -1.0
<b>p</b>	parity (unique). If the parity of the level was unknown, positive or negative was chosen with equal probability. Parities were determined up to $E_{max}$ as in the case of spins. The method of choice is not coded.
<b>T<sub>1/2</sub></b>	half-life of the level (if known). All known half-lives or level widths were converted into seconds. Half-lives of stable nuclei are represented as -1.0E+0.
<b>Ng</b>	number of gamma rays de-exciting the level.
<b>J</b>	flag for spin estimation method.
<b>unc</b>	flag for an uncertain level energy. When impossible to determine, the relative energy of the band, the energy of these band heads were set to 0.0 keV or, if the level order is known, to the preceding level energy with a note that an unknown energy X should be added. The notation uses X+, Y+, Z+ etc. for different bands.
<b>spins</b>	original spins from the ENSDF file. Can be used to adjust spin-parity values by hand.
<b>nd</b>	number of decay modes of the level (if known). Values from 0 through 10 are possible; 0 means that the level may decay via $\gamma$ -emission, and other decay modes are not known.

- m** decay percentage modifier; informs a user about major uncertainties. The modifiers are copied out of ENSDF with no modification, and can have the following values: =, <, >, ? (unknown, but expected), AP (approximate), GE (greater or equal), LE (less or equal), LT (less then), SY (value from systematics).
- percent** percentage decay of different decay modes. As a general rule the various decay modes add up 100%. There are, however, two exceptions: (i) when a small percentage decay is present, the sum may be slightly more then 100% due to rounding error, (ii) when  $\beta$ -decay is followed by a heavier particle emission, the percentage of the  $\beta$ -delayed particle emission is given as a portion of the  $\beta$ -decay and the sum can be substantially larger then 100%. Naturally, when the modifier is “?” the sum is indefinite.
- mode** short indication of decay modes of a level (see Table 3.1).

Two typical examples of the gamma records are given below ( $^{94}\text{Nb}$ ):

<i>Nf</i>	<i>Eg</i> [MeV]	<i>Pg</i>	<i>Pe</i>	<i>ICC</i>
3	0.055	4.267E02	1.301E01	2.050E+00
1	0.113	7.499E01	8.699E01	8.699E01

The format is (39x,i4,1x,f10.3,3(1x,e10.3)) and the columns contain:

- Nf** sequential number of the final state
- Eg**  $\gamma$ -ray energy in MeV
- Pg** Probability that a level decays through the given  $\gamma$ -ray emission. Pg is the ratio of the total electromagnetic decay of the level to the intensity of the  $\gamma$ -ray. If no branching ratio is given in the ENSDF file, Pg=0.
- Pe** Probability that a level decays with the given electromagnetic transition, i.e., ratio of the total electromagnetic decay of the level to the intensity of the given electromagnetic transition. The sum of electromagnetic decays is normalized to 1. If no branching ratio is given in the ENSDF file, Pe =0.
- ICC** Internal conversion coefficient of a transition. A modified version of the Nuclear Data Center program HSICC.FOR was used to calculate values not provided in ENSDF. When calculating ICCs the first multipole mixing ratio was used. If there was no multipole mixing ratio available for the mixed E2+M1 transitions, M1 was assumed in case of odd and E2 in case of even mass nuclei. No attempt was made to include possible E0 decays. For other mixing possibilities, the lowest multipole order was used unless the mixing ratio was provided. Below A=10, ICCs are only calculated for Li and C. The ICCs are set to zero if the transition energy exceeded a certain, mass-dependent limit.

Table 3.1: Coding of decay modes. Some minor possibilities, such as decay through the emission of  $^{20}\text{Ne}$ , are neglected.

Code	Meaning
%B	$\beta^-$ decay
%EC	electron capture
%EC+%B+	electron capture and $\beta^+$ decay
%N	neutron decay
%A	$\alpha$ decay
%IT	isomeric transition
%P	proton decay
%3HE	$^3\text{He}$ decay
%B+P	$\beta^+$ delayed proton decay
%BN	$\beta^-$ delayed neutron decay
%SF	spontaneous fission
%ECP	electron capture delayed proton decay
%ECA	electron capture delayed $\alpha$ decay
%G	$\gamma$ decay
%B2N	$\beta^-$ delayed double neutron decay
%B+2P	$\beta^+$ delayed double proton decay

### 3.4.3 Optical model parameters (`empire/RIPL-2/optical/om-data/om-parameter-u.dat`)

R. Capote has greatly simplified the use of EMPIRE by incorporating the preliminary version of the RIPL-2 optical model parameters (omp) library, which was compiled within an IAEA Coordinated Research Project [47]. The library contains 409 sets of omp for nuclei up to Lr ( $Z=103$ ) for neutrons, protons,  $\alpha$ -particles, d, t, and  $^3\text{He}$  up to 400 MeV (mass and energy ranges vary for different target-projectile combinations). The library contains omp for single isotopes (or for a limited range of isotopes) and global systematics valid over a wide range of masses. The RIPL-2 omp can easily be invoked by assigning omp index (**with negative sign!**) through the input keyword OMPOT and/or DIRPOT for Coupled-Channels calculations (see Section 3.10.1). List of omp indexes is available from the EMPIRE graphic interface under Help→ RIPL-omp (see Section 3.7.7).

The format of the omp library accommodates all functional forms of mass and energy dependencies encountered in the literature accounting for Coupled-Channels and dispersive<sup>1</sup> potentials and includes the relativistic option. Each set is divided into sections describing:

- real volume potential,

<sup>1</sup>ORION has been extended by R. Capote to accept dispersive omp. Therefore, these potentials can be used in EMPIRE calculations in a same way as all the others.

- imaginary volume potential,
- real surface derivative potential,
- imaginary surface derivative potential,
- real spin-orbit potential,
- imaginary spin-orbit potential.

Because of its universality the format is rather complicated, and is best described by using a FORTRAN-like representation.

iref

author

reference

summary

emin,emax

izmin,izmax

iamin,iamax

imodel,izproj,iaproj,irel,idr

-----LOOP: i=1,6

jrange(i)

-----LOOP: j=1,jrange

epot(i,j)

(rco(i,j,k), k=1,11)

(aco(i,j,k), k=1,11)

(pot(i,j,k), k=1,25)

-----END i AND j LOOPS

jcoul

```

-----LOOP: j=1,jcoul
ecoul(j),rcoul0(j),rcoul(j),rcoul1(j),rcoul2(j),beta(j)
-----END j LOOP
(1)-----SKIP TO (2)----- IF IMODEL NOT EQUAL TO 1
nisotopes
-----LOOP: n=1,nisotopes
iz(n),ia(n),ncoll(n),lmax(n),idef(n),bandk(n),[def(j,n),
j=2,idef(n),2]
-----LOOP: k=1,ncoll(n)
ex(k,n),spin(k,n),ipar(k,n)
-----END k AND n LOOPS
(2)-----SKIP TO (3)----- IF IMODEL NOT EQUAL TO 2
nisotopes
-----LOOP: n=1,nisotopes
iz(n),ia(n),nvib(n)
-----LOOP: k=1,nvib(n)
exv(k,n),spinv(k,n),iparv(k,n),nph(k,n),defv(k,n),thetm(k,n)
-----END k LOOP
-----END n LOOP
(3)-----SKIP REMAINING LINES IF IMODEL NOT EQUAL TO 3
nisotopes
-----LOOP: n=1,nisotopes
iz(n),ia(n),beta0(n),gamma0(n),xmubeta(n)
-----END n LOOP

```

Definitions of the symbols and functional forms are listed below.

<b>iref</b>	unique index for this potential (used for referencing through the OMPOT and/or DIRPOT keywords in input)
<b>author</b>	authors of this potential (up to 80 characters, 1 line)
<b>reference</b>	reference for this potential (up to 80 characters, 1 line)
<b>summary</b>	short description of the potential (320 characters, 4 lines)
<b>emin,emax</b>	minimum and maximum energies for validity of this potential
<b>izmin,izmax</b>	minimum and maximum Z values for this potential
<b>iamin,iamax</b>	minimum and maximum A values for this potential
<b>imodel</b>	= 0 for spherical potential = 1 for coupled-channel, rotational model = 2 for coupled-channel, vibrational model = 3 for non-axial deformed model
<b>izproj</b>	Z for incident projectile
<b>iaproj</b>	A for incident projectile
<b>irel</b>	= 0 for non-relativistic parametrization = 1 for relativistic parameterization
<b>idr</b>	= 0 dispersion relations not used = 1 dispersion relations used with equivalent volume real potential = 2 exact dispersion relations used, i.e., volume + surface real potential
<b>index <i>i</i></b>	= 1 real volume potential (Woods-Saxon) = 2 imaginary volume potential (Woods-Saxon) = 3 real surface derivative potential = 4 imaginary surface derivative potential = 5 real spin-orbit potential = 6 imaginary spin-orbit potential
<b>jrange</b>	= number of energy ranges over which the potential is specified = positive for potential strengths = negative for volume integrals = 0 if potential of type <i>i</i> not used
<b><i>epot(i,j)</i></b>	upper energy limit for $j^{th}$ energy range for potential <i>i</i>

**$rco(i,j,k)$**  coefficients for multiplying  $A^{1/3}$  for specification of radius  $R$  in fm where:

$$\begin{aligned} R(i,j) = & \{|rco(i,j,1)| + rco(i,j,2)E + rco(i,j,3)\eta \\ & + rco(i,j,4)/A + rco(i,j,5)/\sqrt{A} + rco(i,j,6)A^{2/3} \\ & + rco(i,j,7)A + rco(i,j,8)A^2 + rco(i,j,9)A^3 \\ & + rco(i,j,10)A^{1/3} + rco(i,j,11)A^{-1/3}\} A^{1/3} \end{aligned}$$

and

if  $rco(4,j,1) > 0.0$ : Woods-Saxon derivative surface potential

if  $rco(4,j,1) < 0.0$ : Gaussian surface potential.

[Note that the  $A$  dependence of  $rco(i,j,11)$  cancels out so that  $rco(i,j,11)$  is equivalent to adding a constant of that magnitude to the radius  $R(i,j)$ ].

**$aco(i,j,k)$**  coefficients for specification of diffuseness  $a$  in fm where:

$$\begin{aligned} a(i,j) = & |aco(i,j,1)| + aco(i,j,2)E + aco(i,j,3)\eta + aco(i,j,4)/A \\ & + aco(i,j,5)/\sqrt{A} + aco(i,j,6)A^{2/3} + aco(i,j,7)A \\ & + aco(i,j,8)A^2 + aco(i,j,9)A^3 + aco(i,j,10)A^{1/3} \\ & + aco(i,j,11)A^{-1/3} \end{aligned} \quad (3.1)$$

**$pot(i,j,k)$**  - strength parameters in MeV when  $aco(i,j,1) > 0$ .

- volume integral of strength in  $\text{MeVfm}^3$  when  $aco(i,j,1) < 0$ , and are given as follows:

if  $pot(i,j,k > 21) = 0$ , standard form:

$$\begin{aligned} V(i,j) = & pot(i,j,1) + pot(i,j,7)\eta + pot(i,j,8)E_{coul1} + pot(i,j,9)A \\ & + pot(i,j,10)A^{1/3} + pot(i,j,11)A^{-2/3} + pot(i,j,12)E_{coul2} \\ & + [pot(i,j,2) + pot(i,j,13)\eta + pot(i,j,14)A] E \\ & + pot(i,j,3)E^2 + pot(i,j,4)E^3 + pot(i,j,6)\sqrt{E} \\ & + [pot(i,j,5) + pot(i,j,15)\eta + pot(i,j,16)E] \ln(E) \\ & + pot(i,j,17) \frac{E_{coul1}}{E^2} \end{aligned} \quad (3.2)$$

if  $pot(i,j,22) \neq 0$ , Smith form:

$$\begin{aligned} V(i,j) = & pot(i,j,1) + pot(i,j,2)\eta \\ & + pot(i,j,3) \cos \left[ 2\pi \frac{A - pot(i,j,4)}{pot(i,j,5)} \right] \\ & + pot(i,j,6) \exp [pot(i,j,7)E + pot(i,j,8)E^2] \\ & + pot(i,j,9)E \exp [pot(i,j,10)E^{pot(i,j,11)}] \end{aligned} \quad (3.3)$$

if  $pot(i,j,23) \neq 0$ , Varner form:

$$V(i,j) = \frac{pot(i,j,1) + pot(i,j,2)\eta}{1 + \exp \left[ \frac{pot(i,j,3) - E + pot(i,j,4)E_{coul2}}{pot(i,j,5)} \right]} + pot(i,j,6) \exp \left[ \frac{pot(i,j,7)E - pot(i,j,8)}{pot(i,j,6)} \right] \quad (3.4)$$

if  $pot(i,j,24) \neq 0$ , Koning form:

$$\begin{aligned} V(i,j) = & b(i,j,1) [1 - b(i,j,2)(E - EF) + b(i,j,3)(E - EF)^2 - b(i,j,4)(E - EF)^3] \\ & + b(i,j,5) + b(i,j,6) \left[ \frac{(E - EF)^{n(i,j)}}{(E - EF)^{n(i,j)} + b(i,j,7)^{n(i,j)}} \right] \\ & + b(i,j,8) \exp [-b(i,j,9)(E - EF)] \frac{(E - EF)^{n(i,j)}}{(E - EF)^{n(i,j)} + b(i,j,10)^{n(i,j)}} \\ & + b(i,j,11) \exp [-b(i,j,12)(E - EF)] \end{aligned} \quad (3.5)$$

if  $pot(i,j,25) \neq 0$ , Engelbrecht form:

$$V(i,j) = pot(i,j,1) + pot(i,j,4) \exp [pot(i,j,5)E^{pot(i,j,2)} + pot(i,j,6)E^{pot(i,j,3)}] \quad (3.6)$$

where

**$E$**  projectile laboratory energy in MeV

$\eta = (N-Z)/A$

**$E_{coul1}$**  =  $0.4Z/A^{1/3}$

**$E_{coul2}$**  =  $1.73Z/RC$

**$EF$**  - Fermi energy in MeV [for above case when  $pot(i,j,24) \neq 0$  or when  $idr=2$ ].  
=  $pot(i,j,18) + pot(i,j,19)*A$

If  $pot(6,j,18) = pot(6,j,19) = 0$ ,

$EF = -0.5*[SN(Z,A) + SN(Z,A+1)]$  (for incident neutrons)

$EF = -0.5*[SP(Z,A) + SP(Z+1,A+1)]$  (for incident protons)

where

$SN(Z,A)$  = neutron separation energy for nucleus (Z,A)

$SP(Z,A)$  = proton separation energy for nucleus (Z,A).

For cases where  $idr=2$ :



- EP** =  $pot(i,j,20)$   
 - average energy of particle states. If  $pot(i,j,20)=0$ , use default value of  $EP=EF$ .
- EA** =  $pot(i,j,21)$   
 - energy above which non-locality of the absorptive potential will be assumed.  
 If  $pot(i,j,21)=0$ , use default value of  $EA=1000$  (MeV).

For  $pot(i,j,24) \neq 0$ , the  $b(i,j,m)$  are defined as:

$b(i,j,m)$  = 0 for  $i=1,6$ ,  $j=1,jrange(i)$ ,  $m=1,12$ , except for the following:

$$b(1,j,1) = pot(1,j,1) + pot(1,j,2)A + pot(1,j,8)\eta$$

$$b(1,j,2) = pot(1,j,3) + pot(1,j,4)A$$

$$b(1,j,3) = pot(1,j,5) + pot(1,j,6)A$$

$$b(1,j,4) = pot(1,j,7)$$

$$b(1,j,5) = pot(1,j,9)*(Z/A**(1./3.))$$

$$b(1,j,11) = pot(1,j,10) + pot(1,j,11)A$$

$$b(1,j,12) = pot(1,j,12)$$

$$b(2,j,6) = pot(2,j,1) + pot(2,j,2)A$$

$$b(2,j,7) = pot(2,j,3) + pot(2,j,4)A$$

$$b(4,j,8) = pot(4,j,1) + pot(4,j,8)\eta$$

$$b(4,j,9) = pot(4,j,2) + pot(4,j,3)/(1. + exp((A-pot(4,j,4))/pot(4,j,5)))$$

$$b(4,j,10) = pot(4,j,6)$$

$$b(5,j,11) = pot(5,j,10) + pot(5,j,11)A$$

$$b(5,j,12) = pot(5,j,12)$$

$$b(6,j,6) = pot(6,j,1)$$

$$b(6,j,7) = pot(6,j,3)$$

$$n(i,j) = int(pot(i,j,13))$$

And, continuing the definitions:

**jcoul** number of energy ranges to specify Coulomb radius and non-locality range

**ecoul(j)** maximum energy of Coulomb energy range  $j$

$rcoul_0(j)$ , $rcoul(j)$ , $rcoul_1(j)$ , $rcoul_2(j)$	coefficients to determine the Coulomb radius, RC: $RC = (rcoul_0(j)A^{-1/3} + rcoul(j) + rcoul_1(j)A^{-2/3} + rcoul_2(j)A^{-5/3}) A^{1/3}$
$beta(j)$	non-locality range. Note that when $beta(j) \neq 0$ , the imaginary potential is purely the derivative Woods-Saxon for energy range $j$ .
<b><i>nisotopes</i></b>	number of isotopes for which deformation parameters and discrete levels are given
<b><i>iz, ia</i></b>	Z and A for the deformation parameters and discrete levels that follow
<b><i>ncoll</i></b>	number of collective states in the coupled-channel rotational model for $iz$ , $ia$
<b><i>lmax</i></b>	maximum $l$ value for multipole expansion
<b><i>idef</i></b>	largest order of deformation
<b><i>bandk</i></b>	$k$ for the rotational band
<b><i>def</i></b>	deformation parameters, $l=2,4,6,\dots$ through $lmax$
<b><i>ex</i></b>	rotational level excitation energy (MeV)
<b><i>spin</i></b>	rotational level spin
<b><i>ipar</i></b>	rotational level parity
<b><i>nvib</i></b>	number of vibrational states in the model for $iz$ , $ia$ (first level must be ground state)
<b><i>exv</i></b>	vibrational level excitation energy (MeV)
<b><i>spinv</i></b>	vibrational level spin
<b><i>iparv</i></b>	vibrational level parity
<b><i>nph</i></b>	= 1 for pure 1-phonon state = 2 for pure 2-phonon state = 3 for mixture of 1- and 2-phonon states
<b><i>defv</i></b>	= vibrational model deformation parameter
<b><i>thetm</i></b>	mixing parameter (degrees) for $nph=3$
<b><i>beta0</i></b>	beta deformability parameter
<b><i>gamma0</i></b>	gamma deformability parameter
<b><i>xmubeta</i></b>	non-axiality parameter

### 3.4.4 Excited-level deformation parameters (`empire/RIPL-2/optical/om-data/om-deformations.dat`)

Recommended deformation parameters ( $\beta_2$  and  $\beta_3$ ) for 1643 collective levels. The dynamical deformation parameters given for the vibrational nuclei and some vibrational band-heads in rotational nuclei assume vibrational states to be of a one-phonon type. For the rotational nuclei the ground-state static deformation parameters are given. The fictitious levels, used in the JENDL-3.2 evaluations, are also included.

$\beta_2$  and  $\beta_3$  have been retrieved from the JENDL-3.2 evaluations, ENSDF and the literature. In the case of ENSDF the quantities such as a quadrupole moment (Q), B(E2) and B(E3) were retrieved and converted into the deformation parameters  $\beta_2$  and  $\beta_3$

Each record of the file contains:

<b>Z</b>	atomic number
<b>A</b>	mass number
<b>El</b>	element symbol
<b>Ex</b>	energy of the excited-level in MeV
<b>J</b>	spin of the excited-level (if the spin is unknown, this field is left blank)
<b>P</b>	parity of the excited-level (if the parity is unknown, P=0)
<b>L</b>	order of the deformation parameter, $\beta$
$\beta_L$	deformation parameter $\beta$ (of the order L)
Reference	indication of the data origin

### 3.4.5 Experimental Giant Dipole Resonance parameters (`empire/RIPL-2/gamma/gdr-parameters-exp.dat`)

Giant Dipole Resonance parameters representing Lorentz curves fit to the total photo-neutron cross section data as compiled by S.S. Dietrich and B.L. Berman [65] for 102 nuclides ranging from 51-V to 239-Pu in 1987. Data for 12-C, 14-N, 16-O, 27-Al and 28-Si were estimated by Liu Jianfeng and Su Zongdi in 1995.

Each record of the file contains:

<b>Z</b>	atomic number
<b>A</b>	mass number (0 stands for natural element)
<b>El</b>	element symbol
<b>N</b>	number of parameter sets for the same nucleus

<b>M</b>	1 for single peak GDR; 2 for double-hump GDR
<b>E1</b>	energy of the first peak
<b>CS1</b>	peak cross section of the first peak
<b>W1</b>	full width at half-maximum for the first peak
<b>E2</b>	energy of the second peak
<b>CS2</b>	peak cross section of the second peak
<b>W2</b>	full width at half-maximum for the second peak
<b>Ref</b>	reference

### 3.4.6 Calculated Giant Dipole Resonance energies and widths (`empire/RIPL-2/gamma/gdr-parameters-theor.dat`)

Predictions of the Giant Dipole Resonance (GDR) energies and widths for about 6000 nuclei with  $Z$  starting with 14 up to 110 lying between the proton and the neutron driplines. The GDR is represented in the Goldhaber-Teller model [81] where the neutron and proton densities perform an out-of-phase vibration around their center of mass. The dynamics of the oscillation is assumed to be dominated by the np-interaction [82]. The present table gives the GDR energies predicted by [82] with a renormalized np-interaction of strength derived from a least-square fit to the experimental GDR energies [83]. The nucleon density distribution and ground-state deformation are taken from the Extended Thomas-Fermi plus Strutinsky Integral (ETFSI) compilation [84, 85]. The expression for the shell-dependent GDR width is taken from [86] using the newly-determined GDR energies and the ETFSI shell corrections. Such predictions include the shell-dependent GDR broadening due to the coupling between the dipole oscillations and the quadrupole surface vibrations. Comparison between predicted and experimental GDR energies and widths can be found in [83]. In case of deformed nuclei, the GDR splits into two peaks for oscillations parallel to the axis of rotational symmetry and perpendicular to it.

Each record of the file contains:

<b>Z</b>	atomic number
<b>A</b>	mass number
<b>E1</b>	element symbol
$\eta$	deformation parameter (diameter along the nuclear symmetry axis / diameter along an axis perpendicular to it) predicted by ETFSI-2
<b>E1</b>	GDR energy for oscillation parallel to the axis of rotational symmetry, in MeV

<b>W1</b>	GDR width for oscillation parallel to the axis of rotational symmetry, in MeV
<b>E2</b>	GDR energy for oscillations perpendicular to the axis of rotational symmetry, in MeV
<b>W2</b>	GDR width for oscillations perpendicular to the axis of rotational symmetry, in MeV

### 3.4.7 Tabulated HF-BCS level densities

(*empire/RIPL-2/densities/total/level-densities-hfbc/zxxx.dat*)

This directory contains tabulated level densities and is a part of the RIPL-2 library. It consists of separate files for 103 elements between  $Z=8$  and  $Z=110$ , each of them containing a number of isotopes. The level densities were calculated using Hartree-Fock-BCS model and adjusted to discrete levels schemes and neutron resonance spacings. The maximum numbers of discrete levels up to which the scheme was considered to be complete are listed in the file `Nmax_Umax` placed in the same directory. The level densities are given for spins up to  $30\hbar$  and excitation energies up to 150 MeV. More details about the calculations can be found in Ref. [56]. `LEV DEN=3` option in the EMPIRE optional input permits the use of these results directly in the EMPIRE calculations. An excerpt from a typical file is reproduced below.

```
*****
Z= 10 A= 18: Total and Spin-dependent Level Density [MeV-1] for Ne 18
*****
U[MeV] T[MeV] NCUMUL RHO OBS RHOTOT J=0 J=1 J=2 J=3 ...
0.25 0.001 1.00E+00 0.00E+00 0.00E+00 0.00E+00 0.00E+00 0.00E+00 0.00E+00 ...
0.50 0.001 1.00E+00 0.00E+00 0.00E+00 0.00E+00 0.00E+00 0.00E+00 0.00E+00 ...
0.75 0.001 1.00E+00 0.00E+00 0.00E+00 0.00E+00 0.00E+00 0.00E+00 0.00E+00 ...
1.00 0.001 1.00E+00 0.00E+00 0.00E+00 0.00E+00 0.00E+00 0.00E+00 0.00E+00 ...
1.25 0.297 1.05E+00 3.89E-01 6.57E-01 2.62E-01 1.20E-01 7.14E-03 7.23E-05 ...
1.50 0.358 1.14E+00 3.71E-01 8.85E-01 1.67E-01 1.55E-01 4.35E-02 4.83E-03 ...
1.75 0.402 1.24E+00 4.01E-01 1.15E+00 1.43E-01 1.63E-01 7.39E-02 1.81E-02 ...
— cut —
```

In addition to spin-dependent level densities, the file also reports the nuclear temperature ( $T$ ), cumulative number of levels (`NCUMUL`) and observed (`RHO OBS`) as well as total (`RHOTOT`) level densities. These quantities are not used by EMPIRE at present.

### 3.4.8 Experimental fission barriers

(*empire/RIPL-2/fission/fis-barrier-exp.dat*)

Fission barrier parameters recommended for the trans-thorium nuclei by V.M.Maslov and for the pre-actinides by G.N.Smirenkin. Each record of the file contains:

<b>Z</b>	charge number of the fissioning nucleus
----------	-----------------------------------------

<b>A</b>	mass number of the fissioning nucleus
<b>El</b>	element symbol of the fissioning nucleus
<b>Ea</b>	inner barrier height in MeV
<b>SymA</b>	symmetry of the inner-barrier saddle point
<b>Eb</b>	outer barrier height in MeV
<b>SymB</b>	symmetry of the outer-barrier saddle point
<b>Delf</b>	correlation function of the fission channel recommended for the fission level density calculation in MeV

### 3.4.9 Fission barriers and saddle point deformations based on the ETFSI model (empire/RIPL-2/fission/fis-barrier-etfsi.dat)

Predictions of the fission barriers and saddle point deformations obtained within the Extended Thomas-Fermi plus Strutinsky Integral (ETFSI) method. The ETFSI approach is a semi-classical approximation to the Hartree-Fock method in which the shell corrections are calculated with the 'integral' version of the Strutinsky theorem. BCS corrections are added with a delta-pairing force. The fission barriers are derived with the SkSC4 Skyrme force on which the ETFSI-1 mass formula is based. The experimental primary barriers can be reproduced within 1.5 MeV (except for the elements with  $Z < 87$  having barriers above 10 MeV).

The present ETFSI compilation includes 2301 nuclei with  $Z=78$  through 120. Their masses range from slightly neutron deficient to very neutron rich nuclei (close to or up to the calculated neutron drip line), up to  $A = 318$ . This compilation contains the nuclei considered in [87], for which experimental barriers are known, and a slightly extended version of the set published in [88]. Also included are the experimental fission barriers compiled in [87] and those originating principally from [89].

For each nucleus a maximum of two barriers are given, one "inner" and one "outer". They correspond to the highest saddle point among the "slightly" and the "strongly" deformed ones. Those two groups of saddle points correspond to well separated values of the elongation parameter  $c$ ,  $c_{in}$  and  $c_{out}$  (see below). In most cases  $c_{in} < 1.6$  and  $c_{out} > 1.6$  (in some cases  $1.5 < c_{out} < 1.6$ ).

In addition to the calculated inner and outer barriers, the deformation parameters at the corresponding saddle points are included. The nuclear shapes are limited to axially symmetrical deformations. These are described by the so-called Brack parametrization  $(c, h, \alpha)$  where  $c$  is the elongation parameter ( $c < 1$ ,  $=1$  and  $>1$  for oblate, spherical and prolate shapes, resp.) and  $h$  is related to the "necking" of the nuclear surface. The shapes corresponding to different regions of the  $(c, h)$  plane are described in detail in [87]. The parameter  $\alpha$  measures the left-right asymmetry ( $\alpha = 0$  for symmetric shapes). The

asymmetry parameters  $ain$  and  $aout$  listed in the file refer not to  $\alpha$  but to the  $\tilde{\alpha}$  quantity defined in [87] as  $\alpha c^3$ .

Each record of the file contains:

<b>Z</b>	atomic number
<b>A</b>	mass number
<b>El</b>	element symbol
<b>cin</b>	$c$ of the inner barrier
<b>hin</b>	$h$ of the inner barrier
<b>ain</b>	$\tilde{\alpha}$ of the inner barrier
<b>Bin</b>	inner barrier in MeV
<b>Bexp</b>	inner experimental barrier in MeV
<b>cout</b>	$c$ of the outer barrier
<b>hout</b>	$h$ of the outer barrier
<b>aout</b>	$\tilde{\alpha}$ of the outer barrier
<b>Bout</b>	outer barrier in MeV
<b>Bexp</b>	outer experimental barrier in MeV

### 3.4.10 Tabulated level densities at saddle points

**(*empire/RIPL-2/fission/fis-levden-hfbcs-inner/zxxx.dat* and  
*empire/RIPL-2/fission/fis-levden-hfbcs-outer/zxxx.dat*)**

Nuclear Level Densities (NLD) at fission saddle points for some 2300 nuclei with  $78 \leq Z \leq 120$  included in the ETFSI compilation [88]. The fission barriers and saddle point deformations are determined within the Extended Thomas-Fermi plus Strutinsky Integral (ETFSI) method. For each nucleus a maximum of two barriers are given, one "inner" and one "outer". They correspond to the highest saddle point among the "slightly" and the "strongly" deformed ones. Those two groups of saddle points correspond to well separated values of the elongation parameter  $c$ . In most cases, for the inner barrier  $c < 1.6$  and the outer  $c > 1.6$ . The nuclear shapes are limited to axially symmetrical deformations. These are described by the so-called Brack parametrization ( $c, h, \alpha$ ) where  $c$  is the elongation parameter ( $c < 1, = 1$  and  $> 1$  for oblate, spherical and prolate shapes, resp.),  $h$  is related to the "necking" of the nuclear surface and  $\alpha$  measures the left-right asymmetry ( $\alpha = 0$  for symmetric shapes). The calculated inner and outer barriers as well as the deformation parameters at the corresponding saddle point can be found in the "fis-barrier-etfsi.dat" file.

At each saddle point, the NLD is estimated within the statistical partition function approach. The NLD calculation is based on the realistic microscopic single-particle level scheme determined within the HF-BCS mass model obtained with the MSk7 Skyrme force [90]. For each saddle point, the single-particle level scheme is calculated consistently by the HF-BCS model constrained on the corresponding quadrupole, octupole and hexadecapole moments. The same pairing strength (within the constant-G approximation) as the one used for the NLD calculation at the ground-state equilibrium deformation is used [90] (the ground-state NLD can be found in the level-densities-hfbcsc" sub-directory of the densities Segment). No damping of the collective effects at increasing excitation energies is considered. The NLD for nuclei with left-right asymmetric fission barriers is increased by a factor of 2.

As for the ground-state description, the NLD model includes

- BCS pairing (in the constant-G approximation) with a renormalized strength and blocking effect for odd-mass and doubly odd nuclei
- Gaussian-type spin dependence with microscopic shell and pairing effect on the spin cut-off parameter
- Deformation effects are included in the single-particle spectrum and the collective contribution of the rotational band on top of each intrinsic state
- Improved description at very-low energies.

The NLD are provided, separately at the inner and outer saddle points, in a table format for the 2300 nuclei with  $78 \leq Z \leq 120$  included in the ETFSI compilation of fission barriers. Each table includes spin-dependent NLD for energies up to  $U = 150$  MeV and spin up to  $J = 29(59/2)$ . Also included in the tables are the nuclear temperature, the cumulative number of levels and the total level and state densities.

Each isotopic chain is included in one unique file named by the elemental symbol  $Z$ . A title line includes for each isotope, in addition to the charge and mass number, the saddle point deformation in the  $(c, h, \alpha)$  parametrization and the fission barrier height in MeV. In each file, the NLDs are given for each isotope in a table format with an excitation energy grid ranging from  $U = 0.25$  MeV up to  $U = 150$  MeV. At each excitation energy  $U$  (in MeV), are provided:

**T** the nuclear temperature in MeV

**NCUMUL** the cumulative number of predicted levels

**RHO OBS** the total level density in  $1/\text{MeV}$  ( $\Sigma \rho(U, J)$ )

**RHOTOT** the total state density in  $1/\text{MeV}$  ( $\Sigma(2J+1)\rho(U, J)$ )

**RHO(J)** the spin-dependent level density for  $J=0$  ( $1/2$ ) up to 29 ( $59/2$ ).



### 3.4.11 Level density parameters (*empire/data/ldp.dat*)

This file contains level density data taken from Ilijinov *et al.* [50]. Furthermore, the first column reports the maximum number of discrete levels up to which level schemes are supposed to be completed according to RIPL-1. Since version 2.17beta, these data are not used but have been superseded by RIPL-2 estimates contained in the library of discrete levels. The *ldp.dat* file consists of the following columns:

Z\*1000+A nuclide identification

NLEVC number of levels in a complete scheme (NLEVC=1 for g.s., taken from RIPL-1 [17])

AROGC *a*-parameter without collective effects according to Ilijinov *et al.* [50](used with the Gilbert-Cameron approach),

AROC *a*-parameter including collective effects (to be used with the EMPIRE-specific level densities)

QN neutron binding energy (according to Ilijinov *et al.* [50] not used by the code),

DOBS observed spacings of neutron resonances (according to Ilijinov *et al.* [50] used to derive AROC, but not used by the code).

The last four items differ from zero only for the nuclei reported in Ref. [50].

NOTE: This file will be replaced by RIPL-2 equivalents in future releases.

### 3.4.12 Ground state deformations (*empire/data/deflib.dat*)

Deformation parameters from the *empire/RIPL-2/masses/mass-frdm95.dat* file converted into  $\beta_2$  and  $\beta_3$  representation. Apart of the 4 comment lines at the beginning, each line contains nucleus identification (Z and A) and two deformations.

### 3.4.13 Fission barriers (*empire/data/fisbar.dat*)

Set of fission barrier parameters obtained from fitting EMPIRE calculations to experimental fission cross sections. At present, it contains a very limited number of nuclei. It is expected to grow in future and its format may change to incorporate more details about calculations. Current format consists of one line per nuclide containing the following parameters

Z atomic number

A mass number

Npar number of parabolas describing the barrier (number of humps plus number of wells)

$N_w$	number of wells
$V_i$	maxima (and minima) of the real part of the fission potential
$\hbar\omega_i$	associated barrier's width (the latter pair appears for each parabola, i.e., $N_{par}$ times)

### 3.4.14 Neutron resonances (empire/data/resonances.endf)

This file contains full set of evaluated neutron resonance parameters (329 materials) extracted from the ENDF/B-VII.0 library. The file is in the ENDF-6 format and contains descriptive part.

## 3.5 Flow of the calculations

Listed below are the essential steps in the execution of the general case involving MSD and MSC calculations:

1. read EMPIRE input file (*.inp*)
2. construct table of nuclei involved
3. read from the input parameter library (or input/output files if they exist)
  - a) discrete levels,
  - b) binding energies,
  - c) level density parameters,
  - d) shell corrections,
  - e) ground state deformations ,
4. calculate
  - a) transmission coefficients ,
  - b) level densities,
  - c) fission barriers
5. retrieves experimental data from the EXFOR library.
6. writes input/output files
  - a) .exf
  - b) -omp.dir
  - c) -omp.rtpl

- d) .lev
  - e) -lev.col
7. determine fusion cross section and direct inelastic scattering (code ECIS06 might be invoked twice if CC and DWBA calculations are requested)
  8. select the compound nucleus for consideration.
  9. calculate double-differential cross sections for inelastic scattering in terms of the MSD mechanism, populate residual nucleus continuum and discrete levels, store recoil spectra (first CN only).
  10. calculate second-chance preequilibrium emission following MSD mechanism, store spectra of particles and recoils and increment residuals' populations. Although MSD is limited to a single type of nucleon, both neutron and protons are emitted in the second-chance process (first CN only).
  11. calculate neutron, proton, and  $\gamma$  emission spectra in terms of the exciton model (code DEGAS), populate residual nuclei continuum and discrete levels (first CN only).
  12. calculate neutron, proton, and  $\gamma$  emission spectra in terms of the HMS model (code DDHMS), populate residual nuclei continuum and discrete levels, store recoil spectra (first CN only).
  13. calculate neutron, proton,  $\alpha$ , and  $\gamma$  emission spectra in terms of the exciton model (code PCROSS), populate residual nuclei continuum and discrete levels, store recoil spectra (first CN only).
  14. calculate neutron, proton, and  $\gamma$  emission spectra in terms of the MSC mechanism, populate residual nuclei continuum and discrete levels (first CN only).
  15. calculate neutron, proton,  $\alpha$ ,  $\gamma$ , and eventually light ion emission widths in the frame of the Hauser-Feshbach model.
  16. calculate fission according to the selected fission model.
  17. normalize emission and fission widths with the Hauser-Feshbach denominator and fusion cross section to obtain compound nucleus spectra and population of continuum and discrete levels in residual nuclei.
  18. print results for the decay of the nucleus considered.
  19. select new nucleus and repeat steps 15 through 19 until all requested nuclei have been processed. The selection scheme is the following: starting from the compound nucleus, neutrons are subtracted until the number of neutron emissions specified in the input is reached. Then one proton is subtracted from the compound nucleus, and all nuclei with decreasing neutron number are considered again. In the Z-N plane the

calculations are performed row-wise from the top-right corner (compound nucleus) to the left. When a row is completed the one below is considered.

20. print inclusive spectra, read new incident energy from the input file (*.inp*) and repeat steps 4 and 7 through 20.

## 3.6 List of EMPIRE modules

The EMPIRE source is divided into modules which generally correspond to nuclear reaction mechanism or certain physical quantity. Communication among the modules is assured by a set of COMMONS located in the *global.h* file that is included whenever necessary. Each of the modules is described shortly below.

### **empire\_ctl.f**

*empire\_ctl.f* prepares files and input for optical model fitting or sensitivity calculations and controls these calculations. It calls the module *main.f*, which controls the nuclear model calculations, as many times as needed to perform the desired operation.

### **main.f**

*main.f* calls the module *input.f* for reading the input data and parameters, controls flow of calculations and prints final results. Also contains the RECOIL subroutine, which constructs recoil spectra when the ENDF=2 option is selected.

### **input.f**

Sets default values of input parameters, reads mandatory input and calls READIN for optional reading. Accesses data bases to retrieve discrete levels, binding energies, deformations and shell-corrections as well as experimental data from the EXFOR library. Defines the collective levels to be used by CCFUS and TRISTAN. Retrieves optical model parameters from the RIPL library and reads level density parameters. Finally, prints out input parameters to the output file (*\*.lst*).

### **ccfus.f**

Calculates fusion cross section for heavy ions in terms of a simplified Coupled-Channels approach. Collective states in target and projectile are identified in *input.f* and used in the CC calculations. As a first guess ground state deformation is assumed for all the collective states, and these can be modified by the user in subsequent runs. CCFUS also provides the fusion barrier used by other routines (e.g., distributed barrier model)

**tl.f**

This module determines the optical model transmission coefficients. Optical model parameters are retrieved from the RIPL-2 library and subroutine ECIS06 is called. The transmission coefficients are calculated inside the *tl.f* for heavy ions only. For light particles this task is delegated to ECIS06, and *tl.f* module ensures the proper transfer of calculated transmission coefficients to the rest of the system.

**subecis06m.f**

This module contains the ECIS06 Coupled Channel code by J. Raynal, which calculates total, elastic and absorption cross sections, elastic angular distribution, inelastic cross sections to collective levels and their respective angular distributions, as well as transmission coefficients. ECIS06 also provides analyzing powers but these are not used by the current version of EMPIRE. ECIS06 implements Coupled-Channels and DWBA models into EMPIRE. We note that ECIS06 has been converted into a subroutine in EMPIRE-3.1.

**fusion.f**

Calculates initial Compound Nucleus population after projectile absorption using transmission coefficients obtained either from the optical model or the distributed barrier model (for heavy ions). Also handles additional possibilities (reading absorption cross section for each partial wave from the external file, reading total absorption cross section from input, and reading critical value of angular momentum  $l_{cr}$ ) that are available for heavy ion induced reactions (see Section 2.1).

**MSD-orion.f**

Calculates two step Multi-step Direct amplitudes in the frame of the TUL theory. The results are later used by TRISTAN to produce Multi-step Direct cross sections. ORION is called from *main.f* and all input parameters are transferred through formal parameters rather than global common (too many conflicts in variable names). Communications with *MSD-tristan.f* occur through TAPE15.

**MSD-tristan.f**

Calculates two step Multi-step Direct cross sections from the results of ORION stored on TAPE15 folding them with the QRPA response functions (vibrational collectivity).

The module distributes the MSD spectrum over the residual nucleus continuum assuming that the spin distribution is proportional to the spin distribution of the 2-exciton states. MSD contribution is also distributed over discrete levels although in a very approximate and arbitrary way, feeding mostly 2+ and 3- levels (4+ to lesser extent) that are possibly close to the collective states of these multipolarities.

### MSC-NVWY.f

Calculates Multi-step Compound decay in terms of the NVWY theory. Neutrons, protons, and  $\gamma$ s are taken into account. Number of considered steps is fixed in the *dimension.h* file as a value of the NDMSCS parameter. If this number of steps is high enough, whole decay of the first CN is calculated within the MSC model, and Hauser-Feshbach calculations (*HF-comp.f*) are not invoked.

### ph-lev-dens.f

Contains a number of routines for the calculation of particle-hole state densities to be used by the MSC model. These routines also include accessible level densities for different type of transitions and take into account the binding condition.

### ddhms.f

Computes preequilibrium spectra with Hybrid Monte Carlo (HMS) simulation formalism developed by Blann and implemented by Chadwick. Treatment of the angular momentum transfer has been developed by Chadwick and Oblozinsky. The original code has been converted into a subroutine. Transfer of input data and results is undertaken by the EMPTRANS subroutine.

### degas.f

The Master Equation approach to the exciton model taking into account  $\gamma$  emission. The original stand-alone code has been converted into a subroutine. Input data are transferred to *SUBDEGAS* from the *main.f* via common blocks DEGASINPUT and DEGASINP. Decay is restricted to the first Composite Nucleus and the number of excitons is limited to  $n = 1, 3, 5$ , and  $7$ . The primary spectra of  $\gamma$ s, neutrons and protons, and population of respective residual nuclei are produced. Gamma cascade is blocked and left to the Hauser-Feshbach calculations, thus only the primary emission of  $\gamma$ s is allowed in the exciton model.

### pcross.f

The exciton model module, developed especially for EMPIRE, which takes into account emission of nucleons, primary gammas and clusters. The latter are treated within the Iwamoto-Harada formalism. PCROSS adopts the never come-back approximation, allows for incident clusters and gammas but ignores spin coupling and does not provide angular distributions.

### HRTW-comp.f

Calculates decay of the Compound Nucleus in terms of the HRTW theory (width fluctuation correction). Uses modified routines of standard Hauser-Feshbach (DECAY, DECAYG,

FISSION) and HRTW\_MARENG to decompose capture cross sections into partial wave components. In addition, contains a number of subroutines which are specific to the HRTW theory, and used to calculate the elastic enhancement factor, effective transmission coefficients, and bookkeeping of reaction channels.

### HF-comp.f

This Hauser-Feshbach module performs the bulk of Compound Nucleus calculations. Follows decay of states in the continuum in the parent nucleus to the continuum and to discrete levels in the residual nucleus through emission of light particles (neutrons, protons,  $\alpha$ s, and eventually a single type light ions). Also calculates full  $\gamma$ -cascade to the continuum and to discrete levels as well as discrete transitions between low lying levels, along with fission widths in which two viscosity effects are taken into account.

Intermediate results are stored on scratch arrays SCRT (continuum) and SCRTL (discrete levels) and are normalized with the initial CN population and divided by the Hauser-Feshbach denominator. The results are accumulated in the population array POP. Note, that particle emission from discrete levels is not considered.

If ENDF=1 option is specified *HF-comp.f* module decomposes particle and  $\gamma$ -spectra into components related to individual reactions. For example, a piece of the first-emission double-differential spectrum corresponding to the subsequent neutron emission is moved to the second-emission spectrum. Under these circumstances, it is assumed that no  $\gamma$ s are emitted between the two subsequent neutron emissions. At present, only two emissions are considered with ENDF=1 option, i.e., (n,3n) reaction spectra can not be processed into the ENDF format. One should invoke ENDF=2 option, which makes use of the cumulative representation (MT=5), to overcome this limitation.

### bar\_mom.f

Contains subroutines BARFIT and MOMFIT that were written by Sierk. The first one provides fission barrier height, ground-state energy, and angular momentum at which fission barrier disappears. The second subroutine calculates the three principal-axis moments of inertia.

The results arise from fits of fission barriers and moments of inertia calculated by Sierk in 1983-1985 using Yukawa plus exponential double folded nuclear energy, exact Coulomb diffuseness corrections and diffuse-matter moments of inertia. The calculated barriers are accurate to a little less than 0.1 MeV but the fit is a little less accurate. Worst errors might be as large as 0.5 MeV.

### lev-dens.f

Contains all subroutines used to calculate the level densities for all approaches used in EMPIRE. Includes retrieval of level density parameters and HF-BCS level densities and

functions for damping the collective effects. Cumulative plots of discrete levels and their comparison with the level density predictions are also performed within this module.

### **gamma-strgth.f**

Prepares deformation-dependent Giant Multipole Resonance parameters (for GDR, GQR and GMR) using built-in systematics and calculates  $\gamma$ -ray strength functions. Allows for a combination of the GMR and Weisskopf estimates. In the case of E1, uses generalized Lorentzian including energy-dependent GDR width and the non-zero limit at  $E_\gamma=0$ .

### **gamma-strength-analytic.f**

Calculates dipole radiative strength functions for  $\gamma$ -decay and photo-absorption using one of the following approaches MLO1, MLO2, MLO3, EGLO, GFL, SLO (adapted from the code provided by V. Plujko to RIPL-2).

### **print.f**

A small module, which prints histograms of spectra emitted from subsequent nuclei, and provides energy integrated cross section for these emissions.

### **pipe.c/pipe.f**

A small subroutine to execute UNIX command line from a FORTRAN or C code. The FORTRAN version *pipe.f* file is provided for the systems on which the C compiler is not installed (typically MS Windows).

### **auxiliary.f**

Set of auxiliary subroutines that contain general algorithms or perform numerical operations not related to any particular physical model. The module includes subroutines for fitting Legendre polynomials, integration, matrix inversion, interpolation, finding nucleus and ejectile index and setting to zero variables in EMPIRE.

## **3.7 Executing EMPIRE**

EMPIRE can be executed using scripts or through Graphic User Interface (GUI). The Graphic User Interface mode is the most convenient, and is recommended on UNIX systems with Tcl/Tk. Where the Tcl/Tk interpreter is not available, the user is advised to use the script mode. The manual mode should be the last choice if scripts can not be translated. For the sake of clarity these modes are described below in the reverse order.

EMPIRE execution may involve the following operation sequences, which are described in more detail below:



- "runE" sequence prepares data, runs the main calculation and prepares ZVView plots of pre-defined cross sections.
- "format" sequence generates the ENDF formatted file.
- "verify" sequence checks the ENDF file for formal correctness and internal consistency.
- "process" sequence performs post-processing to prepare a derived ENDF file, from which more advanced plotting is done.

The complete sequence is intended for the production of evaluated files in ENDF-6 format, but for theoretical modelling, execution of "runE" is sufficient. However, in this case automatic plotting is limited to the cross sections. A more detailed description of the task sequences is described below.

### 3.7.1 "runE" sequence (Run EMPIRE)

The script sequence sets up the environment for a new EMPIRE calculation and cleans-up the directories before launching a new EMPIRE calculation. More specifically, the following tasks are performed:

- Unnecessary files from a previous run are deleted.
- Locally modified files containing input parameters are retrieved.
- EMPIRE is executed; case-related files are renamed as appropriate.
- If the experimental data in computational C4 format are not available, they are generated from the EXFOR file, if present.

The "project name" is defined at this step. Usually this identifies the nuclide that is being processed (e.g. mn55, w182, u235, etc.). The project name is used in the filenames and is implied in the sections below whenever the "\*" appears in the filename.

### 3.7.2 "format" sequence

The following tasks are performed:

- EMPEND is executed to produce an ENDF file from the "short" EMPIRE output (with extension \*.OUT). The input file for EMPEND is generated within the script. The output file \*-e.endf is produced.

- ENDRES is executed (conditionally, if the new resonance file file `*-res.endf` is present on the local directory). The dummy resonance file in the ENDF file generated by EMPEND is replaced with the resonance data on the `*-res.endf` file. The comments from the specified file are appended after the original comments. All resonance data in ENDF File 2 are replaced. The background cross sections in the total, elastic, fission (if present) and radiative capture are set to zero from  $10^{-5}$  eV to the upper energy covered by the resonance parameters in the selected file. The lower energy of the elastic angular distribution is extrapolated to  $10^{-5}$  eV, if needed. The resonance covariance data in MF=32 are also copied, if available. The ENDRES input file is taken from the standardised input file ENDRES.INP, which can be modified by the user, if needed. The main parameters that can be changed are the filename from which the resonances are taken and the value of the LSSF flag, which defines how the unresolved resonance parameters are used (LSSF=0 to use URR to calculate cross sections; LSSF=1 to use URR for selfshielding only). The output ENDF file is `*-endres.endf` and the log file is `*-log.endres`.
- STANEF is executed to update the dictionary section in the new ENDF file. The STANEF input file is generated within the script.

The final output ENDF file from this sequence of operations is `*.endf`.

### 3.7.3 "verify" sequence

The ENDF Utility codes CHECKR, FIZCON and PSYCHE are executed to verify formal correctness and internal consistency of the final ENDF file. The input files are generated within the script. The output files are `*-log.checkr`, `*-log.fizcon` and `*.log.psyche` for the corresponding checking code.

### 3.7.4 "process" sequence

The Pre-Pro codes and some of the codes from the ENDVER package are executed to prepare the ENDF-formatted data for plotting. The output file `*-s.endf` is produced. The following codes and scripts are executed on the ENDF file:

- LINEAR is used to linearise any cross sections, which are not defined with log interpolation in energy or cross section.
- RECENT is used to reconstruct the resonance parameters into tabular cross section values.
- SIGMA1 numerically Doppler-broadens the cross sections to 300 K.
- LEGEND converts angular distributions in ENDF File 4, given by Legendre polynomial representation, into tabular form.

- SIXTAB converts double-differential data into angle-energy sets in tabular form (ENDF option LAW=7).
- "plotlst" script prepares the experimental data for plotting. It checks for the presence of the C4 file of experimental data and links auxilliary dictionary files for local use.
- PLTLST code generates a table of available types of nuclear data that can be reconstructed and compared with the information in the evaluated nuclear data files.

### 3.7.5 "run" sequence

All the main processing sequences are executed one after another.

### 3.7.6 Script mode

The EMPIRE distribution contains several scripts located in the *empire/scripts* directory. These scripts use UNIX bash-shell, which must be installed on the systems. Each script performs one or several steps, including those described in the previous section, taking care of moving, renaming and deleting the files and invoking the execution of appropriate codes. Scripts assume certain naming convention for the files, in particular, all input files must end with *.inp* extension. Unless specified differently, each script is invoked with a single parameter; the name of the input file without *.inp* extension (file root-name). For example, calculations with the input file *Mo100.inp* can be performed using *runE* script and typing

```
../scripts/runE Mo100
```

in the *empire/work* directory (or any other directory at the same level as *work*). General philosophy is that the root-name of the input file (*Mo100* in the example above) defines a project name. Scripts modify generic file names produced by the codes, renaming them by the project name plus the specific extension. These extensions must not be modified as they define the contents of the file (see Table 3.2) and are used as identifiers by the system. The project is set up by creating the EMPIRE input file with arbitrary root-name and *.inp* extension. In the following, we replace root-name with the asterisk '\*' and refer to the files through their extensions .

The following scripts are provided:

- |                |                                                                    |
|----------------|--------------------------------------------------------------------|
| <b>runE</b>    | executes the "runE" sequence described in the previous section.    |
| <b>format</b>  | executes the "format" sequence described in the previous section.  |
| <b>process</b> | executes the "process" sequence described in the previous section. |
| <b>verify</b>  | executes the "verify" sequence described in the previous section.  |

Table 3.2: Possible files for a given project (generally not all of them will be used). User created files are marked with ♣.

extension	generic name	contents of the file
*.inp ♣	INPUT.DAT	EMPIRE input
*.fus ♣	FUSION	set of $l$ -dependent transmission coefficients (one per each line) used for determination of the fusion cross section (optional)
*.lst	LIST.DAT	EMPIRE output (long )
*.out	OUTPUT.DAT	EMPIRE output (short )
*.lev	LEVELS	discrete levels for all nuclei involved in the run
*-lev.col	TARGET_COLL.DAT	characteristics of collective levels used for ECIS06 calculations
*.-omp.ripl	OMPAR.RIPL	optical model parameters read from the RIPL database
*.-omp.dir	OMPAR.DIR	optical model parameters used for DWBA or CC calculations with ECIS06
*-inp.fis	FISSION.INP FISSION.OUT	input parameters related to fission channel detailed output of fission calculations including intermediate results for purpose of checking
*.endf		results in the ENDF format including neutron resonance region and processed with FIXUP and STANEF (this is the final ENDF file for distribution)
*-e.endf		results in the ENDF format as produced by EMPEND (not yet fit for distribution)
*-s.endf		results in the ENDF format after processing with PREPRO codes (ready for plotting but not legal ENDF file for distribution!)
*.exf	EXFOR.DAT	relevant experimental data retrieved from EXFOR (if EXFOR installed)
*.c4		relevant EXFOR data translated into computational format
*.ps		full set of PostScript plots comparing calculations against experimental data
*-cum.ps	CUMULPLOT.PS	cumulative plots of discrete levels in PostScript format
*-MT.zvd		ZVView file for plotting MT (MT=2, 4, 16,...)
*.x42c4_lst		output of X4TOC4 code
*.x42c4_errs		list of EXFOR entries not translated by the X4TOC4 code
*.war		warnings extracted from the EMPIRE output *.lst

Table 3.3: List of log-files

extension	contents of the file
*-log.empend	produced by EMPEND when converting EMPIRE output into ENDF-6 format
*-log.endres	produced by ENDRES when merging EMPIRE results with the resonance region
*-log.checkr	results of format checking with code CHECKR
*-log.fizcon	results of physics checking with the code FIZCON
*-log.psyche	results of format checking with code PSYCHE
*-log.legend	produced by the PREPRO code LEGEND
*-log.linear	produced by the PREPRO code LINEAR
*-log.recent	produced by the PREPRO code RECENT (resonance reconstruction)
*-log.sigma1	produced by the PREPRO code SIGMA1 (Doppler broadening)
*-log.plotc4	produced by the code PLOT4 (cross section plotting)

<b>run</b>	executes all of the above sequences one after the other.
<b>staneF</b>	runs ENDF-6 format standardization code STANEF
<b>c4</b>	converts EXFOR data in the *. <i>exf</i> file into the computational format (file *. <i>c4</i> ) (included in <b>runE</b> )
<b>sortc4</b>	sorts experimental data in the computational format (*. <i>c4</i> file) (included in <b>runE</b> )
<b>plot</b>	runs PLOT4 to create comparison plots of experimental and calculated cross sections; the log-file from PLOT4 is an index of experimental data that can be compared to quantities derived from evaluated nuclear data files (obsolete)
<b>plotlst</b>	produces the index of experimental data without doing the lengthy PLOT4 run
<b>storemul</b>	moves all files matching pattern za*\$2* to the directory ../\$1 (creates ../\$1 if it does not exists). \$1 and \$2 are the parameter of the script, e.g., to move files obtained related to isotopes of iron (using input files of the type za260xx.inp) to the directory ../default_om one should issue a command ../scripts/storemul default_com 260
<b>clean</b>	removes all files related to a given project (except the input file *. <i>inp</i> ) and any <i>core</i> file. This script must be run each time a project is changed by adding new channels or by modifying projectile or target in the input file <i>.inp</i> .
<b>cleansel</b>	removes selected files related to the given project
<b>cleanall</b>	removes <b>all</b> output files for all projects in a current directory; only input files (*. <i>inp</i> ) are retained

**store** moves *.inp*, *.lst*, *.out*, *.ps*, *.endf*, and *.res* files for all projects (*.inp* files are copied rather than moved) to a subdirectory specified as a parameter to *store*. If the subdirectory does not exist, one will be created, which avoids old files being overwritten by new ones (e.g., when calculations are repeated with modified parameters). For example, the results of calculations with the Moldauer’s optical-model parameters can be saved in the subdirectory *OM-Moldauer* by issuing the command:

```
../scripts/store OM-Moldauer
```

**grepawk** handy tool for extracting specific excitation function from the EMPIRE output *.lst* and arranging into two columns (incident energy, cross section). Such a representation allows any standard package to be used (e.g., gnuplot or xmgr) to plot excitation functions for any calculated cross section (e.g., population of a certain discrete level). The user must create a file with the project root-name and extension *.pat* containing two line pattern as in the example below:

```
incident energy
.3350 MeV      7.0 level
```

The first line must be left intact. The second should be changed according to the needs, and has to be the exact string that uniquely identifies a line of the output from which the cross section is to be extracted. A convenient method is to cut and paste between *.lst* and *.pat* files. As usual, script is invoked with the project name as a parameter. UNIX package “awk” is used to scan the *.lst* output. Each time a line is encountered that matches “incident energy”, the projectile energy is extracted. When a match occurs to the second line of *.pat* file, the requested cross section is identified as the word immediately before the “mb” string and extracted. The resulting excitation function is written to the file *.res*. Note that each use of *grepawk* will overwrite the *.res* file. Starting with version 2.16, similar functionality can be achieved with the *zvpl* script which produces *\*.zvd* and calls ZVView to display this file.

**run-piece-wise** runs up to three different inputs for the same reaction, combines the results and processes them through the utility codes to produce a single ENDF file and relevant plots. Different models and/or model parameters are allowed in three separate energy ranges. Users have to ensure that incident energies are monotonically increasing across the three sets of input parameters.

**zvd** plots comparisons of calculated and experimental data using ZVView graphic package. Script is called with MT number and project name as parameters. For example, to plot (n, $\gamma$ ) reaction for the *100mo* project one should type:

Table 3.4: Most frequently used MT numbers and corresponding reactions

Reaction	MT
tot	1
elastic	2
inelastic	4
(n,2n)	16
(n,3n)	17
(n,f)	18
(n,n $\alpha$ )	22
(n,np)	28
(n,np $\alpha$ )	45
(n, $\gamma$ )	102
(n,p)	103
(n, $\alpha$ )	107
(n,p $\alpha$ )	112

```
../scripts/zvd 102 100mo
```

in which zvd script uses *\*-s.endf* file for plotting. If this does not exist, script invokes the **process** script to reconstruct (n,inl), (n,p) and (n, $\alpha$ ) reactions and produce File 6 in a form suitable for plotting. This file is processed along with *\*.c4* that contains experimental data to produce *\*-MT.zvd* file (*MT* is any legal ENDF-6 format MT number). List of typical MT numbers is given in the Table 3.4

- zvcomb** allows an arbitrary number of existing zvd plots to be combined into one. If zvcomb is called without any parameter, a list of available *\*.zvd* files is displayed on the terminal, so that the names can be pasted onto the command line.
- zvpl** similar to grepawk but produces *\*.zvd* file and displays by calling ZVView. Can be operated from the Graphic User Interface *Xrun.tcl*.
- zvv** combines and displays various ZVView plots as a single plot, e.g.,  

```
../scripts/zvv nb93*.zvd
```
- zvvddx** create a ZVView plot of excitation functions, angular distributions, spectra, or double-differential cross sections (intended for use within the Graphic User Interface *Xrun.tcl*)
- mtacomp** produces ZVView plots that compare experimental data with the results of up to three sets of calculations (or evaluations) in the ENDF format for a given MT number and target. The syntax is:

```
../scripts/mtacomp MT comp root dir1 name1 file2 name2 file3 name3
```

where: *MT* stands for the ENDF reaction code (see Table 3.4), *comp* is an arbitrary string added to names of plot files, *dir1* points to the directory containing the first ENDF file, *file1* and *file2* indicate the remaining two ENDF files and *namei* are labels of the respective curves. Note, that *dir1* must contain the ENDF file named *root-s.endf* and optionally EXFOR data in the computational format in the file named *root.c4*. The naming convention is automatically ensured if the files were created by EMPIRE. There are no restrictions on the names of the remaining two ENDF files. The script is intended for use within the GUI but can also be run manually.

**acomp** same as *mtacomp* but does the job for the whole list of MTs in Table 3.4; therefore, *MT* is omitted from the list of parameters. The script is intended for use within the Graphic User Interface but can also be run manually.

**showzvd** calls ZVView package for each *.zvd* file from the argument list.

Note that EXFOR library must be installed in order to compare calculations with experiment and that in most cases plots are created from the ENDF formatted file. The detailed description of the X4TOC4 input is given in the source file *empire/util/plotc4/plotc4.f* and in the manual *empire/util/plotc4/manual.txt*.

### 3.7.7 GUI mode

The Graphic User Interface (GUI) mode is the most convenient way of running EMPIRE, and requires Tcl/Tk to be installed on the computer. Actually, the Tcl scripting language and the related graphic Tool kit (Tk) are available freely for practically any operating system [91]. On most Linux distributions Tcl/Tk is installed by default. For convenience of the user EMPIRE-3.1 comes with the ActiveTcl package, which is easy to install and seems to run on various flavors of Linux (version for Windows is also available from <http://www.activestate.com/Products/ActiveTcl/>).

Standard GUI of EMPIRE-3.1 is a Tcl script *Xrun.tcl* that can be started in any 'working' directory by typing

```
$EMPIREDIR/scripts/Xrun.tcl &
```

We start discussion of the GUI with a few features that apply across the entire interface:

- Action of many buttons is simply calling an appropriate script with a project name as an argument.
- Double-click on the file in the list will generally open it with the default application (i.e., text files will be open with the selected editor, PostScript files with the selected viewer, and \*.zvd files will be displayed using ZVView). Within lists typical mouse



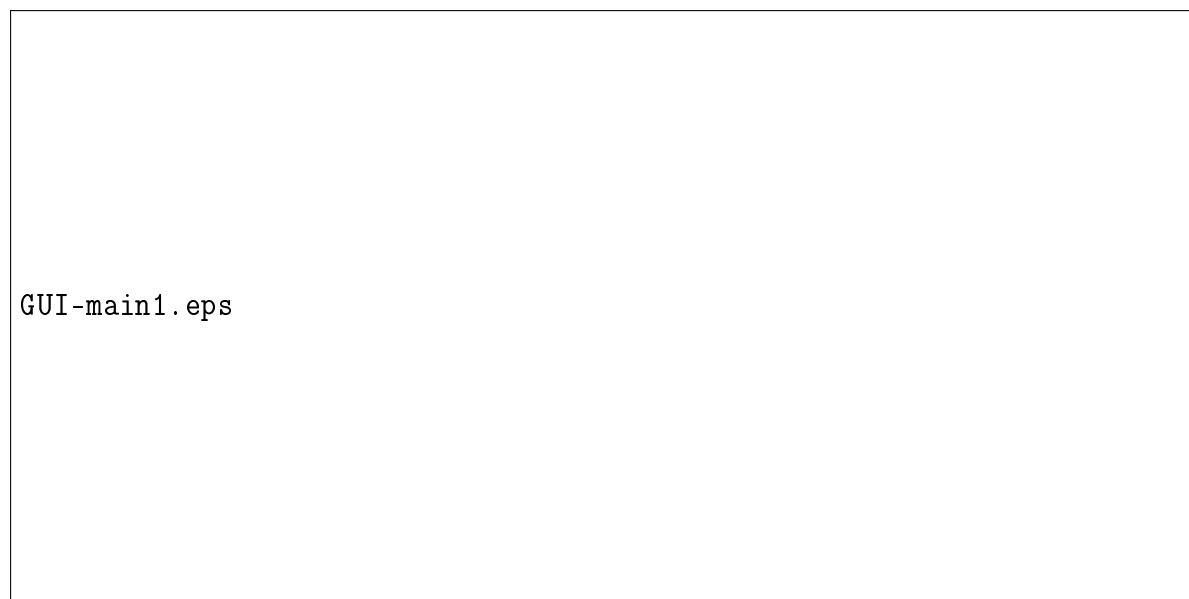


Figure 3.1: EMPIRE GUI - Main1 panel

selection modes are usually available (although the first file only will be open for editing):

- a single-click selects the file,
  - continuous selection by dragging mouse with the left button pressed,
  - continuous selection by clicking left mouse button while holding shift key pressed at the end of the region,
  - arbitrary multiple selection by clicking left mouse button while holding 'Ctrl' key pressed.
- Whenever Tcl/Tk allows a 'balloon-help' is showed when cursor remains above the button or icon for a short period of time. This help is hoped to be sufficient to operate the interface without additional instructions. Note that if cursor is moved fast across the interface the 'balloon-help' which appears on the screen might refer to a button different from the one to which the cursor actually points. To be sure that the help is correct keep in mind that help string always starts exactly below the middle of a button or icon.
  - Colours on the GUI buttons follow 'traffic light scheme' - green means that pressing button at any time will not make any damage, red warns that some data or files that have been obtained before or manually edited might be lost (overwritten). Generally, all buttons involving editor calls are green while button involving execution of codes or deleting files are red. Similar distinction is introduced between the files - red is

used for those which are likely to have been manually edited and green or orange for those which are easy to recreate by rerunning the code .

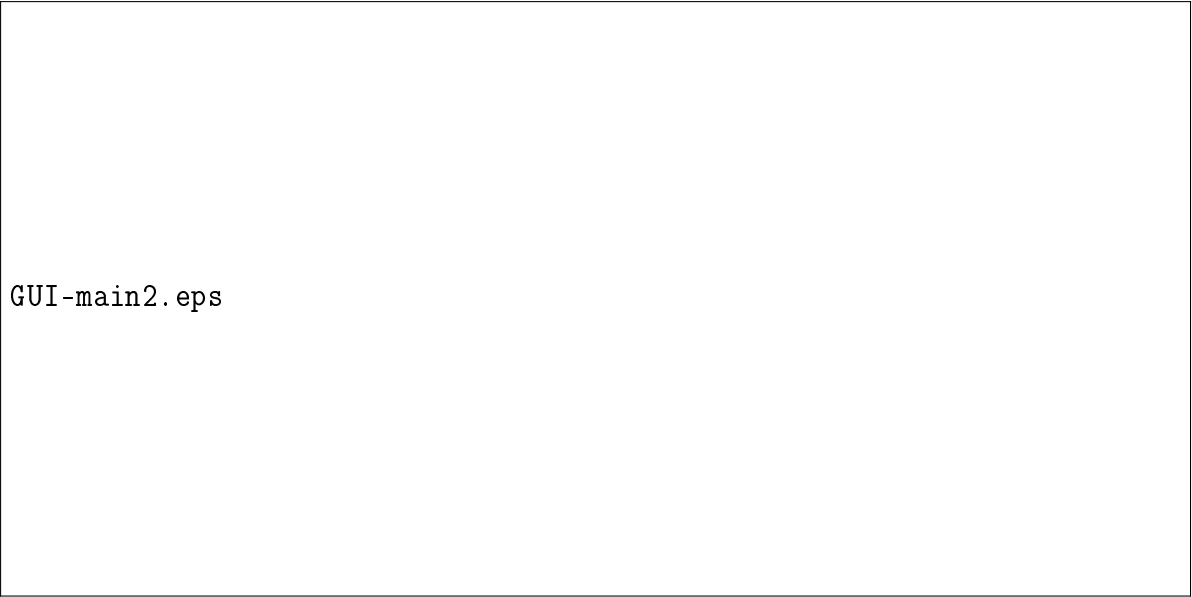
Due to a large number of operations and extended lists the new GUI is organized in a form of a notebook with several panels. Generally, there are several equivalent ways of performing the same operation and the user may choose the one which suits him best. All basic functions, such as running the code and viewing the results can be achieved from the pull-down menus and icon-denoted buttons below the menu bar. On the other hand, more advanced features such as plotting and file management can only be accessed from the various panels.

All operations (except multiple run) begin with the selection of the project name that will be used as a root of the input file name (say 56Fe). Existing project can be selected by clicking on the 'open folder' icon to the left of the GUI. The following icons (from left to right) allow to (i) edit input, (ii) launch full chain of calculations, (iii) run EMPIRE only, (iv) view long EMPIRE output, (v) view short EMPIRE output, (vi) view ENDF-6 formatted file, (vii) view EXFOR data, (viii) view EXFOR data in computational format, (ix) view PLTC4 plots, (x) refresh list of files, (xi) change working directory, and (xii) remove all files related to the project except input. More operations are possible from individual GUI panels.

**Main1 panel** - (Fig. 3.1) provides for essential control of calculations. It allows to create a new input file (clicking on the "Create" button copies the standard input file *skel.inp* to *56Fe.inp* and opens it for editing), executing selected parts of the system (physics calculations, formatting, verification, preprocessing and plotting). One should keep in mind, that format verification and preprocessing can only be performed if EMPIRE calculations and ENDF-6 formatting were carried out before, and plotting is only possible starting from the preprocessed file. Main1 panel gives also access to output and output/input files produced by EMPIRE in the first run.

**Main2 panel** - (Fig. 3.2) provides additional four features for which there was not enough room on the Main1 panel.

- Piece-wise run allows to run calculations using different input in three non-overlapping energy ranges. Clicking on the 'Create 3...' button makes 3 copies of the main EMPIRE input. These 3 copies can be modified allowing for use of different parameters or models providing that they refer to the same combination of target and projectile and allow for the same number of emissions. The energy ranges must be chosen in such a way that input *a* covers the lower part, input *b* intermediate and input *c* the upper part of the requested energy range. When 'run-pieewise' button is hit calculations are executed for all three input files, respective outputs are merged and the resulting file is formatted and processed as if obtained in a single run. Note that use of different parameters and models in the three energy ranges will generally produce discontinuities at the borders. The piece-wise calculations are also possible with 2 input files only (the third one should be deleted in such a case).



GUI-main2.eps

Figure 3.2: EMPIRE GUI - Main2 panel

- OMP fit section allows to run manual fit of the optical model potential. EMPIRE provides limited support by producing plots of selected cross sections (angular distributions) and comparing them with the best previous set. Input option FITOMP should be set to 1 to restrict calculations to those relevant to optical parameter fitting (e.g., second neutron emission will not be followed even though specified in the input). After the first calculation is completed user should create up to 2 plots using the right part of panel 'ZVV plots' (each of them may contain a number of curves) and name them in the 'List name' field as *omp1* and *omp2*. Then, optical model parameters can be adjusted manually by editing respective files and calculations re-run. This will automatically produce previously defined plots overlayed with those obtained in the first run. If the new calculation performs better it can be set as a temporary reference set by hitting the 'Store as ref.' button. Next results will be compared to this reference until a new reference is defined.
- EXFOR section provides access to the stand alone EXFOR retrieval that is graphically similar and functionally identical to the one available from the IAEA and NNDC web sites. Under normal circumstances this retrieval is not necessary as it is performed internally by EMPIRE during the first run. However, user may choose to use manual retrieval interface in order to exercise direct control on the retrieved data. When the EXFOR interface is closed the resulting file with experimental data is automatically renamed to conform to the current project. It is up to the user to ensure that the data retrieved are actually relevant to the calculations. Once retrieved, the data have to be converted into the computational format ('Run X4TOC4' button) and sorted ('Sort C4' button). The same sequence of buttons should also be used if



GUI-ZVV.eps

Figure 3.3: EMPIRE GUI - ZVView plots panel

users decides to modify the existing *\*.exf* file (e.g., by removing or adding certain entries)

- ECIS section allows to view the most recent input and output of ECIS06 code (note that these files are overwritten in each calculation for each incident energy)

**ZVV plots panel** (Fig. 3.3) provides for a powerfull interface to the ZVView plotting package. The window to the left lists all ZVView plots (*\*.zvd* files) that have been previously created. User can display them by double-clicking on any of them. Selecting several plots and double-clicking on the last one will combine all the selected curves into a single plot. Note that 'Filter' field allows to restrict displayed files to those containing filter string in the name (by default Filter is set to the project name). There are 4 possibilities of creating ZVView files:

- Selecting MT number and hitting 'Plot selected MT' (note that any valid ENDF-6 MT number can be typed into the field in addition to those which can be selected from the predefined list). The MT number is included in the plot filename for identification (e.g., *56Fe-102.zvd* for capture). This method allows to plot only excitation functions (cross sections) for the current calculations (ENDF-6 formatted file must exist).
- Hitting 'Launch ZVV Interface' will start more powerfull GUI that allows to create the same type of plots as before but including up to 3 additional ENDF-6 formatted files for comparison.

- 'ZVV plots from EMPIRE' is a bit cumbersome way of creating a cross section ZVView plot by selecting unique string identifying output line containing the cross section of interest, pasting it into the other window and filling additional information (next line, title, etc.) as requested. The advantage of this method is that the ENDF-6 formatted file is not required and any cross section (number followed by 'mb') in the long output (\*.lst) can be plotted. This includes quantities that can not be plotted with the previous methods since not stored in the ENDF-6 formatted file (such as cross sections for the population of discrete levels in any nucleus or intensities of  $\gamma$ -rays).
- Selecting plots from the window to the right of the GUI (list created by PLOT4 or *pltlst* script). This is the only possibility of plotting angular distributions, and energy spectra with the ZVView package. For the relevant line being included in the list there must be a match between experimental data and calculations (i.e., plots are only possible if adequate experimental data are available). Multiple selection can be plotted and each of such selections can be stored by specifying its name in the 'List name' field. When multiple selection is plotted the individual curves are offset from each other by a number of decades specified in the 'Shift 10\*\*' field. It implies that the  $y$ -scale be logarithmic unless shift is set to 0. 'Eres (rel)' is the experimental relative energy resolution used to spread discrete lines (e.g., elastic) and to smooth continuum in the plotted energy spectra. The 'Comapre to' field allows to select another ENDF-6 formatted file to be included in the plots. Note that in order to obtain correct plots the additional file should be preprocessed in a way analogous to the original EMPIRE file (resonances will not be plotted unless the cross sections are reconstructed from the resonance parameters and double-differential data will not be plotted unless converted into the right format).

**Logs panel** (Fig. 3.4) provides access to various output files that should be inspected for possible errors encountered during EMPIRE execution, EXFOR translation into computational format, ENDF-6 formatting, format verification and preprocessing.

**Files panel** (Fig. 3.5) offers file management functions tailored to facilitate operation of the EMPIRE code. Large number of files produced in a single EMPIRE run might result in a very crowded working directory if the latter contains several projects. Files panel is designed to facilitate access to files belonging to a current project by setting default value of the filter to the root-name of the project. User can modify filter value to restrict further list of the files (e.g., filter set to *56Fe\*endf* will show only files with extension \*.endf belonging to the *56Fe* project) or relax it to display more files (e.g., filter set to *inp* will show input files for all projects). We note that, selecting a file with a name consisting only of the root-name and extension (e.g., *56Fe.exf* but not *56Fe-log.psyche*) and hitting 'Change to its project' button is a convenient way of redirecting GUI toward another project. The left part of the panel provides for a convenient removal of the selected types

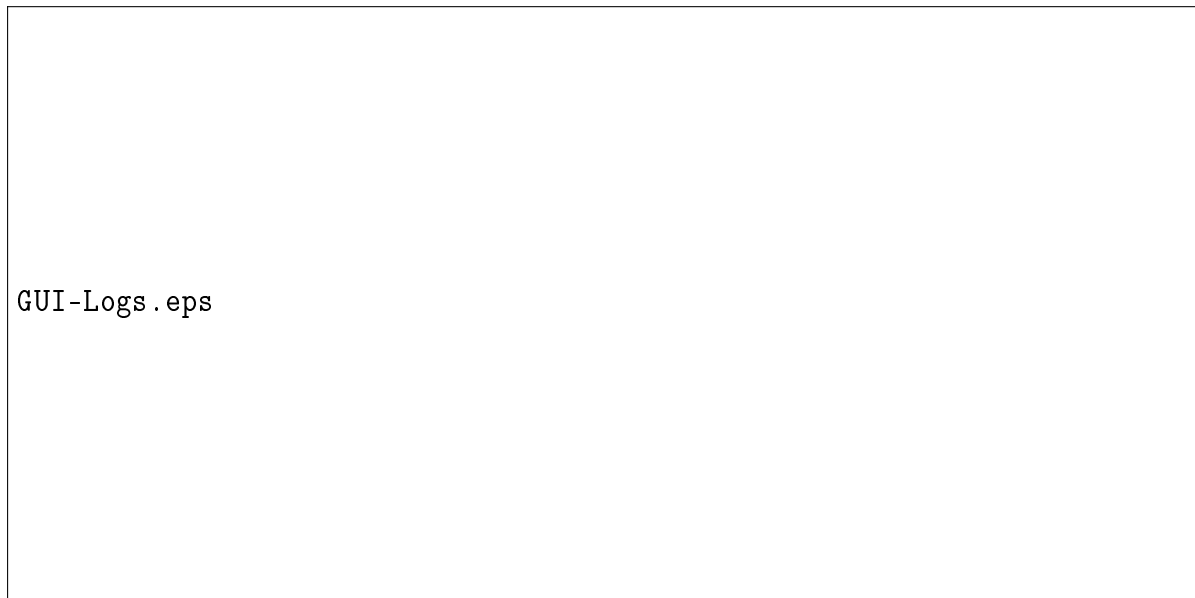


Figure 3.4: EMPIRE GUI - Logs panel

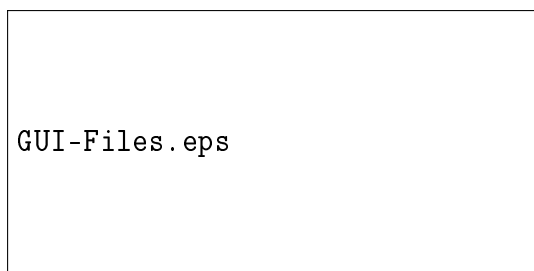


Figure 3.5: EMPIRE GUI - Files panel

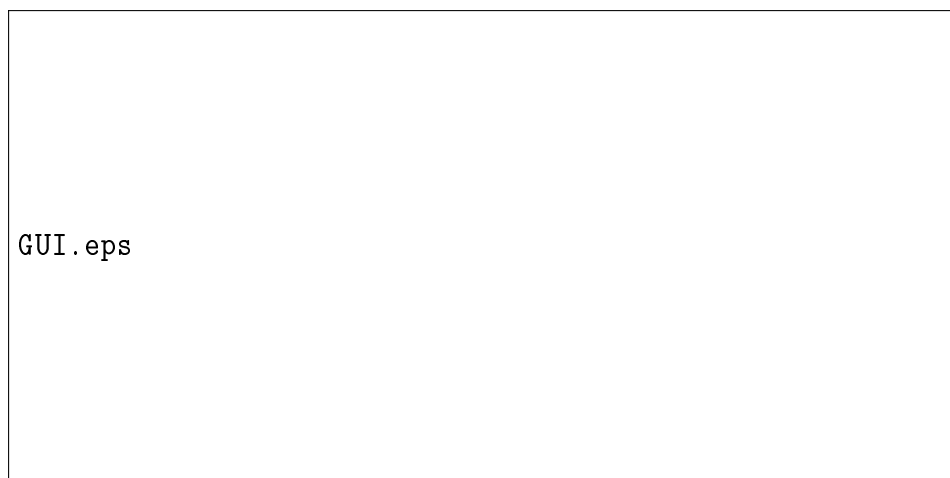


Figure 3.6: Old EMPIRE GUI

of files belonging to the current project. In addition, individual files can be removed by clicking on the 'Delete all selected' button. A double-click on any of the listed files will open it with an appropriate application.

**Folders panel** - (Fig. )

**Multirun panel** - (Fig. )

**Source panel** - (Fig. )

*To be completed*

## 3.8 ENDF formatting

The ENDF formatted file is created by the user selecting the ENDF option in the input file (\*.inp). This instructs EMPIRE to write all necessary information to the output file \*.out, which may actually become very long, depending to some extent on the choice of input options in the EMPIRE calculations. This file is processed by the utility code EMPEND written by Trkov, which creates the ENDF-6 formatted file.

Rather than providing exclusive cross sections and associated spectra for each of the reactions separately, EMPIRE can output inclusive cross sections, spectra and double-differential cross sections. This means that the total emission spectra of neutrons, protons,  $\alpha$ -particles and  $\gamma$ s are printed, instead of individual contributions from the reactions, with the exception of some distinct reactions that are always treated exclusively (e.g. inelastic, (n,2n), (n,p), etc.) This is the preferred mode of EMPIRE execution when ENDF formatting is required. EMPEND automatically recognizes the calculation options from the contents and acts accordingly.

EMPIRE also calculates cross sections for the production of metastable isomers. EMPEND recognises these and stores them in ENDF File 10. Cross sections for radionuclide

production, which can not be uniquely associated with any specific reaction (i.e. an ENDF MT number) are lumped into File 3 MT 5, but to preserve the complete information, the radionuclide production is stored in File 10, MT 5. This can be done because according to ENDF-6 rules the cross sections in File 10 by definition are not required for the reconstruction of redundant reactions.

The ENDF file has to obey the rules of sorting the data in increasing order by data type (MF number) and reaction type (MT number), so several sweeps of the EMPIRE output file must be made, which may slow down the formatting process considerably. In general, the required operations are described as follows:

- In the first sweep the cross sections and the corresponding reaction Q-values are extracted. All reading is done with the REAMF3 routine.
- In the next sweep all reactions for which particle spectra are given are identified. All reading is done with the SCNMF6 routine.
- Another sweep is made for each reaction having angular distributions. This applies to the elastic and all discrete level reactions (inelastic neutron, alpha and proton emission).
- Next follows a sweep for each reaction having energy-angle correlated outgoing particle distributions.
- Finally, a sweep is made for the remaining reactions, particularly the  $(n,\gamma)$  reaction, for which the particle distributions are coded in ENDF File-6.

In the first sweep radionuclide production cross sections are located and the MT numbers are assigned, when possible. Cross sections, which can not be identified uniquely by an MT number are assigned  $MT=10(Z*1000+A)+LFS$  where LFS is the final isomeric state of the nuclide. The spin of the target nucleus, the  $S_0$ -strength function, the average gamma width, the average level spacing and the energy-dependent scattering radius are also extracted to enable the assembly of the dummy resonance parameter file.

In the second sweep, all reactions that do not have explicitly given spectra are identified. When many exclusive spectra are requested in the EMPIRE calculation, there may be cases where particle spectra are given but no MT number is assigned. The spectra are ignored, the cross sections are added to MT=5 and particle production cross sections for this MT are incremented. This preserves particle multiplicities, but spectral shapes may become distorted. After the second sweep, all necessary information is available to write the comments-section (MF=1) and the prompt nu-bar (if the nuclide is fissile). For incident neutrons a dummy resonance file (File 2) is constructed. The cross section data found on the file are fitted by a cubic spline and entered into the output ENDF file on a user-defined dense energy grid, thinned to the specified tolerance and taking reaction thresholds into account. If desired, the spline interpolation may be suppressed and the energy points found on the file are entered directly into the ENDF formatted file.



The angular distributions for discrete level reactions that appear in the ENDF File 4 sections are extracted from the spectra on the EMPIRE output file, interpolated to the appropriate energy, if necessary. Legendre polynomial coefficients in the centre-of-mass are fitted to the distributions. For elastic scattering the Legendre coefficients are copied directly from the EMPIRE output; If more than 64 Legendre coefficients are required, formatting switches automatically to pointwise representation.

The correlated energy-angle distributions for continuum reactions that appear in ENDF File-6 sections are entered in Legendre polynomial representation in the centre-of-mass coordinate system. The maximum Legendre order is limited to 64. For reactions with relatively smooth angular distributions, the number of coefficients is reduced accordingly.

Photon production information for discrete levels can be stored in ENDF Files 12 and 14. The spectra for the continuum are included in File-6 (rather than File 15). File 12 contains photon transition probabilities and photon emission probabilities for discrete level reactions, while File 14 contains the corresponding angular distributions, which are assumed isotropic. The gamma spectra of the (n,gamma) reaction are presently stored in File-6. Primary gammas, which are optionally printed in the Empire output explicitly are not formatted. This option should not be used when ENDF formatting is required. By default, primary gammas are included in the photon spectrum in tabular form.

### 3.8.1 EMPEND Input instructions

The program can be executed interactively from a terminal screen. The required input is entered in response to the prompts, which are the following:

- The name of the EMPIRE output file to be processed.
- The name of the ENDF formatted file to be written.
- Number of subintervals per incident neutron energy interval on the EMPIRE output file. The subintervals define the fine energy mesh for the cross sections on the ENDF formatted file. The following are applicable:
  - 0 Only the points on the EMPIRE output are entered to the ENDF formatted file.
  - 1 The points at reaction thresholds are added. The energy points above threshold are as found in the EMPIRE output file.
  - n Threshold points are entered, but in addition, each interval on the EMPIRE output is subdivided into "n" subintervals. Cross section values at intermediate points are defined by a cubic spline fit.
- Thinning tolerance limit [%] to reduce the number of cross section points. Data points, which can be reproduced from the neighbouring points by linear interpolation to within the specified tolerance, are removed. Entering a negative value for the thinning tolerance limit causes thinning to be suppressed.

- ENDF material number identifier.
- NLIB number assigned to the evaluation (see ENDF-6 manual). The parameter is optional.
- ALAB, EDATE, AUTHOR string, where each of the listed parameters occupies 11 columns (see ENDF-6 manual for details). The parameters are optional.

## NOTES:

- Extensive exclusive spectra calculations in EMPIRE should be avoided when ENDF formatting is needed, since for complex reactions when a residual nuclide can be produced from more than one reaction, the assignment of spectra can not be done uniquely. It is recommended to allow up to 4 emitted neutrons and only a single charged particle.
- All text preceeding the printout for first energy is transferred to the comments section in the ENDF file (FM=1, MT=451). The easiest way to insert customised comments into the ENDF file is to modify (manually) the EMPIRE output.
- The resonance file (MF=2) that is generated for files with incident neutrons is by no means a realistic cross section representation. It is given for completeness, when no information on the resonances (other than from the systematics is available). The code places resonances spaced uniformly around the thermal value according to the given average level spacing. The neutron width is defined from the S0 strength function and the gamma-widths are the average gamma widths. The assigned resonance formalism is the Multi-level Breit-Wigner formalism with energy-dependent scattering radius.

To monitor the formatting process for quality assurance purposes, the EMPEND.LOG file is written in which the details of the formatting process are recorded. A limited amount of checking is done. An entry to the log file is added in the following cases:

- The cross section obtained by integrating the spectrum should agree with the value given directly in the EMPIRE output file. If the difference exceeds 2% a warning message is written, giving the reaction MT number, the incident particle energy, the expected cross section (i.e. the value given directly in the EMPIRE output file) and the percent difference.
- The angular distributions are fitted to determine the Legendre polynomial expansion coefficients. If the distribution reconstructed from the Legendre polynomial coefficients differs from the pointwise values on the EMPIRE output file by more than 5% is written, giving the reaction MT number, the outgoing particle ZA identifier, the incident and the outgoing particle energies and the percent difference in the fitted distribution from the pointwise value on the file.

Additional messages monitor the progress of the data formatting process.

## 3.9 Fitting Optical Model Parameters

When the FITOMP option is selected in the input, EMPIRE will perform automatic fitting of parameters in the direct optical model parameter file, OMPAR.DIR (\*-omp.dir), and of deformation parameters in the file containing the collective target levels, TARGET\_COLL.DAT (\*-lev.col). The fitting procedure also uses the experimental data file in C4 format, C4.dat (\*.c4). To ensure the existence of these files, EMPIRE should be executed at least once before fitting begins and should be executed with the DIRECT option selected and an incident channel optical potential (initially) defined using the DIRPOT option, both in the initial run and during fitting. At the moment, the FITOMP option only works for neutron or proton scattering.

All data relevant to an optical model fit - total, elastic and collective inelastic cross sections and elastic and collective inelastic angular distributions - within the requested energy range are selected from the C4.dat file and included in the  $\chi^2$  to be minimized. The data points in the  $\chi^2$  are weighted in the standard manner using the experimental uncertainties given in the C4.dat file. Natural element data can be inserted in the C4.dat file and used in the fit. In the case of neutron scattering, the file *empire/RIPL-2/resonances/resonances0.dat* is also searched for an s-wave strength function, which is included in the experimental data set when found.

The lower limit of the energy range for calculations used in a fit is initially taken to be 1 keV while the upper limit is taken to be 30 MeV, unless modified using the FITEMX option in the input. All relevant experimental data within this range in the C4.dat are included in the  $\chi^2$ . The incident energies given in the input file define the grid of energies used for calculations, unless the FITGRD option is used. When the input file energies are used, the data points outside of the energy interval they define are not taken into account. That is, the fitting procedure will interpolate calculations but will not extrapolate them. When the FITGRD option is used, the energy interval is extended to include all data points in the initial energy range. In both cases, the grid of incident energies is compared with those of the experimental data and superfluous values are eliminated to speed up the calculation.

The parameters to be adjusted are specified by using the FITabc or FITDEF options, described in more detail below. The RIPL-2 parametrization described in Section 3.4.3 is used to identify the optical model parameters, any of which may be adjusted. The adjustable deformations are simply those of the collective level file. Quadrupole and hexadecupole deformations are permitted for nuclei identified as rotational, while quadrupole and octupole deformations are permitted for those identified as vibrational. The FITabc and FITDEF options typically identify the desired parameter and furnish a shift in its initial value and the maximum variation allowed during the fit with respect to its (shifted) initial value. If no parameter adjustment is requested or all adjustable (possibly shifted) parameters have a maximum allowed variation of zero, the  $\chi^2$  is calculated but no fitting is performed. At most 20 parameters may be shifted and/or adjusted simultaneously.

At present, the optical model fitting is performed using a simple numerical gradient search to minimize the  $\chi^2$ . The adjusted parameters are stored in the modified OMPAR.DIR (\*-omp.dir) and TARGET\_COLL.DAT (\*-lev.col) files. Information on the fit

is written in the FIT.OUT (\*-ompfit.lst) file. When a fit is complete, EMPIRE is run one last time with all options and energies given in the input file, excepting the fit ones.

## 3.10 Input/Output files

### 3.10.1 \*.inp (INPUT.DAT; main input)

EMPIRE is set up to read as much data as possible from the input parameter library (*empire/data*). The user has to supply only those input parameters that the code can not know. These are the incident energy, the projectile, the target and the number of neutron, proton,  $\alpha$ , and light-ion emissions to be followed. In principle, the number of emissions could be eliminated by following the compound nucleus de-excitation until all the energy is exhausted. However, this is not very practical, as in most cases a very large amount of memory would have to be allocated and a lot of CPU time consumed to calculate exit channels that might be of no interest.

With the default library of input parameters it is possible to execute a 'first-shot' calculation with minimal effort. In the second step, the user may wish to regain control over the input in order to make appropriate adjustments to the parameters. This can be done in a selective way in the optional part of the EMPIRE input.

It should be noted that there is a difference in the way EMPIRE accesses general input library in the first and subsequent runs of a given project. In the first run the code extracts relevant data from the input parameter library and creates files with discrete levels (\*.lev), collective levels (\*.lev.col), optical model parameters (\*.omp.rtpl, and \*.omp.dir) and relevant EXFOR data (\*.exf and \*.c4). Once these files exist the code uses them instead of the files contained in the general input library. This has two advantages: (i) time is spared because the case specific files are small and can be read fast, (ii) the user may edit \*.lev, \*.omp.\*, and \*.c4 files and modify them without affecting files in the general input library. Editing the \*.omp.\* files is a convenient method of adjusting some of the optical model parameters without the necessity of typing the whole set from scratch.

Input data are taken from different sources in the following order (those listed above overwrite those listed below):

1. case specific files (\*.lev, \*.lev.col, \*.fus, \*.omp.\*)
2. input file (\*.inp)
3. general input parameter library

Note, that all the files, except \*.inp, are created by the code during the first run, and therefore the user has to create only the \*.inp file described below.

### Mandatory input

Input to EMPIRE consists of two parts. The first is mandatory and contains basic data necessary to specify the case, and the structure is illustrated by the following example:

```

14.8                ;INCIDENT ENERGY (IN LAB)

56.  26.            ;TARGET A , Z

1.   0.              ;PROJECTILE A, Z

3                ;NUMBER OF NEUTRONS TO BE EMITTED

1                ;NUMBER OF PROTONS TO BE EMITTED

1                ;NUMBER OF ALPHAS TO BE EMITTED

0  0.  0.           ;NUMBER OF L.I. TO BE EMITTED AND ITS A AND Z

```

The first line specifies the incident energy in the laboratory system (in MeV). The second and third are used to specify the masses and atomic numbers of a target and a projectile respectively. The next three lines define the number of emissions to be followed for each ejectile. In the above example, all reactions up to  $(n,3np\alpha)$  will be calculated. The code automatically sums over all possible decay sequences to reach the given residual nucleus. Accordingly,  $\sigma_{(n,3np\alpha)} = \sigma_{(n,2npn\alpha)} + \sigma_{(n,np2n\alpha)} + \sigma_{(n,p3n\alpha)} + \sigma_{(n,\alpha3np)} + \dots$  includes all possible permutations of ejectiles. The last line of the input provides for the inclusion of the emission of one type of light ion. The library of optical model parameters allows for d, t,  $^3\text{He}$ ,  $^6\text{Li}$ ,  $^7\text{Li}$ , and  $^7\text{Be}$  ejectiles. Use of the light ion ejectile option requires the code to be compiled with NDEJC set to 4 in the file *dimension.h*. If the last line of the mandatory input consists of three zeros (as in the example) the light ion emission channel is closed regardless of the NDEJC value used in the compilation. The mandatory part of the input is in a free format, while the comments following the semicolon only serve to facilitate input preparation and are ignored by the code.

### Optional input

The mandatory input is followed by optional input, which allows modifications to the default model parameters. Optional input consists of an arbitrary number of records, entered in any order and closed with the GO record, which indicates the end of the input. In the simplest case (all defaults), only the GO record must be entered. Each record starts with an alphanumeric keyword NAME which is followed by the value VAL and the positional parameters. The keyword indicates a physical quantity, such as the binding energy or level density parameter or an option. VAL takes the numerical value of the quantity or option. The positional parameters are typically used to specify to which nucleus the quantity should be applied. Each record must be in the format:

```
FORMAT (A6,G10.5,4I5) NAME,VAL,I1,I2,I3,I4
```

The GO record may be followed by an unlimited list of incident energies (one per record) terminated with a record containing a negative value. Anything below this line will be ignored by the code. The distribution of EMPIRE contains a number of sample inputs.

A complete list of model parameters and options that can be controlled through the optional input entries is given below.

### Calculation control

- NEX        Maximum number of energy steps in the integration set to VAL (default: min(50, NDEX)).
- LTURBO    Step in the angular momentum set to VAL. This option can be used to speed up heavy ion calculations. For example, setting LTURBO to 2, only each second spin in the Compound Nucleus and in all residual nuclei will be considered. The result is appropriately normalized so that no flux is lost (default: 1).
- ENDF       Controls output for ENDF formatting,  
              = 1 output for the ENDF formatting will be created,  
              = 0 no output for the ENDF formatting will be created (default).
- FITPOT    Controls optical model fitting (only total, elastic, capture and inelastic cross sections and elastic and inelastic angular distributions can be fit),  
              = 1 automatic optical model fitting will be performed,  
              = 0 no optical model fitting will be performed (default).
- KALMAN    Controls calculation of a sensitivity matrix,  
              = 1 sensitivity matrix will be calculated,  
              = 0 no sensitivity matrix will be calculated (default).

### Output control

- IOUT       Main output control set to VAL ,  
              = 0 no output except warnings,  
              = 1 input data and essential results (all cross sections) (default),  
              = 2 as IOUT=1 plus fusion spin distribution, yrast state population,  $\gamma$ -transition parameters, fusion barrier, inclusive spectra,  
              = 3 as IOUT=2 +  $\gamma$  and particle spectra + discrete levels' decay + double differential cross sections (if MSD>0),  
              = 4 as IOUT=2 + ORION output + residual nuclei continuum population (up to spin 12),  
              = 5 as IOUT=2 + ORION output + transmission coefficients (up to l=12),  
              = 6 as IOUT=2 + ORION output + level densities (up to spin 12).
- NOUT       MSC calculation output control set to VAL (default: 0).

**Fusion**

- FUSRED Fusion cross section will be multiplied by VAL (default: 1.).
- CSREAD Controls HI fusion cross section determination,  
 > 0 HI fusion cross section is set to VAL [in mb],  
 = -1 distributed barrier model used ,  
 = -2 Coupled-Channels CCFUS-code used (default for HI).  
 Note: CSREAD has no effect if *.fus* file (*FUSION* in manual mode) exists.
- BFUS Fusion barrier height in the distributed barrier model (Eq. 2.2) set to VAL (default:  $B_{fus}$  calculated by CCFUS).
- SIG SIGMA in the distributed barrier model (Eq. 2.2) set to VAL (default:  $0.05B_{fus}$ ).
- TRUNC Truncation in the distributed barrier model (Eq. 2.2) set to VAL (default: 2.).
- EXPUSH Extra-push energy set to VAL (default: 0.).
- CRL Critical  $l$ -value for HI fusion (Eq. 2.5) set to VAL (default: 0).
- DFUS Diffuseness in the transmission coefficients for HI fusion (Eq. 2.5) set to VAL (default: 1.).
- TRGLEV Excited level of the target is set to VAL (default: 1 (ground state)).

**Width fluctuations (HRTW)**

- HRTW Controls HRTW calculations  
 = 0 no HRTW  
 = 1 HRTW up to 5 MeV incident energy, and no HRTW above this value (default)  
 = 2 HRTW for all incident energies

**CCFUS input**

- DV DV barrier parameter in CCFUS set to VAL. This parameter can be used to adjust the fusion barrier. Typical range for changes  $-10 < DV < 10$ . (default: 10).
- FCC FCC parameter in CCFUS set to VAL,  
 =0 diagonalization of the coupling is performed at the barrier position  $r_b$ ,  
 =1 exponential character of the form factor is taken into account. A second order estimation of the position and height of the effective barriers is carried out within a one-Fermi distance from  $r_b$ . This option is recommended for strong coupling (default).

NSSC	Number of inelastic surface channels in CCFUS set to VAL (default: 4).
NACC	Number of additional channels set to VAL (default: 0).
BETCC	Deformation of the I2 <sup>th</sup> collective mode set to VAL.
FLAM	Multi-polarity of the I2-th collective mode set to VAL (entered with positive sign for target modes and negative sign for projectile modes) (default: 2, 3, -2, -3, needs NSSC numbers).
QCC	Q-value of the I2 <sup>th</sup> collective channel set to VAL - excitation energy of the collective level adopted with a negative sign (default: - energies of the first 2+ and 3- levels in the target and the projectile).
FCD	Strength of the coupling at the barrier for I2 <sup>th</sup> collective mode set to VAL. For FCC=1 the characteristic radial dependence of the one-particle transfer form factor is assumed. Used only if NACC>0 (no default).

### Coupled-Channels (ECIS)

DIRECT	Controls use of ECIS06 =0 spherical OM used (default) =1 Coupled Channel method used for calculation of inelastic scattering to collective levels. If a selected OM potential is of CC type, the elastic and reaction cross sections are also taken from ECIS06. Otherwise, spherical OM results are used. In any case, transmission coefficients for all emissions are calculated with spherical OM =2 as above but all transmission coefficients for the incident nucleon emission are calculated within Coupled Channel approach with ECIS06 (extensive calculation time). =3 as DIRECT=1 but DWBA is used instead of CC. All transmission coefficients calculated with spherical OM NOTE: OM potential to be used by ECIS06 might be different from the one used in the rest of the calculations and can be specified with the DIRPOT option.
EcDWBA	Selects all levels with energy below VAL and spin equal or less than I1 to be used in DWBA calculations performed parallel to CC.

### Multi-step Direct

MSD	Controls Multi-step Direct calculations , = 0 no MSD calculations (default), = 1 MSD calculations selected - ORION + TRISTAN will be executed, = 2 MSD calculations selected but only TRISTAN will be executed using the
-----	-----------------------------------------------------------------------------------------------------------------------------------------------------------------------------------------------------------------------------------



most recent results of ORION. WARNING! there is no check whether the last and the current run match with regard to the projectile, the target and the incident energy; this option can be used for a single incident energy only.

- WIDEX    Experimental energy resolution set to VAL (default: 0.2).
- GAPP    Proton pairing gap for target set to VAL (default:  $12/\sqrt{A}$  ).
- GAPN    Neutron pairing gap for target set to VAL (default:  $12/\sqrt{A}$  ).
- HOMEGA  $\hbar\omega$  oscillator energy (default:  $41.47/A^{1/3}$  MeV ).
- EFIT    Coupling constants of multi-polarity I1 fitted to the level at energy VAL (defaults: -1 for  $\lambda = 0$ ,  $E_{GDR}$  for  $\lambda = 1$ , energies of the first low-lying 2+, 3-, and 4+ levels for  $\lambda = 2, 3, 4$ , respectively).
- RESNOR    Response function for multi-polarity I1 will be normalized by factor VAL (default: 1).
- ALS    spin-orbit coupling strength in the harmonic oscillator (default: 1.5).

### Multi-step Compound

- MSC    Controls Multi-step Compound calculations,  
       = 0 no MSC calculations (default),  
       = 1 MSC calculations selected.
- XNI    Initial exciton number set to VAL (default set internally depending on the case, 3 for nucleon induced reactions).
- GDIV    Single particle level densities in MSC set to  $A/VAL$  (default: 13.0).
- TORY    Ratio of unlike to like nucleon-nucleon interaction cross section set to VAL. Used for the determination of the relative share between neutron and protons in the exciton configurations (default: 4.).
- EX1    Initial number of excitons that are neutrons set to VAL (default set internally depending on the case and on TORY).
- EX2    Initial number of excitons that are protons set to VAL (default set internally depending on the case and on TORY).
- D1FRA    Ratio of the spreading GDR width to the total GDR width set to VAL (default: 0.8).
- GST    Controls  $\gamma$ -emission in MSC,  
       = 0 no  $\gamma$ -emission in MSC (default),  
       = 1  $\gamma$ -emission in MSC selected.

STMRO Controls  $p$ - $h$  level density calculations,  
 = 0 closed form  $p$ - $h$  state densities selected (default),  
 = 1 microscopic  $p$ - $h$  state densities selected (not yet implemented).

### Exciton model (DEGAS)

DEGAS Controls exciton model calculations,  
 = 0 DEGAS code disabled (default),  
 = 1 DEGAS code enabled.

GDIVP Sets single-particle level density parameter ( $g$ ) for protons to  $A/VAL$  (default 13).

### Monte Carlo preequilibrium model (HMS)

HMS Controls Monte Carlo preequilibrium calculations,  
 = 0 HMS disabled (default),  
 = 1 HMS enabled.

NHMS Number of events in HMS set to VAL

CHMS Default damp rate in HMS multiplied by VAL

### Exciton model with cluster emission (PCROSS)

PCROSS Controls calculations with PCROSS  
 = 0 PCROSS disabled (default)  
 = 1 PCROSS enabled (with default 1.3 multiplier for mean free path)  
 >1.05 and <2 PCROSS enabled with mean free path multiplier set to VAL

GTILNO Single particle level density parameter  $g$  (in PCROSS) multiplied by VAL

### Level densities

LEVDPEN Selects level density approach,  
 = 0.0 EMPIRE-specific level densities, BCS + Fermi gas with deformation-dependent collective effects, adjusted to experimental  $a$  values and to discrete levels (default),  
 = 1.0 Fermi gas with deformation-dependent collective effects and  $a$  parameters derived from the shell-model,  
 = 2.0 Gilbert-Cameron level densities, adjusted to experimental  $a$  values and to discrete levels,  
 = 3.0 microscopic HF-BCS level densities,  
 > 2.0 Fermi gas with deformation-dependent collective effects and  $a = A/VAL$ .

- ATILNO    systematics value of the level density parameter  $\tilde{a}$  will be multiplied by VAL for the nucleus with Z=I1 and A=I2. NOTE: if the experimental value of the level density parameter exists, the term is ignored while it *is* used to define the normalization factor when ATILNO does not appear in the input or is set to 0. Therefore, using ATILNO set to a higher (or lower) value than 1 may actually result in a lower (or greater)  $\tilde{a}$  than in the default calculations.
- GCROA    Level density parameter  $a$  in Gilbert-Cameron approach  
            $> 0$  parameter  $a$  in nucleus Z=I1, A=I2 set to VAL ,  
            $= 0$  parameter  $a$  in all nuclei according to Ignatyuk systematics,  
            $= -1$  parameter  $a$  in all nuclei according to Arthur systematics,  
            $= -2$  parameter  $a$  in all nuclei according to Ilijnov systematics (default for Gilbert-Cameron).
- GCROUX    Level density parameter  $U_x$  in Gilbert-Cameron approach for nucleus Z=I1, A=I2 set to VAL (default calculated internally).
- GCROD    Pairing shift  $\Delta$  in Gilbert-Cameron approach for nucleus Z=I1, A=I2 set to VAL (default determined internally according to Gilbert-Cameron table, for  $Z > 98$  and/or  $N > 150$   $\Delta = 12/\sqrt{A}$  is taken).
- GCROE0    Level density parameter  $E_0$  in Gilbert-Cameron approach for nucleus Z=I1, A=I2 set to VAL (default calculated internally).
- GCROT    Level density parameter  $T$  in Gilbert-Cameron approach for nucleus Z=I1, A=I2 set to VAL (default calculated internally).
- FITLEV     $> 0$  cumulative plots of discrete levels will be displayed. If LEVDEN=0 the energy range of the plot will extend VAL MeV above the last discrete level,  
            $= 0$  no cumulative plots (default).
- NIXSH     $= 0$  shell-corrections calculated according to Myers-Swiatecki (default),  
            $= 1$  shell-corrections according to Nix-Moller tables.

### Fission

- FISSHI    Controls treatment of the fission channel for nucleus Z=I1, A=I2  
            $= 0$  advanced fission (multi-humped barrier, optical model for fission) recommended for light particle or photon induced fission (default)  
            $= 1$  fission over single-humped barrier (good only for heavy ion induced reactions)  
            $= 2$  fission ignored

**The following options are valid only when FISSHI = 0**

FISBAR	Controls origin of fission barrier data for nucleus Z=I1, A=I2 = 0 Ripl-2 (microscopic calculations by Goriely with internally set barrier widths taken from Lynn - default), = 1 internal EMPIRE library = 2 Ripl-1 (compilation of Maslov, model dependent!)
FISDEN	Controls level densities at saddle points for nucleus Z=I1, A=I2 = 0 Ripl-2 (microscopic calculations by Goriely) = 1 Empire specific
FISOPT	Controls subbarrier effects for nucleus Z=I1, A=I2 = 0 no subbarrier effects = 1 subbarrier effects considered (only with FISBAR=1) = 2 subbarrier effects & isomeric fission considered (only with FISBAR=1)
FISMOD	Controls multimodality of fission for nucleus Z=I1, A=I2 = 0 single-modal fission = 1 multimodal fission (2 modes) = 2 multimodal fission (3 modes)
FISDIS	Controls discrete transitional states =0 no discrete states above fission barrier for nucleus Z=I1, A=I2 =1 discrete states above fission barrier for nucleus Z=I1, A=I2

**The following options are valid only when FISSHI = 1**

QFIS	Liquid drop fission barriers multiplied by VAL (default: 1).
BETAV	Viscosity parameter in Eqs. 2.156, 2.157 and 2.158 set to VAL ( $10^{-21}s^{-1}$ ) (default: 4).
SHRJ	Shell correction to fission barrier damped (Eq. 2.155) to 1/2 at spin VAL (default: 24).
SHRD	Diffuseness of the shell correction damping (Eq. 2.155) set to VAL (default: 2.5).
TEMP0	Temperature at which shell correction fade-out (Eq. 2.154) space starts set to VAL (default: 1.65).
SHRT	Parameter in the temperature shell correction fade-out (Eq. 2.154) set to VAL (default: 1.066).
DEFGA	$d$ (amplitude) in the Gaussian term of Eq. 2.155 set to VAL (default: 0. - no correction).
DEFGW	$\Delta J_G$ (width) in the Gaussian term of Eq. 2.155 set to VAL (default: 10).

DEFGP  $J_G$  (position) in the Gaussian term of Eq. 2.155 set to VAL (default: 40).

### Gamma-ray strength functions

GSTRFN = 0 EGLO enhanced generalized Lorentzian (Uhl-Kopecki) as in the 2.18 version and earlier (default)  
 = 1 MLO1 modified Lorentzian version 1 (Plujko, RIPL-2)  
 = 2 MLO2 modified Lorentzian version 2 (Plujko, RIPL-2)  
 = 3 MLO3 modified Lorentzian version 3 (Plujko, RIPL-2)  
 = 4 EGLO EGLO enhanced generalized Lorentzian (RIPL-2)  
 = 5 GFL (Mughabghab)  
 = 6 SLO standard Lorentzian

### GDR parameters

GDRGFL Selects source of GDR parameters  
 = 0 Messina systematics  
 = 1 experimental or systematics of RIPL-2 (default)

GDRDYN Controls GDR treatment,  
 = 0 GDR shape depends on the ground state deformation (default),  
 = 1 GDR shape dependence accounts for the rotation induced deformation (spin dependent, Eq. 2.143).

EGDR1 GDR energy of first peak set to VAL (default calculated internally from systematics).

GGDR1 GDR width of first peak set to VAL (default calculated internally from systematics).

CSGDR1 GDR cross section of first peak set to VAL (default calculated internally from systematics).

EGDR2 GDR energy of second peak set to VAL (default calculated internally from systematics).

GGDR2 GDR width of second peak set to VAL (default calculated internally from systematics).

CSGDR2 GDR cross section of second peak set to VAL (default calculated internally from systematics).

GDRWP Factor  $c$  in the energy increase of the GDR width (Eq. 2.175) set to VAL (default: 0.0026).

GDRWA1 GDR width of first peak increased by VAL (default: 0).

- GDRWA2 GDR width of second peak increased by VAL (default: 0).
- GDRESH GDR position shifted by VAL (default: 0).
- GDRSPL Splitting of GDR peaks increased by VAL (default: 0).
- GDRST1 GDR cross section of first peak multiplied by VAL (default: 1).
- GDRST2 GDR cross section of second peak multiplied by VAL (default: 1).
- GDRWEI relative contributions of the GDR and Weisskopf estimates to the  $\gamma$ -strength set to  $VAL \cdot GDR + (1 - VAL) \cdot Weiss$ . Note that the condition  $0 \leq VAL \leq 1$  must be fulfilled (default: 1).
- GCASC =0 no full  $\gamma$ -cascade in the first Compound Nucleus (only primary transitions),  
 =1 full  $\gamma$ -cascade in the first Compound Nucleus  
 (default: full  $\gamma$ -cascade in the first Compound Nucleus if the initial excitation energy is less or equal to 20 MeV, otherwise primary transitions only).

### Photo-absorption

- E1 = 0 E1 photo-absorption blocked  
 = 1 E1 photo-absorption selected
- M1 = 0 M1 photo-absorption blocked  
 = 1 M1 photo-absorption selected
- E2 = 0 E2 photo-absorption blocked  
 = 1 E2 photo-absorption selected
- QD Quasideuteron photo-absorption cross section normalized by a factor VAL

### Optical Model Potential

- OMPOT Selects optical model parameters for neutrons (I1 = 1), protons (I1 = 2), or alphas (I1 = 3); VAL must be set to a RIPL-2 catalog number (Lib. No.) of the potential as it appears in the empire/RIPL-2/optical/om-data/om-index.txt file or in Help => 'RIPL omp' when using GUI. For backward compatibility this number must be entered with a negative sign.
- DIRPOT Optical model parameters to be used by ECIS06. The same as above, except that I1 need not be specified (refers to inelastic channel by default).
- EFERMI Fermi Energy for dispersive OM potential (default: -10.392 MeV).
- EAVERP Average energy of particle states for dispersive OM (default:-5.66 MeV).
- EANONL Threshold energy for non-locality in dispersive OM (default: 60 MeV).

ALPHA Mahaux non-locality parameter in dispersive OM (default: 1.65).

RELKIN Controls kinematics,  
       = 0 classical (default),  
       = 1 relativistic.

### Optical model fitting

FITOMP When set to 1, permits automatic or manual adjustment of the optical model potential and collective deformation parameters (default value is 0).

FITabc Selects an optical model parameter for adjustment. The letter a can be R (real) or I (imaginary) and the letter b can be V (volume), S (surface) or O (spin-orbit). Thus the combinations RV, IV, RS, IS, RO and IO specify the 6 different terms in the RIPL-2 optical potential described in Section 3.4.3. The letter c can be V (potential strength), R (radius) or D (diffuseness). The initial shift in the parameter is given by VAL and the maximum allowed variation is given by  $0.01 \cdot I1$ . I2 specifies which of the parameters in the potential strength, radius or diffuseness is to be adjusted.

FITDEF Selects the deformation parameter of multipole I2 for adjustment. The initial shift in the parameter is given by VAL and the maximum allowed variation is given by  $0.01 \cdot I1$ . The value of I2 can be 2 or 4 for rotational nuclei and 2 or 3 for vibrational nuclei.

FITWT Multiplies weights of experimental data of type MF=I1 and MT=I2 in  $\chi^2$  by VAL.

FITWT0 Multiplies weights of natural element experimental data in  $\chi^2$  by VAL.

FITITR Sets the number of iterations in the gradient  $\chi^2$  minimization to  $VAL = \text{maxitr} + 0.01 \cdot \text{itmax}$ , where maxitr is the number of times the gradient is calculated and itmax is the number of iterations along each gradient (default is 3.05).

FITEMX Maximum incident energy of experimental data used in fitting set to VAL (default is 30 MeV).

FITGRD Defines the initial grid of incident energies of nuclear model calculations used to obtain  $\chi^2$ . When set, the first interval is VAL, the second  $VAL + 0.001 \cdot I1$ , the third  $VAL + 0.002 \cdot I1$ , etc. (The default incident energy grid is the one given in the input file.)

### Miscellaneous

BNDG Binding energy of ejectile I3 in nucleus Z=I1, A=I2 set to VAL (default calculated internally from nuclear masses).

- DEFPAR  $b$  coefficient in dynamic deformation expression (Eq. 2.139) set to VAL (default: 1).
- JSTAB Stability limit with respect to spin for the nucleus  $Z=I1$  and  $A=I2$ ,  
 $=0$  set at a spin at which fission barrier (including shell correction) disappears (default),  
 $>0$  set to VAL.

### 3.10.2 \*.lst (LIST.DAT; lengthy output)

As the main output of EMPIRE, the size of the file depends on the controls IOUT and NOUT specified in input (\*.inp). In the extreme case, no output except warnings is produced (note that all essential results are written to the file \*.out, which is not affected by IOUT and NOUT).

The file begins with the code banner and printout of the parameters specified in the optional input. Lack of a message regarding any given parameter means that the default value has been used in the calculations. The next segment of the output specifies the incoming channel and model parameters such as binding energies, fission barriers, shell corrections, ground state deformations and list of optical model systematics used in the calculations. The message is printed to notify the user on eventual re-normalization of the internal level density systematics to the experimental results. Re-normalization is performed only if experimental values of the  $a$ -parameter for at least 3 nuclei involved in the calculations are found in *empire/data/ldp.dat*. The introductory part of the output is followed by the results of calculations for each decaying nucleus.

In the case of Compound Nucleus all calls to the ORION code are listed and the outputs of TRISTAN and ORION codes (the latter only if  $IOUT > 3$ ) are printed. Next, the fusion cross section and associated spin/parity distributions are given. For each decaying nucleus (including Compound Nucleus) the production cross section, population of discrete levels, intensities of discrete  $\gamma$ -lines and emitted spectra of  $\gamma$ s, neutrons, protons,  $\alpha$ s and eventually light ions are printed. Output for a given incident energy is completed by inclusive spectra of all  $\gamma$ s and particles emitted along the de-excitation chain. This scheme is repeated for each incident energy apart from the code banner and optional input printout. The general structure of the output can be summarized as follows (depending on input options some items might be missing in an output):

- code banner
- optional input
- matrix of models usage
- 1<sup>st</sup> incident energy
  - Compound Nucleus



- 
- input parameters
  - elastic, reaction and total cross sections
  - inelastic scattering to collective levels from ECIS06
  - ORION results
  - TRISTAN results
  - fusion cross section
  - MSC results
  - spectra summed over all preequilibrium mechanisms
  - discrete level population before their  $\gamma$ -de-excitation
  - intensities of discrete  $\gamma$ -lines
  - residue (CN) production cross section
  - fission cross section
  - $\gamma$ , n, p,  $\alpha$  and light ion spectra
  - 1<sup>st</sup> residue
    - model parameters
    - discrete level population before their  $\gamma$ -de-excitation
    - intensities of discrete  $\gamma$ -lines
    - residue production cross section
    - second-chance fission cross section
    - $\gamma$ , n, p,  $\alpha$  and light ion spectra
  - 2<sup>nd</sup> residue
    - ...
  - last residue
    - ...
  - inclusive  $\gamma$ , n, p,  $\alpha$  and light ion spectra
  - 2<sup>nd</sup> incident energy
    - ...
  - last incident energy
    - ...
    - inclusive  $\gamma$ , n, p,  $\alpha$  and light ion spectra

### 3.10.3 \*.out (OUTPUT.DAT; short output)

The short version of EMPIRE output is provided to facilitate reading of essential results. No warning messages or details are given. An example of the short output (with ENDF option set to 0) is reproduced below.

```

REACTION  6-C - 12 + 13-Al- 27 INCIDENT ENERGY  50.1      MeV
COMPOUND NUCLEUS ENERGY  51.295 MeV
FUSION CROSS SECTION =    1285.1      mb
19-K - 39 production cross section 0.566424E-08 mb
  fission cross section 0.0000      mb
g  emission cross section 0.15879    mb
n  emission cross section 250.52     mb
p  emission cross section 247.58     mb
He emission cross section 786.84     mb

REACTION  6-C - 12 + 13-Al- 27 INCIDENT ENERGY  100.      MeV
COMPOUND NUCLEUS ENERGY  85.841 MeV
FUSION CROSS SECTION =    1653.8      mb
19-K - 39 production cross section 0.558363E-11 mb
  fission cross section 0.0000      mb
g  emission cross section 0.14045    mb
n  emission cross section 195.79     mb
p  emission cross section 186.42     mb
He emission cross section 1271.4     mb

```

When the ENDF option is activated this file serves to transmit the results along with all necessary data to the EMPEND code. Under such circumstances the file becomes extremely lengthy and is not suitable as a quick reference.

### 3.10.4 \*.fus (FUSION)

This file is used to input arbitrary fusion cross sections, overriding any other options regarding fusion determination that might be contained in the input. The file is a simple column of fusion cross sections for subsequent partial waves starting with  $l = 0$  (one cross section per line in a free format). Cross sections for any number of partial waves can be introduced but the code will consider only those below the actual value of NDLW (see Section 3.3). Other limitations on the number of partial waves can be set in the input or internally by the code (e.g., stability of a liquid drop against rotation or disappearance of the fission barrier, see Section 3.10.1).

### 3.10.5 \*.lev (LEVELS)

File \*.lev contains discrete levels for all nuclei involved in a given calculation. This file is produced by EMPIRE during the first run by extracting relevant information from the RIPL-2 library (files empire/RIPL-2/levels/z\*.dat) retaining the original format (see Section 3.4.2)

File \*.lev most probably requires modification. For certain applications, missing branching ratios, uncertain spins, parities and levels may have to be supplied or modified. However, most likely some levels may need to be cut-off in order to make the scheme consistent

with the level density parameterization. The user has to set  $N_{max}$  (6<sup>th</sup> item in the first line of the isotope section) to the required value. Contrary to 2.17 and earlier versions of EMPIRE, excess levels **must not** be removed.

### 3.10.6 \*-lev.col (TARGET\_COLL.DAT)

The first run with the DIRECT option different from zero results in EMPIRE creating a file that contains collective levels to be used in the Coupled-Channels or DWBA calculations. Whenever possible the data are taken from the optical segment of the RIPL library (note that CC potentials in RIPL contain the necessary information on the levels to be coupled). If the necessary information is not available in RIPL (spherical optical potential is being used), the code tries to identify collective levels internally among those available in *\*.lev* file. In such circumstances, the g.s. deformation is assigned to the g.s. rotational band, and default dynamic deformations are ascribed to each collective level (note that band deformation is used in the rotational model and dynamic deformations are used in the vibrational model). The format of the *\*-lev.col* file is analogous to the one used in the optical segment of the RIPL library (see Section 3.4.3). An example, containing 8 collective levels in <sup>244</sup>Am is reproduced below.

```

95 243 nucleus is treated as deformed

Ncoll Lmax IDef Kgs (Def(1,j),j=2,IDef,2)
8 4 4 2.5 0.150E+00 0.000E+00

N E[MeV] J pi Nph L K Dyn.Def.
1 0.0000 2.5 -1. 0 0 0 0.100E-01
2 0.0422 3.5 -1. 0 0 0 0.100E-01
4 0.0964 4.5 -1. 0 0 0 0.100E-01
7 0.1623 5.5 -1. 0 0 0 0.100E-01
9 0.2380 6.5 -1. 0 0 0 0.100E-01
53 0.0840 2.5 1. 0 0 0 0.500E-01
55 0.1092 3.5 1. 0 0 0 0.500E-01
56 0.1435 4.5 1. 0 0 0 0.500E-01

```

The sequential number N corresponds to the position of each level in the *\*.lev* file. Note that levels with  $N < 50$  will be considered in CC calculations (if such were selected), while those with  $N > 50$  will be used in the additional DWBA run of ECIS06. The actual positions of these levels in the decay scheme are N-50. The remaining symbols are explained below:

Ncoll	number of collective states in the coupled-channel rotational model for a particular <i>iz</i> , <i>ia</i>
Lmax	maximum <i>l</i> value for multipole expansion
IDef	largest order of deformation
Kgs	<i>k</i> for the rotational band
Def	deformation parameters, $l=2,4,6,\dots$ through Lmax

E	level excitation energy (MeV)
J	level spin
pi	level parity
Nph	1 for pure 1-phonon state 2 for pure 2-phonon state 3 for mixture of 1- and 2-phonon states
L	level orbital momentum
K	level spin projection
Dyn.Def.	vibrational model deformation parameter

Users may choose to modify the *\*-lev.col* file to fit experimental data. In fact, such modifications are expected to be necessary if the file was created internally rather than copied from the RIPL library. In particular, deformation parameters should be given appropriate attention since cross sections are very sensitive to their values. Deformation parameters can be modified automatically using the FITOMP option.

### 3.10.7 \*-inp.fis (FISSION.INP)

This file collects all incident energy independent input parameters related to fission. It follows general EMPIRE philosophy of input/output files: it is created by the code if missing and it is read by the code if it exists. Users can edit it to modify default fission parameters. The file is divided into sections corresponding to each fissioning nucleus. Below we reproduce one such section of the file. The format is self-explanatory and users should have no problems to understand content of the file.

```
Isotope:
-----
Z= 95 A=244
-----
FISBAR =1. Fundamental barriers from Internal library
Nr.parabolas =3 Nr.wells=1
FISMOD =0.
Va ha Vb hb Vi hi (in Mev)
6.000 0.700 6.100 0.470 2.500 1.000
h2/2J(A) h2/2J(B) h2/2J(I) (in MeV)
0.0050 0.0025 0.0035
Beta2(A) Beta2(B) Beta2(I)
0.4519 0.9519 0.6707
FISOPT=1. Subbarrier effects considered
Parabolic energy dependent imaginary potential in the isomeric well Wimag = W0 + W1*E + W2*E^2, where E is
excitation energy with respect to the isomeric well
W0 W1 W2
1.0000 0.0000 0.0000
Number of discrete states at barrier 1 = 4
Jdis Pidis Edis homega
6.0 -1 0.000 0.700
0.0 -1 0.030 0.700
2.0 1 0.040 0.700
```

```

4.0 1 0.050 0.700
Number of discrete states at barrier 2 = 4
Jdis Pidis Edis homega
6.0 -1 0.000 0.470
0.0 -1 0.050 0.470
2.0 1 0.070 0.470
4.0 1 0.090 0.470
Number of discrete states at barrier 3 = 4
Jdis Pidis Edis homega
6.0 -1 0.000 1.000
0.0 -1 0.050 1.000
2.0 1 0.070 1.000
4.0 1 0.100 1.000
FISDEN=1.Level densities at the saddle points EMPIRE specific
Asymmetry shell-corr delta gamma atilf/atil at saddles
Barrier 1 2 2.600 0.896 0.030 1.000
Barrier 2 3 0.640 0.896 0.030 1.000
Coefficients of a linear energy dependent factor adjusting the fission level densities
(a0 + a1*E + a2*E**2) * rho(E,J) where E stands for excitation energy above the barrier
a0 a1 a2
Barrier 1 1.000 0.000 0.000
Barrier 2 1.000 0.000 0.000

```

### 3.10.8 FISSION.OUT

Contains details of the fission calculations such quantities as level densities at saddles, fission transmission coefficients and fission probabilities, that are usually beyond interest of the typical user of the code. Therefore, the file exists only under generic name and is overwritten each time the code is run. The format of the file is self-explanatory.

### 3.10.9 \*-omp.ripl (OMPAR.RIPL)

Set of optical model parameters for all nucleus-ejectile combinations involved in the calculations extracted from the RIPL library. This file is created by EMPIRE if RIPL potential is requested in the input and the \*-omp.ripl file does not already exist (typically during the first run). The format is identical to the RIPL optical segment (see Section 3.4.3). Optical model parameters contained in the \*-omp.ripl file can be modified manually if desired.

### 3.10.10 \*-omp.dir (OMPAR.DIR)

Used to store optical model parameters that are input to ECIS06 for Coupled-Channels or DWBA calculations. The format is the same as that of the \*-omp.ripl file described above, and coincides with the RIPL format (see Section 3.4.3) used to represent optical model parameters. The reason for creating \*-omp.dir file, in addition to the \*-omp.ripl, is in order to use the Coupled-Channels optical model potential for the incident channel, in which CC or DWBA calculations are performed, and the spherical potential for the calculation of transmission coefficients when DIRECT=1 or 2 options are used. Depending on the combination of input options, \*-omp.dir can be empty. Optical model parameters contained in the \*-omp.dir file can be modified manually if desired or automatically using the FITOMP option.

### 3.10.11 \*.endf (OUTPUT.ENDF)

EMPIRE results (in ENDF format) from processing with the EMPEND, FIXUP, ENDRES and STANEF codes. This is the final properly formatted ENDF-6 file.

### 3.10.12 \*-s.endf

\*.endf file processed with a chain of codes: FIXUP, LINEAR, RECENT, SIGMA1, LEGEND and SIXTAB. Intermediate files are removed by the *process* script. Note, that this file is intended only for plotting and does not respect certain limits imposed by the ENDF-6 format.

### 3.10.13 \*.exf (EXFOR.DAT)

This file contains all relevant experimental data retrieved from the EXFOR library. The format is 'human readable', and provides the user with sufficient information about the experiment. A typical excerpt is given below

```

SUBENT      10827001      861124
BIB          13          46
INSTITUTE    (1USALRL)
REFERENCE    (J,PR/C,19,2127,7906)
              (C,80BNL,1,245,8007) UPDATED VALUES.
AUTHOR       (S.M.GRIMES,R.C.HAIGHT,K.R.ALVAR,H.H.BARSCHALL,
              R.R.BORCHERS)
TITLE        CHARGED PARTICLE EMISSION IN REACTIONS OF 15-MEV
              NEUTRONS WITH ISOTOPES OF CHROMIUM, IRON, NICKEL, AND
              COPPER.
INC-SOURCE   (D-T) 400-KEV DEUTERONS ON ROTATING TITANIUM TRITIDE
              TARGET
SAMPLE       2.5-CM DIAMETER FOIL WITH DIAPHRAGM TO AVOID CONTAMIN-
              ANTS FROM FOIL HOLDERS.
DETECTOR      (SOLST) PAIR OF SILICON SURFACE BARRIER DETECTORS, 15
              AND 1500 MICRO-METERS THICK, SPACED 19-MM APART.
METHOD        TRIPLE LENS MAGNETIC QUADRAPOLE SPECTROMETER USED.
              DIFFERENT REACTION ANGLES OBTAINED BY MOVING TRANSPORT
              SYSTEM ALONG ITS AXIS. NINE DIFFERENT CURRENT SETTINGS
              USED FOR MAGNETS TO COVER ENERGY RANGE OF EMITTED
              PARTICLES
MONITOR       (1-H-1(N,EL)1-H-1,,SIG)
              (1-H-2(N,EL)1-H-2,,SIG)
CORRECTION    ENERGY SPECTRA CORRECTED FOR ENERGY LOSS IN TARGET
ERR-ANALYS    ERRORS IN PRODUCT OF SPECTROMETER SOLID ANGLE AND
              ABSOLUTE NEUTRON FLUX DUE TO-
              -ERRORS IN POLYETHYLENE STOPPING POWER, LESS THAN
              3-PERCENT
              -ERRORS IN ELASTIC CROSS SECTIONS FROM HYDROGEN, LESS
              THAN 1-PERCENT
              -ERRORS IN ELASTIC CROSS SECTIONS FROM DEUTERIUM, LESS
              THAN 10-PERCENT
              -ERROR IN SOLID ANGLE OF TARGET TO NEUTRON SOURCE
              RATIO FOR CH(2) OR CD(2) COMPARED TO THAT OF SAMPLE
              FOILS, 8-PERCENT
              OTHER ERRORS DUE TO-
              -TARGET FOIL THICKNESS ERRORS, 2.5-PERCENT
              -EFFECT OF STATISTICS AND THE LEGENDRE POLYNOMIAL FIT,
              7-PERCENT (FOR PROTONS, ALPHAS) TO 15-PERCENT (DEUT-
```

```

ERONS)
STATUS      (APRVD) APPROVED BY S.M.GRIMES, 86/11/21.
            PARTIAL CROSS SECTIONS TAKEN FROM PRIVATE COMM.,
            GRIMES, 79/5.
HISTORY     (790605C)
            (820819A) REFERENCE UPDATE, BIB CORRECTIONS.
            (830830A) BIB CORRECTIONS.
            (860422A) BIB UPDATES.
            (860709A) BIB UPDATED, SUBENTS 71-103 ADDED.
ENDBIB      46
COMMON      1          3
EN
MEV
14.8
ENDCOMMON   3
SUBENT      10827012    790716
BIB         4          6
REACTION    (24-CR-52(N,D)23-V-51,PAR,SIG)
SAMPLE      SAMPLE IS 2.1 MILLI-GMS/SQ-CM THICK, ENRICHED TO
            99.9-PERCENT CR-52
MONITOR     (1-H-2(N,EL)1-H-2,,SIG) NEUTRONS ON THICK CD(2) RAD-
            IATOR
ERR-ANALYS  COMBINED ERROR IS 20-30 PERCENT
ENDBIB      6
NOCOMMON    Usually
DATA        4          11
E-MIN      E-MAX      DATA      DATA-ERR
MEV         MEV        MB         MB
1.5         2.0        0.2        0.15
2.0         2.5        0.5        0.2
2.5         3.0        0.7        0.25
3.0         3.5        0.6        0.2
3.5         4.0        1.0        0.3
4.0         4.5        0.3        0.15
4.5         5.0        0.9        0.3

```

### 3.10.14 \*.c4 (empire/util/x4toc4/c4.dat)

This file contains relevant EXFOR data translated into computational format by the X4TOC4 code. An excerpt from the .c4 file of experimental data for the (n,2n) reaction on  $^{124}\text{Sn}$  is shown below.

```

1 24052  3 16  1.2722+7 8000.000 0.038800 1.5000-3
1 24052  3 16  1.2744+7 8000.000 0.041200 1.6000-3
1 24052  3 16  1.3251+7 10000.00 0.121900 5.0000-3
1 24052  3 16  1.3271+7 10000.00 0.123700 5.1000-3
1 24052  3 16  1.3888+7 9000.000 0.240600 9.7000-3
1 24052  3 16  1.3902+7 9000.000 0.250600 0.010100
1 24052  3 16  1.4251+7 8000.000 0.322000 0.012500

```

The original file also contains information on the EXFOR sub-entry number, the first author and the year of publication. These data are placed far to the right and are not displayed here. The user may wish to modify this file by deleting or adding some lines. A detailed description of the format is given in the source of the X4TOC4 code, while we list only the most important columns (fields).

Field #	Contents
2	Z*1000+A
3	ENDF File (3-cross sections)
4	ENDF MT number (here MT=16 stands for (n,2n))
5	incident energy (in eV)
6	incident energy resolution (in eV)
7	cross section (in b)
8	cross section error (in b)

### 3.10.15 \*.ps (empire//util/plotc4/plot.ps)

PostScript plots compare calculations with experimental data produced by the PLOT4 code. Note that the results must be ENDF formatted for graphical plots.

### 3.10.16 \*-cum.ps

PostScript plots compare cumulative number of discrete levels and level densities fitted to reproduce the last level. Plots are only produced for Gilbert-Cameron or EMPIRE-specific level densities when FITLEV>0 is specified in the input. All nuclei involved in a calculation and with at least 3 known discrete levels are included.

### 3.10.17 \*-ompfit.lst (FIT.OUT)

Information about variations in optical model or deformation fit parameters and the minimization of  $\chi^2$  is written here. This file is written only when FITOPT>0 is specified in the input.

### 3.10.18 \*.x42c4 \_lst (empire/util/x4toc4/x4toc4.lst)

Output of the X4TOC4 code for the last run. Provides a log of the translation from EXFOR to computational format.

### 3.10.19 \*.x42c4 \_errs (empire/util/x4toc4/errors)

List of EXFOR entries not translated by the X4TOC4 code to the computational format, for example, when X4TOC4 is not able to resolve the reaction string.

### 3.10.20 Log files

Full EMPIRE run will, in general, produce a number of *\*-log* files, which report summary of results and eventual problem encountered during formatting, format checking preprocessing, and plotting. These files, named after codes that generated them, include:



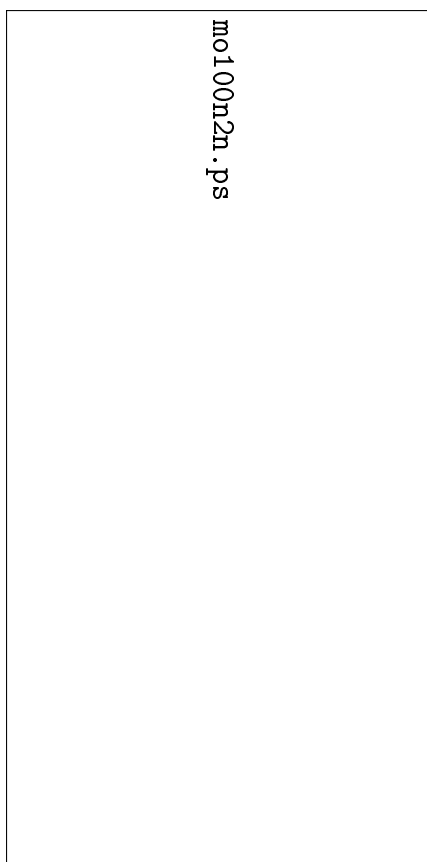


Figure 3.7: Comparison of the experimental data extracted from the EXFOR library with the results of EMPIRE calculations using default parameters. This plot is produced automatically when running EMPIRE with the *run* script or clicking the Run+Format+Plot button in GUI mode.

*\*-log.checkr \*-log.empend \*-log.endres \*-log.fixup \*-log.fixup2 \*-log.fizcon \*-log.legend \*-log.linear \*-log.plotc4 \*-log.psychc \*-log.recent \*-log.sigma1* and should be inspected as a part of the Quality Assurance.

## 3.11 Plotting capabilities

All pertinent experimental data in EXFOR are retrieved during the first run of the code and plotted against the ENDF-formatted file using a chain of ENDF Pre-Processing codes (PREPRO [12]) and X4TOC4 [13] and PLOT4 [13]. These codes are called by EMPIRE in a transparent way by bash scripts. Fig. 3.7 shows typical example of such a plot. High quality plots can be produced interactively using the ZVView package of Zerkin [14].

### 3.11.1 ZVView

The plotting capabilities of EMPIRE have been greatly enhanced by incorporating the graphic package ZVView of Zerkín [14]. This software is operated from the EMPIRE GUI and produces publication quality plots. The scale can be changed, selected data sets can be excluded from the plot, and data points values displayed; changes can also be made to the plot title, subtitle, symbols and colors, data fitting, smoothing and others. Plots can be exported to the PostScript or encapsulated PostScript format for inclusion in the L<sup>A</sup>T<sub>E</sub>X document.

Contrary to PLOT4, ZVV plots are not generated automatically. The user has to select a desired reaction from the EMPIRE GUI () button or type MT number in the entry box at the bottom of the GUI) and click on the  button. Internal scripts and components of the ZVView package process the ENDF and \*.c4 files to produce the \*-MT.zvd file, which is then displayed with the ZVView.

ZVV plots can also be combined to include different reactions on the same graph. Clicking on the  button will open the terminal with a list of all ZVV plots available in the *work* directory. The user may select any number of them to be included in a single plot. Usually, the plot title has to be set within the ZVView environment before saving.

Additional functionality is offered by the ZVView GUI (see Fig. 3.8), which permits comparison of up to three calculations (or ENDF files), and experimental data (see Fig. 4.3, 4.4 and 4.5). It is primarily intended as a tool for checking the effect of different options used in the calculations or comparing the results with other evaluations. Usually, one would undertake a set of calculations and use the script *store* to move (or copy) all the relevant files to a specified directory. For example, to store the project with root-name "fe56" in a *case1* directory, one should type:

```
../scripts/store ../case1 fe56
```

inside the *work* directory (note that *case1* will be on the same level as *work*). Thus, the working directory is free to run new calculations with the modified input. These results can again be stored in another directory (e.g., *case2*) and the third set of calculations executed in the *work* directory. If experimental data are to be plotted, the \*.c4 file with the same root-name should be present in the first directory, which is ensured if EXFOR data were extracted by EMPIRE. Clicking the  button of the EMPIRE GUI launches ZVV GUI, as shown in Fig. 3.8. Note that the root-name of the project and *work* directory are by default transferred to ZVV GUI. Comparisons can be made by pointing the "File 2:" and "File 3:" fields to other files containing ENDF formatted data (e.g., stored in *case1* and *case2* directories). We stress that while the first set is referenced through its directory and default names \*-s.endf and \*.c4 the other two are identified by respective arbitrary file names. An arbitrary suffix identifying the comparison plots and labels for each curve should be entered in the respective fields. At this stage the system is ready to create the requested plots () button). One can also choose to create all plots at once () button), although they can be viewed one by one or

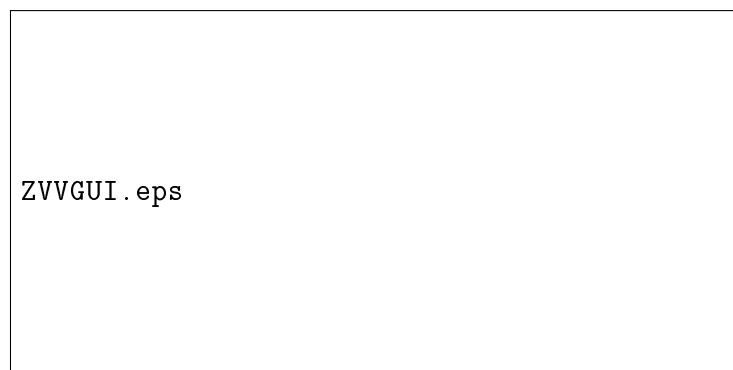


Figure 3.8: Graphic User Interface to ZVView to compare up to three calculations (or ENDF files) and merge different reactions on a single ZVV plot.

merged together. ZVV GUI can also be used to create simple ZVV plots by replacing the EMPIRE GUI function. Leaving labels related to "File 2:" and "File 3:" fields and suffix blank, simple ZVV plots can be created for all the reactions with just one mouse click. Setting the project field to "\*" (without " ") creates plots for all reactions and targets for which *\*-s.endf* files exist in the *work* directory. This comparison capability is not limited to the EMPIRE results; any evaluated file in the ENDF format can be compared with another ENDF file or with EMPIRE calculations, providing that the first file is named (or linked) as *\*-s.endf* and placed in the *work* directory.

As a rule, only the ENDF-formatted files can be plotted with PLOT4 or ZVView. This choice is not only a matter of convenience but was deliberately selected to validate the final (ENDF-formatted) product. The only exception to this rule is provided by the Create ZVV GUI button, which allows the user to construct and plot any excitation function directly from the EMPIRE output. Hence, the user has to supply a string which unambiguously identifies the cross section. The *gawk* script scans EMPIRE output (*\*.lst*) for the lines containing the specified string and extracts a number (cross section) followed by the "mb" string along with the respective incident energy value. The results are sent to ZVView for plotting.

## 3.12 Plans for further development

Following extensions are foreseen in the future releases of the EMPIRE code:

1. Inclusion of isospin,
2. Width fluctuation correction for reactions on excited targets,
3. Improved parametrization of the elastic enhancement factor,
4. ENDF-formatting of primary gammas.

5. Improved description of direct reactions (e.g. breakup, pickup, etc.) for reactions with incident complex particles (e.g. deuteron, triton and  $^3\text{He}$ ),
6. Implement particle decay of discrete levels that is relevant for the treatment of direct reactions (e.g.  $^{12}\text{C}(\text{n},\text{n}+3\alpha)$  ) in the outgoing channels.
7. Inclusion of heavy-ion optical potential (Sao Paulo potential).

## 4 Working notes

### 4.1 Avoiding problems

Consideration and observation of the following remarks will help to avoid problems when running the EMPIRE code:

- Each modification of the EMPIRE input file (*\*.inp*) that involves a change of projectile, target, or the number of emitted particles must be followed by the execution of the *clean* script in order to remove input/output files that do not match the new case. One should keep in mind that *clean* will also remove all the files that might have been modified manually (such as *\*.lev*, *\*-omp.dir*, etc.). If these files are compatible with the new input and are to be preserved they have to be renamed by adding a prefix before executing the *clean* script.
- Any serious calculations should be preceded by a test run using FITLEV set to a positive value in order to check the completeness of the discrete level schemes and their consistency with the level densities. Such calculations should be repeated after each change of the input file (*\*.inp*) that requires running the *clean* script (see above). Calculation times for such runs are very short.
- If the ENDF option is selected, the incident energies should be in increasing order.
- Log files *\*.war*, *\*.x42c4\_errs* and *empend.log* should be checked for possible warnings and error messages.
- Irregularities in the excitation functions such as (n,2n) or (n,p) are usually due to improper level density parametrization (check cumulative plots of discrete levels) or to the overestimated MSD contribution (check response functions and ensure that the levels to which they are adjusted are actually the collective ones).
- Irregularities in the increasing part of the excitation function for inelastic scattering are usually due to insufficiently dense mesh of incident energies.

### 4.2 Fitting discrete levels

Running EMPIRE with the FITLEV option is strongly recommended before any cross section calculations are attempted. This allows a check of whether the discrete level schemes for the involved nuclei are complete and consistent with the level density parametrization.

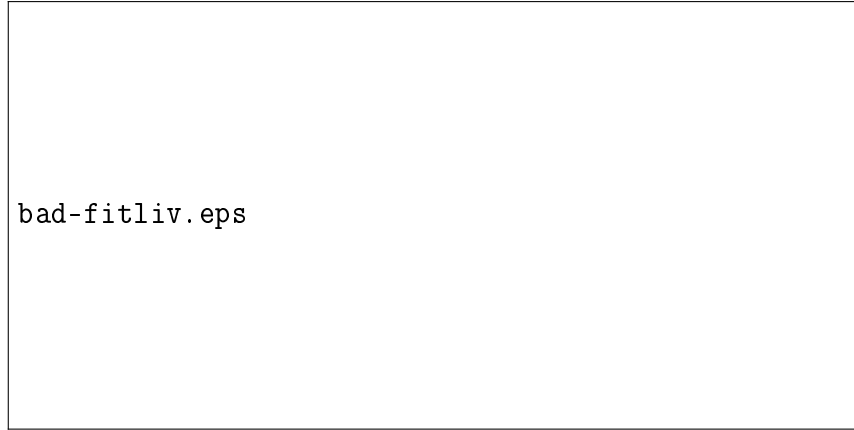


Figure 4.1: Cumulative plot of 10 discrete levels in  $^{96}\text{Pd}$  which could not be reproduced by the level density calculations (EMPIRE-specific level densities with default parametrization were used).

If the whole package is properly installed, plots of cumulative number of levels will be stored in the *\*-cum.ps* file and can be inspected in the PostScript viewer (ghostview) by clicking on the Levels button in the "Plots:" section of the GUI. Two somewhat extreme examples of such plots are shown in Fig. 4.1 and 4.2. Fig. 4.1 demonstrates 10 levels in  $^{96}\text{Pd}$ , which could not be matched with the level densities, which usually happens when the levels are over extend. Then, levels that were not detected experimentally are missing in the spectrum, and the resulting high energy end of the cumulative plot is too low. Missing levels are more likely in the high-energy region of the spectrum and reducing the number of levels considered may restore agreement; neglecting the highest 4 levels in  $^{96}\text{Pd}$  leads to a reasonable fit, as shown in the Fig. 4.2. Graphical representation helps to identify the level at which cumulative plot starts to bend, and levels lying above this point should be excluded from consideration. One should edit *.lev* file and decrease  $N_{max}$  parameters (6<sup>th</sup> entry in the first line of a given isotope section) to remove levels in excess. The next step after the modified *\*.lev* file is saved is to rerun the code and check whether the applied cuts are sufficient. If this is not the case, the whole procedure should be repeated and further levels removed. Note, levels are only removed from the local file of the specific case being calculated, and that *Zxxx.dat* files in the parameter library are not affected.

There are no restrictions on the contents of the input file (*\*.inp*) used for displaying the cumulative plots except that the FITLEV record must be included with VAL different from 0. Dispositions that do not consider level densities are ignored as the code exits after the plots are completed without performing any cross section calculations.

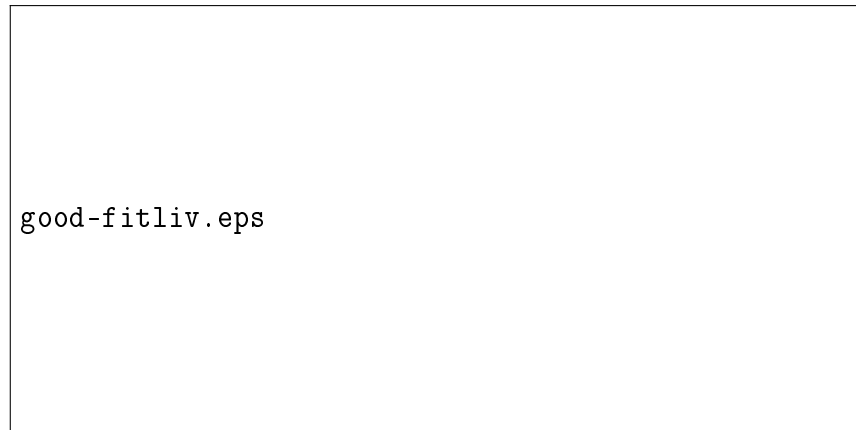


Figure 4.2: Same as Fig. 4.1 but after restricting the fit to the first 6 levels only. Note the difference of two orders of magnitude in the level densities around 6 MeV.

### 4.3 Handling OM potentials

Interface to the RIPL-2 optical model segment has been developed by Capote. This interface allows the use of any type of Optical Model Potential (OMP) contained in the library (including dispersive ones) by specifying the OMP catalog number in the optional input (list of available OMPs can be accessed from the EMPIRE GUI through the menu `Help`  $\Rightarrow$  `RIPL-omp`). The OMPOT record contains two numerical values in addition to the usual keyword. The first value is the OMP catalog number entered with a **negative** sign, which indicates that the potential is going to be taken from RIPL rather than from the internal sets coded in EMPIRE. The second value defines the type of particle. For example,

OMPOT	-401.	1	selects RIPL-2 Wilmore-Hodgson global potential (RIPL-2 number 401) for neutrons,
OMPOT	-4004.	2	selects RIPL-2 CC potential for protons (to be used for $^{197}\text{Au}$ only).

The code will create `*-omp.ripl` file containing parameters for the selected potentials for all nuclei and particles involved in the calculations. This file can be edited in order to adjust OMP parameters extracted from RIPL. RIPL Coupled-Channels Optical Model Potentials (CC-OMP) include collective discrete levels and related deformations, and thus the `*-omp.ripl` contains all information needed to run Coupled-Channel (CC) calculations.

The ECIS06 module, along with the RIPL interface, bring into EMPIRE an easy access to a large number of optical model potentials. However, the related input keywords (DIRECT, DIRPOT and OMPOT) must be used with considerable care. In the following, we will explain different combinations of these keywords, focusing on the use of optical model parameters within EMPIRE. To this end we will discuss several examples of neutron induced reactions on a spherical nucleus ( $^{54}\text{Fe}$ ) with dynamic deformation (vibrational case),

and on a deformed one ( $^{153}\text{Eu}$ ) with static deformation (rotational case). The general input file may contain the following lines:

```
DIRECT      x.          call ECIS for CC, CC full or DWBA
DIRPOT      -xx.        RIPL OMP for direct (inelastic) channel
OMPOT       -xx.      z  RIPL OMP for particle z
```

In the following examples we use case-specific file names as created when script or GUI modes are used to run the code. We recall that the correspondence between the case specific names and those generated by the code is the following:

*\*-omp.dir*  $\iff$  *OMPAR.DIR*

*\*-omp.ripl*  $\iff$  *OMPAR.RIPL*

*\*-lev.col*  $\iff$  *TARGET\_COLL.DAT*

with "\*" standing for the actual root-name of the file.

### 4.3.1 DWBA with RIPL OMP

Apply the DWBA model to the spherical vibrational nucleus  $^{54}\text{Fe}$ . Our goal is to perform calculations using default spherical RIPL potentials for all channels, but including inelastic scattering calculated by ECIS06 with the DWBA option using RIPL spherical OMP catalog number 10. The input file must contain two lines:

```
DIRECT  3.
```

```
DIRPOT  -10.
```

Resulting OMP files:

*\*-omp.ripl* default RIPL OMP used for all the channels in the HF calculations.

*\*-omp.dir* spherical OMP employed in the DWBA calculations of the inelastic scattering to collective discrete levels, in this case RIPL OMP potential catalog number 10.

We can adjust the inelastic scattering cross sections in subsequent runs by changing OMP inside the *-omp.dir* file and/or by changing dynamic deformations inside the *\*-lev.col* file (initial deformation values are 0.15 for quadrupole and 0.05 for octupole vibrations).



### 4.3.2 Coupled-Channels with RIPL spherical OMP

Our goal is to perform calculations for  $^{54}\text{Fe}$  using default RIPL potentials for all the channels, but including inelastic scattering calculated by the ECIS06 CC option using RIPL spherical OMP potential catalog number 10. The input file must contain 2 lines:

```
DIRECT 1.
```

```
DIRPOT - 10.
```

Resulting OMP files:

*\*-omp.ripl* RIPL OMP used for all the channels in the HF calculations.

*\*-omp.dir* spherical OMP employed for the CC calculations of the inelastic scattering to collective discrete levels, in this case RIPL OMP catalog number 10.

We can adjust the inelastic scattering cross sections in subsequent runs by changing OMP inside the *\*-omp.dir* file or by changing dynamic deformations inside the *\*-lev.col* file.

### 4.3.3 Coupled-Channels with RIPL Coupled-Channels OMP for inelastic scattering

We intend to perform calculations for  $^{153}\text{Eu}$  using RIPL spherical potential catalog number 221 for all neutron channels (local potential for  $^{153}\text{Eu}$ ) except the inelastic channel, for which we are going to calculate cross sections with the CC method using the RIPL CC-OMP potential catalog number 2004. The input file must contain 3 lines:

```
DIRECT 1.
```

```
DIRPOT -2004.
```

```
OMPOT -221. 1
```

Resulting OMP files:

*\*-omp.dir* deformed (CC) OMP employed for the CC calculations of the inelastic channel, (RIPL potential catalog number 2004 in this case (contains collective levels and respective deformations)).

*\*-omp.ripl* RIPL spherical OMP catalog number 221 used in the HF calculations of neutron channels.

The inelastic scattering cross sections can be adjusted in subsequent runs by changing OMP inside the *\*-omp.dir* file or by changing the static deformation of the ground state band inside the same file. We are using a true CC-OMP from RIPL and collective levels are stored together with the potential parameters inside the *\*-omp.dir* file.

### 4.3.4 Complete Coupled-Channels with RIPL CC OMP for inelastic scattering

Our aim is to performing exact calculations for  $^{153}\text{Eu}$  using default EMPIRE potentials for all charged particle channels and the RIPL spherical OMP catalog number 221 (local potential for  $^{153}\text{Eu}$ ) for all neutron channels except inelastic, for which we are going to calculate cross sections and transmission coefficients consistently using the CC method and the RIPL CC-OMP catalog number 2004. The input file must contain three lines:

DIRECT 2.

DIRPOT -2004.

OMPOT -221. 1

Resulting OMP files are:

*\*-omp.ripl* CC-OMP employed for the CC calculations of the fusion and inelastic channels (RIPL CC-OMP number 2004 (contains collective levels and respective deformations)). In addition, the file contains RIPL S-OMP number 221 employed for all other neutron channels except inelastic.

*\*-omp.dir* is not created since a true CC-OMP is used consistently and all relevant parameters are contained in the *\*-omp.ripl* file.

The inelastic scattering cross sections can be adjusted in subsequent runs by changing either S-OMP inside the *\*-omp.ripl* file or the static deformation of the ground state band inside the *\*-lev.col* file (initial value is the experimental g.s. quadrupole deformation). Note that the CC-OMP and the CC method are also used for the calculation of the fusion cross section.

## 4.4 Use of level densities

The variety of nuclear level densities available in EMPIRE calls for additional guidance on their use. Only three options are recommended: Empire-specific, Gilbert-Cameron (GC) and HF-BCS; all remaining options (such as Rocol with level density parameter  $a=A/8$ ) are included for comparison but their accuracy is much lower than the three recommendations. The GC level densities, especially when adjusted to known experimental data, may be the most accurate at excitation energies up to the neutron binding and slightly above. However, GC level densities do not lend themselves to extrapolation to higher excitation energies and to nuclei far from the stability line. Energy extrapolation in GC might be dangerous because of the collective effects which are implicitly contained in the level density parameter  $a$ . While this can be an acceptable approximation at low excitation energies for which level densities are fixed by fitting experimental data (discrete

levels and neutron resonance spacings), there is no physical justification for extending such a treatment to higher energies. In fact, collective effects, as implicitly accounted for in the GC approach, increase exponentially with excitation energy instead of decreasing and eventually disappearing. In this respect, EMPIRE-specific and microscopic HF-BCS densities behave properly and should be preferred at excitation energies well above neutron binding.

EMPIRE-specific level densities, in addition to explicit treatment of the collective effects and their damping, also include the effects of dynamic deformation, which is induced by the rotation of a nucleus at high spin. This deformation affects level densities through the modification of nuclear moments of inertia. The yrast line is taken into account by setting level densities to zero whenever the thermal energy available for single particle motion is negative. Thermal energy is calculated as the difference between the total excitation energy and the energy needed for rotation. Spin and energy ranges are also formally unlimited in the EMPIRE-specific level densities. These features make the approach particularly suited for the heavy ion and high-energy nucleon-induced reactions. On the other hand, EMPIRE-specific level densities are fitted to the experimental data in a manner similar to the GC, suggesting that their predictions at low energies should be comparable to those of GC or even better due to the use of the BCS model below critical energy. Therefore, EMPIRE-specific level densities are generally recommended, and are used as a default in the EMPIRE.

However, EMPIRE-specific level densities suffer the same uncertainty as GC when extrapolating from the stability line, because both rely on experimental parameterization of the level density parameter  $a$ , which is only possible for stable or close to stable nuclei. For nuclei far from the stability line, the HF-BCS densities based on realistic schemes of single particle levels offer higher reliability. The physics involved in this approach is clearly superior to the treatment used in the two models discussed above, which makes HF-BCS densities more suitable for extrapolation. In addition, the tabulated values provided by Goriely for RIPL-2 and available in EMPIRE were adjusted to the same experimental data as the other two phenomenological approaches. Therefore, results of the HF-BCS model at low energies should not differ significantly from those provided by the GC or EMPIRE-specific models. Comparisons of cross section calculations for about 300 reactions on targets from  $^{40}\text{Ca}$  to  $^{208}\text{Pb}$  show that microscopic level densities can compete with the phenomenological ones to the extent that makes them the preferred choice far from the stability line. On the other hand, one should keep in mind that tables of level densities are limited to excitation energies below 150 MeV and spins up to  $30\hbar$ , which prevents their use for the Heavy Ion induced reactions well above the Coulomb barrier.

## 4.5 Parameter tuning

The parameter libraries and internal systematics contained in the EMPIRE code perform reasonably well in reproducing cross sections for major neutron induced reactions up to 20 MeV. However, one can not expect that global parametrization will provide perfect fits to

all channels and at all incident energies. Weak reaction channels may differ substantially from the experimental data. In view of the uncertainties associated with the model parameters, certain adjustments were made in order to fit measured cross sections. Guidance is given below on parameter tuning, indicating the most sensitive methods and, if possible, describing the effect of their modification.

It is strongly recommended that various available options in the code are exploited before any attempt is made to change the parameters. This guarantees that physically meaningful parameters are used. For example, the user may try different optical model potentials, various formulations and/or parameterizations of level densities and eventually different preequilibrium models. These attempts should, at least, provide the user with the best starting point for parameter adjustment. We note that various options may provide very different results as illustrated by the following three sets of calculations:

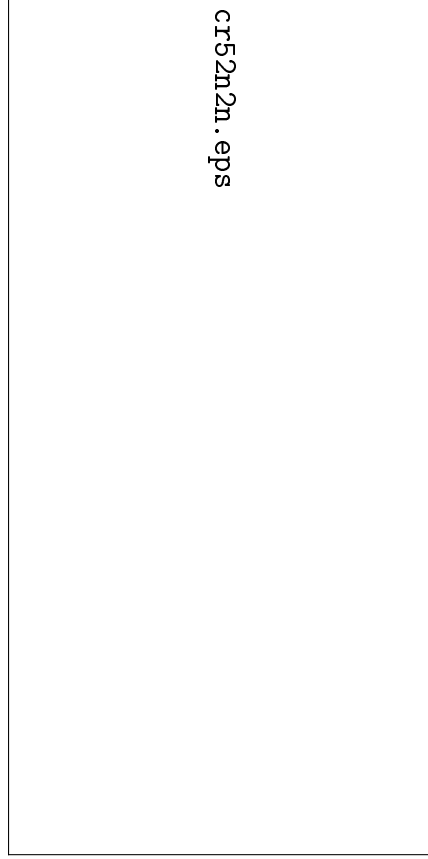


Figure 4.3: Comparison of experimental data with results calculated using three sets of parameters for the  $^{52}\text{Cr}(n,2n)$  reaction (see text).

- |          |                                                                                                                                                                                                                                                 |
|----------|-------------------------------------------------------------------------------------------------------------------------------------------------------------------------------------------------------------------------------------------------|
| standard | Wilmore-Hodgson S-OMP for neutrons and Becchetti-Greenlees for protons, EMPIRE-specific level densities with internal systematics, and discrete levels up to $N_{max} = 10$ (note that in EMPIRE-3.1 Koning-DeLaroche potential is a standard), |
| Ko-Be    | Koning-DeLaroche S-OMP for neutrons and protons, discrete levels up to the $N_{max}$ recommended by RIPL-2 (limited to 40 by the ENDF-6 format), and EMPIRE-specific level densities,                                                           |
| Ko-Be-Go | as above but using HF-BCS microscopic level densities[56] instead of the EMPIRE-specific ones.                                                                                                                                                  |

Fig. 4.3, 4.4 and 4.5 show comparison of the results obtained using the above sets of parameters in three sample cases. Differences of a factor of 2 are observed, and therefore changing the default options may considerably improve the comparison with experimental data. However, this approach may still not be sufficient in some cases, and the next step would be to determine which reaction mechanism is most likely to be responsible for the

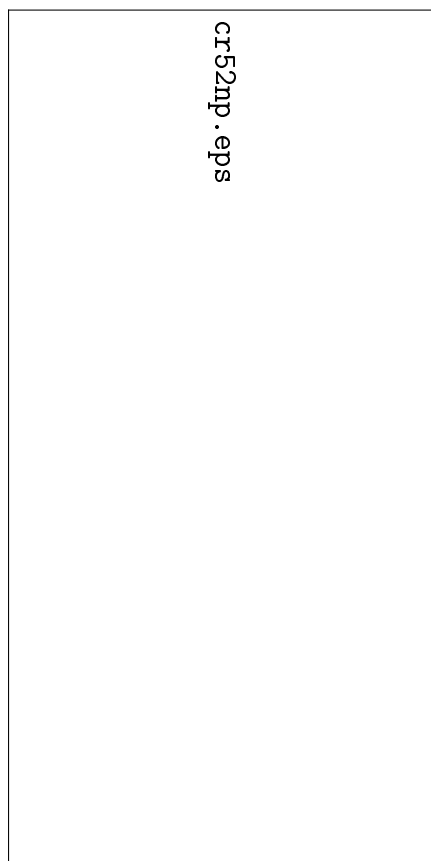


Figure 4.4: Comparison of experimental data with results calculated using three sets of parameters for the  $^{52}\text{Cr}(\text{n,p})$  reaction (see text).

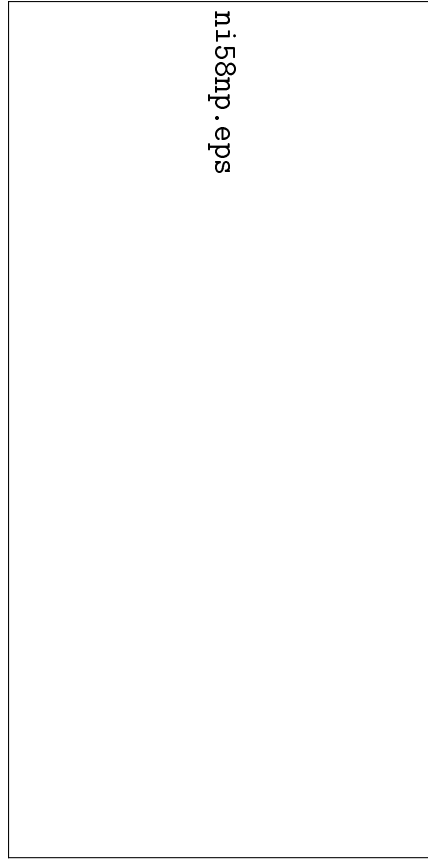


Figure 4.5: Comparison of experimental data with results calculated using three sets of parameters for the  $^{58}\text{Ni}(n,p)$  reaction (see text).

disagreement, remembering that neutron capture below 10 MeV and the low energy part of the particle spectra are essentially due to Compound Nucleus decay. The high energy part of particle spectra is dominated by the preequilibrium emission, and population of the collective discrete levels in inelastic scattering arises mainly from the direct reactions. We also note that at incident energies below 50 MeV the multiple-chance preequilibrium emission is rather small and multiple particle emission is governed by the statistical decay. The list below should help pinpoint the mechanism that might be causing a problem:

- **Nucleon spectra at high ejectile energies underestimated (overestimated)** - these are usually related to the underestimated (overestimated) preequilibrium emission.
- **Tails of the inelastic scattering cross sections underestimated (overestimated)** - again caused by too low (too high) preequilibrium contribution.
- **Inelastic cross sections to discrete levels underestimated (overestimated)** - lack of or too low (too high) contribution from the direct reactions is the most likely

reason. In case of under-estimation, user should ensure that Coupled-Channel or DWBA option is turned on (DIRECT=1, 2, or 3). Generally, the Coupled-Channel option will provide higher cross sections than DWBA.

- **Capture cross sections below 10 MeV underestimated (overestimated)** - as mentioned before, the Compound Nucleus is responsible. The discrepancy might be traced to  $\gamma$ -ray strength function being too low (too high) or to the ratio of level densities in the daughter nuclei and the Compound Nucleus being too low (too high) ( $\rho_n/\rho_{CN}$  - note that the neutron channel is usually the main competitor).
- **Capture cross sections above 10 MeV underestimated** - be sure that the exciton model DEGAS is turned on. The preequilibrium emission of  $\gamma$ s (or the Direct-Semidirect mechanism) is responsible for more than 90% of the capture cross section in this energy range.
- **Cross sections underestimated (overestimated) in all channels** - can be traced to an inadequate optical potential that provides too low (too high) absorption cross section.
- **Wrong total cross section** - obviously an inadequate optical potential.
- **Wrong angular distributions for elastic scattering** - again would assume an inadequate optical potential to be the main reason. At low energies where few inelastic channels are open, there might be a non-negligible contribution from the symmetric compound elastic, which could be affected by the wrong  $\rho_n/\rho_{CN}$  ratio.
- **Cross sections for the  $\alpha$ -channel underestimated** - for nuclei with masses larger than about 100, the discrepancy is not due to wrong parameters but to the lack of a preequilibrium emission of clusters in the present version of EMPIRE. One may compensate for this deficiency by increasing level densities in the residue after  $\alpha$  emission or by increasing the diffuseness of the optical model potential for  $\alpha$ -particles. However, the resulting parameters will be unphysical. Such an intervention may only be justified for lighter nuclei, for which preequilibrium emission of  $\alpha$ -particles is relatively unimportant.
- **Fission cross sections underestimated (overestimated)** - for neutron induced fission, the current fission model coded in EMPIRE is too crude. One may try to cure the problem by decreasing (increasing) the fission barrier or increasing (decreasing) level densities at the saddle point, but this should be considered as an arbitrary fitting exercise without much physical meaning. Tuning fission cross sections in the HI induced reactions will be discussed later on.
- **Excitation functions shifted in energy** - for nuclei far from the stability line (typical for HI induced reactions), this effect can be traced to incorrect binding energies (masses). A modest change of binding energies (of the order of 0.5 MeV)



can be justified as being within the uncertainty of the theoretical masses. However, this argument does not hold for nuclei close to the stability valley since experimental nuclear masses are known with a rather high accuracy.

- **Structure in the continuum part of the inelastic scattering spectrum "out of phase"** - this structure originates from the MSD contribution. When the spectrum does not match experiment, the user may attempt to tune calculations by changing the positions of collective levels to which the response functions are fitted.
- **Double-differential spectra for inelastic scattering to continuum at small angles ( $<40^\circ$ ) underestimated** - MSD mechanism is responsible for the major part of the cross section in this range. Choosing the compressional form factor for the  $l = 0$  transfer (default is the surface form factor) should bring substantial improvement. In fact, from the physical standpoint this *is* the factor that should be used for the  $l = 0$  transfer. The different default is being used due to the numerical instabilities that happen occasionally when this physically-correct option is selected.
- **Wrong ratio between two competing channels (e.g.,  $\sigma(\mathbf{n},\mathbf{n}) / \sigma(\mathbf{n},\mathbf{p})$ )** - at low incident energies this ratio is governed by the Compound Nucleus decay and may be distorted by an inappropriate ratio of level densities in the two competing channels. Actually, the cross section ratio is approximately proportional to the level density ratio in the respective residual nuclei. Also, the optical model potential may have a significant effect. At higher incident energies, the preequilibrium contribution starts to play a role, and a reference for one of the preequilibrium channels may provide a solution.
- **Wrong slope of the increasing part of the excitation function** - a crucial role is played by the discrete levels in the residual nucleus and the optical model potential (transmission coefficients), of which the discrete levels are easier to control. Changing the number of accepted levels may effectively increase or decrease the available phase space for the particular decay mode.
- **Production of residues in HI induced reaction underestimated (overestimated)** - for lighter nuclei in which the fission channel is not dominant, the fusion cross section might be too small (or too big). Competition between fission and particle emission may constitute an additional source of error for the highly fissile (heavy) nuclei. In such a case, decreasing (increasing) strength of the fission channel is usually an effective way of increasing (decreasing) residue production.

The mechanisms and parameters that are expected to be the most important and effective in solving a particular problem have been noted in the above discussion. However, we are always dealing with a complicate interplay of different factors and in some cases the major sources of error may differ from those indicated. However, the user should be able to identify the most critical reaction mechanism or a key input quantity in most cases, and be able to avoid a random search for optimal parameters.

So far we have discussed the symptoms and possible reasons for operational problems. Knowing the disease, we should now look for the most appropriate treatment. We will indicate those input parameters to which particular models or input quantities (such as fusion, level densities and,  $\gamma$ -ray strength functions) are most sensitive. However, parameters not mentioned below may also influence the results. Generally, their effect should be less pronounced but they might become one of the key players in particular situations. In addition, these assessments are complicated and most of the parameters are correlated; for example, deficiencies in one parameter can be compensated by a change in another leading to unrealistic values. Therefore, it is important to understand the physical reason for a discrepancy and proceed accordingly, and to fit all available observables rather than a single cross section. Such an approach increases the user's confidence in the final results. Finally, fitting a single experimental point that differs dramatically from the calculated value can be dangerous, especially when the exercise involves a strong channel. The experimental point might simply be wrong. Such cases are known in the EXFOR library, either because of an erroneous experiment or a compilation error. In particular, if the experimental data fall well below the calculated cross section, the user should check whether the measurement concerned the total cross section for the reaction channel or the cross section to the isomeric or ground state.

In the discussion that follows, we group parameters according to the reaction mechanism or input quantity to which they are relevant, and refer to them by keywords defined in the input description (see Section 3.10.1).

## Fusion

We have to distinguish between heavy ion and Light Ion ( $A < 5$ ) of nucleon induced reactions. Heavy ion induced reactions:

- FUSRED scales calculated fusion cross section with an arbitrary factor to set the parameter directly to the desired value, but lacks any physical significance and predictive power. Should be used as the last resource unless the fusion cross section is known from a more microscopic model or experiment.
- BFUS Fusion barrier height in the distributed barrier model  $B_{fus}$  (Eq. 2.2) is by default calculated by the CCFUS and used for the HI induced reactions only. Even a slight decrease of the barrier height can produce a considerable increase of the fusion cross section (and vice versa) when the incident energy (in CM) is close to the barrier height. This effect tends to disappear at higher incident energies.
- SIG SIGMA in the distributed barrier model (Eq. 2.2) is by default set to  $0.05B_{fus}$ . Increase of SIGMA will also increase the fusion cross section. Similarly to BFUS, the effect is most pronounced at low energies and tends to disappear at higher values.

- EXPUSH Extra-push energy (default value is 0) is very effective at decreasing the HI fusion cross section when increased. Physically justified for a fusion of massive systems.
- CRL Critical  $l$ -value for the HI fusion (Eq. 2.5) sets fusion cross section to the required value - much like FUSRED.
- DFUS Diffuseness in the transmission coefficients of HI fusion (Eq. 2.5) does not change the fusion cross section, but defines the spin distribution. Larger DFUS, the higher the spins populated, and this effect may contribute to an increase of the fission cross section and resulting reduction in the evaporation residues.

Most of the parameters discussed above concern HI induced reactions. There are fewer possibilities for nucleons as the fusion (or absorption) cross section is calculated using the optical model. Users may try different parameterizations available in the RIPL library or internal OMP systematics. If this fails, increasing the imaginary part of the OMP will increase the absorption cross section. However, users are advised that blind modification of the OMP can easily produce physically unrealistic results.

### Coupled-Channels (ECIS)

CC calculations are most sensitive to the deformations of collective levels, which can be adjusted by editing the *\*-lev.coll* file (see Section 3.10.6). Actually, if the collective levels are selected internally rather than taken from the RIPL library along with the CC optical model potential, these deformations *should* be adjusted. The code sets them by default to the g.s. deformation for the rotational model and to the arbitrarily fixed values for the vibrational model. These values can only be considered as a first guess. Increasing the band deformation for the rotational model or dynamic deformations for the vibrational model results in an increase of the calculated direct cross sections (opposite is true if the deformations are decreased).

Adding more collective levels to the *\*-lev.coll* file will generally increase the total direct cross section, and may result in a substantial increase of the cross section to the introduced levels. Generally, the overall effect is not very significant as high energy levels are usually only weakly coupled. Substantial increase of the direct cross section, especially for the highly deformed nuclei, can be achieved by using the CC approach instead of DWBA. As a rule, CC model *should* be the preferred choice in such cases.

Obviously, the cross sections calculated with the CC model are sensitive to the OMP. The effect might be considerable but is difficult to predict due to the large number of parameters involved. Generally, deeper imaginary part of the OMP (especially the imaginary surface component) will result in the higher cross sections.

### Multi-step Direct

The microscopic character of the MSD model limits the possibilities of influencing the results compared with the classical models (such as the exciton model). A certain degree

of flexibility is provided by the pairing gap parameters (GAPP for protons and GAPN for neutrons). The dependence is non-linear, and it is difficult to predict the impact of any change. MSD results are slightly more sensitive to the EFIT parameters, which define the energies of the collective levels to which response functions for different multipolarities are fitted. Again, due to the non-linearity, the results of the change are hard to predict, the effect has an oscillating character. However, on average, decreasing the EFIT value for a given multi-polarity results in an increase in strength for the  $l$ -transfer under consideration and a higher MSD cross section. We stress again that EMPIRE sets EFIT values internally to the energy of the lowest discrete level which can be coupled to the ground state with a given  $l$  transfer (except  $l = 0$  transfer for which the self-consistent value is taken by default). This assignment might be erroneous if there happens to be a non-collective and low energy level with a suitable spin. In such a case, the EFIT value should be corrected manually by entering the EFIT keyword with the proper energy of the true collective level. Modifications in the EFIT values will generally affect the structure observed in the MSD spectra by shifting maxima to different energies, and the user is advised to try first the self-consistent values for EFIT before attempting any arbitrary modifications.

Substantial increases in the MSD contribution at *forward angles* can be obtained by switching to the compressional form factor for the  $l = 0$  transfer (COMPFF=1). As already mentioned before, this option is physically sound and strongly recommended.

The last resource involves multiplying the response function by an arbitrary factor through the RESNOR entry. Factors larger than 1 will increase MSD cross sections, and values smaller than 1 will reduce it. This procedure has no physical meaning and may eventually lead to the MSD emission being larger than the absorption cross section.

### Multi-step Compound

The most significant MSC contribution to the nucleon spectra is located between the Compound Nucleus (low energies) and the MSD contributions (middle-high energies). MSC mechanism accounts for about 20-30% of the total emission at incident energies close to 10 MeV and decreases with the increasing incident energy. Therefore, one should not expect too much from tuning this mechanism. Similarly to MSD, the user's freedom to modify MSC is rather limited. The parameters that have the largest effect are as follows:

GDIV	Single particle level densities defining particle-hole level densities in MSC set to $A/13$ by default. Increasing (decreasing) GDIV will result in a higher (lower) MSC cross section. Note that increasing GDIV is justified for nuclei close to the magic numbers, as their level densities are significantly lower.
TORY	Ratio of the cross sections for unlike and like nucleon-nucleon interaction (e.g., $\sigma_{np}/\sigma_{nn}$ ). Can be used for adjusting the relative share between neutron and proton emission. The default value of 4, as derived from the free nucleon scattering, is generally accepted, although some doubts have been expressed as to whether the free scattering value should be applied to the scattering inside

nuclear matter. Increasing (decreasing) this parameters will favor (suppress) the charge exchange channel.

**D1FRA** Ratio of the GDR spreading width to the total GDR width (default: 0.8) is relevant to  $\gamma$ -emission only. While there is not much room for increase, decreasing the ratio will also reduce the already low  $\gamma$ -emission through the MSC mechanism.

### Exciton model (DEGAS)

The above discussion of the GDIV parameter also applies to the exciton model calculations in the neutron channel. DEGAS also offers the possibility to vary independently the single particle level density in the proton channel, which allows modifications to the neutron/proton emission ratio. By default, both single particle densities are taken to be equal.

### Level densities

The Hauser-Feshbach results are very sensitive to the level densities, and more precisely to their ratio in the neighboring nuclei. Generally, changing level densities is the most effective way of adjusting cross sections. As mentioned at the beginning of this Section, various formulations of the level densities provided in EMPIRE should be considered with their default parameterization first. Only if this exercise does not produce sensible results should the user attempt to vary the model parameters. The three recommended and most accurate models are (i) EMPIRE-specific, (ii) Gilbert-Cameron, and (iii) HF-BCS. All of them are fitted to match the discrete levels. While the pre-calculated HF-BCS level densities can not be modified, EMPIRE and Gilbert-Cameron offer more significant flexibility. First of all, they are affected by the number of discrete levels in the calculations (it is assumed that cumulative plots had already been checked for consistency using the FITLEV option). Generally, adopting fewer levels increases the level densities between the last discrete level and neutron binding energy, and considering more levels tends to decrease level densities in the same region (see Fig. 4.1 and 4.2). However, this general statement may not hold in cases with strong irregularities in the cumulative plots. Extending the discrete level scheme too far involves a risk of including the region with missing levels which would lead to an unphysical reduction of level densities. The new RIPL-2 library of discrete levels contains estimates of the completeness of the scheme ( $N_{max}$ ), which is used by EMPIRE as a default. These values have been compared with the EMPIRE level densities (i) and (ii) and were found to be compatible in about 75% of cases. The user should decrease  $N_{max}$  in the remaining 25%. If this reduction is insufficient the discrete level region may extend too far. Another extreme involves too few levels, in which there is a risk of fitting level densities to a bunch of collective levels that are shifted toward lower energies because of their collective nature. The resulting level densities might be considerably overestimated.

Changing the level density models and the number of discrete levels may fail, and the user may be forced to adjust the level density parameters themselves. Depending on the model there are different possibilities for explicit adjustment of level density parameters. EMPIRE-specific level densities:  $a$ -parameter is energy and spin dependent, and can not be read as a single input entry. However, there is a possibility of applying a factor (ATILNO) to the asymptotic value of the  $a$ -parameter, which is equivalent to multiplying each  $a$ -parameter (larger  $a$  values correspond to larger level densities). There are no other parameters in the EMPIRE-specific level densities that can be controlled from the input. The Gilbert-Cameron level densities offer more flexibility: all of the parameters can be specified in the input file. However, it is a responsibility of the user to ensure that these parameters are internally consistent (i.e., fulfill matching conditions and fit discrete levels). A much safer approach involves the introduction of the  $a$ -parameter and one other ( $U_x$ ,  $E_o$ , and  $T$ ), and allows the code to take care of the internal consistency. As usual, level densities increase with  $a$ -parameter. The constant temperature component (low energy) of the level densities increases with decreasing  $T$  and  $E_o$ , and higher values of  $U_x$  correspond to higher level densities. Finally, within the Gilbert-Cameron approach coded in EMPIRE, there are three built in systematics for  $a$ , that can be selected with the GCROA keyword:

GCROA    = 0 Ignatyuk systematics,  
            = -1 Arthur systematics,  
            = -2 Ilijnov systematics (default).

### Fission

Fission can be scaled quite effectively with a number of parameters, especially in the HI induced reactions. The reduced dissipation coefficient  $\beta_v$  is controlled by the keyword BETAV, and decreases the fission channel when moved further out from the 3.2 value (corresponding to  $\beta_v = 3.2 \cdot 10^{-21} \text{ s}^{-1}$ ), separating the under-damped and over-damped motion. All remaining input parameters affect directly (e.g., QFIS) or indirectly the height of the fission barrier, and can be divided into those that control shell correction damping with spin and temperature and those that modify the fission barrier by adding a Gaussian centered at a certain spin. All of them are listed below:

QFIS	Liquid drop fission barrier multiplier. QFIS>1 decreases fission channel.
SHRJ	Shell correction to fission barrier is damped to 1/2 (Eq. 2.155) at the spin defined by SHRJ. For negative shell corrections, lowering SHRJ will increase the fission channel, at least at sufficiently high incident energies. Opposite is true for positive shell corrections.
SHRD	Diffuseness of the shell correction damping (Eq. 2.155). The size and sign of the effect depend on the actual spin population of the fissioning nucleus.
TEMP0	Temperature at which temperature-damping of the shell correction (Eq. 2.154) starts to be effective. Increasing (decreasing) this value will decrease (increase)

fission above the temperature defined as  $\min(\text{TEMP0}, 1.65)$  (1.65 is the default value) and will have no effect on the fission cross sections at incident energies corresponding to lower temperatures.

- SHRT      Multiplier in the exponent of the temperature-damping of the shell correction (Eq. 2.154). Increasing this parameter will increase fission above the temperature selected with TEMP0 (no change below).
- DEFGA      Amplitude of the Gaussian term defined by Eq. 2.155. Setting to a positive value will increase fission barrier and therefore decrease fission channel, but only if the states with spins within the range defined below by DEFGW and DEFGP are populated. On the contrary, a negative value will increase the fission cross section. The Gaussian term is used to simulate irregularities in the shell correction related to the incidental bunching or de-bunching of single particle levels due to the rotation-induced change in nuclear deformation. Generally, the effect will only be observed in the limited range of incident energies.
- DEFGW       $\Delta J_G$  (width in spin) in the Gaussian (term of Eq. 2.155). Increasing DEFGW will magnify the effect described above and enlarge the range of incident energies being affected.
- DEFGP       $J_G$  (spin position) of the Gaussian (term Eq. 2.155). The value of DEFGP defines the mean value of the incident energy range affected by the Gaussian term, which increases with DEFGP. Setting this parameter above the maximum spin for nucleus stability reduces or even eliminates the effect.

### GDR parameters ( $\gamma$ -ray strength functions)

The EMPIRE input file provides the user with a full control of the GDR parameters. This possibility might be worth trying as the present version of the code makes use of the built-in systematics by default. This systematic approach is usually reasonable for nuclei with  $A > 100$ , but for lighter nuclei the experimental data show less regular behavior. GDR widths are particularly widely scattered and their deviation from systematics may reach 3 MeV. Also, peak cross sections for nuclei with  $A > 225$  can differ from the systematics by as much as 100 mb. The experimental values for the GDR parameters can be found in RIPL-2. Other multipolarities can also be modified by entering them explicitly in the input file but their effect on the cross sections is rather small.

The overall increase of the  $\gamma$ -ray strength function can be obtained by increasing the GDR peak cross sections (CSGDR1 and CSGDR2). Increase of the low energy part of the strength function (usually most important for the capture cross sections) can be attained by lowering the positions of the GDR peaks (EGDR1 and EGDR2), especially the lower one (EGDR1). Another effective method leading to a similar result involves increasing the GDR widths (again the lower one is more significant). Opposite actions will reduce the  $\gamma$ -ray strength function. If the dynamic option is selected (i.e., GDR parameters depend

on angular momentum and temperature), shifts with respect to the calculated values can be introduced in place of the explicit values of the parameters. These shifts are coded in the input file under keywords: GDRWA1, GDRWA2, GDRESH, GDRSPL, GDRST1, and GDRST1.

Drastic changes of the default GDR parameters are likely to be unphysical. Thus, the product of the peak cross section and GDR width is constrained by the sum rule, and users should ensure that the inputted values respect this limitation.

## 4.6 Description of test cases

The test cases are intended for the verification of the local installation.

(to be completed by Roberto)

## Acknowledgments

EMPIRE is the result of international cooperation towards open source software as so successfully promoted by the General Public License. A number of authors contributed to the development of the code. The recent developments described in this report would not have been possible without their valuable voluntary contributions. We would also like to acknowledge the authors of the codes that are included in EMPIRE: E. Betak (DEGAS), M.B. Chadwick (DDHMS), C.H. Dasso and S. Landowne (CCFUS), H. Lenske and H. Wolter (ORION and TRISTAN), J. Raynal (ECIS06), and A. Sierk (BARFIT and MOMFIT). We would like to thank M. Mebel for providing the routine for calculation of shell-corrections according to Myers and Swiatecki. We are grateful to G. Giardina and his collaborators A. D'Arrigo, A. Taccone, and A. Lamberto who assisted the project from the very beginning and have tested various versions of the code since 1993. We would also like to thank A.L. Nichols for his continual support of the project. Finally, we are indebted to R. Sturiale for LINUX support at the early stages of the development of EMPIRE development.

M. Pigni (attn. Roberto) ...

RIPL Project ...



# Bibliography

- [1] H. M. Hofmann, J. Richert, J. W. Tepel, and H. A. Weidenmüller, *Ann. Phys.* **90**, 403 (1975).
- [2] H. M. Hofmann, T. Mertelmeier, M. Herman, and J. W. Tepel, *Z. Physik A* **297**, 153 (1980).
- [3] H. Feshbach, A. Kerman, and S. Koonin, *Ann. of Phys.* **125**, 429 (1980).
- [4] H. Nishioka, J. J. M. Verbaarschot, H. A. Weidenmüller, and S. Yoshida, *Ann. Phys.* **172**, 67 (1986).
- [5] J. Raynal, *Notes on ECIS*, CEA-N-2772, Commissariat à l'Energie Atomique, 1994.
- [6] C. H. Dasso and S. Landowne, *Comp. Phys. Comm.* **46**, 187 (1987).
- [7] T. Tamura, T. Udagawa, and H. Lenske, *Phys. Rev.* **C26**, 379 (1982).
- [8] H. Lenske and H. H. Wolter, TRISTAN and ORION codes, private communication to M. Herman.
- [9] E. Běták and P. Obložinský, INDC(SLK)-001, IAEA, Vienna, 1993.
- [10] M. B. Chadwick, DDHMS code, private communication to M. Herman.
- [11] A. J. Sierk, *Phys. Rev.* **C33**, 2039 (1986).
- [12] D. E. Cullen, PREPRO2000: ENDF Preprocessing Codes, Report IAEA-NDS-39, Vienna, 2000, available from <http://www-nds.iaea.org/ndspub/endl/prepro/>.
- [13] A. Trkov, ENDVER - ENDF File Verification Support Package, available from <http://www-nds.iaea.org/ndspub/endl/endver/>.
- [14] V. V. Zerkin, ZVView graphics software for nuclear data analysis version 9.4, 2001, available from <http://www-nds.iaea.org/ndspub/zvview/>.
- [15] K. H. Schmidt and W. Morawek, *Rep. Prog. Phys.* **54**, 949 (1993).
- [16] D. L. Hill and J. A. Wheeler, *Phys. Rev.* **89**, 1102 (1953).
- [17] IAEA-CRP, Reference Input Parameter Library (RIPL), IAEA-TECDOC-1034, Vienna, <http://www-nds.iaea.org/ripl/>, 1998.

- [18] H. Lenske *et al.*, submitted to Nucl. Phys.
- [19] H. Lenske and H. H. Wolter, Nucl. Phys. **A538**, 483 (1992).
- [20] A. Fetter and J. Walecka, *Quantum Theory of Many Body Systems* (McGraw-Hill, New York, ADDRESS, 1971).
- [21] H. Wienke, R. Capote, M. Herman, and M. Sin, Phys.Rev. C **78**, 064611 (2008).
- [22] N. V. G. K. Hagino and H. Sagawa, Nucl. Phys. **A731**, 272 (2004).
- [23] J. W. Negele, *Theory of Many-Body Systems* (Addison-Wesley, New York, 1990).
- [24] A. L. Fetter and J. D. Walecka, *Quantum Theory of Many-Particle Systems* (McGraw-Hill, New York, 1971).
- [25] A. Bohr and B. Mottelson, *Nuclear Structure* (Reading, MA. Addison-Wesley/W.A. Benjamin, Inc., USA, 1975), Vol. Vol.2.
- [26] R. Siudak, Ph.D. thesis, Univ. Cracow (Poland), .
- [27] P. Ring and S. Schuck, *Theoretische Kernphysik* (Springer, Berlin, 1982).
- [28] V. G. Soloviev, Progr. Part. Nucl. Phys. **19**, 107 (1987).
- [29] M. Herman, G. Reffo, and H. Weidenmüller, Nucl.Phys. **A53**, 124 (1992).
- [30] K. Stankiewicz, A. Marcinkowski, and M. Herman, Nucl. Phys. **A435**, 67 (1985).
- [31] P. Obložinský, Nucl. Phys. **A453**, 127 (1986).
- [32] A. Hoering and H. A. Weidenmüller, Phys. Rev. **C46**, 2476 (1992).
- [33] M. Herman, A. Hoering, and G. Reffo, Phys. Rev. **C46**, 2493 (1992).
- [34] P. Axel, Phys. Rev. **126**, 671 (1962).
- [35] D. M. Brink, Ph.D. thesis, Oxford, 1955.
- [36] D. M. Brink, Nucl. Phys. **4**, 215 (1957).
- [37] G. F. Bertsch, private communication to A. Hoering, 1992.
- [38] C. Kalbach, Z. Phys. **A287**, 319 (1978).
- [39] E. Běták, A. L. F. Cvelbar, and T. Vidmar, Nucl. Phys. **A686**, 133 (2001).
- [40] M. Blann, Phys. Rev. **C54**, 1341 (1996).
- [41] M. Blann, Phys. Rev. Lett. **27**, 337 (1971).

- [42] M. Blann and A. Mignerey, Nucl. Phys. **A186**, 245 (1972).
- [43] M. Blann, Phys. Rev. Lett. **28**, 757 (1972).
- [44] M. Blann, Nucl. Phys. **A213**, 570 (1973).
- [45] J. Bisplinghoff, Phys. Rev. C **33**, 1569 (1986).
- [46] A. Gilbert and A. G. W. Cameron, Can. J. Phys. **43**, 1446 (1965).
- [47] IAEA-CRP, Reference Input Parameter Library, Phase II (RIPL-2), to be released in 2002.
- [48] A. V. Ignatyuk, G. N. Smirenkin, and A. S. Tishin, Sov. J. Nucl. Phys. **21**, 255 (1975).
- [49] P. G. Young *et al.*, Trans. Amer. Nucl. Soc. **60**, 271 (1989).
- [50] A. S. Iljinov *et al.*, Nucl. Phys. **A543**, 517 (1992).
- [51] A. R. Junghans *et al.*, Nucl. Phys. **A633**, 633 (1997).
- [52] A. V. Ignatyuk, K. K. Istekov, and G. N. Smirenkin, Sov. J. Nucl. Phys. **29**, 450 (1979).
- [53] I. Gontchar, private communication to M. Herman, 1995.
- [54] P. Moller and J. R. Nix, At. Data Nucl. Data Tables **26**, 165 (1981).
- [55] A. D'Arrigo, G. Giardina, and A. Taccone, Phys. Lett. **B262**, 1 (1991).
- [56] P. Demetriou and S. Goriely, Nucl. Phys. **A695**, 95 (2001).
- [57] S. E. Vigdor and H. J. Karwowski, Phys. Rev. **C26**, 1068 (1982).
- [58] G. Andersson *et al.*, Nucl. Phys. **A268**, 205 (1976).
- [59] W. D. Myers and W. J. Swiatecki, Phys. Rev. **C60**, 014606 (1999).
- [60] A. D'Arrigo *et al.*, J. Phys. **G20**, 305 (1994).
- [61] P. Grange and H. A. Weidenmüller, Phys. Lett. **B96**, 26 (1980).
- [62] E. M. Rastopchin *et al.*, Sov. J. Nucl. Phys. **53**, 741 (1991).
- [63] H. Kramers, Physica **7**, 284 (1940).
- [64] J. M. Blatt and V. Weisskopf, *Theoretical Nuclear Physics* (John Wiley and Sons, Inc., New York, 1952).
- [65] S. S. Dietrich and B. L. Berman, Atomic Nucl. Data Tbl. **38**, 199 (1998).

- [66] A. D'Arrigo *et al.*, Influence of nuclear deformation on photon emission spectra, unpublished.
- [67] D. R. Chakrabarty *et al.*, Phys. Rev. **C36**, 1886 (1987).
- [68] J. Speth and A. van de Woude, Rep. Prog. Phys. **44**, 719 (1981).
- [69] W. V. Prestwich, Z. Phys. **A315**, 103 (1984).
- [70] IAEA-CRP, Handbook on photonuclear data for applications: Cross sections and spectra, IAEA-TECDOC-1178, Vienna, <http://www-nds.iaea.org/photonuclear/>, 2000.
- [71] M. B. Chadwick, P. O. zinský, P. E. Hodgson, and G. Reffo, Phys. Rev. **C44**, 814 (1991).
- [72] U. Brosa, S. Grossmann, and Müller, A. Phys. Rep **197**, 167 (1990).
- [73] B. et al., Phys.Rev. **C 9**, 1924 (1974).
- [74] B.S.Bhandari, Phys.Rev. **C 19**, 1820 (1979).
- [75] S.Bjornholm and J.E.Lynn, Rev. Mod. Phys. **52**, 725 (1980).
- [76] A. Ventura, private communication, 2002.
- [77] G. Audi and A. H. Wapstra, Nucl. Phys. **A595**, 409 (1995).
- [78] P. Moller, J. R. Nix, W. D. Myers, and W. J. Swiatecki, At. Data and Nucl. Data Tables **59**, 185 (1995).
- [79] Evaluated Nuclear Structure Data File (ENSDF), <http://www-nds.iaea.org>.
- [80] R. B. Firestone *et al.*, *Table of Isotopes, 8th Ed.* (John Wiley and Sons, Inc., New York, 1998), Vol. 1, 2.
- [81] E. T. M. Goldhaber, Phys. Rev. **74**, 1046 (1948).
- [82] P. V. I. et al., Phys. Rev. **C45**, R13 (1992).
- [83] S. Goriely, Phys. Lett. **B436**, 10 (1998).
- [84] S. Goriely, in *AIP Conf. Proc. 529*, edited by S. Wender (PUBLISHER, ADDRESS, 2000), p. 28.7.
- [85] A. K. D. Y. Aboussir, J. M. Pearson and F.Tondeur, At. Data and Nucl. Data Tables **61**, 127 (1995).
- [86] M. A. F. K. Thielemann, in *Proc. of the Conf. on Nuclear Data for Science and Technology*, edited by D. K. Bockhoff, Reidel (PUBLISHER, ADDRESS, 1983), p. 762.

- [87] A. Mamdouh, J. M. Pearson, M. Rayet, and F. Tondeur, Nucl. Phys. **A644**, 389 (1998).
- [88] A. Mamdouh, J. M. Pearson, M. Rayet, and F. Tondeur, Nucl. Phys. **A679**, 337 (2001).
- [89] G. N. Smirenkin, Technical report, IAEA-Report INDC(CCP)-359 (unpublished).
- [90] S. Goriely, F. Tondeur, and J. M. Pearson, Atomic Data Nuclear Data Tables **77**, 311 (2001).
- [91] Tcl/Tk software package, available free of charge from <http://dev.scriptics.com/software/tcltk/>.

# Appendix ChangeLog

## Changes in version 3.1 with respect to 2.19

Sao Jose dos Campos, June 2011

1. PREPRO2007 updated to PREPRO2010
2. Merging resonance parameters into the final ENDF file
3. GUI assisted OMP fitting
4. Prompt fission neutron spectra including post-fission neutrons emitted from fully accelerated fragments (Los Alamos or Kornilov model) (M. Sin, R. Capote)
5. DWBA calculations on odd nuclei (discrete levels embedded in the continuum only) (R. Capote)
6. ECIS subroutine modified to allow use of dispersive potentials with different geometry of the imaginary and real parts (R. Capote)
7. MSD-model extended to deformed nuclei (H. Wienke)
8. Recursive treatment of transmission through multi-hump fission barrier (M. Sin, R. Capote)
9. Library of neutron resonances updated to ENDF/B-VII.0
10. Checking codes updated
11. Calculation, formatting and plotting of isomers
12. Options are partially implemented to use average radiation width, neutron width, and resonance spacing, to create fake resonance file (MF=2).
13. EXFOR library updated to January 2011 version
14. MySQL based EXFOR retrieval system moved to more robust FORTRAN implementation
15. Moments of inertia (spin distribution parameter) controlled from the input
16. Parity dependent level densities (HFBCS available)

17. Resonance module added
  - Parameters from Atlas of Neutron Resonances => MF2
  - Parameter uncertainties => MF32
  - Reproducing thermal cross section uncertainties
  - Inclusion of arbitrary correlations among gamma-widths and among neutron-widths
18. New parametrization of EGSM level densities (EGSM = Enhanced/EMPIRE Generalized Superfluid Model)
19. New fission model implemented (Phys. Rev. C 77 (2008) 054601)
20. RIPL-3 updates
  - Discrete levels library
  - Optical model parameters
  - Microscopic level densities (HFBCS) with parity dependence
21. ECIS-2006 implemented
22. Covariance generation capabilities using Monte Carlo approach or Kalman filter
23. Accounting for model uncertainties in covariance generation
24. Correlated sampling in Monte Carlo
25. Scaling factor in Kalman filter
26. Six ejectiles (n, p, alpha, g, d, t, 3He) + arbitrary light ion; includes ENDF-6 formatting (Capote, Trkov)
27. Inclusion of RIPL-3 combinatorial level densities with parity dependence
28. Upgrade of ZVView package with 2-D and 3-D plotting of covariance matrices (Zerkin)
29. DDHMS preequilibrium model extended to produce exclusive spectra
30. KERCEN code incorporated in the EMPIRE system (not linked through GUI)
31. Primary capture gammas isolated and printed separately

## Changes in version 2.19 with respect to 2.18 Brookhaven, March 2005

1. Error in the Wilmore-Hodgson omp corrected. VOM(4, Nejc, Nnuc) set to -0.0018 instead of -0.00018. This coefficient was also found to be wrong in the preliminary version of RIPL-2 (M. Herman).
2. MSD is automatically turned off for non-nucleon incident reactions (M. Herman).
3. Internal conversion coefficients included in the gamma cascade between discrete levels (ICC data from RIPL-2)(M. Herman).
4. Bug in reading branching ratios from the RIPL-2 file corrected (emission probabilities instead of branching ratios were used in the previous RIPL-2 versions) (R. Capote).
5. Bug in DEGAS resulting in lack of the preequilibrium population in the Compound Nucleus continuum corrected (bug has been introduced in version 2.18) (E. Betak).
6. ENDRES code and BNL-325 file with resonance parameters added in order to merge resonance parameters into the final ENDF file (also dxsend.f has been updated) (A. Trkov).
7. LINEAR and RECENT utility codes added in order to reconstruct cross sections from the resonance parameters and enable plotting (M. Herman & A. Trkov).
8. Some potentially empty files removed if actually empty (M. Herman).
9. run, runE, format and plot scripts modified to avoid double coding (M. Herman).
10. Processing with FIXUP split into two runs to avoid redundant data in the final ENDF file (reconstruction of 203 and 207 postponed to the second run) (M. Herman).
11. Last energy point in the gamma spectra from capture included in the file \*.out with energy of the CN excitation energy and respective cross section scaled to preserve spectrum integral.
12. Option for manual OMP fitting added to the new GUI (M. Herman).
13. PSYCHE added to the chain of utility codes (M. Herman).
14. Spectral energies for ENDF formatting printed in F10.5 instead of F9.4 format to improve accuracy (M. Herman).
15. EMPEND revised to eliminate some undesired entries in the ENDF file (A. Trkov).
16. Fission with under-barrier effects in terms of optical model for fission implemented (R. Capote, M.Herman, M. Sin, and A. Ventura).



17. Reactions on excited targets (M. Herman).
18. PostScript (and eps) files produced from within ZVV viewer are stored in the work directory with a name following standard convention (M. Herman).
19. 'mb' printed after gamma emission intensity of discrete transitions in order to be able to plot respective excitation functions directly from the EMPIRE output (\*.lst) (M. Herman).
20. 'zvpl' script for direct plotting from the EMPIRE output modified. Additional window to paste a pattern is being opened. A bit more cumbersome than before but more reliable. Before, many patterns were misunderstood due to skipping blanks in the pattern and garbage plot was produced (M. Herman).
21. Maximum number of aliases in c4sort.f increased to 200.
22. 'reaction' and 'titles' files used by X4TOC4 corrected and extended to cover proton induced reactions (still needs a consistent check) (M. Herman).
23. On-line retrieval of the EXFOR data from the remote database implemented. At the moment works only at nuclear data centers but will be extended to reading from the EXFOR CD-ROM (V. Zerkin & M. Herman).
24. Spectra for the ENDF formatting printed also for the proton induced reactions (M. Herman).
25. File 'titles' in x4toc4 modified to treat properly min and max bin energies in the emission spectra (M. Herman).
26. Correction to DEGAS regarding flux conservation (E. Betak)
27. X4TOC4 replaced with the version available from ENDVER (version 2001-8) (A. Trkov).
28. sixtab.f and dxsend.f modified to enable processing of more advanced formatting used in the recent LANL evaluations (discrete gamma's are still not processed correctly in such cases) (A. Trkov).
29. Archives directories moved from inside 'work' to 'empire' to make 'work' more manageable (change inside Xrun.tcl) (M. Herman).
30. Retrieval of EXFOR data from the relational MySQL database - opens access to the periodically updated EXFOR library issued by the IAEA-NDS on CD-ROMs (V. Zerkin, M. Herman).
31. Preequilibrium emission of clusters (Iwamoto-Harada) coded by R. Capote (PCROSS module).

32. Xrun.tcl GUI updated: selective delete, access to fission input, and generation of three piece-wise input templates (M. Herman).
33. ZVView updated to the zvv97l.exe version (V. Zerkin).
34. Spectra of recoils calculated using 'ENDF=2 prescription' instead of a rough approximation used before (M. Herman).
35. Pre-fission spectra of particles printed in \*.out for ENDF formatting (M. Herman)
36. Zerkin's GUI allowing for customized EXFOR retrieval can be started from the EMPIRE GUI (M. Herman)
37. Confirmation dialogs added to GUI for all 'delete' buttons (M. Herman)
38. CHECKR added to the chain of utility codes (M. Herman).
39. FIZCON added to the chain of utility codes (M. Herman).
40. STANEF added to the chain of utility codes (M. Herman).
41. Printing particle spectra in the \*.out output of EMPIRE rearranged so that transitions to the discrete levels are printed first with negative energies and end points of the spectra are indicated by repeating the line.
42. EMPEND adjusted to accept format of p.41 above - improves energy balance above reaction thresholds (A. Trkov).
43. Suite of gamma-strength functions from RIPL-2 coded by Plujko and implemented by R. Capote and M. Herman.
44. Reaction/MT-number conversion table for X4TOC4 updated to include gammas in the incident channel (A. Trkov & M. Herman).
45. Ordering error in ENDF/MF12 corrected in EMPEND (A. Trkov)
46. Quasideuteron photoabsorption added by B. Carlson
47. Formatting of photonuclear reactions added to EMPEND (A. Trkov)
48. X4TOC4 updated by A. Trkov.
49. Fixed energy balance in exclusive spectra by including missing gamma-ray transitions in the ENDF file (levels without branching ratio assumed to decay to the ground state) (M. Herman).
50. Scripts moved to the empire/scripts/ directory allowing for multiple working directories (M. Herman)

51. Run section in the GUI redesigned to allow for free selection of modules to run (M. Herman)
52. Comparison plots including an arbitrary ENDF-6 file possible also for spectra and double-differential cross sections (M. Herman)
53. Numerical procedure for determining experimental coupling constants, used for construction of QRPA response functions, in MSD-tristan/inelas modified in order to avoid fluctuations with incident energy (H. Wienke)
54. ECIS06 converted into subroutine by R. Capote
55. SCAT2 replaced by ECIS06 (R. Capote)
56. ENDRES updated by A. Trkov

## Changes in version 2.18 with respect to 2.17.1 (Vienna, September 2002)

1. Bug fixed in reading levels file when preparing collective levels for ECIS (R. Capote).
2. Bug fixed in reading Coulomb parameters of o.m.p. from the RIPL-2 file (affects charged particle channels) (R. Capote).
3. Relativistic correction in tl.f removed ( $\gamma=1$ ). It is not needed since SCAT2 and ECIS take care of it (R. Capote).
4. Bug in EMPEND, which caused skipping the last but one energy point fixed (A. Trkov).
5. EMPEND formats branching ratios in the ENDF file (A. Trkov).
6. xterm closes when calculations are done as it was in versions 2.17 and earlier (p.3.iii below removed) since it was inconvenient for running piece-wise and multiple calculations (M. Herman).
7. gamma-strength function uses a temperature consistent with the current level densities for the final state (not for the initial one as erroneously coded before) (M. Herman).
8. Beta version of the new GUI (Xrun.tcl) added (M. Herman).
9. Corrected renormalization of the absorption cross section in DEGAS (E. Betak).
10. Corrected way of restricting exciton configurations used in DEGAS (E. Betak).

11. Maximum number of excitons used in DEGAS set to 5 (3 configurations) (M. Herman).
12. PLOT4 updated to produce  $\gamma$ -spectra (continuum contribution from the capture reaction has not yet been included) (A. Trkov).
13. Bugs in PLOT4 fixed. PLOT4 tested on Linux with g77 and Absoft90 ver. 7.0 compilers and on Ms Windows with Lahey 75 (A. Trkov).
14. If discrete levels are inconsistent with Gilbert-Cameron level densities and LEVFIT is non-negative calculations are continued using nuclear temperature taken from the systematics. Appropriate message is printed and cumulative plot displayed (without blocking further calculations) (M. Herman).
15. Bug in empire-specific level densities at very high energies (close to 200 MeV) when level density exceeds capacity of the 32-bit word has been fixed by ignoring fit to the discrete levels (unfortunately in all nuclei) (M. Herman).
16. File Ko in tl.f is rewound to avoid messages that particular omp is not found in the local file (M. Herman).
17. Number of iterations when fitting discrete levels with Gilbert-Cameron level densities limited to 300 to avoid the possibility of infinite loop (M. Herman).
18. Z=105 name changed to 'Db'; thanks to Erik Strub for pointing it out (M. Herman).
19. Problem with the discontinuity of neutron capture cross section when incident energy becomes lower than the integration bin width has been solved. Capture cross sections, even at very low energies ( $<10$  keV) can now be calculated even with as few as 50 energy bins (tested on 193-Ir) (M. Herman).
20. All collective levels are used in ECIS calculations with DIRECT=1,2, even if they can not be excited because of the too low incident energy. In the previous versions only open channels were taken into consideration and coupling to the closed ones was ignored (R. Capote).
21. Minor corrections of nuclear masses in EMPEND (avoid potentially infinite loop while the ENDF formatted file is processed by SIXTAB) (A. Trkov).
22. Thresholds for particle emission channels corrected in EMPEND (A. Trkov).
23. Discrete level library updated to the RIPL-2 version of September 24, 2002 (M. Herman).
24. LSTTAB corrected to allow for plotting spectra at  $90^\circ$  with ZVView (A.Trkov).

## Changes in version 2.17.1 with respect to 2.17 (Vienna, April 2002)

1. Bug in reading RIPL discrete levels fixed by R. Capote.
2. All scripts modified: (i) all links made symbolic to allow for using network drives, (ii) ./ added in front of calls (thus ./ is no longer needed in the PATH), (iii) xterm remains open after calculations are completed so that runtime messages can be inspected (M. Herman).
3. GUI background color changed to gray (M. Herman).
4. guizvv.tcl for graphical comparison of up to three calculations/evaluations (already present in 2.17) modified (nonstandard Tcl/Tk widget replaced) (M. Herman).

## Changes in version 2.17 with respect to 2.17beta (Vienna, February 2002)

1. Bug corrected: adding CN contribution to angular distributions for discrete levels. Gammas were added to CSAlev(...,0) in HFcomp.f with 0 being out of dimension. Adding of gammas is now blocked. Thanks to V. Plujko for pointing this out.
2. PLOT4 updated by A. Trkov to produce spectra (including double-differential) for outgoing protons and alphas. Structure of the PostScript files improved.
3. RIPL files placed in the empire/RIPL-2 directory following RIPL-2 structure and naming convention (compatibility with the RIPL-2 CD-ROM).
4. Optical model database updated to the preliminary RIPL-2 version.
5. EXFOR library updated to version of 18.05.2001 (NOTE: previous EXFOR database will NOT work with EMPIRE-2.17 due to a different directory structure).
6. Case specific file with extracted discrete levels (file 14) closed at the end of calculations.
7. The new script “*setup-emp*” assists installation procedure and allows to use EXFOR library and/or HF-BCS level densities directly from the installation CD-ROM without copying them onto hard disk.

## Changes in version 2.17beta with respect to 2.16.2 (Vienna, November 2001)

1. Dispersive optical model potential implemented (SCAT2, ECIS, ORION3) (R. Capote)
2. Optical model database updated to the preliminary version from RIPL2 (including 4 dispersive omp) (R. Capote)
3. Discrete levels database updated to the preliminary version of RIPL2 (R. Capote)
4. Number of discrete levels constituting a complete scheme taken from the preliminary version of RIPL2 (R. Capote)
5. Elastic is calculated in all cases on the  $2.5^\circ$  grid, while all the rest are on the  $10^\circ$  grid. Previous inconsistency removed (transfer of elastic when  $DIRECT > 0$  was used) (M. Herman)
6. GUI starts with gvim editor selected by default (M. Herman)
7. Two compilation warnings in tl.f fixed (M. Herman)
8. Cumulative plots of discrete levels created as a PostScript file rather than being dumped onto the screen. The file is stored as \*cum.ps and available through GUI (M. Herman)
9. Damping of the rotational level density enhancement below BCS critical energy made consistent with the one above critical energy. Removes discontinuity at critical energy for perfectly spherical nuclei ( $\beta=0$ ) (M. Herman)
10. List of warnings available through the GUI (M. Herman)
11. Tabulated HFBCS levels densities, as provided to RIPL-2 by S. Goriely, included as additional level density option (M. Herman)

## Changes in version 2.16.2 with respect to 2.16 (Vienna, 21 August 2001)

1. Implementation of the HMS model completed
2. New version of V. Zerkhin viewer (zv94l.exe) provides eps format and interaction with plot titles (use A + right shift)
3. Duplicate use of file 33 removed (36 used in levdens.f)

## Changes in version 2.16 with respect to 2.15 (Vienna, July 2001)

1. EXFOR retrieval using FORTRAN instead of UNIX 'grep'.
2. Fission barrier set to 1000 MeV for  $Z < 19$ .
3. GDR second peak energy set to 0 for spherical nuclei.
4. Temperature in the generalized Lorentzian protected against 0 excitation energy.
5. Plotc4.f improved (A. Trkov) to allow for up to 23 data sets to be drawn on a single plot. Plotc4 input modified to include whole energy range.
6. Orion calculations performed up to 99% of the maximum energy loss (instead of 90% that cause problems with extrapolation to low outgoing energies).
7. Plotc4.f improved (A. Trkov) to allow for energy spectra and angular distributions plots.
8. Legend and lsttab added for future improvements but not fully implemented yet.
9. ENDF=2 option added (lumped channel representation MT=10 or 5). SO FAR DDX ARE NOT SUPPORTED BY EMPEND!!!!
10. Exact treatment of recoil spectra with ENDF=2 option.
11. Call to Monte Carlo preequilibrium model HMS coded by M.B. Chadwick. NO TRANSFER OF THE RESULTS!!!!
12. Exciton model code DEGAS implemented by P. Oblozinsky
13. Fixed bug in flux conservation when GST option selected but MSC gamma channel closed.
14. New version of SCAT2 introduced by R. Capote
15. Link to ECIS for calculation of the elastic, absorption and cross sections to discrete collective levels within rotational and vibrational CC model. Includes automatic selection of collective levels (R. Capote).
16. Link to the omp segment of RIPL introduced by R. Capote. NOTE: change in the format and name of the local file with internal omp. New name is \*omp.int and two columns are added in definition of om potentials (just before radii). RIPL potentials are stored in the file \*omp.ripl.
17. New version of V. Zerkov viewer (zv93l.exe)

18. List of RIPL omp added to the GUI under Help menu
19. DWBA option with ECIS added by R. Capote
20. pol20, pol21 and pol22 variables in SCAT2 initialized with 0.
21. Bug fixed in ACCUMSD when MSD transitions to continuum were energetically closed (seems to have had no effect on the results).
22. Total cross section added to EXFOR retrieval, and together with fission to the MT list for ZVView plotting.
23. “zvpl” script added for plotting excitation function for any cross section from the main EMPIRE output (\*.lst).
24. “runpiecewise” script added for running up to 3 different inputs for the same case in the 3 non-overlapping energy ranges (incident energies inside and among the 3 ranges must increase monotonically).
25. Division by 0 in fitting field parameters in MSD tristan.f protected.
26. GUI modified to include 'zvpl' script and allow for merging ZVV plots.
27. Form factor for the  $l=0$  transitions in MSD controlled from the optional input (default: standard surface form factor).
28. Provision for use of combined preequilibrium models in a single run.
29. “zvcomb” script added to combine various existing ZVView plots.
30. Utility code manuals and Frequently Asked Questions (FAQ) added to the GUI under Help menu.
31. Utility code inputs accessible from the GUI Options menu.
32. Utility code c4sort added to sort \*.c4 file in ascending energy. Actually, disabled (commented) in run and runE scripts as sorting takes too long for large files.

## **Changes in version 2.15 with respect to 2.14.1 (Vienna, November 2000)**

1. Adding of plotting of double differential cross sections for neutron production using PLOT4 (modified by A. Trkov). This involves modification of EXFOR retrieval (new REAC\\_SIG.TXT file, changes in the 'sel' script and input.f), as well as modifications in the util/x4toc4/reaction file.



2. Activated printout of total and shape elastic cross sections, shape elastic angular distributions, strength functions, and scattering radius from SCAT2.
3. Minimum Tl set to 1.0E10 to avoid underflow in the calculations. This limit might be changed in line 761 of tl.f

## Changes in version 2.14.1 with respect to 2.14 (Vienna, October 2000)

1. Bugs fixed:
  - a) flux conservation at very low incident energies (in HRTW),
  - b) mismatch of elastic channels for negative parity targets (in HRTW),
  - c) division by zero 1p0h level density in MSC gamma emission,
  - d) undefined variables in MSC NVWY.f and MSD tristan.f defined (KASE in MSD orion.f still remains undefined, Z1 and Z2 are not problems since they are unused).
2. MATIN1 replaced by MTXINV in MSC gamma emission.
3. VMS specific statements marked with \*IF VMS in input.f and io.h
4. Print of C.M. incident energy to standard output added in main.f

## Changes in version 2.14 with respect to 2.13 (Vienna, September 2000)

1. Second chance preequilibrium emission applying Chadwick model to the result of the MSD.
2. Bug fixed in clearing the population of discrete levels when using ENDF option.
3. Bug fixed in writing optical model parameters for the incident channel on the ompar file.
4. SHC(2)=SHC(1) bug fixed in main.f
5. Misprint for 95Zr in data/ldp.dat(7676) fixed by setting the value to 0.
6. Removed redundant FLOAT in ORION2.
7. Collective level densities with  $a=A/\text{LEV DEN}$  used whenever  $\text{LEV DEN} > 2.0$
8. Star format for recoil mass replaced by fixed format.

9. Alphanumeric branching ratios in orsi.liv replaced by numbers and input.f changed appropriately (BCDNUM removed).
10. HRTW formulation of the statistical model included (width fluctuation correction).
11. Bug fixed that caused use of Weisskopf estimates for gamma strength at all incident energies except the first one.
12. Bug removed in passing GDR parameters through input.
13. Zerkin's zvd plotting capability added (through zvd script and tcl/tk GUI).
14. EXFOR entries for neutron capture coded as SIG,,AV (averaged cross sections) included in plots.

## **Changes in version 2.13 with respect to 2.12.2 (Vienna, March 2000 )**

1. General cleanup of the FORTRAN source.
2. New organization of modules that reflects physical contents.
3. Check whether MSD cross section is not larger than the fusion cross section.
4. Gamma cascade in the first CN is default if CN excitation energy is below 20 MeV and can be controlled with GCASC in optional input.
5.  $l=0$  transfer strength in MSD-orion set to the self-consistent value by default (rather than to GMR energy as before).
6. Fusion cross sections read from the file name.fus are treated as fusion cross sections at subsequent  $l$  values (starting with  $l=0$ ) rather than fusion cross sections to a given spin of CN. Transmission coefficients are calculated from the read values and a proper angular momentum and parity coupling is performed to obtain Compound Nucleus spin distribution.
7. Error removed in BCS blocking in TRISTAN.
8. BCS blocking in TRISTAN made automatic (no input required).
9. pipe.c replaced with coding by Capote.
10. Automatic retrieval of EXFOR data.
11. Link to EMPEND to create ENDF formatted file.
12. Link to X4TOC4 and PLOT4 to produce plots at the end of the run.

13. Fission barriers for  $Z > 102$  according to Myers&Swiatecki, Phys. Rev. C60 1999.
14. FITLEV creates a whole set of cumulative plots without interaction.
15. Fusion barrier can be read from input (BFUS).
16. Bass option for fusion disabled.
17. Distributed fusion barrier mode now relies on the CCFUS fusion barrier.
18. OMPAR (.omp) file with optical model parameters produced and used for input.

## **Changes in version 2.12.2 with respect to 2.12.1 (Vienna, 11 April 1999)**

1. Energy shift used to fit low-energy discrete levels gradually decreased between  $E_{cut}$  and neutron binding to recover agreement with Dobs.
2. Entire code checked with FTNCHEK and some errors corrected (undefined variables, unreferenced variables removed).
3. All DO loops given separate endings (END DO, no labels).
4. Entire code consistently indented.

## **Changes in version 2.12.1 with respect to 2.12 (Vienna, 07 Dec. 1998)**

1. Dsource directory added with explicit double precision source (no compiler -r8 option required).
2. roign.f routine replaced by roemp.f. Fits dynamic level densities (BCS approach below critical energy) to discrete levels by applying an energy shift. ATTENTION: these shifts destroy agreement with Dobs at neutron binding.

## **Changes in version 2.12 with respect to 2.11 (Vienna, 15 Sept. 1998)**

1. Error removed in the determination of pairing corrections in readnix.f (for Gilbert-Cameron).
2. Errors removed in coding of the dynamic level densities.

3. New, EMPIRE-specific systematics of level density parameter  $a$  for dynamic level densities introduced and set as default if dynamic level density chosen. This systematics fits Ilijnov-Mebel  $D_{obs}$  using EMPIRE formulae for level densities. If an experimental value for a given nucleus is present in the *ldp.dat* file, this value is adopted. The average normalization factor is calculated from these cases and applied to those for which there are no experimental data. All nuclei are treated as deformed as far as collective enhancement is concerned. Damping of the collective effects has been temporarily removed, i.e. level densities are calculated by means of an adiabatic approach.